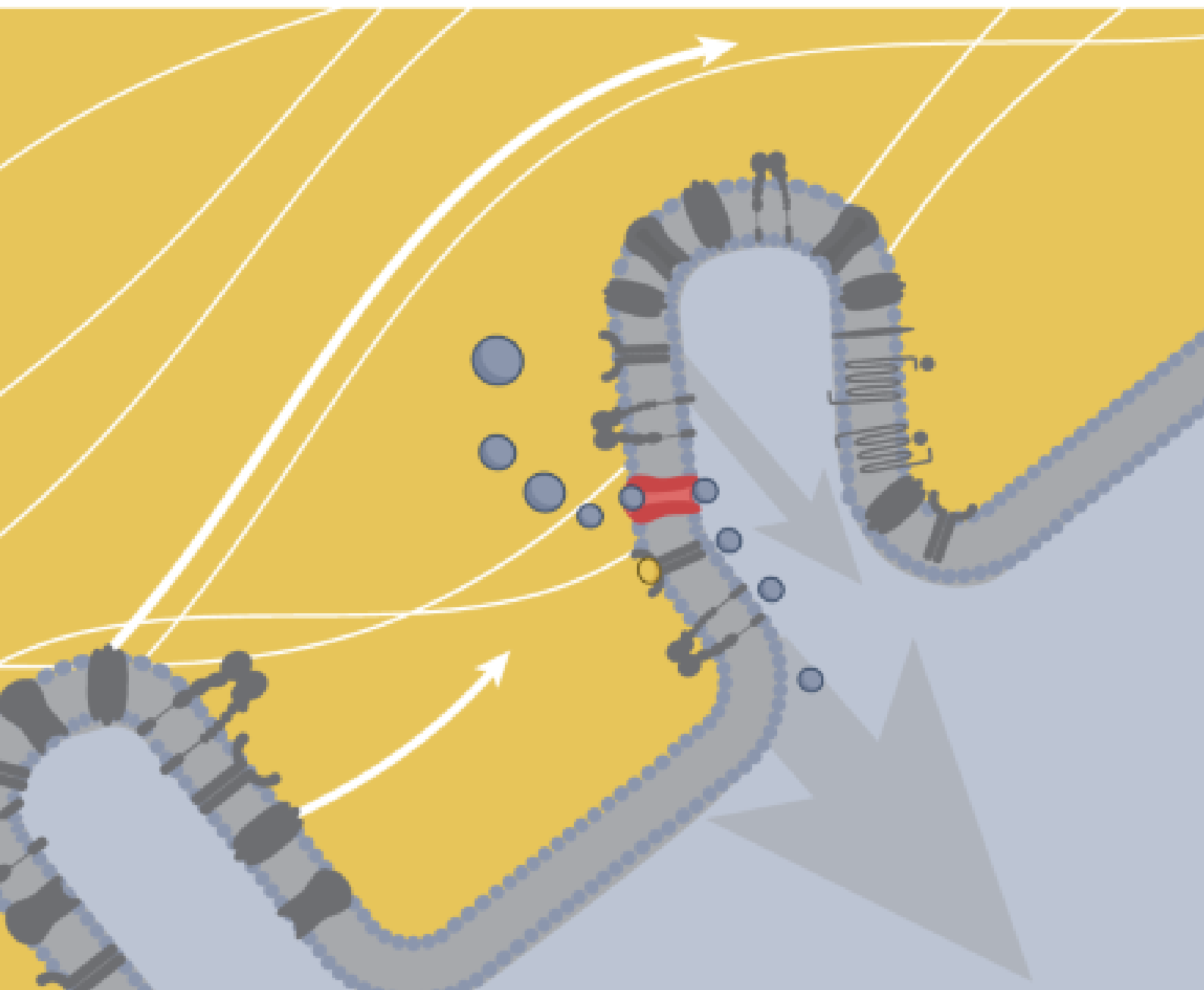


nature reviews rheumatology



MECHANOSIGNALLING

An emerging target for osteoarthritis therapy

Acute exacerbation of interstitial lung disease

Features and management

OSTEOARTHRITIS

Use of platelet-rich plasma for knee OA not supported by RCT results

Intra-articular injection of platelet-rich plasma (PRP) is increasingly used in the management of osteoarthritis (OA). Despite showing promise in preclinical studies and some randomized controlled trials (RCTs), high-quality evidence of its efficacy is lacking. The results of a rigorous RCT now reported in *JAMA* do not support the use of PRP injections for knee OA.

The RESTORE RCT enrolled 288 patients with mild-to-moderate radiographic knee OA. “We found PRP resulted in clinically meaningful improvements in knee pain over 12 months; however, these improvements were no greater than those observed in people who received saline injections,” reports co-lead author Kade Paterson. “There was also no benefit of PRP over saline for 12-month change in cartilage thinning, and

there was no additional improvement with PRP over saline on 29 of our 31 clinical and structural secondary outcomes.”

The discrepancy between these results and those of previous RCTs could be attributable to differences in methodology, including the PRP preparation used. However, the findings from the RESTORE study support those of an earlier RCT published in *JAMA* ($n = 100$), which used a PRP preparation with a platelet concentration reportedly higher than that of the preparation used in the RESTORE trial. In that earlier RCT, PRP injections did not have any benefit over saline injections for symptoms of ankle OA over 26 weeks. “A promising avenue for future research would be to compare the clinical effects of PRP containing lower versus

“The results of a rigorous RCT ... do not support the use of PRP injections for knee OA”



Credit: RUNSTUDIO/DigitalVision

higher concentrations of platelets in people with OA, to determine whether platelet concentration does indeed affect the clinical response to PRP injections,” notes Paterson.

Sarah Onuora

ORIGINAL ARTICLE Bennell, K. L. et al. Effect of intra-articular platelet-rich plasma vs placebo injection on pain and medial tibial cartilage volume in patients with knee osteoarthritis: the RESTORE Randomized Clinical Trial. *JAMA* **326**, 2021–2030 (2021)

RELATED ARTICLE Paget, L. D. A. et al. Effect of platelet-rich plasma injections vs placebo on ankle symptoms and function in patients with ankle osteoarthritis: a randomized clinical trial. *JAMA* **326**, 1595–1605 (2021)

SJÖGREN SYNDROME

New hope for B cell-targeting therapy in pSS

B cells are known to be important in the pathogenesis of primary Sjögren syndrome (pSS), which is characterized by oral and ocular dryness, systemic manifestations and an increased risk of developing B cell lymphoma. However, attempts to treat pSS by targeting B cells have failed to show efficacy in large, randomized controlled trials, possibly owing to the choice of inclusion criteria and outcome measures.

Following years of disappointing trial results in pSS, a phase IIb study of the anti-B cell-activating factor (BAFF) receptor antibody ianalumab has reported positive results in patients with moderate-to-severe pSS. The study, published in *The Lancet*, met its primary outcome measure of an improvement in the EULAR Sjögren's Syndrome Disease Activity Index (ESSDAI) score at week 24.

“a phase IIb study of ... ianalumab has reported positive results in patients with moderate-to-severe pSS”

“This is the first fully powered study in pSS to demonstrate improvement in systemic disease measured by the ESSDAI,” states corresponding author Simon Bowman. “Furthermore, there was a clear dose response, which supports the positive outcome of this study.”

In the study, 190 participants were randomly assigned 1:1:1:1 to receive placebo or ianalumab at 5 mg, 50 mg or 300 mg doses for 24 weeks. The agent was delivered by subcutaneous injection every 4 weeks, and disease activity, symptom severity and quality of life were recorded using a variety of scoring systems. Overall, a statistically significant change in the ESSDAI score from baseline was reported at week 24 for the 300 mg dose of ianalumab, along with an improvement in salivary flow rate. However, patient-reported outcomes for

symptom severity, fatigue and health-related quality of life did not show improvements at week 24.

In addition to trial design elements such as the choice of outcome measures and the careful selection of participants with disease that was severe but still potentially amenable to improvement, the positive results of this trial compared with previous trials of B cell-targeting therapies in pSS could also be related to the dual mode of action of ianalumab, which both depletes B cells and blocks BAFF signalling.

“These results represent a paradigm shift in demonstrating that successful disease-modifying therapy is possible in this condition,” concludes Bowman, adding that further studies are planned for ianalumab.

Joanna Clarke

ORIGINAL ARTICLE Bowman, S. J. et al. Safety and efficacy of subcutaneous ianalumab (VAY736) in patients with primary Sjögren's syndrome: a randomised, double-blind, placebo-controlled, phase 2b dose-finding trial. *Lancet* [https://doi.org/10.1016/S0140-6736\(21\)00251-0](https://doi.org/10.1016/S0140-6736(21)00251-0) (2021)

RELATED ARTICLE Seror, R. et al. Current and future therapies for primary Sjögren syndrome. *Nat. Rev. Rheumatol.* **17**, 475–486 (2021)

THERAPY

DRESS linked to HLA alleles

Drug reaction with eosinophilia and systemic symptoms (DRESS) occurs in some patients with systemic-onset juvenile idiopathic arthritis (sJIA) or adult-onset Still's disease (AOSD) treated with IL-1 or IL-6 inhibitors, according to the findings of a case-control study. Notably, these delayed hypersensitivity reactions were strongly associated with a common HLA class II haplotype.

The multicentre study included 66 patients with sJIA or AOSD who had a probable drug reaction to the IL-1 inhibitors anakinra, canakinumab, rilonacept and/or the IL-6 tocilizumab; a further 65 patients enrolled in the study were considered drug-tolerant. In a retrospective analysis of clinical data, the researchers verified 65 of 66 of the drug-reactive cases to be DRESS according to RegiSCAR criteria.

Features of DRESS included peripheral blood eosinophilia, rash and elevated concentrations of liver enzymes. Macrophage activation syndrome, which can be a feature of DRESS, was far more common among patients with sJIA or AOSD who had DRESS than in those who were drug-tolerant (64% versus 3%; $P = 1.2 \times 10^{-14}$). The researchers also observed that many patients continued cytokine inhibitor therapy after DRESS criteria were met, suggesting that the drug reactions were often not recognized.

HLA data were available for 94 of the 131 patients in the study. The researchers found that *HLA-DRB1*15* haplotypes were enriched in those with DRESS as compared with self-identified ancestry-matched drug-tolerant study participants ($P = 6.3 \times 10^{-10}$) and also compared with ancestry-matched individuals in the International Childhood Arthritis Genetics Consortium (INCHARGE) sJIA cohort ($P = 7.5 \times 10^{-13}$). Common *HLA-DRB1*15* alleles were also linked with suspected delayed anakinra reaction in a small cohort of patients with Kawasaki disease in a phase I-IIa trial ($n = 19$).

The researchers suggest that HLA testing should be considered as part of pre-prescription risk assessment, and that vigilance for DRESS is needed during treatment with IL-1 and IL-6 inhibitors.

Sarah Onuora

ORIGINAL ARTICLE Saper, V.E. et al. Severe delayed hypersensitivity reactions to IL-1 and IL-6 inhibitors link to common *HLA-DRB1*15* alleles. *Ann. Rheum. Dis.* <https://doi.org/10.1136/annrheumdis-2021-220578> (2021)

SYSTEMIC SCLEROSIS

Evaluating early diagnostic criteria for SSc

Early diagnosis of systemic sclerosis (SSc) potentially enables therapeutic intervention to avoid the progression of skin fibrosis and organ damage. Researchers have previously evaluated criteria for Very Early Diagnosis of SSc (VEDOSS) in retrospective analyses of single-centre cohorts, but whether these criteria are generalizable is not yet known.

In the VEDOSS international, multicentre, longitudinal registry study, 553 participants had Raynaud phenomenon at enrolment without fulfilling the 2013 ACR-EULAR classification criteria for SSc or the criteria for any other definite connective tissue disease, and had data for at least one annual follow-up visit for assessment of the VEDOSS criteria of positivity for antinuclear antibodies (ANAs), puffy fingers, SSc-specific autoantibodies and abnormal findings on nailfold capillaroscopy. In these patients, the mean age was 45.9 years, 91.7% were women, the median time since onset of Raynaud phenomenon was 4.0 years, and the median duration of follow-up was 3.6 years.

The primary end point of the study was progression to SSc from enrolment to follow-up. Among the 254 participants who

progressed or completed 5 years of follow-up, 133 (52.4%) met the end point. The baseline status of each VEDOSS criterion was assessed for association with progression. Notably, only four of 37 individuals (10.8%) with an absence of ANAs at baseline progressed within 5 years. By contrast, 16 of 17 participants (94.1%) with the baseline combination of SSc-specific autoantibodies and puffy fingers progressed to SSc. Other combinations of VEDOSS criteria were associated with intermediate risks of progression, enabling the researchers to propose a reference scale that might be useful for risk stratification in clinical practice, to assess requirements for screening and early intervention. Risk stratification might also facilitate sample-size calculation in clinical trials investigating prevention of progression to SSc.

Robert Phillips

ORIGINAL ARTICLE Bellando-Randone, S. et al. Progression of patients with Raynaud's phenomenon to systemic sclerosis: a five-year analysis of the European Scleroderma Trial and Research group multicentre, longitudinal registry study for Very Early Diagnosis of Systemic Sclerosis (VEDOSS). *Lancet Rheumatol.* **3**, e834–e843 (2021)

INFLAMMATORY ARTHRITIS

Inflammatory arthritis affects men's fertility

Reproductive outcomes are influenced by many factors, both maternal and paternal. Conditions that affect the number, quality and delivery of sperm are related to fertility, and systemic inflammation is known to contribute to the occurrence of abnormalities in sperm DNA. Researchers have now found that pre-conception paternal inflammatory arthritis is negatively associated with pregnancy rates and outcomes.

Perez-Garcia and colleagues have reported results from the Dutch iFAME-Fertility multicentre cross-sectional study of the effects of inflammatory arthritis on male fertility. They analysed data from self-reported questionnaires completed by 408 men ≥ 40 years old who had rheumatologist-diagnosed inflammatory arthritis and who had, at some point, reported a positive pregnancy test. Of the 897 singleton pregnancies that were reported by these men, 677 occurred pre-diagnosis and 220 post-diagnosis, and 794 resulted in live births.

Post-diagnosis pregnancies differed from pre-diagnosis pregnancies in several notable aspects, including a longer time to pregnancy

and a greater proportion involving assisted reproductive technology, suggesting effects of inflammatory arthritis on conception. Furthermore, the rate of miscarriage (but not stillbirth) was greater in post-diagnosis pregnancies (adjusted OR 2.03; 95% CI 1.12–3.69, $P = 0.015$). In a subgroup analysis, the risk of miscarriage was particularly high following diagnoses of psoriatic arthritis (adjusted OR 4.35; 95% CI 1.65–11.49) or rheumatoid arthritis (adjusted OR 2.96; 95% CI 1.19–7.36).

Demonstration of an association between paternal inflammatory arthritis and miscarriage suggests that pre-conception counselling should be offered to men with this diagnosis. The relative contributions of the paternal inflammatory arthritis itself, associated comorbidities and anti-rheumatic therapies to the risks of adverse pregnancy outcomes remain to be determined.

Robert Phillips

ORIGINAL ARTICLE Perez-Garcia, L.F. et al. Paternal inflammatory arthritis is associated with a higher risk of miscarriage: results of a large multicentre study (iFAME-Fertility). *Rheumatology* <https://doi.org/10.1093/rheumatology/keab910> (2021)

ANTIPHOSPHOLIPID SYNDROME

Defibrotide inhibits NET-mediated thrombosis in APS models

Defibrotide, a heterogeneous mixture of polyanionic oligonucleotides, was first suggested as a treatment for antiphospholipid syndrome (APS) nearly 20 years ago, when it was successfully used to treat a patient with catastrophic APS (CAPS), but this possibility has not been investigated in clinical trials or preclinical studies.

A new study sheds light on how defibrotide might interfere with antiphospholipid antibody-mediated thrombosis.

Defibrotide is approved for the treatment of transplant-associated veno-occlusive disease, but its mechanisms of action are poorly understood. The new research suggests that it mitigates neutrophil extracellular trap (NET) formation in vitro and in mouse models of APS.

In the study, published in *Arthritis & Rheumatology*, defibrotide suppressed NET formation by neutrophils stimulated with antibodies isolated from patients with APS. The researchers found that this suppression was attributable at least in part to activation of adenosine A_{2A} receptors. In vivo, defibrotide attenuated APS-mediated venous thrombosis in wild-type mice but was not able to prevent venous thrombosis or NET formation in adenosine A_{2A} receptor knockout mice.

“defibrotide could be repurposed for the treatment of APS”

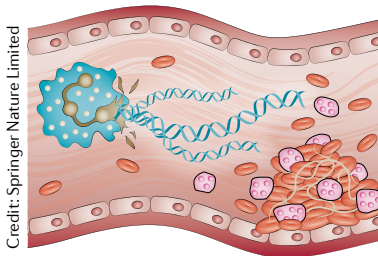
In a related paper published in *JCI Insight*, the researchers reported a potentially complementary mechanism of the polyanionic agent. “Defibrotide might also protect the endothelium from NETs that are already formed,” reports Jason Knight, corresponding author of both papers.

Together, the findings of these preclinical studies support the possibility that defibrotide could be repurposed for the treatment of APS. “We hope that the role of defibrotide will be further explored in a carefully selected subgroup of patients with APS with microvascular disease that does not necessarily respond to anti-coagulation,” says Doruk Erkan, co-author of the *Arthritis & Rheumatology* paper.

Sarah Onuora

ORIGINAL ARTICLE Ali, R. A. et al. Defibrotide inhibits antiphospholipid antibody-mediated NET formation and venous thrombosis. *Arthritis Rheumatol.* <https://doi.org/10.1002/art.42017> (2021)

RELATED ARTICLE Shi, H. et al. Endothelium-protective, histone-neutralizing properties of the polyanionic agent defibrotide. *JCI Insight* <https://doi.org/10.1172/jci.insight.149149> (2021)



Credit: Springer Nature Limited

PAEDIATRIC RHEUMATOLOGY

Tofacitinib a promising oral therapy for JIA

Current therapies for juvenile idiopathic arthritis (JIA) are not effective in all patients and often require administration by injection, which is not an ideal route for children. A phase III study in *The Lancet* has reported promising results for the oral Janus kinase inhibitor tofacitinib in children with JIA, which could broaden the treatment options for children who prefer to avoid injections.

“JIA is an umbrella term that groups together several JIA categories,” explains corresponding author Nicolino Ruperto. “In the present study, the categories included were polyarthritis (rheumatoid factor negative and positive), extended oligoarthritis and systemic arthritis without active systemic symptoms and signs at enrolment, as well as a small group of patients with enthesitis related arthritis or psoriatic arthritis.”

The researchers enrolled 225 children and young people between the ages of 2 and 17 years from 64 centres around the world that are part of the Paediatric

“rate of flare at 44 weeks was significantly lower in children with polyarticular-course JIA ... who received tofacitinib”

Rheumatology International Trials Organisation (PRINTO) and Pediatric Rheumatology Collaborative Study Group (PRCGS) networks, and used a double-blind, withdrawal design in which all participants received the active therapy for 18 weeks in the open-label part of the trial, followed by a double-blind randomized part that lasted for 26 weeks in which half of the participants were switched to placebo. The primary outcome measure was time to disease flare in the second part. “This peculiar study design, invented for JIA, has obvious ethical advantages (all children get the experimental drug from day 1) and is based on prior knowledge from trials performed in the adult population,” says Ruperto.

The rate of flare at 44 weeks was significantly lower in children with polyarticular-course JIA (polyarthritis, oligoarthritis or systemic JIA) who received tofacitinib than in those who received placebo ($P=0.0031$), and the safety profile of tofacitinib was consistent



Credit: Roman Miller/Alamy Stock Photo

with that seen in adults. Importantly, no thrombotic events were reported.

“A second phase III trial of tofacitinib is currently ongoing dedicated to systemic JIA,” states Ruperto. “Other trials with other Janus kinase inhibitors in JIA are also currently ongoing.”

Joanna Clarke

ORIGINAL ARTICLE Ruperto, N., Brunner, H. I. et al. Tofacitinib in juvenile idiopathic arthritis: a double-blind, placebo-controlled, withdrawal phase 3 randomised trial. *Lancet* **398**, 1984–1996 (2021)

Credit: Prostock-Studio/iStock/Getty Images Plus



QUALITY OF LIFE

Let's talk about sex, rheumatology!

Caroline A. Flurey

New research reports that men with inflammatory arthritis experience an impact on sexual health beyond erectile dysfunction, affecting their emotional, mental, and social health. Training to empower health professionals to have conversations about sex could improve support for people with rheumatic diseases.

Refers to Fernando Perez-Garcia, L. et al. It is not just about sex: viewpoints of men with inflammatory arthritis on the overall impact of the disease on their sexual health. RMD Open 7, e001821 (2021).

The World Health Organisation states that sexuality is “a central aspect of being human throughout life and encompasses sex, gender identities and roles, sexual orientation, eroticism, pleasure, intimacy and reproduction”. However, the focus on sexual health in the rheumatology literature has largely been limited to function, specifically fertility issues in women, and erectile dysfunction in men. Perez-Garcia and colleagues² have used Q-methodology to explore the impact of inflammatory arthritis on sexual health

“ Sex is an important aspect of quality of life, but it is still widely considered a taboo topic ”

in 30 men with rheumatoid arthritis or polyarticular juvenile idiopathic arthritis. The results provide important insights into their experiences.

Q-methodology combines qualitative and quantitative techniques to identify groups of people with similar opinions. Participants sort statements of opinion according to how much they agree with each statement across a grid representing a normal distribution. The participants are then grouped according to their views. In the study conducted by Perez-Garcia et al.², three viewpoints were identified: “Arthritis negatively affects my sexual health”, “I am keeping up appearances”, and “I am satisfied with my sexual health”. Consistent with reported prevalence of sexual problems in inflammatory arthritis, 43% of the participants populated the “I am satisfied with my

“ social barriers remain in discussing sex in relation to eroticism, pleasure, and intimacy ”

sexual health” viewpoint, reporting limited impact on sexual health. Q-methodology aims to gather opinions, and is not powered for epidemiological claims; nevertheless, it is notable that those satisfied with their sexual health reported lower disease activity than those in the other two groups.

In the new study, participants forming the first two viewpoints all reported experiencing an impact on their sex lives due to inflammatory arthritis, but they differed in their specific experiences². Men in both groups reported physical symptoms (such as pain) having a negative impact, causing sex to become less spontaneous or less frequent. However, those who formed the “Arthritis negatively affects my sexual health” viewpoint experienced a broader impact on their sexual health, including erectile dysfunction and relationship issues such as feeling guilty towards their partners, and not feeling fully understood. Men who formed the “I am keeping up appearances” viewpoint described a negative impact on self-esteem due to inflammatory arthritis, with physical differences (such as swollen joints) and inability to demonstrate physical prowess (both in general and during sex) affecting their feelings of attractiveness.

In a systematic review (published in 2020) of the impact of inflammatory arthritis on intimate relationships and sexual function³, among 55 eligible studies, only five were qualitative, and of these only one focused solely on men. In this study, men with systemic lupus erythematosus reported struggling to fulfil expected obligations as sexual partners, leading to feelings of guilt and emasculation. These findings are consistent with those reported by Perez-Garcia et al.². Similarly, my own qualitative findings in men with systemic sclerosis⁴ indicate that they worry about the impact of systemic sclerosis on intimacy and on their sexual partner's satisfaction. Women with inflammatory arthritis describe feeling pressure to maintain a normal sex life, to protect their relationships³. These findings suggest either a real or perceived pressure on both men and women to subscribe to traditional

gender roles in relation to sex, with the potential for psychological impact if inflammatory arthritis prevents these roles being fulfilled.

Perez-Garcia et al. found that men reported experiencing an impact of inflammatory arthritis on masculinity, translating to lack of confidence with sex². Some men reported hiding symptoms from their partners and trying to keep up appearances, which is consistent with the idea that men try to behave according to traditional masculine ideals and can subscribe to a learnt 'boy code' of hiding feelings of vulnerability⁵. Research in patients with rheumatoid arthritis has identified the need for clinicians to explicitly ask men about psychosocial and emotional issues⁶, which should be extended to include asking about issues related to sex. An indirect approach can often be effective, such as asking about how partners are coping, as opposed to direct questioning about feelings of masculinity.

Evidence suggests that providing information to men with long-term conditions offers reassurance and increases feelings of control⁷. However, Perez-Garcia et al. found that men reported difficulties accessing information related to sex, finding online information inadequate and health-care professionals too busy to address this issue². A study conducted in Denmark found 93.5% of women and 85.5% of men with rheumatoid arthritis had not discussed sexual issues with health professionals in the preceding 5 years⁸. This finding may be a result of social taboos relating to sex causing health professionals to feel uncomfortable raising the topic. Multidisciplinary health professionals in rheumatic diseases report that they seldom discuss sexual health with patients, despite considering it important⁹. However, those professionals who had received relevant training in sexual

health reported feeling more comfortable and raising it as an issue more frequently than staff without such training⁹. Providing training to empower health professionals to discuss sexual-health issues with patients should therefore be a key consideration.

The majority of research on the psychosocial impact of inflammatory arthritis has either addressed gender differences or focused solely on women⁶. Perez-Garcia et al. therefore make an important contribution to understanding an overlooked aspect of men's experiences of such conditions². However, it is worth noting that experiences of sex and intimacy also remain under-researched in women with inflammatory arthritis³. Further research is needed to understand the support needs and preferences for sexual health, and how these differ between men and women.

For sexuality in general, it is worth noting that the majority of rheumatology research is conducted through a broadly heterosexual lens. In this context it is important to highlight that patients from LGBTQ+ communities experience considerable health inequalities due to individual or institutional heteronormativity, as well as discrimination or victimization¹⁰. Future research in rheumatology should address whether the support needs of people from LGBTQ+ communities are appropriately served, not only in relation to sexual health, but also more broadly.

Sex is an important aspect of quality of life, but it is still widely considered a taboo topic. Although discussing sex in relation to reproduction is generally considered appropriate, social barriers remain in discussing sex in relation to eroticism, pleasure, and intimacy. However, appetite seems to be growing for more open discussion of sex and intimacy among health-care professionals, as illustrated by the inclusion of a session entitled "Myths

and taboos around relationships: strategies for a sexy life" at the 2021 EULAR European Congress of Rheumatology. Further research is needed to explore how health-care professionals can support people with rheumatic diseases to have healthy sex lives.

Caroline A. Flurey

Faculty of Health & Applied Sciences, University of the West of England, Bristol, UK.

e-mail: Caroline2.Flurey@uwe.ac.uk

<https://doi.org/10.1038/s41584-021-00722-y>

1. World Health Organisation. Sexual and reproductive health: Gender and human rights: Sexual health https://www.who.int/reproductivehealth/topics/gender_rights/sexual_health/en/ (2014).
2. Fernando Perez-Garcia, L. et al. It is not just about sex: viewpoints of men with inflammatory arthritis on the overall impact of the disease on their sexual health. *RMD Open* **7**, e001821 (2021).
3. Restoux, L. J. et al. Systematic review of the impact of inflammatory arthritis on intimate relationships and sexual function. *Arthritis Care Res.* **72**, 41–62 (2020).
4. Flurey, C. A. 'I've handed back my man card': experiences, coping styles, and support preferences of men with systemic sclerosis [abstract]. *Rheumatology* **60** (Suppl. 1) <https://doi.org/10.1093/rheumatology/keab246.027> (2021).
5. Pollack, W. S. Real boys: Rescuing our sons from the myths of boyhood (Henry Holt and Company, 1998).
6. Flurey, C. A. et al. "You obviously just have to put on a brave face": a qualitative study of the experiences and coping styles of men with rheumatoid arthritis. *Arthritis Care Res.* **69**, 330–337 (2017).
7. Galdas, P. et al. The accessibility and acceptability of self-management support interventions for men with long term conditions: a systematic review and meta-synthesis of qualitative studies. *BMC Public Health* **14**, 1230 (2014).
8. Bay, L. T. et al. Sexual health and dysfunction in patients with rheumatoid arthritis: a cross-sectional single-center study. *Sex. Med.* **8**, 615–630 (2020).
9. Helland, Y., Garratt, A., Kjekshus, I., Kvien, T. K. & Dagfinrud, H. Current practice and barriers to the management of sexual issues in rheumatology: results of a survey of health professionals. *Scand. J. Rheumatol.* **42**, 20–26 (2013).
10. Zeeman, L. et al. A review of lesbian, gay, bisexual, trans and intersex (LGBTI) health and healthcare inequalities. *Eur. J. Public Health* **29**, 974–980 (2019).

Competing interests

The author declares no competing interests.

Mechanosignalling in cartilage: an emerging target for the treatment of osteoarthritis

Tom Hodgkinson^{1,2,5}, Domhnall C. Kelly^{1,3,5}, Caroline M. Curtin^{1,2,4} and Fergal J. O'Brien^{1,2,3,4}✉

Abstract | Mechanical stimuli have fundamental roles in articular cartilage during health and disease. Chondrocytes respond to the physical properties of the cartilage extracellular matrix (ECM) and the mechanical forces exerted on them during joint loading. In osteoarthritis (OA), catabolic processes degrade the functional ECM and the composition and viscoelastic properties of the ECM produced by chondrocytes are altered. The abnormal loading environment created by these alterations propagates cell dysfunction and inflammation. Chondrocytes sense their physical environment via an array of mechanosensitive receptors and channels that activate a complex network of downstream signalling pathways to regulate several cell processes central to OA pathology. Advances in understanding the complex roles of specific mechanosignalling mechanisms in healthy and OA cartilage have highlighted molecular processes that can be therapeutically targeted to interrupt pathological feedback loops. The potential for combining these mechanosignalling targets with the rapidly expanding field of smart mechanoresponsive biomaterials and delivery systems is an emerging paradigm in OA treatment. The continued advances in this field have the potential to enable restoration of healthy mechanical microenvironments and signalling through the development of precision therapeutics, mechanoregulated biomaterials and drug systems in the near future.

¹Tissue Engineering Research Group, Department of Anatomy and Regenerative Medicine, Royal College of Surgeons in Ireland, Dublin, Ireland.

²Advanced Materials and Bioengineering Research Centre (AMBER), RCSI and Trinity College Dublin, Dublin, Ireland.

³Centre for Research in Medical Devices (CÚRAM), National University of Ireland, Galway, Ireland.

⁴Trinity Centre for Biomedical Engineering, Trinity Biomedical Sciences Institute, Trinity College Dublin, Dublin, Ireland.

⁵These authors contributed equally: Tom Hodgkinson, Domhnall C. Kelly.

✉e-mail: fjobrien@rcsi.com

<https://doi.org/10.1038/s41584-021-00724-w>

Mechanical signalling is an important mediator of numerous physiological and pathophysiological processes in the cells and tissues of the joint. In cartilage, chondrocytes synthesize, and are surrounded by, a highly specialized extracellular matrix (ECM) that enables low friction movement and protects the tissue during mechanical loading¹. In healthy cartilage, the mechanical forces generated by movement are an essential component of maintaining the homeostatic balance of chondrocyte-mediated ECM deposition and remodelling — a dynamic, continuous process of adaptation to the local mechanical environment, involving both sensation and transduction of forces. Some movement is required for healthy cartilage maintenance and joint disuse can lead to detrimental cartilage atrophy¹; however, excessive mechanical loading is a risk factor for the pathogenesis and progression of osteoarthritis (OA)², a disease that can affect all joint tissues and results in the functional failure of the joint³.

In OA, pathological changes in the cartilage ECM, including degeneration of the functional matrix (most notably type II collagen and proteoglycans), loss of tissue

hydration and production of incorrect fibrous ECM, occur concomitantly with aberrant chondrocyte proliferation, senescence, inflammation and hypertrophy⁴. Similarly, remodelling processes are dysregulated in the subchondral bone, resulting in changes to cortical plate thickness and local trabecular bone mass and architecture. These changes are dependent on the degree of OA severity and, in the later stages of disease, can be accompanied by bony outgrowths (osteophytes) at the joint margins⁵. At present, the timing of, and relationship between, these bone and cartilage tissue phenomena are not clear from a pathophysiological perspective (reviewed elsewhere^{3,5}). A number of factors are known to increase the risk of developing OA, including ageing, obesity and trauma or joint destabilization (post-traumatic OA)^{6–8}. Although OA tissues seem qualitatively similar in different types of OA, the mechanisms of disease can vary substantially⁹. For example, the composition and mechanical properties of cartilage ECM alter with increasing age, along with a broader drift in the chondrocyte transcriptome, both of which are thought to increase the propensity for OA

Key points

- Mechanical forces are a critical environmental factor for maintaining joint homeostasis, determining cell phenotype, inflammatory responses and the tightly regulated anabolic–catabolic signalling axis essential for cartilage homeostasis.
- Chondrocytes sense their mechanical environment through numerous direct and indirect mechanisms that regulate cell function in health and degenerative diseases, such as osteoarthritis.
- Targeted inhibition of mechanoinflammatory signalling pathways or restoration of functional chondroprotective extracellular matrix environments in osteoarthritis could prevent extracellular matrix degradation and promote reparative anabolic processes.
- Development of self-regulating and mechanically responsive biomaterials and drug delivery systems offer advanced ‘on-demand’ therapeutic approaches for the treatment of osteoarthritis.

development^{10,11}. Conversely, post-traumatic OA arises following injury to the joint tissue, most commonly in the form of fracture, cartilage damage, acute ligament injury or chronic ligament instability. As post-traumatic OA tends to affect a younger, more active population who place more rigorous demands on their joints, surgical interventions are more commonly used to treat this type of OA than other types¹².

Decades of research have demonstrated that the role of mechanical loading in the pathobiology of OA goes beyond tissue ‘wear and tear’ and is in fact a dynamic force that promotes the disease through the activation of mechanoresponsive cell signalling (mechanosignalling) and the resultant production of pro-inflammatory mediators and catabolic enzymes^{13–17}. This pathological signal transduction, which can be viewed as a corruption of chondrocyte mechanoadaptive processes, occurs when chondrocytes experience excessive physical forces, or when the chondroprotective ECM is compromised. In the latter situation, inadequate distribution of loads means that even within normal physiological ranges, excessive stress can be exerted on chondrocytes. In addition, the loss of important ECM molecules and structures also substantially affects mechanically controlled chondroprotective mechanisms^{18,19}. Despite the diverse aetiology of OA, the dysregulation of mechanosignalling seems to have a central role in the related processes that underlie disease progression and the phenotypic drift of chondrocytes in all types of OA.

Although the mechanisms by which degenerative or reparative signalling programmes are initiated within chondrocytes have not been fully elucidated, important molecular pathways and signalling mechanisms have been identified. In OA, targeting these pathways is an emerging strategy to reduce the release of the pro-inflammatory cytokines and catabolic enzymes that promote the progression of the disease^{20,21}. Furthermore, mechanosignalling and inflammatory mediators can directly interact, highlighting the potential for mechanobiology approaches that can boost repair and simultaneously reduce mechanoinflammation²². The correction of pathological mechanosignalling, either through adjustment of the cellular mechanical environment or through control over mechanosignalling, is likely to enhance the clinical effect of locally delivered anabolic factors such as fibroblast growth factor 18 (FGF18), which has shown

promise in clinical trials for the treatment of OA²³. In addition, regenerative biomaterials offer the opportunity to restore repair-stimulating mechanical environments while potentially, through additional functionalization, delivering disease-modifying OA drugs (DMOADs) or nucleic acids. Systems currently under development, such as stimuli-responsive release systems, can provide sophisticated control over this delivery, highlighting the potential for closed-loop therapeutic delivery²⁴. Similarly, synthetic gene circuits that respond to OA-associated stimuli such as inflammation by upregulating the production of anti-inflammatory agents represent an exciting development to enable in situ self-regulating therapeutic cell reprogramming^{21,25}.

In this Review, we focus on advances in the understanding of the complex role of specific mechanosignalling mechanisms in chondrocytes in healthy and OA cartilage. We highlight several important molecular processes and discuss strategies to target these therapeutically to interrupt pathological feedback loops, including the potential for combining these mechanosignalling targets with the rapidly expanding field of smart mechanoresponsive biomaterials and drug delivery systems.

Cartilage mechanoadaptation

Articular cartilage has a structure that is highly specialized for low friction movement and weight bearing. Cartilage itself can be subdivided into three overlapping zones moving from the subchondral bone towards the articulating surface — the deep zone, the intermediate zone and the superficial zone²⁶. Within these zones, the ECM composition and architecture reflect the forces experienced during movement. In the deep zone, type II collagen fibres are thick and arranged perpendicular to the joint surface to resist compressive loads, and proteoglycan concentrations are high to promote water retention. The intermediate zone experiences both compressive and shear forces, so type II collagen fibres are arranged randomly to resist forces from a number of directions. In the superficial zone, chondrocytes and type II collagen fibres are orientated transversely to disperse shear forces during articulation and secrete proteoglycan 4 (also known as lubricin) for lubrication²⁶ (FIG. 1).

At the tissue scale, the physical properties of cartilage are determined by the composition of the ECM; a network consisting predominantly of type II collagen, which traps high concentrations of proteoglycans (such as aggrecan, lubricin and perlecan) and glycosaminoglycans (GAGs; such as hyaluronan)^{27–29}. These proteoglycans and GAGs impart a fixed negative charge on the ECM, thereby promoting water retention and conferring remarkable shock-absorbing and low-friction properties. When compressed, any interstitial fluid is forced from the tissue, only to return upon unloading via charge interactions. Concurrently, hydrostatic pressure generated by ECM obstruction of interstitial fluid movement protects the tissue from compressive forces²⁸. Chondrocytes therefore experience a range of loading modes (including compression, stretch, shear and pressure), often simultaneously, which at the cellular level

Shear

A force or stress that is applied coplanar with the cross-section of the tissue.

Stretch

Deformation resulting in the final length of a material being greater than the initial length.

Pressure

A force applied acting inwards normal to any surface divided by the area of the surface.

are transduced and modified by the inherent properties of the ECM in which they are embedded. In combination with the magnitude of force and how frequently it is experienced, the integrity of the ECM has an important role in determining if an experienced load initiates catabolic signalling cascades in tissue-resident chondrocytes. Evidence indicates that ECM degradation not only affects the transmission of forces across the tissue, but can also alter the type of loading experienced by a chondrocyte in a particular zone, substantially affecting cell responses¹⁴.

The ECM in which chondrocytes reside does not have a homogeneous structure and composition. Surrounding the chondrocytes, a distinct region termed the pericellular matrix (PCM) has perhaps the most influence on cell mechanotransduction. Together with the cell itself, this region, which is around 2–4 µm thick, forms the structural, functional and metabolic unit commonly referred to as the ‘chondron’³⁰. The PCM can be around an order of magnitude softer than the bulk tissue ECM (in humans 0.04–0.1 MPa and 0.1–2 MPa, respectively), and is characterized by the presence of type VI collagen, but also contains other important components, including perlecan, aggrecan, hyaluronan, biglycan, type IX collagen, laminin and fibronectin^{30,31}. Moving outwards from the cell, the PCM integrates with the territorial matrix, a region characterized by a network of tightly packed proteoglycan, fibronectin and fine, fibrillar collagen^{32–34}. In turn, the territorial matrix integrates with the interterritorial matrix (the bulk tissue ECM; FIG. 1).

Although the integrity of all of these ECM regions is important for tissue function, the PCM directly modulates the forces experienced by the cell. Considering this function, it is perhaps not surprising that the PCM, and in particular the destruction of the PCM, has been implicated in OA¹⁸. Indeed, PCM degeneration is one of the earliest events in OA, altering both the transmittance and mode of mechanical forces experienced by chondrocytes^{35,36}. Notably, experimental and in silico models show that the forces experienced by chondrocytes are comparable across various species, and are independent of animal mass as a result of variations in PCM and ECM properties between species^{1,37}. When a mechanical stimulus is beyond a threshold that is perceived to be injurious, ECM remodelling is initiated. Targeting chondrocyte mechanosensing therefore offers the opportunity to retune cell thresholds in disease to re-establish the dynamic homeostatic balance.

Mechanosignalling mechanisms

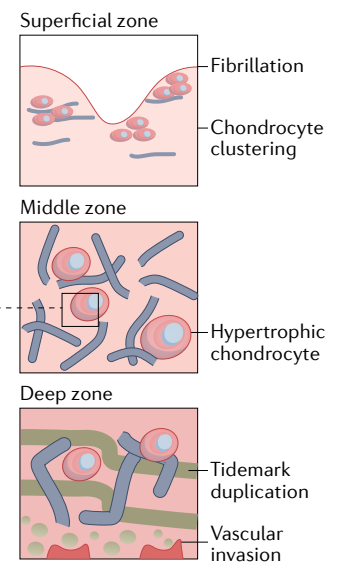
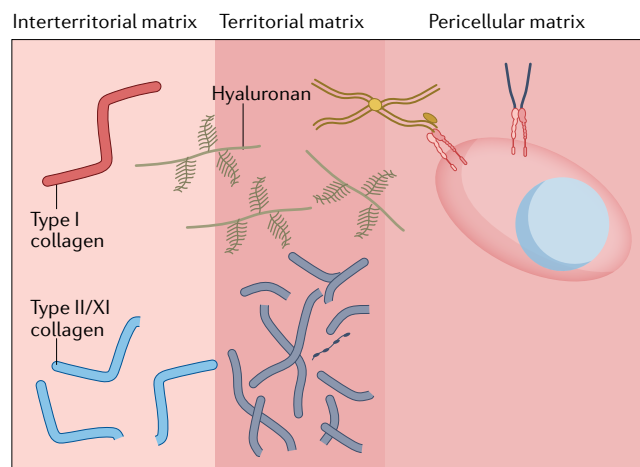
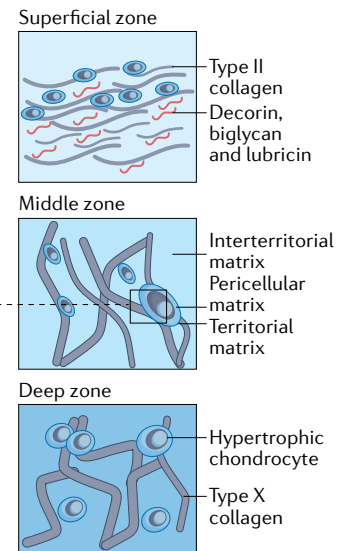
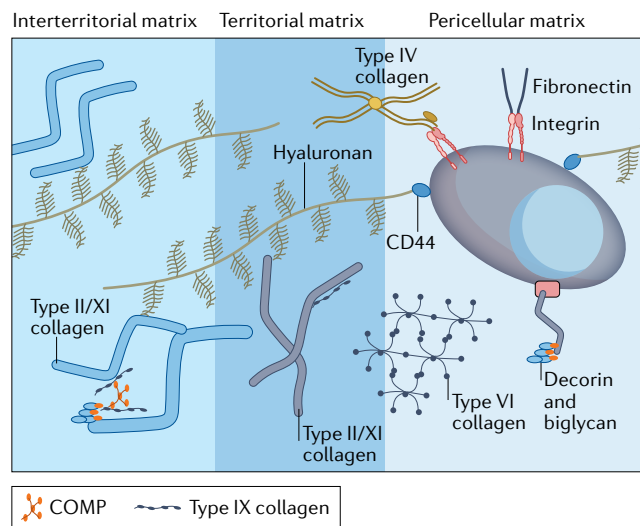
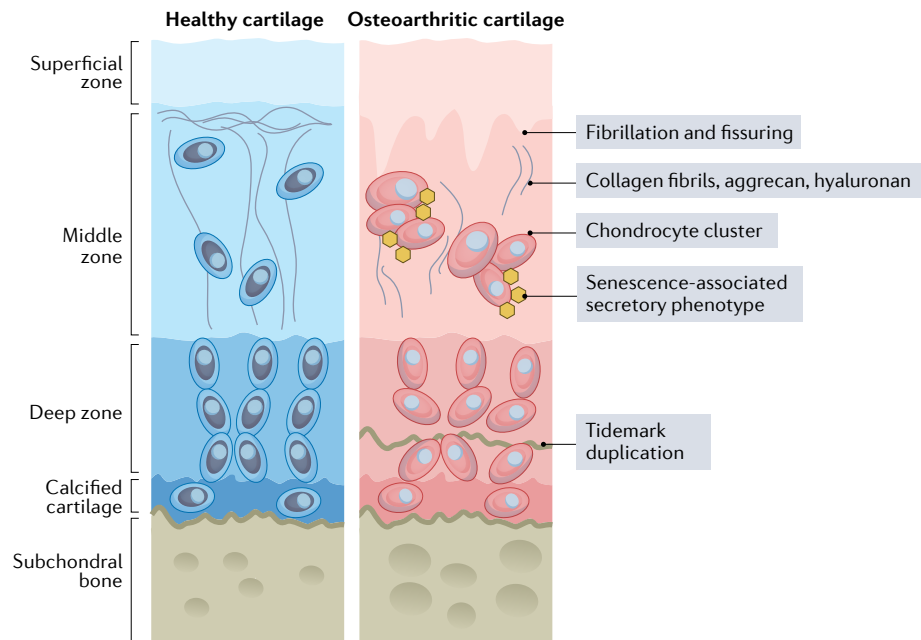
Chondrocytes effectively respond to mechanical stresses either ‘directly’ through sensing PCM deformation via cell–ECM adhesions and/or cell sensory structures, or ‘indirectly’ following the mechanically induced release of sequestered growth factors and their interaction with cell receptors (FIGS 2,3). In this section, we discuss indirect mechanosignalling via growth factors and several important direct chondrocyte mechanosignalling molecules and mechanisms, including integrins^{38–40}, cytoskeletal and nucleoskeletal constituents⁴¹, the chondrocyte ‘channelome’ (including mechanosensitive ion channels^{42–44}) and the primary cilium^{45,46}.

Growth factor-mediated mechanosignalling. Alterations in the composition and architecture of the PCM and territorial matrix lead to altered bioavailability of sequestered growth factors, such as FGFs, bone morphogenetic proteins (BMPs) and transforming growth factor-β (TGFβ)^{19,47–49}. Following deformation or destruction, ECM-sequestered factors are released to interact with cell membrane receptors, thereby activating downstream intracellular signalling pathways (FIG. 2).

A well-studied example of growth factor-mediated mechanosignalling is PCM and/or territorial matrix involvement in FGF signalling^{19,50–53}. All FGFs depend on heparin sulfate as an obligate co-receptor to bind, dimerize and activate FGF receptors (FGFRs)⁵⁴. In the PCM and territorial matrix, FGFs bind to perlecan, a heparin sulfate proteoglycan, and form an FGF reservoir that is released to activate FGFRs upon mechanical stimulation. FGF signalling can activate multiple intracellular signalling pathways, including those associated with protein kinase C (PKC), mitogen-activated protein kinase (MAPK) and phosphoinositide 3-kinase (PI3K)–protein kinase B (AKT)⁵⁴. A healthy PCM and territorial matrix composition is likely to have a substantial effect on both the availability of sequestered FGFs and the type of FGFs that are present, as members of the FGF family exhibit differing affinities for heparin sulfate binding. With FGFs, the balance between the deleterious and beneficial effects of signalling is dependent on the specific family members and receptors that are activated⁵⁵. Notably, recombinant human FGF18 (sprifermin), which activates FGFR3, is the only FGF therapy currently undergoing clinical trials, and has shown encouraging results by increasing cartilage thickness and reducing loss when administered by intra-articular injection to patients with OA^{56–58}.

Several other growth factor families have mechanical elements to their activity and regulation, including members of the TGFβ superfamily, which are activated by mechanical stress in an integrin-dependent manner (discussed in the following section)⁵⁹. Further understanding of how the initiation of anabolic, catabolic or pro-inflammatory signalling is regulated, the signalling proteins released under injurious and non-injurious conditions, and their effect on the anabolic–catabolic axis in cartilage tissue will provide valuable information to guide the development of pharmacological treatments for OA.

Integrin-mediated mechanosignalling. Integrins, the most well studied of the cell adhesion molecules, are important components in determining the responses of cells to their environment. The activity of integrins is tightly controlled via both biochemical and mechanical regulatory pathways (reviewed elsewhere^{60–62}). Briefly, upon ligand binding, integrins undergo conformational changes that expose regions in their cytoplasmic tails that promote binding to the actin cytoskeleton and integrin adhesion complex formation^{63,64} (FIG. 3a). The maturation of these nascent adhesion complexes into focal complexes, focal adhesions and fibrillar adhesions is tightly regulated⁶². Integrin-mediated force generation and mechanotransduction occurs through the



◀ **Fig. 1 | Articular cartilage composition and structure.** The structure of articular cartilage can be divided into three distinct zones moving from the articular surface towards the bone (superficial, middle and deep), followed by the calcified cartilage. Each zone exhibits a characteristic extracellular matrix (ECM) composition and organization that reflect the forces experienced. Chondrocytes and type II collagen fibres are orientated transversely in the superficial zone, enabling the dispersion of shear forces during articulation. The presence of lubricin within this zone further facilitates lubrication of the joint. In the middle zone, type II collagen fibres resist compressive and shear forces from a number of directions, as exemplified by the random arrangement of the fibres. By contrast, thick collagen fibres arranged perpendicular to the articulating joint surface in the deep zone resist compressive loads and high concentrations of proteoglycan in this zone enable water retention. The ECM in which chondrocytes reside also differs in composition and structure and can be divided into three regions moving from the chondrocyte outwards; the pericellular matrix (PCM), territorial matrix and the interterritorial matrix. The PCM, characterized by the presence of type VI collagen, surrounds the chondrocyte and influences chondrocyte mechanotransduction. The PCM also contains other important components such as hyaluronan, biglycan and fibronectin. The PCM integrates with the territorial matrix, a region characterized by tightly packed fibrillar collagen and proteoglycan. The outermost region, termed the interterritorial matrix, is the bulk tissue ECM. Although the integrity of the ECM as a whole has a role in the transmission of forces across the tissue, each specific zone determines the type of loading experienced by a chondrocyte, thereby influencing the cell response. In osteoarthritis, degeneration of the functional ECM, loss of tissue hydration and the production of incorrect fibrous ECM components occurs, along with fibrillation and fissuring. These pathological changes are accompanied by an altered chondrocyte phenotype, chondrocyte clustering, senescence and inflammation. Thickening of calcified cartilage and vascular invasion contribute to the characteristic histological feature of tidemark duplication. COMP, cartilage oligomeric matrix protein.

‘molecular clutch’ mechanism⁶⁵ in a substrate stiffness-dependent and integrin type-dependent manner (reviewed elsewhere^{62,66,67}).

In articular cartilage, several integrin heterodimers are present, including $\alpha 1\beta 1$, $\alpha 5\beta 1$, $\alpha 10\beta 1$, $\alpha 11\beta 1$ and $\alpha V\beta 1$, with a weaker expression of $\alpha 3\beta 1$ and $\alpha V\beta 3$ (REFS^{68–70}). The integrin profile of human OA chondrocytes is altered and difficult to interpret. For example, the expression of $\alpha 1\beta 1$, $\alpha 3\beta 1$, $\alpha 2\beta 1$, $\alpha 4\beta 1$ and $\beta 2$ integrins is increased, but the full implications of these expression changes are currently unclear^{71–73}. The expression of some integrin subunits is responsive to mechanical stimulation (such as $\alpha 5$, the expression of which increases upon loading⁷⁴) and several have been linked with both healthy and pathological chondrocyte mechanosignalling. For example, the αV integrin subunit has a critical role in the activation of TGF β signalling in regions of cartilage subjected to mechanical stress in human OA⁵⁹, suggesting a mechanism by which pathological ECM destruction is localized in the tissue. Under low mechanical stress, αV integrin is in an inactive state and latent TGF β is deposited into the PCM and territorial matrix bound to latency-associated peptide. Under conditions of high mechanical stress, integrin activation leads to the generation of cytoskeletal stress, increased cell stiffness and exertion of contractile forces by chondrocytes on the surrounding matrix. If this force is sufficient (>40 pN), latency-associated peptide undergoes a conformational change that results in the release of active TGF β ⁵⁹ (FIG. 3a). Therefore, in regions of high mechanical stress in the cartilage (generated by altered subchondral bone architecture in OA), talin-mediated increases in cytoskeleton contractile forces and chondrocyte stiffness trigger αV integrin-mediated activation of TGF β . Through this mechanism, regions of TGF β activation

can be correlated with regions of high mechanical stress where TGF β activation dysregulates chondrocyte metabolism and homeostasis, thereby promoting ECM degradation. Knockout of αV integrin in mice substantially attenuated this TGF β activation and downstream ECM degradation⁵⁹.

Other integrins with interesting expression profiles in articular chondrocytes include the $\alpha 10$ and $\alpha 11$ subunits and $\beta 1$ -containing integrins^{72,75–79}. The $\alpha 10$ integrin subunit is the dominant collagen-binding subunit in healthy chondrocytes^{80,81}, whereas the $\alpha 11$ subunit, which also binds collagen, is expressed at low levels in human and mouse chondrocytes^{68,70,82}. Expression of the $\alpha 11$ subunit is increased in OA cartilage and correlates with poorer chondrogenic differentiation of mesenchymal stem cells (MSCs)⁸³. Chondroprotective factors such as FGF2 and BMP2 increase the expression of the $\alpha 10$ subunit, whereas the $\alpha 11$ subunit is increased by TGF β ^{68,83}. Intriguingly, a 2020 study found that treatment with MSCs that had been selected for high $\alpha 10\beta 1$ integrin expression resulted in the production of less subchondral bone sclerosis and cartilage fibrillation in horses with injury-induced OA than treatment with saline⁸⁴. Mechanistic details of how these integrin subunits exert their effects on chondrocyte phenotypes is yet to be determined, although a link to cell stiffness and cytoskeletal contractility seems likely.

Clearly, the considerable influence of integrins $\alpha 1\beta 1$, $\alpha 5\beta 1$, $\alpha 10\beta 1$, $\alpha 11\beta 1$ and $\alpha V\beta 1$, among others, on chondrocyte behaviour make them potential targets for the treatment of OA. An attractive approach to targeting integrins in OA could be the repurposing of integrin receptor antagonists that are currently available or undergoing clinical examination for other indications. For example, cilengitide, a selective inhibitor of $\alpha V\beta 3$ and $\alpha V\beta 5$ integrins, is currently in clinical trials for the treatment of glioblastoma and is capable of suppressing pro-inflammatory and catabolic mediators (such as IL-1 β , TNF and matrix metalloproteinases (MMPs)) in ATDC5 cells (a mouse chondrogenic cell line)⁸⁵, suggesting potential for testing in OA.

Cytoskeletal and nucleoskeletal elements. The cytoskeleton has a substantial effect on mechanotransduction and a fundamental role in physiological and pathological chondrocyte phenotypes⁴¹. The actin cytoskeleton undergoes reorganization with deformative loading (such as compression) and non-deformative loading (such as osmotic or hydrostatic pressure), and disruption of F-actin is associated with altered cell viscoelastic properties and nuclear deformation following compression^{86–89}. Mechanical regulation of thymosin $\beta 4$, an inhibitor of F-actin polymerization, results in increased expression of catabolic mediators (MMPs), leading to increased cartilage catabolism. Treatment with thymosin $\beta 4$ peptide corroborates these downstream effects indicating that thymosin $\beta 4$ is involved in the mechanoregulation of MMPs⁹⁰. Cytoskeletal elements are abnormally distributed and assembled (or even absent altogether) in OA chondrocytes, compromising cell metabolic activities and biomechanical integrity^{91,92}. Moreover, in human OA chondrocytes cultured in

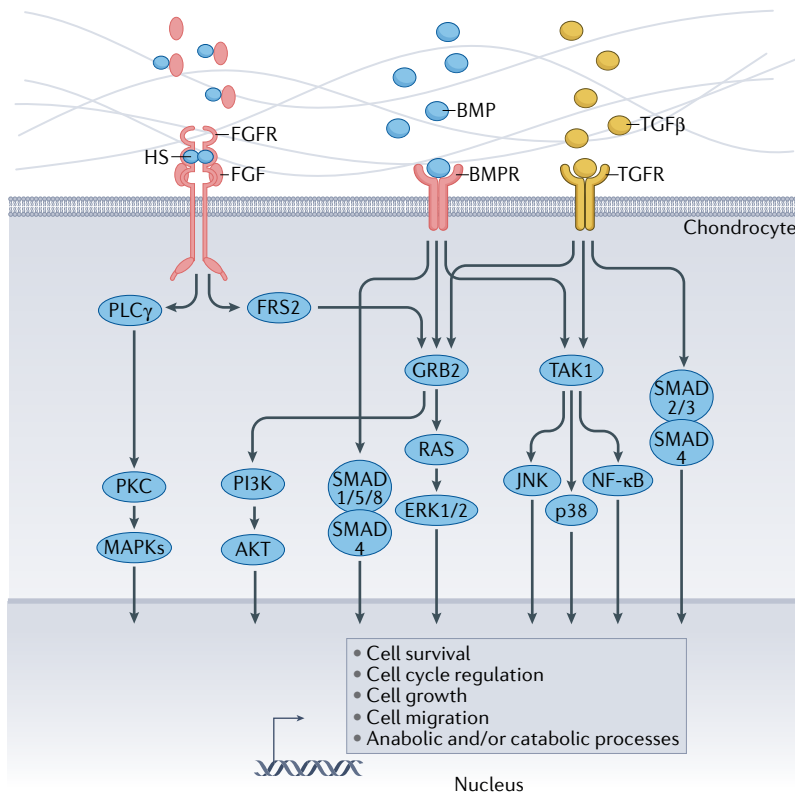


Fig. 2 | Growth factor signalling in chondrocytes. Upon deformation, growth factors sequestered in the extracellular matrix, including fibroblast growth factor (FGF), bone morphogenetic protein (BMP) and transforming growth factor- β (TGF β) activate cell surface receptors. FGF binds to FGF receptors (FGFRs), causing phospholipase C γ (PLC γ) to be recruited to the kinase domains of FGFRs and activated and, in turn, to stimulate protein kinase C (PKC) activity and downstream activation of mitogen-activated protein kinases (MAPKs). FGFR ligand binding also activates growth factor receptor-bound protein 2 (GRB2) through FGF receptor substrate 2 (FRS2), which activates RAS, resulting in the activation of extracellular-signal-regulated kinase 1 (ERK1) and ERK2. ERK1 and ERK2 translocate to the nucleus and affect the activity of numerous transcription factors. FGFR signalling via GRB2 also triggers the phosphoinositide 3-kinase (PI3K)–protein kinase B (AKT) pathway. BMPs and TGF β bind to cell surface heterodimer BMP receptors (BMPRs) and TGF receptors (TGF β R). In the SMAD signalling pathway, either SMADs 1, 5 or 8 (for BMPRs) or SMADs 2 or 3 (for TGF β R) are phosphorylated and activated upon ligand–receptor binding, recruiting SMAD4 and translocating to the nucleus to affect transcription. Non-SMAD signalling pathways are activated through TGF β activated kinase (TAK1), which can activate c-Jun amino terminal kinase (JNK), p38 MAPK and NF- κ B. Activation of these pathways results in context-dependent expression of genes associated with anabolic and/or catabolic chondrocyte processes, as well those controlling chondrocyte hypertrophy. HS, heparan sulfate.

alginate gel, the application of an anabolic cyclical loading regime alone is unable to reverse these cytoskeletal changes, suggesting that a combined intervention approach that re-establishes an anabolic extracellular mechanical environment while simultaneously rebalancing dysregulated intracellular mechanotransductive signalling is required⁹².

Direct mechanotransduction relies, in part, on a physical link between the ECM, the cytoskeleton and the nucleus. The cytoskeleton transmits external forces to the nucleus via linker of nucleoskeleton and cytoskeleton (LINC) complexes associated with nuclear lamins. These deformations influence chromatin dynamics, epigenetics and gene transcription^{93,94} (FIG. 3a). For example,

compression of articular cartilage explants results in chondrocyte deformation and nuclear deformation, with the corresponding reduction in nuclear volume mediating alterations in ECM synthesis⁹⁵. Additionally, the role of the nucleus in chondrocyte mechanotransduction can be observed in studies of the osmotic environment of chondrocytes. Application of osmotic challenge to chondrocytes alters chondrocyte gene expression patterns, protein production and calcium signalling^{96–98}. Chondrocyte nuclei subjected to hyperosmotic or hypoosmotic challenge, within a physiological range of osmolalities, undergo chromatin condensation or decondensation, respectively⁹⁶. Interestingly, studies performed on isolated nuclei have demonstrated that chromatin condensation can occur in the absence of a functional plasma membrane, suggesting a direct mechanotransduction link between this physical cue and downstream alterations in gene expression and cellular metabolism⁹⁶. Furthermore, dysregulation of nuclear mechanosensing can occur in OA subchondral bone, where it has a role in the epigenetic regulation of MSC osteogenic potential by histone deacetylases (HDACs)⁹⁹. Mechanically, cellular tension produced by the cytoskeleton also directly regulates the translocation of the mechanosignalling protein Yes-associated protein (YAP) to the nucleus, where it can promote the transcription of target genes. This direct mechanical activation has been demonstrated experimentally in a two-dimensional set up in which cytoskeletal tension stretched the cell nucleus and nuclear pores, thereby facilitating YAP movement into the nucleus¹⁰⁰. This direct mechanism of nuclear entry might have important implications for controlling YAP activity in the altered mechanical environment of the OA joint (see section *Mechanotherapeutics for osteoarthritis* for further discussion of YAP signalling).

The chondrocyte channelome. Chondrocytes express a diverse array of ion channels and porins that are collectively referred to as the ‘chondrocyte channelome’ (reviewed elsewhere^{42,44}). The activity of channelome proteins is associated with fluctuations in ion signalling, one of the earliest cellular events in chondrocyte responses to various modes of mechanical stimulation¹⁰¹. Ion channels can be classified on the basis of their gating mechanisms into categories including voltage-gated, ligand-gated and mechanically gated. Although each type of channel can be found in the chondrocyte channelome, mechanically gated ion channels are of particular interest as they are capable of inducing rapid mechanosensory transduction. Calcium, a ubiquitous second messenger, has an important role in activating multiple intracellular signalling pathways in mechanotransduction (FIG. 3). Any initial ion influx can also be amplified further by the subsequent release of ions from intracellular stores. Understanding the mechanisms linking mechanically mediated calcium signalling and downstream responses can provide valuable information on therapeutic targets¹⁰¹.

In cartilage, particular attention has been paid to members of the vanilloid subfamily of transient receptor potential (TRPV) channels, which are regulators of

intracellular calcium ion concentration in non-excitable cells. Although chondrocytes express various transient receptor potential channels, interest in the TRPV4 non-specific cation channel has increased owing to its role in controlling the mechano-osmotic transduction

cascade^{102–104} (FIG. 3). TRPV4-mediated intracellular calcium signalling is an important mechanosignalling pathway in chondrocytes, and is involved in the regulation of ECM biosynthesis¹⁰². Deletion of *Trpv4* in mice results in a severe OA-like presentation¹⁰⁴ and, strikingly, loss

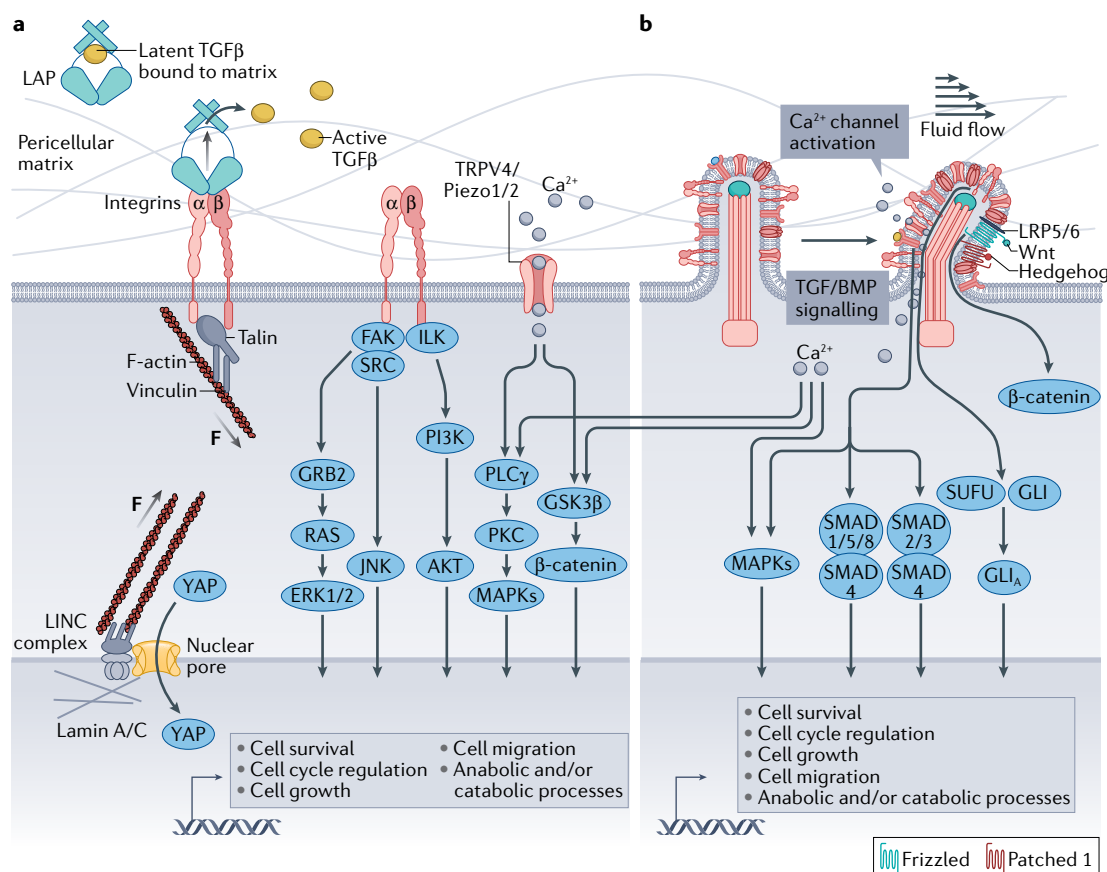
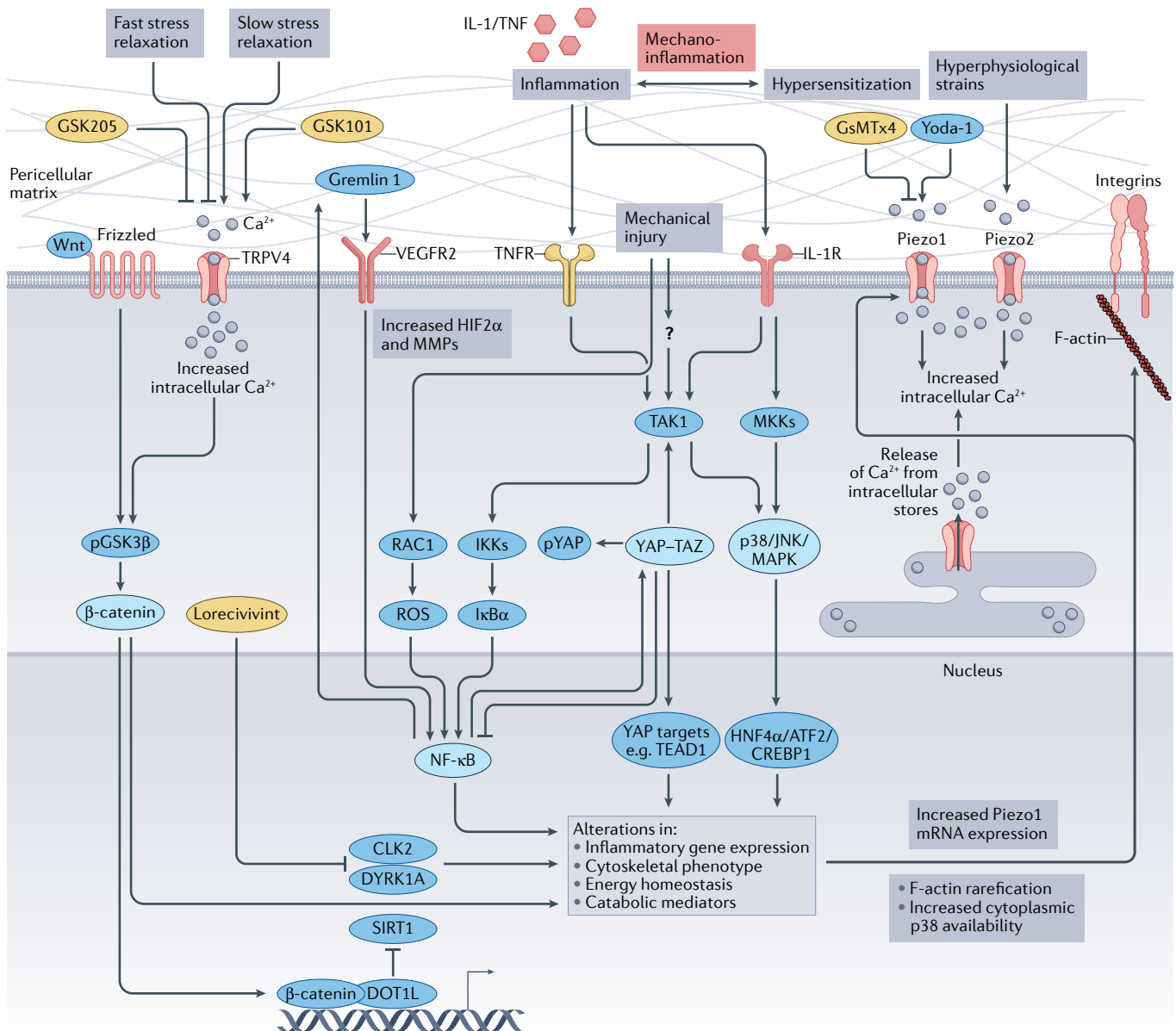


Fig. 3 | Chondrocyte mechanosignalling. a | Integrin activation can trigger biochemical signal transduction and direct mechanical deformation of the cell through cytoskeletal contraction. Contraction of the actin cytoskeleton following integrin activation also regulates growth factor activation and signalling. Actin cytoskeleton contraction increases cell tension and pulling forces exerted by chondrocytes on the surrounding matrix. If this force is sufficient, latency-associated peptide (LAP) undergoes a conformation change resulting in the release of activated transforming growth factor- β (TGF β). The actin cytoskeleton is also connected to the nucleus through linker of nucleoskeleton and cytoskeleton (LINC) complexes. These complexes link the actin cytoskeleton to the nucleoskeletal components such as lamin A and lamin C. When contractile force is generated, nuclear pore entry of Yes-associated protein (YAP) into the nucleus is increased by physical stretching of the pore. Upon integrin binding, SRC kinase and focal adhesion kinase (FAK) recruitment results in growth factor receptor-bound protein 2 (GRB2) binding and downstream activation of extracellular-signal-regulated kinase 1 (ERK1), ERK2 and c-Jun amino terminal kinase (JNK) signalling. Integrin binding also triggers phosphoinositide 3-kinase (PI3K)–protein kinase B (AKT) pathway activation through integrin-linked protein kinase (ILK). Mechanically regulated ion channels, such as transient receptor potential cation channel subfamily V member 4 (TRPV4), Piezo1 and Piezo2, regulate calcium ion influxes into cells, thereby activating numerous downstream signalling pathways, including phospholipase C γ (PLC γ)–protein kinase C (PKC)–mitogen-activated protein kinase (MAPK) signalling and glycogen synthase kinase-3 β (GSK3 β)– β -catenin signalling. **b** | Primary cilia house large amounts of many different mechanosensory receptors and channels that are involved in direct and indirect mechanosensing. Upon mechanical stimulation, for example through deflection when experiencing fluid flow, these receptors and channels are activated, resulting in downstream activation of multiple signalling pathways. Mechanically active ion channels, such as Piezo1, Piezo2 and TRPV4, initiate calcium signalling, which interacts with multiple downstream pathways including PLC γ , GSK3 β and MAPKs. Numerous receptors for growth factors are concentrated on the primary cilia. Activated TGF β and bone morphogenetic protein (BMP) signalling activate downstream SMADs and MAPKs, which translocate to the nucleus and regulate genes related to chondrogenic phenotype and anabolic or catabolic processes. Hedgehog and Wnt signalling can also occur through receptors positioned on the primary cilia. When Hedgehog binds to its receptor Patched 1, it no longer suppresses smoothened, which promotes suppressor of fused negative regulator of hedgehog signalling (SUFU) and glioma-associated oncogene (GLI) trafficking and dissociation of active GLI (GLI_A), which translocates to the nucleus and leads to the upregulation of Hedgehog target genes. When Wnt binds to Frizzled and its co-receptor LRP5/6, the β -catenin destruction complex is inactivated, enabling β -catenin to regulate Wnt target gene transcription. F, force.



of TRPV4 in chondrocytes prevents OA development in an age-related mouse model but not in a mechanical load-dependent model¹⁰⁵. These anabolic roles for TRPV4 suggest it could be a promising therapeutic target for OA. In addition, the transient receptor potential proteins TRPA1 and TRPP2 have well-established mechanosensory properties in other mechanosensitive cells, and also seem likely to be involved in chondrocytes¹⁰⁶.

Whereas physiological loading can induce an anabolic response in chondrocytes through the activity of TRPV4 ion channels, another family of mechanosensitive ion channels have been implicated in the mechanotransduction of injurious mechanical stimuli. Piezo channels, specifically Piezo1 and Piezo2, are cation-permeable ion channels that are also involved in chondrocyte mechanotransduction (reviewed elsewhere¹⁰⁷) and are linked to several downstream processes in chondrocytes, including cell cycle progression, that are relevant for OA¹⁰⁸. Both Piezo1 and Piezo2 are present in chondrocytes, where they provide high strain

mechanosensitivity and the ability to respond to hyperphysiological levels of mechanical stress¹⁰⁹. Briefly, high strain (compressive loading that is >45% strain) increases calcium ion influx via Piezo channels. Knockdown of either Piezo1 or Piezo2 in porcine chondrocytes via small interfering RNA prevented mechanically induced calcium ion release, suggesting a synergistic action for these two channels¹⁰⁹. Furthermore, inhibition of Piezo activity with GsMTx4 protected chondrocytes in cartilage explants from mechanically induced death^{107,109}. However, further elucidation of the effects of Piezo inhibition are required, as GsMTx4 is a non-selective inhibitor of cation-permeable mechanosensitive channels and does not exclusively inhibit Piezo channels^{110,111} (FIG. 4).

Primary cilia. The primary cilium is a non-motile cellular organelle that protrudes from the cell surface and contains a high concentration of mechanosensory machinery and growth factor receptors for signaling pathways important in OA pathology, such as the

Strain
The deformation of a material from stress.

◀ Fig. 4 | **Mechanoinflammation signalling pathways in chondrocytes in osteoarthritis.**

Mechanoinflammation in osteoarthritis (OA) involves several signalling pathways that can be activated by both pro-inflammatory cytokines, such as TNF and IL-1, and mechanical stimuli. Mechanical regulation of downstream pathway activity controls both anabolic and catabolic processes, thereby offering a number of promising therapeutic targets that could halt the progression of OA while concomitantly stimulating anabolic repair. Activation of mechanoinflammatory signalling contributes to increased pro-inflammatory gene expression, alterations in cytoskeletal phenotype and energy homeostasis, and an increase in catabolic mediators. Important mediators of mechanoinflammation include transforming growth factor- β -activated kinase 1 (TAK1), Yes-associated protein (YAP)—transcriptional coactivator with PDZ-binding motif (TAZ), NF- κ B, c-Jun amino terminal kinase (JNK), p38 mitogen-activated protein kinase (MAPK) and downstream mediators of the Wnt signalling pathways. TAK1 activation occurs upstream of p38 MAPK, JNK and NF- κ B. Pro-inflammatory cytokines promote the destruction of YAP through TAK1-mediated phosphorylation, and YAP can also interact with TAK1 to attenuate NF- κ B signalling. Induction of gremlin 1 as a result of excessive mechanical loading occurs via the Ras-related C3 botulinum toxin substrate 1 (RAC1)—reactive oxygen species (ROS)—transcription factor p65 (a subunit of the NF- κ B complex) axis and NF- κ B signalling. Gremlin 1 then exerts a pro-inflammatory effect through the gremlin 1—vascular endothelial growth factor receptor (VEGFR) axis and is linked to the upregulation of hypoxia-inducible factor 2 α (HIF2 α) and matrix metalloproteinase (MMP) expression. Mechanoinflammation predisposes chondrocytes to a state of hypersensitization, rendering them susceptible to pro-inflammatory and mechanical stimuli present within normal physiological ranges. IL-1 α induces the upregulation of Piezo1, leading to increased calcium concentrations, and contributes to F-actin rarefaction via the transcription factors CREBP1, ATF2 and HNF4 α . Treatment of chondrocytes with Yoda-1, a specific Piezo1 activator, results in enhanced calcium signalling in chondrocytes pretreated with IL-1 α , which in turn affects cytoskeletal organization through F-actin rarefaction. Conversely, inhibition of Piezo activity with GsMTx4, a non-selective inhibitor of cation-permeable mechanosensitive channels, protects cartilage explants from mechanically induced death. In addition to calcium ion influx from extracellular space, calcium can also be released from intracellular stores, such as the endoplasmic reticulum, further altering intracellular calcium concentrations. Chondrocytes sense and respond to changes in matrix viscoelasticity through the transient receptor potential cation channel subfamily V member 4 (TRPV4)—glycogen synthase kinase-3 β (GSK3 β) axis, in which TRPV4 activation, either pharmacologically (GSK101) or through culturing of cells on slow-relaxing gels, results in increased calcium, GSK3 β phosphorylation (pGSK3 β) and increased inflammation. The opposite holds true for fast-relaxing hydrogels or treatment with a small molecule inhibitor of TRPV4 (GSK205). Therapeutic targeting of mechanoinflammation and its signalling pathways holds promising potential. Lorecivint, a Wnt pathway modulator, inhibits CDC-like kinase enzyme (CLK2) and dual-specificity tyrosine phosphorylation-regulated kinases enzymes (DYRK1A) activity, thereby enhancing chondrogenesis and reducing inflammation. Additionally, DOT1-like histone lysine methyltransferase (DOT1L) interacts with sirtuin 1 (SIRT1), thereby preventing Wnt pathway hyperactivation and maintaining cartilage homeostasis. Wnt signalling in the absence of DOT1L results in high SIRT1 activity and disrupts homeostasis. IKKs, inhibitor of NF- κ B kinases; IL-1R, IL-1 receptor; MKKs, MAPK kinases; pYAP, phosphorylated YAP; TEAD1, TEA domain family member 1; TNFR, TNF receptor.

TGF β family, Wnt and Hedgehog. For example, in OA, Hedgehog signalling is activated through binding of its receptor Patched 1, which is localized at the base of the primary cilium. This activation results in aberrant expression of hypertrophic markers such as type X collagen and the upregulation of MMPs¹¹². In chondrocytes, the primary cilia have an important role in mechanotransduction^{113,114} (FIG. 3b). Experiments using cartilage from cows with OA have shown that primary cilia exhibit cartilage zone-dependent variation (in both occurrence and length, which both increase with distance from the articulating surface), which is thought to be a result of the differences in stress, strain and fluid flow that are present throughout each zone¹¹⁵. Interestingly, both cilium length and the percentage of ciliated chondrocytes in the cartilage samples increased with OA severity. Additionally, the orientation of

primary cilia was towards the articular surface rather than away from it, as occurred in chondrocytes from healthy cartilage¹¹³. In *Col2a1Cre;Ift88^{fl/fl}* transgenic mice, which lack primary cilia, cartilage stiffness is decreased, whereas cartilage thickness and the expression of several genetic markers of OA (such as *COLX*, *RUNX2*, *MMP13* and *ADAMTS5*) are increased^{114,116}. Furthermore, transgenic mice with mutant Polaris, an essential cilium protein, fail to initiate mechanosignalling, and compression of IFT88^{orp^{pk}}-mutant chondrocytes, which lack primary cilia, does not initiate intracellular calcium signalling, ECM synthesis or ATP release^{106,117,118}. The localization of mechanosensors to the primary cilia facilitates the mechanical activation of purinergic signalling in the form of ATP and intracellular calcium release¹¹⁹. This ATP release is mediated by the mechanically stimulated opening of hemichannels (connexons), which are present in high densities in the primary cilia, and is linked to several anabolic activities including an increase in proteoglycan production and cell proliferation^{120–122}.

Mechanotherapeutics for osteoarthritis

The term mechanotherapeutics originally referred to the use of physiotherapy to treat a disease but now also encompasses interventions that target molecular, cellular and tissue level mechanosignalling to repair tissue damage or treat disease^{123,124}. In short, mechanotransduction can be targeted in a therapeutic manner to either promote anti-catabolic, anabolic pathways and repair processes, or to block pathways that are central to OA. However, underlying the complex nature of OA pathogenesis is an equally complex signalling network. For example, a study aimed at characterizing the response of human articular cartilage explants to mechanical injury revealed the significant regulation (more than twofold change) in 690 genes¹²⁵. These genes are involved in pathways that are implicated in regulating inflammation, the production of catabolic and degradative enzymes (such as MMPs and proteins from the disintegrin and metalloproteinase with thrombospondin motifs family), cellular apoptosis and bone dysfunction within the joint. Although in the previous section of this Review we separated out chondrocyte mechanosensors for clarity, it is important to note that the overlap and crosstalk between corresponding signalling mechanisms is considerable (FIGS 2–4). Furthermore, several of the pathways discussed can be activated by an individual mechanical stimulus; for example, cell stretching can activate integrin signalling but also results in direct deformation of the cytoskeleton and nucleoskeleton in an integrin-dependent manner⁶⁰. The activation of, and interaction between, these pathways can also have a considerable effect on how a cell interprets other stimuli, such as growth factor signalling⁵⁹. Although this complexity makes understanding cell responses to mechanical stimuli challenging, it also affords the opportunity to simultaneously control multiple cellular processes with carefully designed interventions. In the following sections, we highlight some of the prominent mechanosignalling pathways that have been implicated in the pathogenesis and progression of OA and how these pathways might be targeted therapeutically (FIG. 4).

The MAPK pathway. The MAPKs have important roles in the regulation of various cell signalling pathways that are implicated in cellular proliferation, ECM synthesis, cell survival and mediation of pain¹²⁶. In chondrocytes, MAPKs are involved in regulating gene expression in response to mechanical stimulation. Activation of the MAPKs extracellular signal-regulated kinase 1 (ERK1), ERK2, p38 MAPK and SAPK/ERK kinase 1 occurs following compression, as demonstrated in mechanically stimulated bovine cartilage explants¹²⁷. Furthermore, in human chondrocytes, integrin activation via ECM molecule fragments activates MAPKs and results in the upregulation of catabolic signalling. For many years, $\alpha 5 \beta 1$ integrin has been known to mediate ECM degradation induced by fibronectin fragments¹²⁸, and the signalling proteins downstream of $\alpha 5 \beta 1$ integrin have now been identified. In short, activation of proline-rich tyrosine kinase 2 by PKC δ and downstream activation of the MAPKs ERK1, ERK2, c-Jun amino terminal kinase 1 (JNK1), JNK2 and p38 α leads to heightened activity of the transcription factors NF- κ B and AP-1 (REFS^{129–131}). This signalling cascade also requires the production of reactive oxygen species (ROS) and the presence of active Ras-related C3 botulinum toxin substrate 1 (RAC1)^{132,133}. In addition, MAPKs are required for stimulation of nitric oxide, MMP3 and MMP13 production, which further potentiates the progression to OA^{134–136}. Compression or shear stress activate ERK1, ERK2 and p38 MAPK, thereby contributing to an increase in the expression of pro-inflammatory cytokines and molecules while also regulating the expression of mechanoresponsive anabolic genes¹³⁷ (FIG. 4).

Although therapeutic inhibition of MAPKs holds great potential for slowing the progression of OA, safety

concerns exist around the use of general MAPK inhibitors in humans¹³⁸. Considering that MAPKs operate within a complex signalling network, it is likely that a system offering long-term feedback for the controlled delivery of therapeutics will be required. Furthermore, targeting the deleterious processes downstream of MAPK activation might be a more attractive therapeutic option than targeting MAPKs themselves. Aside from these considerations, the use of targeted, biomaterial-based approaches typically utilized in tissue engineering applications could enable increased specificity and efficacy for selective modulation of MAPKs in a therapeutic manner. For example, the application of highly versatile functionalized scaffolds, which have previously demonstrated success in modulating JNK3 to enhance the osteogenic potential of MSCs in rat calvarial defects¹³⁹, might provide the basis of a platform for targeted regulation of MAPK signalling pathways in other tissues such as cartilage.

Mechanoinflammation and NF- κ B signalling. In addition to being activated by cytokine signalling, NF- κ B can also be regulated by physical forces in chondrocytes. For example, low magnitude mechanical strain can block the nuclear translocation of NF- κ B in human periodontal ligament cells, thereby preventing the upregulation of pro-inflammatory genes¹⁴⁰. Conversely, high magnitude mechanical strain, representative of that experienced during injury, can induce transactivation of the NF- κ B signalling complex and lead to the expression of pro-inflammatory genes, cartilage destruction and inhibition of ECM synthesis, as demonstrated in rat models of OA¹⁴¹. These findings indicate a central role for mechanoinflammation in the progression of OA (BOX 1) and, perhaps more importantly, open the door to a number of promising therapeutic targets.

A well-described mechanoinflammation pathway involves activation of TGF β -activated kinase 1 (TAK1), upstream of p38 MAPK, JNK and NF- κ B signalling¹⁴² (FIG. 4). Notably, although TAK1 can be activated by pro-inflammatory cytokines and Toll-like receptor ligation, the pattern of ubiquitination of TAK1 that occurs during mechanoinflammation is distinct from that which occurs following cytokine stimulation¹⁴³. Gremlin 1, a secreted BMP agonist, has also been identified as a mediator of NF- κ B signalling following excessive mechanical loading in chondrocytes². Inhibition of vascular endothelial growth factor receptor 2 or NF- κ B attenuated gremlin-1-induced pro-inflammatory and catabolic activity. Moreover, in mouse models of OA, chondrocyte-specific knockdown of gremlin 1 or the use of an anti-gremlin-1 antibody suppressed OA development, whereas the delivery of recombinant gremlin 1 accelerated disease. Further investigations revealed that gremlin 1 production in response to mechanical loading occurs through the RAC1–ROS–NF- κ B pathway² (FIG. 4).

In a 2021 study that utilized porcine chondrocytes, inflammation predisposed cells to becoming hypersensitive to injurious levels of mechanical loading as a result of IL-1 α -induced upregulation of Piezo1 and subsequent increased basal calcium ion concentrations¹⁴⁴. Interestingly, the presence of IL-1 α also increased

Box 1 | Mechanoinflammation in osteoarthritis

Mechanoinflammation can be described as the inflammatory response to mechanical injury. Beyond wear and tear, excessive mechanical loading of the cartilage activates receptors and signalling pathways that result in the production of the catabolic enzymes that degrade functional cartilage extracellular matrix. Evidence from osteoarthritis (OA) and other forms of arthritis also indicates that mechanical strain is important in determining the localization of inflammation and tissue degradation^{59,201}. Deletion or inhibition of mechanically induced proteases, or the inflammatory signalling pathways that control them, prevents OA progression in animal models, even when joints are destabilized^{13,59}. Similarly, progression of OA is prevented when joints are immobilized following induction of OA or when superficial zone chondrocytes are specifically destroyed prior to joint destabilization^{14,16}. Mechanoinflammation involves several signalling pathways, including transforming growth factor- β (TGF β), p38 mitogen-activated protein kinase (MAPK), c-Jun amino terminal kinase, Yes-associated protein (YAP)–transcriptional coactivator with PDZ-binding motif (TAZ) and NF- κ B. TGF β -activated kinase 1 (TAK1), which can be activated by both pro-inflammatory cytokines and mechanical stimuli, seems to be involved in a number of these signalling pathways¹⁴³. TAK1 mediates mechanical activation of MAPK cascades and is central to YAP–TAZ anabolic activity and reciprocal inhibitory interaction with NF- κ B²². Thus, control of mechanoinflammation in the OA joint has the potential to both control catabolic processes and promote anabolic repair processes. Interestingly, along with the magnitude and duration of force and how frequently it is applied to the joint, the type of loading experienced by chondrocytes situated in the different zones of cartilage seems to be important in determining whether mechanoinflammatory pathways are activated or anabolic processes are stimulated¹⁴. Targeting mechanoinflammation, either through restoration of a functional mechanical environment (for example, by use of biomaterials) or by controlling signalling mechanisms and receptors, might be one of the most promising strategies for improving the efficacy of therapies for OA.

F-actin rarefaction

A process resulting in a reduction in F-actin abundance within a cell.

chondrocyte deformation in response to the same loading magnitude owing to F-actin rarefaction. Enhanced calcium signalling and altered organization of the chondrocyte F-actin cytoskeleton also occurred following treatment with a specific Piezo activator compound, Yoda-1. Further to these findings, a signalling pathway has been delineated from the IL-1 receptor type I complex on the cell membrane to MAPK kinase 3 (MKK3) and MKK6, which phosphorylate p38 MAPK, leading to nuclear signalling of the transcription factor CREBP1, which together with other transcription factors (including ATF2 and HNF4 α) upregulates Piezo1 (FIG. 4). This proposed feedforward mechanism indicates that mechanoinflammation contributes to the maladaptive reprogramming of chondrocytes and provides a rational set of informed mechanotransduction targets for therapeutic approaches to OA¹⁴⁴. In the same study, TRPV4 expression and function were not altered by the presence of IL-1 α , suggesting that inflammation has a selective effect on the expression of cell mechanosensory machinery. However, TRPV4 has been identified as an important mechanoreceptor in mechanoinflammation. In another 2021 study, in which pathway analysis was carried out following TRPV4 activation (mechanical or pharmacological), both inflammatory and anabolic signalling networks were activated by TRPV4 signalling, suggesting that TRPV4 mechanotransduction involves the activation of a rapidly resolving inflammatory pathway as part of a broader anabolic response following physiological loading²⁵. The transient, resolving nature of this inflammatory response might be a differentiating factor between anabolic responses and chronic inflammation.

Studies have also shown how ECM viscoelasticity modulates the function of human healthy and OA chondrocytes, and have shown that under static conditions, healthy chondrocytes interact with the ECM of fast-relaxing and slow-relaxing alginate hydrogels by regulating their volume and phenotype²⁰. In hydrogels that exhibit stress relaxation, the force or strain a cell applies to the surrounding hydrogel over time is initially resisted with a certain stiffness (defined by the initial elastic modulus of the hydrogel), followed by a decreasing resistance over time. In fast-relaxing gels, chondrocyte cell volume expands and ECM expression is upregulated, whereas the opposite is true for slow-relaxing gels. Inflammation predisposes cells to mechanical stress; however, the reverse has been observed in chondrocytes cultured in slow-relaxing gels, in which they undergo a pro-inflammatory phenotypic shift that makes them more sensitive to extrinsic inflammatory cues^{20,144}. Mechanistically, one way chondrocytes might sense and respond to changes in matrix viscoelasticity is through the TRPV4–glycogen synthase kinase-3 β (GSK3 β) molecular axis²⁰. Treatment of healthy chondrocytes embedded in slow-relaxing gels with a selective TRPV4 inhibitor reduced inflammation and shifted the cells towards the phenotype they acquire in fast-relaxing gels. Similarly, treatment of healthy chondrocytes cultured in fast-relaxing gels with a TRPV4 activator resulted in an increase in intracellular calcium, GSK3 β phosphorylation and a subsequent increase in inflammation²⁰ (FIG. 4).

Notably, a TRPV4–PI3K–AKT–p27 signalling axis controls proliferation of the MDA-MB-231 tumour cell line, which is promoted in fast-relaxing hydrogels but arrested in slow-relaxing gels¹⁴⁵. Although demonstrated in a different cell type, this discovery highlights the central role of TRPV4 in mechanosensation and regulating cell behaviour. In a study in bovine chondrocytes, cell confinement in fast-relaxing hydrogels enhanced cell proliferation, ECM production and anabolic gene expression¹⁴⁶. Furthermore, in the same study, restricted cell volume expansion in slower relaxing hydrogels induced IL-1 β signalling, highlighting the interplay between cell volume expansion and pro-inflammatory pathways associated with OA progression. Unlike healthy chondrocytes, which can sense and transduce changes in ECM viscoelasticity, OA chondrocytes are unable to do so. Interestingly, treatment of human OA chondrocytes with a TRPV4 inhibitor failed to change calcium ion concentrations, suggesting a dysregulation of the TRPV4–GSK3 β molecular axis in OA chondrocytes²⁰. Although TRPV4 has an important role in responses to mechanical signals in healthy chondrocytes, its impairment in OA chondrocytes could limit its use as a therapeutic target (at least in the later stages of OA). Such findings highlight the importance of not only understanding the mechanism of phenotype drift in chondrocytes, but also the timing of the molecular events governing this drift, and will be invaluable in determining treatment strategies.

The Wnt signalling pathway. Wnt signalling has established roles in embryonic development, tissue homeostasis and growth, and is implicated in the onset and progression of various pathologies¹⁴⁷. In cartilage, Wnt activity is essential for cartilage homeostasis; however, controlled activity is required, as a moderate amount of Wnt activity is essential for chondrocyte proliferation, whereas excessive activity contributes to hypertrophy and increased expression of MMPs¹⁴⁸. In OA, the expression of Wnt pathway members is dysregulated, which increases the expression of catabolic enzymes¹⁴⁹, and mechanical injury of human articular cartilage leads to the upregulation of Frizzled-related protein (FRZB), a Wnt-binding protein¹⁵⁰. In a study in mouse chondrocytes, knockout of *Frzb* led to an increase in MMP expression and the accumulation of β -catenin upon stimulation with IL-1 β ¹⁵¹. In the same study, a microarray and systematic analysis revealed distinct differences between healthy and injured cartilage, including the upregulation of Wnt16, downregulation of FRZB, upregulation of Wnt target genes and the nuclear localization of β -catenin. Furthermore, Wnt16 and β -catenin were upregulated in areas of the joint that had moderate-to-severe OA scores compared with those areas with preserved cartilage¹⁵¹. In a mouse model of post-traumatic OA, Wnt16 protein and mRNA were also upregulated in a transient manner; however, Wnt16-deficient mice had more severe OA than wild-type mice, suggesting a homeostatic role for Wnt16 (REF.¹⁵²). Interestingly, Wnt16-deficient mice failed to upregulate lubricin, a low friction proteoglycan and chondroprotective agent¹⁵².

The Wnt signalling pathway thus presents potential therapeutic targets for the treatment of OA^{149,153,154} (FIG. 4). However, the involvement of Wnt signalling in so many important biological processes makes targeting these pathways a daunting task. Any such intervention should aim to fine-tune Wnt signalling activity (reviewed elsewhere¹⁵⁵). The strong performance of lorecivint (SM04690), a Wnt pathway modulator, in phase I (NCT02095548) and phase II (NCT02536833 and NCT03122860) clinical trials is encouraging. In these studies, lorecivint demonstrated safety and efficacy in patients with knee OA and produced substantial improvements in patient-reported pain and functionality compared with placebo^{156,157}. Lorecivint inhibits the activity of CDC-like kinase 2 and dual-specificity tyrosine phosphorylation-regulated kinase 1A, thereby enhancing chondrogenesis and chondrocyte function, and reducing inflammation¹⁵⁸. Another promising therapeutic is DOT1-like histone lysine methyltransferase (DOT1L), which limits Wnt activation. DOT1L seems to have a chondroprotective role in cartilage, and intra-articular delivery of a DOT1L inhibitor triggered the development of OA in mice^{159–161}.

YAP–TAZ and Hippo signalling pathway. The transcriptional cofactors YAP and transcriptional coactivator with PDZ-binding motif (TAZ) form an important mechanosignalling complex and are involved in regulating chondrogenesis, chondrocyte maturation and hypertrophy¹⁶². YAP–TAZ activity is tightly regulated by biochemical and mechanical regulation. Biochemically, YAP and TAZ are members of the Hippo signalling pathway, which can be activated by cadherin–cadherin interactions and leads to YAP phosphorylation and retention in the cytoplasm, where it cannot influence transcription¹⁶³. Mechanical stimulation can also control YAP activity independently of Hippo signalling, for example through Rho GTPase activation and the generation of cytoskeletal tension¹⁶⁴. This regulation demonstrates that YAP–TAZ activity can be controlled by cell structure and polarity, cell–ECM interactions and physical cues from the microenvironment, and that these signals can be directly converted into altered gene expression profiles enabling cells to adapt their phenotypes rapidly. However, YAP–TAZ regulation is not fully understood in complex or in vivo 3D environments, and responses that diverge from well-established responses in a two-dimensional environment have been reported^{165,166}. YAP is downregulated in human MSCs during in vitro chondrogenesis¹⁶⁷, and can also inhibit terminal chondrocyte maturation and hypertrophy by suppressing type X collagen production through interaction with the transcription factor RUNX2, an important regulator of chondrocyte hypertrophy and osteogenesis¹⁶². In OA, deletion of YAP promotes cartilage disruption, whereas pro-inflammatory cytokines that are typically upregulated in the OA joint (such as IL-1 β and TNF) promote the destruction of YAP through TAK1-mediated phosphorylation²². YAP also interacts with TAK1 and attenuates NF- κ B signalling by inhibiting substrate accessibility, which establishes a reciprocal antagonism between YAP–TAZ and NF- κ B that is important in regulating pro-inflammatory responses in OA²² (FIG. 4).

Central energy metabolism and metabolites. Metabolism has an important role in OA progression, and studies from the past few years have begun to reveal links between chondrocyte mechanotransduction and metabolic pathways¹⁶⁸. Central energy metabolism pathways such as glycolysis, the pentose–phosphate pathway and the tricarboxylic acid cycle are how cells harvest energy and generate the precursors to non-essential amino acids. Strong evidence supports the idea that mechanosignalling can regulate cell metabolism and that metabolic processes respond differently to mechanical stimuli in healthy and OA chondrocytes¹⁶⁹. For example, in OA chondrocytes, cyclic loading reduces phosphorylation of AKT, a regulator of signalling by the transcription factor FOXO in energy homeostasis¹⁷⁰. Conversely, mechanical stimulation induces AKT phosphorylation in healthy porcine chondrocytes¹⁷¹. These different metabolic responses have implications for downstream anabolic responses to mechanical loading in healthy human chondrocytes, which are fuelled by a glycolytic energy flux that is reduced in OA¹⁷². Additionally, mounting evidence suggests that mitochondria are central mediators of the early cellular response to cartilage injury, and mitochondrial respiratory dysfunction is considered a peracute (within minutes) response to mechanical injury¹⁷³. Further evidence for this idea is illustrated in *Prg4*-knockout mice, in which increased whole-joint friction was linked to evidence of mitochondrial dysregulation, including increased ROS and caspase activation¹⁷⁴.

Therapeutic approaches that use mitoprotective drugs such as Szeto–Schiller peptides can help to protect mitochondrial structure and function, indicating the potential of mitoprotection as an emerging therapeutic strategy¹⁷⁵. Investigating the effects of mechanically induced changes on both the cellular metabolome and mitochondrial structure and function could enable the identification of therapeutic targets and metabolites involved in mediating cell mechanotransduction and cell phenotypes, thereby opening the possibility of harnessing these ‘activity metabolites’ to control cell behaviour or developing chemical analogues with enhanced therapeutic action^{176–178}. Metabolomic data obtained to date has highlighted the role of various signalling pathways associated with mechanotransduction, including decreased energy flow to the pentose phosphate pathway and increased flux through the tricarboxylic acid cycle, suggesting a redirecting of cellular energy in response to mechanical loading¹⁷⁶. Considering the multifactorial nature of OA and the distinct shift in chondrocyte metabolism during disease, it is likely that further elucidation of the role of central energy metabolism and mitochondrial structure and function in mechanotransduction will yield promising therapeutic targets via the comparison of mechanically-induced metabolite expression in both healthy and OA chondrocytes^{176,177}.

Future directions

Understanding mechanosignalling is vital for the development of therapies that control cellular responses, halt disease progression and enable the regeneration of cartilage tissue. Physiotherapy is commonly used as part of

Tribology

The science and engineering of interacting surfaces (wear, friction and lubrication) and how they behave in relative motion.

the non-pharmacological treatment of OA, albeit often without a comprehensive understanding of the underlying cellular mechanosensory and signalling mechanisms involved¹²³. Cellular mechanosignalling in the cartilage as a result of joint movement is proportional to cell and tissue strain¹⁷⁹. Considering the role of articular cartilage in facilitating low friction movement, therapeutic approaches that target tissue lubrication properties could lessen tissue strain and, in turn, reduce aberrant downstream signalling (FIG. 5). A study from 2020 demonstrated that synovial fluid from patients with different forms of arthritis is characterized by distinct tribology endotypes, with synovial fluid samples from patients with inflammatory arthritis having lower amounts of lubricin and higher amounts of neutrophils and IL-8 than

samples from patients with OA¹⁸⁰. Interestingly, these distinct endotypes demonstrate differential modification by viscosupplementation; hyaluronan is more effective at reducing friction in the synovial fluid from patients with inflammatory arthritis than in synovial fluid from those with OA. More recently, advanced biomimetic cartilage lubricating polymers consisting of a hyaluronan backbone covalently linked to either lubricin-like sulfonate-rich polymers or lipid-like phosphocholine-rich polymers have been developed and have demonstrated excellent lubrication of human cartilage explants as well as the ability to promote cartilage regeneration and reverse OA progression in a rat model of post-traumatic OA¹⁸¹.

Although several potential DMOADs have emerged over the past few years (including cyclooxygenase 2

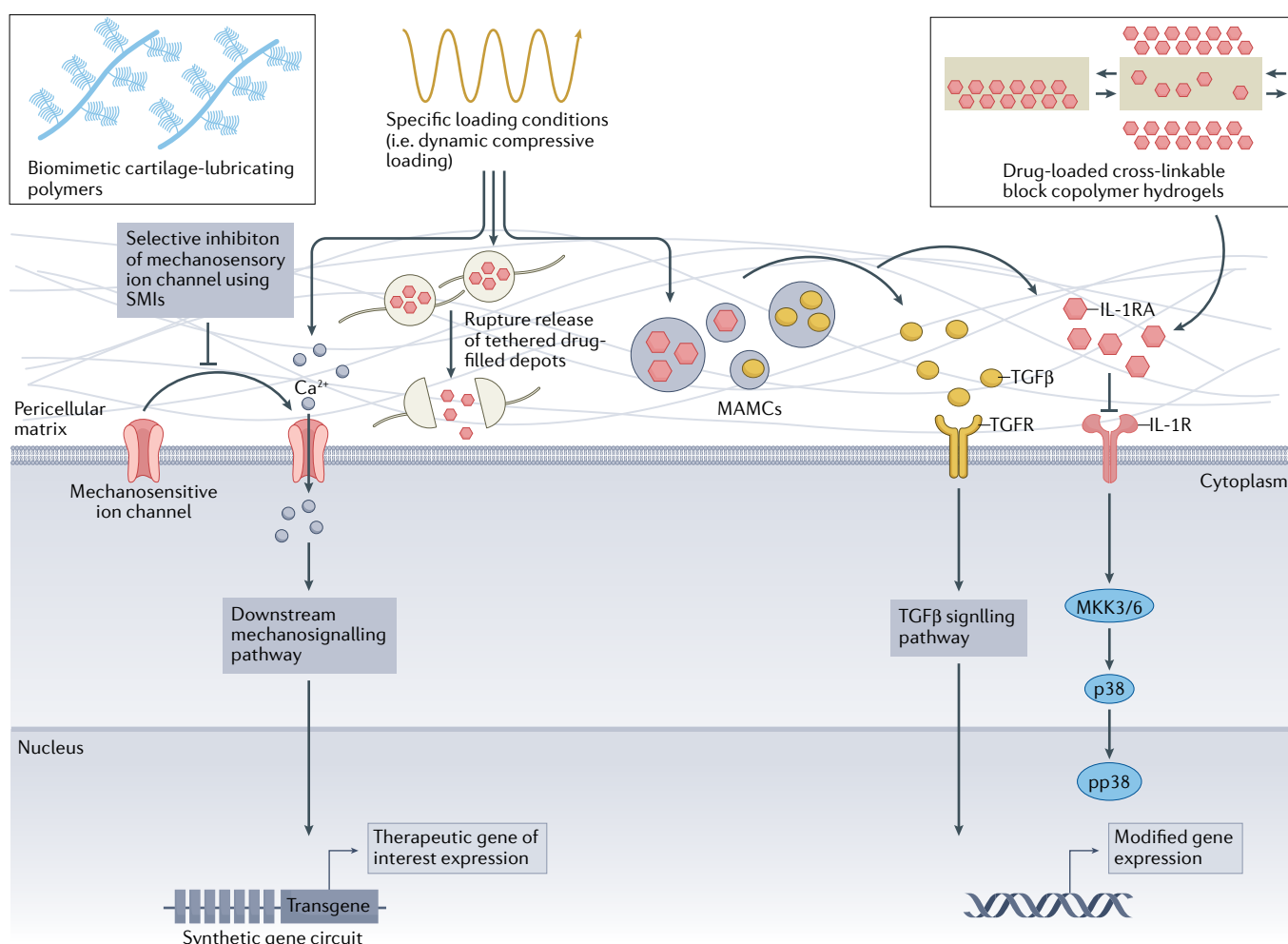


Fig. 5 | Mechanoresponsive therapeutics for the treatment of osteoarthritis. Mechanotherapeutic approaches aim to take advantage of the dynamic physical stimuli present in the joint to deliver biomolecules. Selective small molecule inhibitors (SMIs) offer a promising method of blocking mechanosignalling pathways in the treatment of osteoarthritis. Biomimetic, collagen-lubricating polymers can provide enhanced lubrication, lowering overall friction and tissue strain. Drug-loaded cross-linkable block copolymer hydrogels and tethered drug-filled depots enable delivery of biomolecules in a spatiotemporally controlled manner. Mechanically activated microcapsules (MAMCs) can be tailored to rupture in response to specific loading conditions, thereby enabling delivery of therapeutics in a controllable manner in response to the specific needs

of the tissue at any given time. MAMCs encapsulating chondrogenic molecules (such as transforming growth factor- β ; TGF β) or anti-inflammatory agents (such as IL-1 receptor antagonist; IL-1RA) have shown promise for cartilage regeneration. Advances within the fields of synthetic biology and tissue engineering have enabled the development of autonomously regulated drug delivery systems that can respond in real-time to the ever-changing mechanical microenvironment of the joint, thereby enabling enhanced tissue repair. For example, the development of a synthetic mechanosensitive ion channel-responsive gene circuit has enabled the autonomous production of the anti-inflammatory agent IL-1RA in response to mechanical loading. IL-1R, IL-1 receptor; MKK, MAPK kinase; pp38, phosphorylated p38; TGFR, transforming growth factor receptor.

inhibitors, glucocorticoids, IL-1 β inhibitors and TNF inhibitors), these have not proved to be as effective as hoped, and a rethinking of how therapeutics are developed for OA is required. A good starting point might be the repurposing of selective small-molecule inhibitors that have shown success in blocking mechanosignalling pathways in other mechanosensitive cells and/or tissues. For example, WRG-28 specifically inhibits the receptor–ligand interactions of discoidin domain receptor 2 (DDR2) in tumours¹⁸², but aberrant DDR2 activation has also been implicated in OA, and selective inhibition of this receptor could be a useful starting point for the development of a DMOAD¹⁸³. The continuing development of advanced cartilage-on-a-chip models that are capable of recapitulating in vivo-like physiological and pathological mechanical and biochemical cues in high-throughput systems will also provide a valuable method for rapid and accurate screening of prospective DMOADs prior to in vivo testing¹⁸⁴. It is important that researchers developing these models investigate the divergence in pathological mechanisms between current experimental models of post-traumatic OA and advanced, age-related OA in humans. Nevertheless, destruction of the mechanically functional ECM promotes disease progression in both age-related and post-traumatic OA, and a mechanotherapeutic strategy that is effective in both types of disease remains a possibility. In age-related OA, which has no clear initiation point, patients often present to the clinic with already advanced cartilage damage. For these patients, functionalized biomaterials and tissue-engineered approaches that assist in re-establishing healthy mechanical environments and enable tissue regeneration to proceed are likely to be important.

In addition to the physical impediments to developing and delivering successful DMOADs (such as dense ECM and rapid drug clearance), mechanosignalling and critical catabolic–anabolic signalling axes that underlie the progression of OA are intricately linked. Although research to date has largely focused on controlling one specific parameter (such as ECM stiffness, growth factor presentation, inflammation, mechanical stimulation or biomaterial degradation), this approach often overlooks this complex interplay between stimuli and downstream signalling events. However, researchers should not despair at the overwhelming complexity of these pathways, as continuing advances are resulting in additions to the therapeutic toolbox. For example, the development of biomaterials that are capable of regulating a combination of factors simultaneously has provided valuable insights into this signalling interplay. Investigations into the role of several mechanosignalling pathways (including $\alpha 5 \beta 1$ integrin, YAP, TGF β , MAPKs and Wnt pathways) and their involvement in regulating the differentiation of human MSCs cultured on articular cartilage-promoting or hypertrophic cartilage-promoting hydrogels with cyclic compression have revealed a role for downregulation of Wnt signalling in the promotion of articular-like chondrocyte phenotypes in soft matrices and have confirmed YAP regulation of hypertrophy in stiff matrices^{162,185}. The combination of omics analysis with such biomaterials can be used to map cellular and molecular responses

to tightly controlled biomechanical stimuli (so-called mechanomics), and will hopefully provide even greater insight into responses to specific stimuli¹⁸⁶.

Therapies for OA, a disease that is intricately linked to the ageing process, might require sustained administration over a long time-period to maintain the delicate anabolic–catabolic balance in cartilage. Patients with OA are also likely to have an increase in number and severity of comorbidities as they age, which could further complicate treatment¹⁸⁷. To attempt to overcome these challenges, considerable advances have been made in developing cartilage-specific drug delivery strategies. For example, developments in advanced therapeutic approaches such as gene therapy, in which plasmid DNA-based or RNA-based therapeutics are delivered to the cell of interest might help overcome issues related to target specificity, safety and bioavailability. In the past few years, advances in vector technologies and a greater understanding of the mechanisms of action of delivered nucleic acids or genes have led to a surge in the development of gene therapy approaches. The potential of small interfering RNAs has been demonstrated through the knockdown of modulators of mechanoinflammation, including Wnt, β -catenin, NF- κ B and p38 MAPK^{188–190}. Several microRNAs (miRNAs), highly potent post-transcriptional regulators that can each exert an effect on multiple mRNAs, are mechanically regulated in chondrocytes, and alterations in miRNA expression is associated with OA and with different degrees of mechanical loading in different cartilage zones^{191–195}. miRNA profiling of OA cartilage has revealed unique miRNA signatures and several miRNAs have been identified as potential therapeutic targets¹⁹⁶. One promising candidate is miR-365, which regulates cell hypertrophy through a mechanism involving NF- κ B and HDAC4 (REF.¹⁹³). miR-365 is upregulated by cyclical loading in human and rat chondrocytes and is also upregulated in cartilage from patients with age-related or post-traumatic OA¹⁹³. Itself a potent inhibitor of chondrocyte hypertrophy and MMP expression, HDAC4 activity is inhibited by miR-365, leading to an increase in MMP13 and type X collagen production. Inhibition of miR-365 is able to attenuate this upregulation in human articular chondrocytes in vitro¹⁹³. miR-222 also regulates HDAC4, but in contrast to miR-365, miR-222 is downregulated in OA chondrocytes and is implicated in regulating cartilage destruction and MMP13 expression¹⁹⁷. Intra-articular delivery of miR-222 to mice with OA induced by destabilization of the medial meniscus led to the recovery of chondrocyte numbers and reduced cartilage destruction¹⁹⁷. Furthermore, the study of miRNAs that are regulated by different loading conditions in mature tissue-engineered human cartilage has led to the discovery of several miRNAs (including miR-199b-5p, miR-1229-5p, miR-1275, miR-4459, miR-6891-5p and miR-7150) that are only differentially expressed under catabolic loading conditions¹⁹⁸. These systematic approaches to investigating diverse loading conditions in both healthy and OA cells are likely to lead to further therapeutic avenues in this area¹⁹⁹.

Another approach for cartilage-specific drug delivery is the use of mechanoresponsive smart biomaterials that

Box 2 | Use of mechanoresponsive ‘smart’ biomaterials in cartilage regeneration

Mechanoresponsive biomaterials can be designed to adapt and respond to the changing mechanical microenvironment of the joint during tissue restoration. By harnessing the constant dynamic stimuli present in the joint, mechanoresponsive biomaterials can be used to deliver biomolecules in a spatiotemporally controlled manner²⁰². Drug delivery systems that are responsive to physical stimuli can deliver drugs in a controlled manner in response to compressive, tensile and shear forces²⁰³. For example, drug-loaded cross-linkable block copolymer hydrogels containing mechanoresponsive drug depots enable the delivery of anti-inflammatory drugs (such as dexamethasone) when compressive forces are applied to the gels²⁰⁴ (FIG. 5). Furthermore, the development of ‘smart’ mechanoresponsive biomaterials tailored to use specific mechanical cues present at various stages of the tissue regeneration process would enable therapeutics to be delivered sequentially on the basis of the specific needs of the cells and tissue at any given time. For example, mechanically activated microcapsules tuned to exhibit different rupture profiles could enable the release of specific drugs in a sequential manner in response to the different mechanical forces present throughout the healing process^{24,200} (FIG. 5). As our understanding of the receptors and signalling pathways involved in mechanotransduction increases, so too does the ‘degree of smartness’ of mechanoresponsive approaches. In addition to responding to a particular physical force and delivering a specific drug, the use of advanced tissue engineering and synthetic biology approaches targeting mechanotransduction pathways involved in health and disease can enable ‘mechanobiological reprogramming’ of cells for the creation of autonomous mechanoresponsive constructs for enhanced tissue repair²⁵.

leverage the mechanical environment of the joint during regeneration to facilitate drug delivery according to the needs of the tissue, ultimately enhancing the therapeutic process (BOX 2). For cartilage applications, a suite of mechanically activated microcapsules (MAMCs) capable of releasing TGFβ3 have been developed that have varying thresholds of mechanoactivation²⁰⁰ (FIG. 5). Use of the MAMC system to deliver the anti-inflammatory agent IL-1 receptor antagonist (IL-1RA) has also been demonstrated to successfully reduce ECM degradation in engineered cartilage constructs treated with IL-1β²⁴. However, issues remain around how to prolong delivery in vivo in these systems over timescales that are suitable for cartilage regeneration and how to fine-tune release profiles to mechanical inputs. To overcome these limitations, researchers have begun to develop autonomous

mechanotherapeutics, which can respond in real time to the changing microenvironment, thus overcoming issues with long-term integration, target specificity, timing, homeostatic maintenance and repeated administration. For example, a synthetic TRPV4-responsive gene circuit has been developed by deconstructing the signalling networks downstream of TRPV4 activation²⁵. This gene circuit was effective as an autonomously regulated drug delivery system and is capable of producing IL-1RA in response to mechanical loading²⁵ (FIG. 5). Although only tested to date with the mechanical activation of TRPV4 and the delivery of a specific anti-inflammatory molecule, the framework of this system opens the door to the possibility of using other mechanoreceptors and signalling pathways, enabling the creation of a new generation of mechanotherapeutics. The development of such mechanically responsive biomaterials and closed-loop drug delivery systems could be vital for maintaining treatment efficacy in the changing environment of the joint during regeneration.

Conclusions

Mechanical stimuli are a critical environmental factor for maintaining joint homeostasis. How chondrocytes sense and respond to these mechanical forces determines cellular phenotype, regulates inflammation and tightly controls the anabolic–catabolic axis required for cartilage health. Chondrocytes are equipped to respond to these forces through a variety of mechanosensory mechanisms and signalling pathways. Altered mechanical forces, as a result of trauma or a reduced capacity to withstand normal loading conditions, regulates cell processes central to OA pathology, thus providing a number of effectors that can be targeted to uncouple pathological feedback loops. Coupling these targets with advanced drug delivery systems, ranging from gene therapy to mechanosensitive biomaterials, offers great promise in the development of safe and effective treatments for OA.

Published online 21 December 2021

- Vincent, T. L. & Wann, A. K. Mechanoadaptation: articular cartilage through thick and thin. *J. Physiol.* **597**, 1271–1281 (2019).
- Chang, S. H. et al. Excessive mechanical loading promotes osteoarthritis through the gremlin-1–NF-κB pathway. *Nat. Commun.* **10**, 1442 (2019).
- Goldring, S. R. & Goldring, M. B. Changes in the osteochondral unit during osteoarthritis: structure, function and cartilage–bone crosstalk. *Nat. Rev. Rheumatol.* **12**, 632–644 (2016).
- Pap, T. & Korb-Pap, A. Cartilage damage in osteoarthritis and rheumatoid arthritis — two unequal siblings. *Nat. Rev. Rheumatol.* **11**, 606–615 (2015).
- Burr, D. B. & Gallant, M. A. Bone remodelling in osteoarthritis. *Nat. Rev. Rheumatol.* **8**, 665–673 (2012).
- Collins, K. H. et al. Adipose tissue is a critical regulator of osteoarthritis. *Proc. Natl Acad. Sci. USA* **118**, e2021096118 (2021).
- Watt, F. E. Posttraumatic osteoarthritis: what have we learned to advance osteoarthritis? *Curr. Opin. Rheumatol.* **33**, 74–83 (2021).
- Greene, M. A. & Loeser, R. F. Aging-related inflammation in osteoarthritis. *Osteoarthritis Cartilage* **23**, 1966–1971 (2015).
- McNulty, M. A. et al. Histopathology of naturally occurring and surgically induced osteoarthritis in mice. *Osteoarthritis Cartilage* **20**, 949–956 (2012).
- Lotz, M. & Loeser, R. F. Effects of aging on articular cartilage homeostasis. *Bone* **51**, 241–248 (2012).
- Loeser, R. F. et al. Microarray analysis reveals age-related differences in gene expression during the development of osteoarthritis in mice. *Arthritis Rheum.* **64**, 705–717 (2012).
- Thomas, A. C., Hubbard-Turner, T., Wikstrom, E. A. & Palmieri-Smith, R. M. Epidemiology of posttraumatic osteoarthritis. *J. Athlet. Train.* **52**, 491–496 (2017).
- Glasson, S. S. et al. Deletion of active ADAMTS5 prevents cartilage degradation in a murine model of osteoarthritis. *Nature* **434**, 644–648 (2005).
- Burleigh, A. et al. Joint immobilization prevents murine osteoarthritis and reveals the highly mechanosensitive nature of protease expression in vivo. *Arthritis Rheum.* **64**, 2278–2288 (2012).
- Ismail, H. M. et al. Interleukin-1 acts via the JNK-2 signaling pathway to induce aggrecan degradation by human chondrocytes. *Arthritis Rheumatol.* **67**, 1826–1836 (2015).
- Zhang, M. et al. Induced superficial chondrocyte death reduces catabolic cartilage damage in murine posttraumatic osteoarthritis. *J. Clin. Invest.* **126**, 2893–2902 (2016).
- Gilbert, S. J. & Blain, E. J. In *Mechanobiology in Health and Disease* (ed. Verbruggen, S. W.) 99–126 (Elsevier, 2018).
- Guilak, F., Nims, R. J., Dicks, A., Wu, C.-L. & Meulenbelt, I. Osteoarthritis as a disease of the cartilage pericellular matrix. *Matrix Biol.* **71–72**, 40–50 (2018).
- Vincent, T. L. Targeting mechanotransduction pathways in osteoarthritis: a focus on the pericellular matrix. *Curr. Opin. Pharmacol.* **13**, 449–454 (2013).
- Agarwal, P. et al. A dysfunctional TRPV4–GSK3β pathway prevents osteoarthritic chondrocytes from sensing changes in extracellular matrix viscoelasticity. *Nat. Biomed. Eng.* **5**, 1472–1484 (2021).
- Nims, R. J. et al. A synthetic mechanogenetic gene circuit for autonomous drug delivery in engineered tissues. *Sci. Adv.* **7**, eabd9858 (2021).
- Deng, Y. et al. Reciprocal inhibition of YAP/TAZ and NF-κB regulates osteoarthritic cartilage degradation. *Nat. Commun.* **9**, 4564 (2018).
- Eckstein, F. et al. Intra-articular sprifermin reduces cartilage loss in addition to increasing cartilage gain independent of location in the femorotibial joint: post-hoc analysis of a randomised, placebo-controlled phase II clinical trial. *Ann. Rheum. Dis.* **79**, 525–528 (2020).
- Peredo, A. P. et al. Mechano-activated biomolecule release in regenerating load-bearing tissue microenvironments. *Biomaterials* **265**, 120255 (2021).
- Nims, R. J., Pferdehirt, L. & Guilak, F. Mechanogenetics: harnessing mechanobiology for cellular engineering. *Curr. Opin. Biotechnol.* **73**, 374–379 (2022).

26. Poole, A. R. et al. Composition and structure of articular cartilage: a template for tissue repair. *Clin. Orthop. Relat. Res.* **391**, S26–S33 (2001).
27. Mow, V. C., Ratcliffe, A. & Poole, A. R. Cartilage and diarthrodial joints as paradigms for hierarchical materials and structures. *Biomaterials* **13**, 67–97 (1992).
28. Schätti, O. R., Marková, M., Torzilli, P. A. & Gallo, L. M. Mechanical loading of cartilage explants with compression and sliding motion modulates gene expression of lubricin and catabolic enzymes. *Cartilage* **6**, 185–193 (2015).
29. Melrose, J., Hayes, A. J., Whitelock, J. M. & Little, C. B. Perlecan, the “jack of all trades” proteoglycan of cartilaginous weight-bearing connective tissues. *Bioessays* **30**, 457–469 (2008).
30. Poole, C. A. Articular cartilage chondrons: form, function and failure. *J. Anat.* **191**, 1–13 (1997).
31. Schinagl, R. M., Gurskis, D., Chen, A. C. & Sah, R. L. Depth-dependent confined compression modulus of full-thickness bovine articular cartilage. *J. Ortho Res.* **15**, 499–506 (1997).
32. Xia, Y., Moody, J. B., Alhadad, H. & Hu, J. Imaging the physical and morphological properties of a multi-zone young articular cartilage at microscopic resolution. *J. Mag. Reson. Imaging* **17**, 365–374 (2003).
33. Ratcliffe, A., Fryer, P. R. & Hardingham, T. E. The distribution of aggregating proteoglycans in articular cartilage: comparison of quantitative immunoelectron microscopy with radioimmunoassay and biochemical analysis. *J. Histochem. Cytochem.* **32**, 193–201 (1984).
34. Maroudas, A., Muir, H. & Wingham, J. The correlation of fixed negative charge with glycosaminoglycan content of human articular cartilage. *Biochim. Biophys. Acta* **177**, 492–500 (1969).
35. Wilusz, R. E., Zauscher, S. & Guilak, F. Micromechanical mapping of early osteoarthritic changes in the pericellular matrix of human articular cartilage. *Osteoarthritis Cartilage* **21**, 1895–1903 (2013).
36. Chery, D. R. et al. Early changes in cartilage pericellular matrix micromechanobiology portend the onset of post-traumatic osteoarthritis. *Acta Biomater.* **111**, 267–278 (2020).
37. Simon, W. H. Scale effects in animal joints. I. Articular cartilage thickness and compressive stress. *Arthritis Rheum.* **13**, 244–255 (1970).
38. Loeser, R. F. Integrins and cell signaling in chondrocytes. *Biorheology* **39**, 119–124 (2002).
39. Millward-Sadler, S. J. & Salter, D. M. Integrin-dependent signal cascades in chondrocyte mechanotransduction. *Ann. Biomed. Eng.* **32**, 435–446 (2004).
40. Ross, T. D. et al. Integrins in mechanotransduction. *Curr. Opin. Cell Biol.* **25**, 613–618 (2013).
41. Blain, E. J. Involvement of the cytoskeletal elements in articular cartilage homeostasis and pathology. *Int. J. Exp. Pathol.* **90**, 1–15 (2009).
42. Barrett-Jolley, R., Lewis, R., Fallman, R. & Mobasheri, A. The emerging chondrocyte channelome. *Front. Physiol.* **1**, 135 (2010).
43. Matta, C., Zákány, R. & Mobasheri, A. Voltage-dependent calcium channels in chondrocytes: roles in health and disease. *Curr. Rheumatol. Rep.* **17**, 43 (2015).
44. Mobasheri, A. et al. The chondrocyte channelome: a narrative review. *Jt. Bone Spine* **86**, 29–35 (2019).
45. Ruhlén, R. & Marberry, K. The chondrocyte primary cilium. *Osteoarthritis Cartilage* **22**, 1071–1076 (2014).
46. Tao, F., Jiang, T., Tao, H., Cao, H. & Xiang, W. Primary cilia: versatile regulator in cartilage development. *Cell Prolif.* **53**, e12765 (2020).
47. Guilak, F. et al. The pericellular matrix as a transducer of biomechanical and biochemical signals in articular cartilage. *Ann. N. Y. Acad. Sci.* **1068**, 498–512 (2006).
48. Youn, I., Choi, J., Cao, L., Setton, L. & Guilak, F. Zonal variations in the three-dimensional morphology of the chondron measured in situ using confocal microscopy. *Osteoarthritis Cartilage* **14**, 889–897 (2006).
49. Martin, J., Miller, B., Scherb, M., Lemke, L. & Buckwalter, J. Co-localization of insulin-like growth factor binding protein 5 and fibronectin in human articular cartilage. *Osteoarthritis Cartilage* **10**, 556–563 (2002).
50. Vincent, T., Hermansson, M., Bolton, M., Wait, R. & Saklatvala, J. Basic FGF mediates an immediate response of articular cartilage to mechanical injury. *Proc. Natl Acad. Sci. USA* **99**, 8259–8264 (2002).
51. Vincent, T. L., Hermansson, M. A., Hansen, U. N., Amis, A. A. & Saklatvala, J. Basic fibroblast growth factor mediates transduction of mechanical signals when articular cartilage is loaded. *Arthritis Rheum.* **50**, 526–535 (2004).
52. Vincent, T. L., McLean, C. J., Full, L. E., Peston, D. & Saklatvala, J. FGF-2 is bound to perlecan in the pericellular matrix of articular cartilage, where it acts as a chondrocyte mechanotransducer. *Osteoarthritis Cartilage* **15**, 752–763 (2007).
53. Vincent, T. L. Fibroblast growth factor 2: good or bad guy in the joint? *Arthritis Res. Ther.* **13**, 127 (2011).
54. Xie, Y., Zinkle, A., Chen, L. & Mohammadi, M. Fibroblast growth factor signalling in osteoarthritis and cartilage repair. *Nat. Rev. Rheumatol.* **16**, 547–564 (2020).
55. Makarenkova, H. P. et al. Differential interactions of FGFs with heparan sulfate control gradient formation and branching morphogenesis. *Sci. Signal.* **2**, ra55 (2009).
56. Eckstein, F., Wirth, W., Guermazi, A., Maschek, S. & Aydemir, A. Brief report: intraarticular sprifermin not only increases cartilage thickness, but also reduces cartilage loss: location-independent post hoc analysis using magnetic resonance imaging. *Arthritis Rheumatol.* **67**, 2916–2922 (2015).
57. Lohmander, L. S. et al. Intraarticular sprifermin (recombinant human fibroblast growth factor 18) in knee osteoarthritis: a randomized, double-blind, placebo-controlled trial. *Arthritis Rheumatol.* **66**, 1820–1831 (2014).
58. Hochberg, M. C. et al. Effect of intra-articular sprifermin vs placebo on femorotibial joint cartilage thickness in patients with osteoarthritis: the FORWARD randomized clinical trial. *JAMA* **322**, 1360–1370 (2019).
59. Zhen, G. et al. Mechanical stress determines the configuration of TGF β activation in articular cartilage. *Nat. Commun.* **12**, 1706 (2021).
60. Kechagia, J. Z., Ivaska, J. & Roca-Cusachs, P. Integrins as biomechanical sensors of the microenvironment. *Nat. Rev. Mol. Cell Biol.* **20**, 457–473 (2019).
61. Seetharaman, S. & Etienne-Manneville, S. Integrin diversity brings specificity in mechanotransduction. *Biol. Cell* **110**, 49–64 (2018).
62. Cantini, M., Donnelly, H., Dalby, M. J. & Salmeron-Sanchez, M. The plot thickens: the emerging role of matrix viscosity in cell mechanotransduction. *Adv. Healthc. Mater.* **9**, 1901259 (2020).
63. Parsons, J. T., Horwitz, A. R. & Schwartz, M. A. Cell adhesion: integrating cytoskeletal dynamics and cellular tension. *Nat. Rev. Mol. Cell Biol.* **11**, 633–643 (2010).
64. Puklin-Faucher, E. & Sheetz, M. P. The mechanical integrin cycle. *J. Cell Sci.* **122**, 179–186 (2009).
65. Elosegui-Artola, A. et al. Mechanical regulation of a molecular clutch defines force transmission and transduction in response to matrix rigidity. *Nat. Cell Biol.* **18**, 540–548 (2016).
66. Elosegui-Artola, A. et al. Rigidity sensing and adaptation through regulation of integrin types. *Nat. Mater.* **13**, 631–637 (2014).
67. Franz, F., Daday, C. & Gräter, F. Advances in molecular simulations of protein mechanical properties and function. *Curr. Opin. Struct. Biol.* **61**, 132–138 (2020).
68. Gouttenoire, J. et al. BMP-2 and TGF- β 1 differentially control expression of type II procollagen and α 10 and α 11 integrins in mouse chondrocytes. *Eur. J. Cell Biol.* **89**, 307–314 (2010).
69. Salter, D., Hughes, D., Simpson, R. & Gardner, D. Integrin expression by human articular chondrocytes. *Rheumatology* **31**, 231–234 (1992).
70. Zhang, W.-M. et al. Analysis of the human integrin α 11 gene (ITGA11) and its promoter. *Matrix Biol.* **21**, 513–525 (2002).
71. Loeser, R. F. Integrins and chondrocyte–matrix interactions in articular cartilage. *Matrix Biol.* **39**, 11–16 (2014).
72. Orazizadeh, M. et al. CD47 associates with α 5 integrin and regulates responses of human articular chondrocytes to mechanical stimulation in an in vitro model. *Arthritis Res. Ther.* **10**, R4 (2008).
73. Ostergaard, K. et al. Expression of α and β subunits of the integrin superfamily in articular cartilage from macroscopically normal and osteoarthritic human femoral heads. *Ann. Rheum. Dis.* **57**, 303–308 (1998).
74. Lucchinetti, E., Bhargava, M. M. & Torzilli, P. A. The effect of mechanical load on integrin subunits α 5 and β 1 in chondrocytes from mature and immature cartilage explants. *Cell Tissue Res.* **315**, 385–391 (2004).
75. Millward-Sadler, S. et al. Integrin-regulated secretion of interleukin 4: a novel pathway of mechanotransduction in human articular chondrocytes. *J. Cell Biol.* **145**, 183–189 (1999).
76. Millward-Sadler, S., Wright, M., Davies, L., Nuki, G. & Salter, D. Mechanotransduction via integrins and interleukin-4 results in altered aggrecan and matrix metalloproteinase 3 gene expression in normal, but not osteoarthritic, human articular chondrocytes. *Arthritis Rheum.* **43**, 2091–2099 (2000).
77. Steward, A. et al. Cell–matrix interactions regulate mesenchymal stem cell response to hydrostatic pressure. *Acta Biomater.* **8**, 2153–2159 (2012).
78. Jablonski, C. L., Ferguson, S., Pozzi, A. & Clark, A. L. Integrin α 11 participates in chondrocyte transduction of osmotic stress. *Biochem. Biophys. Res. Commun.* **445**, 184–190 (2014).
79. Wright, M. et al. Hyperpolarisation of cultured human chondrocytes following cyclical pressure-induced strain: evidence of a role for α 5 β 1 integrin as a chondrocyte mechanoreceptor. *J. Ortho Res.* **15**, 742–747 (1997).
80. Camper, L., Hellman, U. & Lundgren-Åkerlund, E. Isolation, cloning, and sequence analysis of the integrin subunit α 10, a β 1-associated collagen binding integrin expressed on chondrocytes. *J. Biol. Chem.* **273**, 20383–20389 (1998).
81. Bengtsson, T., Camper, L., Schneller, M. & Lundgren-Åkerlund, E. Characterization of the mouse integrin subunit α 10 gene and comparison with its human homologue: genomic structure, chromosomal localization and identification of splice variants. *Matrix Biol.* **20**, 565–576 (2001).
82. Lehnert, K. et al. Cloning, sequence analysis, and chromosomal localization of the novel human integrin α 11 subunit (ITGA11). *Genomics* **60**, 179–187 (1999).
83. Varas, L. et al. α 10 integrin expression is up-regulated on fibroblast growth factor-2-treated mesenchymal stem cells with improved chondrogenic differentiation potential. *Stem Cell Dev.* **16**, 965–978 (2007).
84. Delco, M. L. et al. Integrin α 10 β 1-selected mesenchymal stem cells mitigate the progression of osteoarthritis in an equine talar impact model. *Am. J. Sports Med.* **48**, 612–623 (2020).
85. Hirose, N. et al. Protective effects of cilengitide on inflammation in chondrocytes under excessive mechanical stress. *Cell Biol. Int.* **44**, 966–974 (2020).
86. Chao, P. H., West, A. C. & Hung, C. T. Chondrocyte intracellular calcium, cytoskeletal organization, and gene expression responses to dynamic osmotic loading. *Am. J. Physiol. Cell Physiol.* **291**, 718–725 (2006).
87. Erickson, G. R., Northrup, D. L. & Guilak, F. Hypo-osmotic stress induces calcium-dependent actin reorganization in articular chondrocytes. *Osteoarthritis Cartilage* **11**, 187–197 (2003).
88. Grodzinsky, A. J., Levenston, M. E., Jin, M. & Frank, E. H. Cartilage tissue remodeling in response to mechanical forces. *Annu. Rev. Biomed. Eng.* **2**, 691–713 (2000).
89. Guilak, F. Compression-induced changes in the shape and volume of the chondrocyte nucleus. *J. Biomech.* **28**, 1529–1541 (1995).
90. Blain, E. J., Mason, D. J. & Duance, V. C. The effect of thymosin β 4 on articular cartilage chondrocyte matrix metalloproteinase expression. *Biochem. Soc. Trans.* **30**, 879–882 (2002).
91. Fioravanti, A., Nerucci, F., Annefeld, M., Collodel, G. & Marcolongo, R. Morphological and cytoskeletal aspects of cultivated normal and osteoarthritic human articular chondrocytes after cyclical pressure: a pilot study. *Clin. Exp. Rheumatol.* **21**, 739–746 (2003).
92. Fioravanti, A., Benetti, D., Coppola, G. & Collodel, G. Effect of continuous high hydrostatic pressure on the morphology and cytoskeleton of normal and osteoarthritic human chondrocytes cultivated in alginate gels. *Clin. Exp. Rheumatol.* **23**, 847–853 (2005).
93. Isermann, P. & Lammerding, J. Nuclear mechanics and mechanotransduction in health and disease. *Curr. Biol.* **23**, R1113–R1121 (2013).
94. Khilan, A. A., Al-Maslami, N. A. & Horn, H. F. Cell stretchers and the LINC complex in mechanotransduction. *Arch. Biochem. Biophys.* **702**, 108829 (2021).
95. Lee, D. A. et al. Chondrocyte deformation within compressed agarose constructs at the cellular and sub-cellular levels. *J. Biomech.* **33**, 81–95 (2000).
96. Irianto, J. et al. Osmotic challenge drives rapid and reversible chromatin condensation in chondrocytes. *Biophys. J.* **104**, 759–769 (2013).

97. Hopewell, B. & Urban, J. P. Adaptation of articular chondrocytes to changes in osmolality. *Biorheology* **40**, 73–77 (2003).
98. Hung, C. T. et al. Disparate aggrecan gene expression in chondrocytes subjected to hypotonic and hypertonic loading in 2D and 3D culture. *Biorheology* **40**, 61–72 (2003).
99. Killaars, A. R., Walker, C. J. & Anseth, K. S. Nuclear mechanosensing controls MSC osteogenic potential through HDAC epigenetic remodeling. *Proc. Natl Acad. Sci. USA* **117**, 21258 (2020).
100. Elosegui-Artola, A. et al. Force triggers YAP nuclear entry by regulating transport across nuclear pores. *Cell* **171**, 1397–1410 (2017).
101. Delco, M. L. & Bonassar, L. J. Targeting calcium-related mechanotransduction in early OA. *Nat. Rev. Rheumatol.* **17**, 445–446 (2021).
102. O'Connor, C. J., Leddy, H. A., Benefield, H. C., Liedtke, W. B. & Guilak, F. TRPV4-mediated mechanotransduction regulates the metabolic response of chondrocytes to dynamic loading. *Proc. Natl Acad. Sci. USA* **111**, 1316–1321 (2014).
103. Phan, M. N. et al. Functional characterization of TRPV4 as an osmotically sensitive ion channel in porcine articular chondrocytes. *Arthritis Rheum.* **60**, 3028–3037 (2009).
104. Clark, A. L., Votta, B. J., Kumar, S., Liedtke, W. & Guilak, F. Chondroprotective role of the osmotically sensitive ion channel transient receptor potential vanilloid 4: age- and sex-dependent progression of osteoarthritis in Trpv4-deficient mice. *Arthritis Rheum.* **62**, 2973–2983 (2010).
105. O'Connor, C. J. et al. Cartilage-specific knockout of the mechanosensory ion channel TRPV4 decreases age-related osteoarthritis. *Sci. Rep.* **6**, 29053 (2016).
106. Drexler, S. K., Wann, A. K. T. & Vincent, T. L. Are cellular mechanosensors potential therapeutic targets in osteoarthritis. *Int. J. Clin. Rheumatol.* **9**, 155–167 (2014).
107. Lee, W., Guilak, F. & Liedtke, W. Role of Piezo channels in joint health and injury. *Curr. Top. Membr.* **79**, 263–273 (2017).
108. Sun, Y. et al. Mechanism of abnormal chondrocyte proliferation induced by Piezo1-siRNA exposed to mechanical stretch. *BioMed. Res. Int.* **2020**, 8538463 (2020).
109. Lee, W. et al. Synergy between Piezo1 and Piezo2 channels confers high-strain mechanosensitivity to articular cartilage. *Proc. Natl Acad. Sci. USA* **111**, E5114–E5122 (2014).
110. Gnanasambandam, R. et al. GsMTx4: mechanism of inhibiting mechanosensitive ion channels. *Biophys. J.* **112**, 31–45 (2017).
111. Suchyna, T. M. Piezo channels and GsMTx4: two milestones in our understanding of excitatory mechanosensitive channels and their role in pathology. *Prog. Biophys. Mol. Biol.* **130**, 244–253 (2017).
112. Xiao, W. F., Li, Y. S., Deng, A., Yang, Y. T. & He, M. Functional role of hedgehog pathway in osteoarthritis. *Cell Biochem. Funct.* **38**, 122–129 (2020).
113. McGlashan, S. R., Cluett, E. C., Jensen, C. G. & Poole, C. A. Primary cilia in osteoarthritic chondrocytes: from chondrons to clusters. *Dev. Dyn.* **237**, 2013–2020 (2008).
114. McGlashan, S. R., Jensen, C. G. & Poole, C. A. Localization of extracellular matrix receptors on the chondrocyte primary cilium. *J. Histochem. Cytochem.* **54**, 1005–1014 (2006).
115. Chang, C. F., Ramaswamy, G. & Serra, R. Depletion of primary cilia in articular chondrocytes results in reduced Gli3 repressor to activator ratio, increased Hedgehog signaling, and symptoms of early osteoarthritis. *Osteoarthritis Cartilage* **20**, 152–161 (2012).
116. Irianto, J., Ramaswamy, G., Serra, R. & Knight, M. M. Depletion of chondrocyte primary cilia reduces the compressive modulus of articular cartilage. *J. Biomech.* **47**, 579–582 (2014).
117. Wann, A. K. T. et al. Primary cilia mediate mechanotransduction through control of ATP-induced Ca²⁺ signaling in compressed chondrocytes. *FASEB J.* **26**, 1663–1671 (2012).
118. Shao, Y. Y., Wang, L., Welter, J. F. & Ballock, R. T. Primary cilia modulate Ihh signal transduction in response to hydrostatic loading of growth plate chondrocytes. *Bone* **50**, 79–84 (2012).
119. Pingguan-Murphy, B., El-Azzeh, M., Bader, D. & Knight, M. Cyclic compression of chondrocytes modulates a purinergic calcium signalling pathway in a strain rate- and frequency-dependent manner. *J. Cell Physiol.* **209**, 389–397 (2006).
120. Zhang, J. et al. Connexin43 hemichannels mediate small molecule exchange between chondrocytes and matrix in biomechanically-stimulated temporomandibular joint cartilage. *Osteoarthritis Cartilage* **22**, 822–830 (2014).
121. Garcia, M. & Knight, M. M. Cyclic loading opens hemichannels to release ATP as part of a chondrocyte mechanotransduction pathway. *J. Orthop. Res.* **28**, 510–515 (2010).
122. Chowdhury, T. & Knight, M. Purinergic pathway suppresses the release of NO and stimulates proteoglycan synthesis in chondrocyte/agarose constructs subjected to dynamic compression. *J. Cell Physiol.* **209**, 845–853 (2006).
123. Huang, C., Holfeld, J., Schaden, W., Orgill, D. & Ogawa, R. Mechanotherapy: revisiting physical therapy and recruiting mechanobiology for a new era in medicine. *Trends Mol. Med.* **19**, 555–564 (2013).
124. Thompson, W. R., Scott, A., Loughman, M. T., Ward, S. R. & Warden, S. J. Understanding mechanobiology: physical therapists as a force in mechanotherapy and musculoskeletal regenerative rehabilitation. *Phys. Ther.* **96**, 560–569 (2016).
125. Dell'Accio, F., De Bari, C., Eltaoui, N. M., Vanhummelen, P. & Pitzalis, C. Identification of the molecular response of articular cartilage to injury, by microarray screening: Wnt-16 expression and signaling after injury and in osteoarthritis. *Arthritis Rheum.* **58**, 1410–1421 (2008).
126. Loeser, R. F., Erickson, E. A. & Long, D. L. Mitogen-activated protein kinases as therapeutic targets in osteoarthritis. *Curr. Opin. Rheumatol.* **20**, 581–586 (2008).
127. Fanning, P. J. et al. Mechanical regulation of mitogen-activated protein kinase signaling in articular cartilage. *J. Biol. Chem.* **278**, 50940–50948 (2003).
128. Forsyth, C. B., Pulai, J. & Loeser, R. F. Fibronectin fragments and blocking antibodies to $\alpha 2 \beta 1$ and $\alpha 5 \beta 1$ integrins stimulate mitogen-activated protein kinase signaling and increase collagenase 3 (matrix metalloproteinase 13) production by human articular chondrocytes. *Arthritis Rheum.* **46**, 2368–2376 (2002).
129. Im, H.-J. et al. Inhibitory effects of insulin-like growth factor-1 and osteogenic protein-1 on fibronectin fragment- and interleukin-1 β -stimulated matrix metalloproteinase-13 expression in human chondrocytes. *J. Biol. Chem.* **278**, 25386–25394 (2003).
130. Loeser, R. F., Forsyth, C. B., Samarel, A. M. & Im, H.-J. Fibronectin fragment activation of proline-rich tyrosine kinase PYK2 mediates integrin signals regulating collagenase-3 expression by human chondrocytes through a protein kinase C-dependent pathway. *J. Biol. Chem.* **278**, 24577–24585 (2003).
131. Pulai, J. I. et al. NF- κ B mediates the stimulation of cytokine and chemokine expression by human articular chondrocytes in response to fibronectin fragments. *J. Immunol.* **174**, 5781–5788 (2005).
132. Del Carlo, M., Schwartz, D., Erickson, E. A. & Loeser, R. F. Endogenous production of reactive oxygen species is required for stimulation of human articular chondrocyte matrix metalloproteinase production by fibronectin fragments. *Free Radic. Biol. Med.* **42**, 1350–1358 (2007).
133. Long, D. L., Willey, J. S. & Loeser, R. F. Rac1 is required for matrix metalloproteinase 13 production by chondrocytes in response to fibronectin fragments. *Arthritis Rheum.* **65**, 1561–1568 (2013).
134. Gemba, T., Valbracht, J., Alsalam, S. & Lotz, M. Focal adhesion kinase and mitogen-activated protein kinases are involved in chondrocyte activation by the 29-kDa amino-terminal fibronectin fragment. *J. Biol. Chem.* **277**, 907–911 (2002).
135. Ding, L., Guo, D. & Homandberg, G. The cartilage chondrolytic mechanism of fibronectin fragments involves MAP kinases: comparison of three fragments and native fibronectin. *Osteoarthritis Cartilage* **16**, 1253–1262 (2008).
136. Ding, L., Guo, D. & Homandberg, G. Fibronectin fragments mediate matrix metalloproteinase upregulation and cartilage damage through proline rich tyrosine kinase 2, c-src, NF- κ B and protein kinase C δ . *Osteoarthritis Cartilage* **17**, 1385–1392 (2009).
137. Fitzgerald, J. B. et al. Shear- and compression-induced chondrocyte transcription requires MAPK activation in cartilage explants. *J. Biol. Chem.* **283**, 6735–6743 (2008).
138. Zhang, J., Shen, B. & Lin, A. Novel strategies for inhibition of the p38 MAPK pathway. *Trends Pharmacol. Sci.* **28**, 286–295 (2007).
139. González-Vázquez, A. et al. Accelerating bone healing in vivo by harnessing the age-altered activation of c-Jun N-terminal kinase 3. *Biomaterials* **268**, 120540 (2021).
140. Agarwal, S. et al. A central role for the nuclear factor- κ B pathway in anti-inflammatory and proinflammatory actions of mechanical strain. *FASEB J.* **17**, 899–901 (2003).
141. Yang, Y. et al. Mechanical stress protects against osteoarthritis via regulation of the AMPK/NF- κ B signaling pathway. *J. Cell Physiol.* **234**, 9156–9167 (2019).
142. Vincent, T. L. Mechanofluorescence in osteoarthritis pathogenesis. *Semin. Arthritis Rheum.* **49**, S36–S38 (2019).
143. Ismail, H. M., Didangelos, A., Vincent, T. L. & Saklatvala, J. Rapid activation of transforming growth factor β -activated kinase 1 in chondrocytes by phosphorylation and K(63)-linked polyubiquitination upon injury to animal articular cartilage. *Arthritis Rheumatol.* **69**, 565–575 (2017).
144. Lee, W. et al. Inflammatory signaling sensitizes Piezo1 mechanotransduction in articular chondrocytes as a pathogenic feed-forward mechanism in osteoarthritis. *Proc. Natl Acad. Sci. USA* **118**, e2001611118 (2021).
145. Nam, S. et al. Cell cycle progression in confining microenvironments is regulated by a growth-responsive TRPV4-PI3K/Akt-p27(Kip1) signaling axis. *Sci. Adv.* **5**, eaaw6171 (2019).
146. Lee, H. P., Gu, L., Mooney, D. J., Levenston, M. E. & Chaudhuri, O. Mechanical confinement regulates cartilage matrix formation by chondrocytes. *Nat. Mater.* **16**, 1243–1251 (2017).
147. Miller, J. R. The Wnts. *Genome Biol.* **3**, reviews3001.1 (2001).
148. Blom, A. B. et al. Involvement of the Wnt signaling pathway in experimental and human osteoarthritis: prominent role of Wnt-induced signaling protein 1. *Arthritis Rheum.* **60**, 501–512 (2009).
149. De Santis, M. et al. The role of Wnt pathway in the pathogenesis of OA and its potential therapeutic implications in the field of regenerative medicine. *BioMed. Res. Int.* **2018**, 7402947 (2018).
150. Dell'Accio, F. et al. Activation of WNT and BMP signaling in adult human articular cartilage following mechanical injury. *Arthritis Res. Ther.* **8**, R139 (2006).
151. Bougault, C. et al. Protective role of frizzled-related protein B on matrix metalloproteinase induction in mouse chondrocytes. *Arthritis Res. Ther.* **16**, R137 (2014).
152. Nalesso, G. et al. WNT16 antagonizes excessive canonical WNT activation and protects cartilage in osteoarthritis. *Ann. Rheum. Dis.* **76**, 218–226 (2017).
153. Wang, Y., Fan, X., Xing, L. & Tian, F. Wnt signaling: a promising target for osteoarthritis therapy. *Cell Commun. Signal.* **17**, 97 (2019).
154. Lories, R. J. & Montegudo, S. Review article: is Wnt signaling an attractive target for the treatment of osteoarthritis? *Rheumatol. Ther.* **7**, 259–270 (2020).
155. Montegudo, S. & Lories, R. J. Cushioning the cartilage: a canonical Wnt restricting matter. *Nat. Rev. Rheumatol.* **13**, 670–681 (2017).
156. Deshmukh, V. et al. A small-molecule inhibitor of the Wnt pathway (SM04690) as a potential disease modifying agent for the treatment of osteoarthritis of the knee. *Osteoarthritis Cartilage* **26**, 18–27 (2018).
157. Yazici, Y. et al. A phase 2b randomized trial of lorecivint, a novel intra-articular CLK2/DYRK1A inhibitor and Wnt pathway modulator for knee osteoarthritis. *Osteoarthritis Cartilage* **29**, 654–666 (2021).
158. Deshmukh, V. et al. Modulation of the Wnt pathway through inhibition of CLK2 and DYRK1A by lorecivint as a novel, potentially disease-modifying approach for knee osteoarthritis treatment. *Osteoarthritis Cartilage* **27**, 1347–1360 (2019).
159. Montegudo, S. et al. DOT1L safeguards cartilage homeostasis and protects against osteoarthritis. *Nat. Commun.* **8**, 15889 (2017).
160. Cornelis, F. M. F. et al. Increased susceptibility to develop spontaneous and post-traumatic osteoarthritis in Dot1l-deficient mice. *Osteoarthritis Cartilage* **27**, 513–525 (2019).
161. Castaño Betancourt, M. C. et al. Genome-wide association and functional studies identify the DOT1L gene to be involved in cartilage thickness and hip osteoarthritis. *Proc. Natl Acad. Sci. USA* **109**, 8218–8223 (2012).

162. Deng, Y. et al. Yap1 regulates multiple steps of chondrocyte differentiation during skeletal development and bone repair. *Cell Rep.* **14**, 2224–2237 (2016).
163. Gumbiner, B. M. & Kim, N.-G. The Hippo-YAP signaling pathway and contact inhibition of growth. *J. Cell Sci.* **127**, 709–717 (2014).
164. Dupont, S. et al. Role of YAP/TAZ in mechanotransduction. *Nature* **474**, 179–183 (2011).
165. Baker, B. M. & Chen, C. S. Deconstructing the third dimension—how 3D culture microenvironments alter cellular cues. *J. Cell Sci.* **125**, 3015–3024 (2012).
166. Caliri, S. R., Vega, S. L., Kwon, M., Soulas, E. M. & Burdick, J. A. Dimensionality and spreading influence MSC YAP/TAZ signaling in hydrogel environments. *Biomaterials* **103**, 314–323 (2016).
167. Karystinou, A. et al. Yes-associated protein (YAP) is a negative regulator of chondrogenesis in mesenchymal stem cells. *Arthritis Res. Ther.* **17**, 147 (2015).
168. Mobasheri, A. et al. The role of metabolism in the pathogenesis of osteoarthritis. *Nat. Rev. Rheumatol.* **13**, 302–311 (2017).
169. Salinas, D., Mumey, B. M. & June, R. K. Physiological dynamic compression regulates central energy metabolism in primary human chondrocytes. *Biomech. Model. Mechanobiol.* **18**, 69–77 (2019).
170. Lehtinen, M. K. et al. A conserved MST-FOXO signaling pathway mediates oxidative-stress responses and extends life span. *Cell* **125**, 987–1001 (2006).
171. Niehoff, A. et al. Dynamic and static mechanical compression affects Akt phosphorylation in porcine patellofemoral joint cartilage. *J. Orthop. Res.* **26**, 616–623 (2008).
172. Holledge, M. M., Millward-Sadler, S. J., Nuki, G. & Salter, D. M. Mechanical regulation of proteoglycan synthesis in normal and osteoarthritic human articular chondrocytes—roles for $\alpha 5$ and $\alpha v \beta 5$ integrins. *Biorheology* **45**, 275–288 (2008).
173. Delco, M. L., Bonnevie, E. D., Bonassar, L. J. & Fortier, L. A. Mitochondrial dysfunction is an acute response of articular chondrocytes to mechanical injury. *J. Orthop. Res.* **36**, 739–750 (2018).
174. Waller, K. A., Zhang, L. X. & Jay, G. D. Friction-induced mitochondrial dysregulation contributes to joint deterioration in Prg4 knockout mice. *Int. J. Mol. Sci.* **18**, 1252 (2017).
175. Bartell, L. R. et al. Mitoprotective therapy prevents rapid, strain-dependent mitochondrial dysfunction after articular cartilage injury. *J. Orthop. Res.* **38**, 1257–1267 (2020).
176. Jutila, A. A. et al. Candidate mediators of chondrocyte mechanotransduction via targeted and untargeted metabolomic measurements. *Arch. Biochem. Biophys.* **545**, 116–123 (2014).
177. Zignego, D. L., Jutila, A. A., Gelbek, M. K., Gannon, D. M. & June, R. K. The mechanical microenvironment of high concentration agarose for applying deformation to primary chondrocytes. *J. Biomech.* **47**, 2143–2148 (2014).
178. Hodgkinson, T. et al. The use of nanovibration to discover specific and potent bioactive metabolites that stimulate osteogenic differentiation in mesenchymal stem cells. *Sci. Adv.* **7**, eabb7921 (2021).
179. Bonnevie, E. D. et al. Microscale frictional strains determine chondrocyte fate in loaded cartilage. *J. Biomech.* **74**, 72–78 (2018).
180. Irwin, R. M. et al. Distinct tribological endotypes of pathological human synovial fluid reveal characteristic biomarkers and variation in efficacy of viscosupplementation at reducing local strains in articular cartilage. *Osteoarthritis Cartilage* **28**, 492–501 (2020).
181. Xie, R. et al. Biomimetic cartilage-lubricating polymers regenerate cartilage in rats with early osteoarthritis. *Nat. Biomed. Eng.* **5**, 1189–1201 (2021).
182. Grither, W. R. & Longmore, G. D. Inhibition of tumor-microenvironment interaction and tumor invasion by small-molecule allosteric inhibitor of DDR2 extracellular domain. *Proc. Natl Acad. Sci. USA* **115**, E7786–E7794 (2018).
183. Kumar, A., Choudhury, M. D., Ghosh, P. & Palit, P. Discoidin domain receptor 2: an emerging pharmacological drug target for prospective therapy against osteoarthritis. *Pharmacol. Rep.* **71**, 399–408 (2019).
184. Occhetta, P. et al. Hyperphysiological compression of articular cartilage induces an osteoarthritic phenotype in a cartilage-on-a-chip model. *Nat. Biomed. Eng.* **3**, 545–557 (2019).
185. Lee, J. et al. Combinatorial screening of biochemical and physical signals for phenotypic regulation of stem cell-based cartilage tissue engineering. *Sci. Adv.* **6**, eaaz5913 (2020).
186. Wang, J., Lü, D., Mao, D. & Long, M. Mechanomics: an emerging field between biology and biomechanics. *Protein Cell* **5**, 518–531 (2014).
187. Gabriel, S. E., Crowson, C. S. & O’Fallon, W. M. Comorbidity in arthritis. *J. Rheumatol.* **26**, 2475–2479 (1999).
188. Shi, S., Man, Z., Li, W., Sun, S. & Zhang, W. Silencing of Wnt5a prevents interleukin-1 β -induced collagen type II degradation in rat chondrocytes. *Exp. Ther. Med.* **12**, 3161–3166 (2016).
189. Yan, H. et al. Suppression of NF- κ B activity via nanoparticle-based siRNA delivery alters early cartilage responses to injury. *Proc. Natl Acad. Sci. USA* **113**, E6199–E6208 (2016).
190. Rai, M. F. et al. Applications of RNA interference in the treatment of arthritis. *Transl. Res.* **214**, 1–16 (2019).
191. Cheleschi, S. et al. Hydrostatic pressure regulates microRNA expression levels in osteoarthritic chondrocyte cultures via the Wnt/ β -catenin pathway. *Int. J. Mol. Sci.* **18**, 133 (2017).
192. De Palma, A. et al. Hydrostatic pressure as epigenetic modulator in chondrocyte cultures: a study on miRNA-155, miRNA-181a and miRNA-223 expression levels. *J. Biomech.* **66**, 165–169 (2018).
193. Yang, X. et al. Mechanical and IL-1 β responsive miR-365 contributes to osteoarthritis development by targeting histone deacetylase 4. *Int. J. Mol. Sci.* **17**, 436 (2016).
194. Stadnik, P. S. et al. Regulation of microRNA-221, -222, -21 and -27 in articular cartilage subjected to abnormal compressive forces. *J. Physiol.* **599**, 143–155 (2021).
195. Dunn, W., DuRaine, G. & Reddi, A. H. Profiling microRNA expression in bovine articular cartilage and implications for mechanotransduction. *Arthritis Rheum.* **60**, 2333–2339 (2009).
196. Iliopoulos, D., Malizos, K. N., Oikonomou, P. & Tsezou, A. Integrative microRNA and proteomic approaches identify novel osteoarthritis genes and their collaborative metabolic and inflammatory networks. *PLoS ONE* **3**, e3740 (2008).
197. Song, J. et al. MicroRNA-222 regulates MMP-13 via targeting HDAC-4 during osteoarthritis pathogenesis. *BBA Clin.* **3**, 79–89 (2014).
198. Hecht, N., Johnstone, B., Angele, P., Walker, T. & Richter, W. Mechanosensitive MiRs regulated by anabolic and catabolic loading of human cartilage. *Osteoarthritis Cartilage* **27**, 1208–1218 (2019).
199. Lolli, A., Colella, F., De Bari, C. & van Osch, G. J. V. M. Targeting anti-chondrogenic factors for the stimulation of chondrogenesis: a new paradigm in cartilage repair. *J. Orthop. Res.* **37**, 12–22 (2019).
200. Mohanraj, B. et al. Mechanically activated microcapsules for “on-demand” drug delivery in dynamically loaded musculoskeletal tissues. *Adv. Funct. Mater.* **29**, 1807909 (2019).
201. Cambré, I. et al. Mechanical strain determines the site-specific localization of inflammation and tissue damage in arthritis. *Nat. Commun.* **9**, 4613 (2018).
202. Lin, X., Bai, Y., Zhou, H. & Yang, L. Mechano-active biomaterials for tissue repair and regeneration. *J. Mater. Sci. Technol.* **59**, 227–233 (2020).
203. Zhang, Y., Yu, J., Bomba, H. N., Zhu, Y. & Gu, Z. Mechanical force-triggered drug delivery. *Chem. Rev.* **116**, 12536–12563 (2016).
204. Xiao, L. et al. Hyaluronic acid-based hydrogels containing covalently integrated drug depots: implication for controlling inflammation in mechanically stressed tissues. *Biomacromolecules* **14**, 3808–3819 (2013).

Acknowledgements

T.H. is in receipt of a Marie Skłodowska-Curie Individual Fellowship from the European Commission through the Horizon 2020 project ChondroCONNECT (project ID: 894837). The work of D.C.K. is funded by Science Foundation Ireland under the European Regional Development Fund CURAM (13/RC/2073) and the Irish Research Council Government of Ireland Postgraduate Programme (GOIPG/2018/371). C.M.C. recognizes funding from the Irish Health Research Board (ILP-POR-2019-023 and ILP-POR-2017-032). F.J.O.B. acknowledges funding from the European Commission Horizon 2020 research and innovation programme under the European Research Council Advanced Grant (agreement ID: 788753, ReCaP) and from the Irish Health Research Board (ILP-POR-2017-032).

Author contributions

T.H. and D.C.K. wrote the manuscript. All authors researched data for the article, made a substantial contribution to discussion of content and reviewed or edited the manuscript before submission.

Competing interests

The authors declare no competing interests.

Peer review information


Nature Reviews Rheumatology thanks L. Bonassar, F. Guilak and the other, anonymous, reviewer(s) for their contribution to the peer review of this work.

Publisher's note

Springer Nature remains neutral with regard to jurisdictional claims in published maps and institutional affiliations.

© Springer Nature Limited 2021

Acute exacerbation of interstitial lung disease associated with rheumatic disease

Fabrizio Luppi¹ ✉, Marco Sebastiani², Carlo Salvarani^{2,3}, Elisabeth Bendstrup⁴ 
and Andreina Manfredi²

Abstract | Interstitial lung disease (ILD) is a cause of morbidity and mortality in patients with rheumatic diseases, such as connective-tissue diseases, rheumatoid arthritis and systemic vasculitis. Some patients with ILD secondary to rheumatic disease (RD-ILD) experience acute exacerbations, with sudden ILD progression and high mortality during or immediately after the exacerbation, and a very low 1-year survival rate. In the ILD subtype idiopathic pulmonary fibrosis (IPF), an acute exacerbation is defined as acute worsening or development of dyspnoea associated with new bilateral ground-glass opacities and/or consolidations at high-resolution CT, superimposed on a background pattern consistent with fibrosing ILD. However, acute exacerbation in RD-ILD (AE-RD-ILD) currently has no specific definition. The aetiology and pathogenesis of AE-RD-ILD remain unclear, but distinct triggers might include infection, mechanical stress, microaspiration and DMARD treatment. At this time, no effective evidence-based therapeutic strategies for AE-RD-ILD are available. In clinical practice, AE-RD-ILD is often empirically treated with high-dose systemic steroids and antibiotics, with or without immunosuppressive drugs. In this Review, we summarize the clinical features, diagnosis, management and prognosis of AE-RD-ILD, enabling the similarities and differences with acute exacerbation in IPF to be critically assessed.

¹Respiratory Diseases Unit, University of Milano-Bicocca, S. Gerardo Hospital, ASST Monza, Monza, Italy.

²Rheumatology Unit, University of Modena and Reggio Emilia, Azienda Ospedaliero-Universitaria Policlinico di Modena, Modena, Italy.

³Rheumatology Unit, Dipartimento Medicina Interna e Specialità Mediche, Azienda Unità Sanitaria Locale di Reggio Emilia-Istituto di Ricerca e Cura a Carattere Scientifico, Reggio Emilia, Italy.

⁴Center for Rare Lung Disease, Department of Respiratory Medicine and Allergy, Aarhus University Hospital, Aarhus, Denmark.

✉e-mail: fabrizio.luppi@unimib.it

<https://doi.org/10.1038/s41584-021-00721-z>

Interstitial lung disease (ILD) includes various pulmonary parenchymal disorders that are classified together because of similarities in clinical presentation, chest radiographic appearance and physiological features¹. ILD can occur as a result of environmental exposure, as in conditions such as asbestosis and hypersensitivity pneumonitis, or exposure to medication, as in drug-induced ILD. Other forms of ILD include granulomatous disorders such as sarcoidosis, idiopathic interstitial pneumonias (IIPs) and rheumatic disease-associated ILDs (RD-ILDs)². In general, ILD results from de novo fibrosis or excessive accumulation of connective-tissue matrix in the lung interstitium, following an inflammatory process³. In many cases, ILD ultimately leads to irreversible pulmonary fibrosis⁴, and it is an important cause of morbidity and mortality in patients with rheumatic diseases⁴. Currently, specific classification of RD-ILD is not available. Instead, it usually follows the radiological and/or histopathological classifications of IIPs, all the patterns of which reportedly occur in RD-ILD² (TABLE 1). The relative prevalence and prognostic importance of each pattern differs between IIP and RD-ILD.

In IIP, the most prevalent radiological and histopathological pattern is usual interstitial pneumonia (UIP), which clinically corresponds to idiopathic pulmonary fibrosis (IPF)³. Some studies have also identified UIP as the most common pattern in rheumatoid arthritis (RA)-associated ILD (RA-ILD), which has a similarly low survival rate to IPF^{5,6}. By contrast, patients with connective-tissue disease (CTD) and a UIP pattern have better prognoses than those with IIP and UIP⁷. Non-specific interstitial pneumonia (NSIP) is the IIP pattern that is most commonly observed in patients with ILD and systemic sclerosis (SSc)⁸, idiopathic inflammatory myopathies (including antisynthetase syndrome)⁹ or primary Sjögren syndrome¹⁰; generally, these patients have more favourable prognoses than those with IPF or RA-ILD associated with UIP¹¹.

Although patients with IPF typically exhibit progressive clinical, radiological and functional decline¹², they can also experience episodes of acute respiratory decompensation — referred to as acute exacerbation — with worsening dyspnoea and requirement for supplemental oxygen¹³. Acute exacerbation occurs in nearly all types of ILD, and is associated with poor survival^{14–18}.

Key points

- In patients with rheumatic diseases, interstitial lung disease (ILD) is a major cause of morbidity and mortality.
- Some patients with rheumatic disease experience acute exacerbation of ILD (AE-ILD), a sudden worsening that is associated with high short-term mortality and a very low 1-year survival rate.
- Diagnosis of AE-ILD relies on clinical suspicion, symptom worsening and identification of potential triggers combined with imaging and exclusion of other diseases.
- Management strategies for AE-ILD are based on recommendations for idiopathic pulmonary fibrosis, including systemic steroids and broad-spectrum antibiotics.
- Randomized controlled trials of the management of acute exacerbation are lacking.

Dyspnoea

Difficult or laboured breathing.

Pneumothorax

Presence of air between the pleura and the lungs, causing the collapse of the lung.

Pleural effusion

Accumulation of fluid between the pleural layers.

The histological pattern associated with acute exacerbation in RD-ILD (AE-RD-ILD)¹⁹ commonly includes diffuse alveolar damage (DAD), which is similar to that observed in acute respiratory distress syndrome (ARDS), a severe acute respiratory deterioration with similar clinical, radiological and pathological characteristics to AE-RD-ILD, but without a background of ILD^{20–22}.

In this Review, we summarize the definition, epidemiology and key pathogenic mechanisms relating to AE-RD-ILD, with discussion of relevant clinical features, diagnostic criteria, prognostic evaluation, monitoring and management approaches. We also compare AE-RD-ILD with acute exacerbation in IPF (AE-IPF), as IPF is the prototypical ILD in which AE has been described.

Definition of acute exacerbation

In 1993, the occurrence of acute respiratory deterioration in three patients with IPF was described for the first time²³. The patients developed acute influenza-like symptoms, including cough, fever, leukocytosis and progressive hypoxia, with no identifiable infection. Histological findings from tissue obtained by open-lung biopsy indicated both UIP and acute lung injury patterns. In 2007, an international consensus statement was published containing a proposed standard definition of

AE-IPF as an acute, clinically significant deterioration of unidentifiable cause in a patient with underlying IPF, as opposed to acute respiratory deterioration with a known cause²⁴. Although the proposed definition represented a major achievement in AE-IPF diagnosis, it was difficult to apply in clinical practice, mainly because of the challenge of excluding all potential known causes of acute respiratory failure in severely ill patients, such as pulmonary infection²⁵. Hence, a standardized work-up for patients manifesting possible AE-IPF was not proposed. A major controversial diagnostic issue was associated with the role of bronchoalveolar lavage in identifying infectious agents, as bronchoscopy in non-intubated patients with high baseline oxygen requirement poses a risk of hypoxaemia worsening, and most microbiological tests have poor sensitivity²⁶.

Considering the difficulty in classifying AE-IPF using the proposed criteria, and the statement that ‘idiopathic’ AE-IPF might be indistinguishable both clinically and prognostically from that induced by known causes of acute lung injury (such as pulmonary infection, microaspiration and mechanical injury)²⁴, an expert working group was encouraged to revise the previous AE-IPF definition with the aim of updating the diagnostic criteria and facilitating their application in clinical practice²⁷. The updated criteria included a change in the range for diagnosis of acute exacerbation from 30 days to “typically less than 1 month”, as well as exclusion of the term “idiopathic” in relation to the cause of the acute exacerbation, and of the diagnosis of acute respiratory failure caused by cardiac failure or fluid overload (because of its favourable prognosis), and of other extrapulmonary causes (such as pneumothorax, pleural effusion and pulmonary embolism). The revised definition was intended to identify diagnostic criteria that are sufficiently broad and easy to apply both in clinical practice and in clinical trials.

Acute exacerbation is not restricted to IPF, and it can also complicate the course of other ILDs, as in AE-RD-ILD^{28,29}. Unfortunately, acute exacerbation in ILDs

Table 1 | Radiological and histopathological patterns associated with interstitial lung disease secondary to rheumatic disease

Category	Radiological pattern	Histopathological pattern	Description of the pathological pattern
Chronic fibrosing interstitial pneumonia	Usual interstitial pneumonia	Usual interstitial pneumonia	Combination of patchy fibrosis with alternating areas of normal lung, temporal heterogeneity of fibrosis characterized by scattered fibroblastic foci on a background of dense acellular collagen and architectural alteration because of chronic scarring or honeycomb change
	Idiopathic non-specific interstitial pneumonia	Non-specific interstitial pneumonia	Temporally uniform interstitial process with varying proportions of interstitial inflammation and fibrosis
Smoking-related interstitial pneumonia	Respiratory bronchiolitis-interstitial lung disease	Respiratory bronchiolitis	Mainly characterized by the prominent accumulation of pigmented macrophages in the lumen of respiratory bronchioles and adjacent alveoli
	Desquamative interstitial pneumonia	Desquamative interstitial pneumonia	Characterized by the accumulation of numerous pigmented macrophages within most of the distal airspace of the lung and, sometimes, the presence of giant cells
Acute/subacute interstitial pneumonia	Cryptogenic organizing pneumonia	Organizing pneumonia	Histological term characterized by patchy filling of alveoli and bronchioles by loose plugs of connective tissue
	Acute interstitial pneumonia (acute exacerbation of idiopathic pulmonary fibrosis)	Diffuse alveolar damage	Characterized by an initial exudative (acute) phase with oedema, hyaline membranes and interstitial acute inflammation, followed by an organizing (subacute) phase with loose organizing fibrosis mostly within the alveolar septa, and type II pneumocyte hyperplasia

Table 2 | Definitions and diagnostic criteria for acute exacerbation in IPF and in ILD in rheumatic disease

Characteristic	Source of information		
	2007 definition of acute exacerbation in IPF ²⁴	2016 definition of acute exacerbation in IPF ²⁷	2021 proposed definition of acute exacerbation in ILD in rheumatic disease
Definition	An acute worsening of dyspnoea and lung function with an unidentifiable cause	An acute, clinically significant respiratory deterioration characterized by evidence of new widespread alveolar abnormality	An acute, clinically significant respiratory worsening characterized by new widespread alveolar abnormality in a patient with a known or concurrent diagnosis of rheumatic disease
Diagnostic criteria			
Disease	Previous or concurrent diagnosis of IPF	Previous or concurrent diagnosis of IPF	Rheumatic disease with previous or concurrent diagnosis of ILD
Symptoms	Unexplained worsening or development of dyspnoea <1 month duration	Acute worsening or development of dyspnoea typically <1 month duration	Acute worsening or development of dyspnoea typically <1 month duration
Imaging	HRCT with new bilateral ground-glass abnormality and/or consolidation superimposed on a background reticular or honeycomb pattern consistent with UIP	HRCT with new bilateral ground-glass opacity and/or consolidation superimposed on a background pattern consistent with UIP pattern	HRCT with new bilateral ground-glass opacity and/or consolidation superimposed on a background pattern of ILD
Infection	No evidence of pulmonary infection by endotracheal aspirate or bronchoalveolar lavage	Not considered as an exclusion criterion for acute exacerbation	Not considered as an exclusion criterion for acute exacerbation
Triggers	Infections*, gastroesophageal reflux, microaspiration, surgery, bronchoscopy, air pollution	Infections*, gastroesophageal reflux, microaspiration, surgery, bronchoscopy, air pollution	Infections, opportunistic infections, DMARDs, gastroesophageal reflux, microaspiration, surgery, bronchoscopy, air pollution
Alternative causes	Exclusion of alternative causes, including the following: left heart failure, pulmonary embolism, identifiable causes of acute lung injury	Deterioration not fully explained by cardiac failure or fluid overload	Deterioration not fully explained by cardiac failure, fluid overload or DMARD use

*Opportunistic infections should always be considered. HRCT, high-resolution CT; ILD, interstitial lung disease; IPF, idiopathic pulmonary fibrosis; UIP, usual interstitial pneumonia.

other than IPF currently has no separate, specific definition. The diagnostic criteria applied in most studies to define acute exacerbation in non-IPF ILD are based on the criteria indicated for IPF, and extrapolated from the updated AE-IPF statement²⁷. With consideration of the 2007 and 2016 criteria for the definition of AE-IPF, we can also propose an equivalent definition for AE-RD-ILD (TABLE 2) on the basis of specific characteristics of RD-ILD, highlighting notable differences from previous IPF definitions, with the purpose of contributing to the development of an RD-ILD definition for clinical use. A distinguishing feature of the definition of AE-RD-ILD is that the triggers of the condition include treatment with antirheumatic drugs prior to hospitalization³⁰, which can be associated with elevation of the risk of infections, including opportunistic infections³¹. Whether the drug is the cause of a drug-induced ILD or the trigger of an AE-RD-ILD can be difficult to determine, and both possibilities should be taken into consideration. Also, the time-frame for differentiation between an acute deterioration and a progressive disease is arbitrary, and further evidence is required to guide informed decision-making on this issue.

Epidemiology

Most evidence on the epidemiology of ILDs has been derived from prospective registries of data reported by respiratory physicians, showing a prevalence ranging from about 4 to 80 per 100,000 in various European countries and in the USA³². Prevalence estimates for IPF vary from 2 to 29 cases per 100,000 in the general population³³. Data relating to the prevalence of RD-ILD

are scarce and variable for both retrospective studies and heterogeneity of lung involvement in different rheumatic diseases. Reported prevalence of ILD varies from a low range of 4–13% in systemic lupus erythematosus to a higher range of 65–91% in SSC³⁴. In one US study, over a 10-year period, incidence of RA-ILD was quite stable, whereas prevalence increased from 3.2 to 6.0 per 100,000 people³⁵.

The reported annual incidence of AE-IPF ranges from 1% to 20% in patients with IPF, and this wide range of values reflects variation in study design and disease severity²⁷, and the lack of a standard definition for acute exacerbation³⁶. Nonetheless, it represents a considerable disease burden, given the high individual and societal costs associated with these events. In patients with RD-ILD, the estimated 1-year incidence of AE-RD-ILD ranges from 1.25% to 7.2%, which seems to be lower than that in IPF^{19,28}. In patients with rheumatic disease who display a radiological UIP pattern, the incidence of AE-RD-ILD has been estimated as 5.6%, compared with 11.1% in those with RA-ILD with the UIP pattern^{28,37}. The prevalence of UIP is higher in RA-ILD than in CTD-ILD in general, so the high frequency of acute exacerbation in RA-ILD might be explained by the observation that a UIP pattern, *per se*, is associated with a high risk of AE-ILD³⁸. Patients with diffuse SSC and anti-topoisomerase I antibodies have a high incidence of ILD (including AE-RD-ILD), which frequently leads to SSC-related death³⁹. In a retrospective study of 139 patients with SSC, 47.5% had ILD, and among the 9.4% who developed AE-ILD, the incidence of overlap with polymyositis or dermatomyositis was higher,

mortality was higher and the prevalence of antinuclear antibodies was lower than in the patients without AE-ILD⁴⁰. In a single-centre, retrospective study of patients with idiopathic inflammatory myopathies who were admitted to the intensive-care unit, reasons for admission included infection and acute exacerbation, which was secondary to rapidly progressive ILD⁴¹. Results therefore suggest that a UIP pattern, an RA-ILD or SSC-ILD diagnosis and an overlap with polymyositis or dermatomyositis are risk factors for AE-RD-ILD³⁵. Notably, acute exacerbation also occurs in patients with microscopic polyangiitis and ILD, in whom the 1-year acute exacerbation cumulative incidence rate has been estimated to be 7.2%⁴².

Pathophysiology

The aetiology of AE-RD-ILD remains largely unclear, and its onset and development are unpredictable. Similar to ARDS, AE-ILD is associated with higher numbers of neutrophils and lower numbers of macrophages and eosinophils in bronchoalveolar lavage fluid than is non-AE-ILD⁴³. Notably, a response to exposure to pulmonary toxicants is the production of chemokines such as IL-8 and CXCL1 and the accumulation of pro-inflammatory (also known as M1) macrophages at sites of tissue injury⁴⁴. The activated M1 macrophages release various pro-inflammatory cytokines, including TNF, IL-1 β , IL-6, IL-12, IL-15 and IL-23, and generate cytotoxic reactive oxygen and nitrogen species, proteolytic enzymes and bioactive lipids⁴⁴. The response also involves the production of M2 macrophages, which release anti-inflammatory molecules (including IL-10 and TGF β) in response to T helper 2-type cytokines (IL-4 and IL-13), and inhibit pro-inflammatory mediators⁴⁵. Therefore, they have a pivotal role in repairing lung damage⁴⁶. Evidence also exists of increased vascular permeability in the lungs of patients who experience AE-ILD. In patients with fibrotic lung disease, increased vascular permeability, pro-coagulant activity and fibrin turnover correlate with loss of lung compliance⁴⁷. Intra-alveolar fibrin accumulation is a hallmark of lung injury and correlates with disease severity and outcomes in patients with DAD⁴⁸. Similarly, macrophage and neutrophil activation leads to release of reactive oxygen species and proteases. Activation of both M1 macrophages and neutrophils causes lung damage, capillary-alveolar permeability and oxygen deficiency⁴⁶. Notably, neutrophil concentrations in the bronchoalveolar lavage fluid of patients with ARDS correlate with disease severity and poor outcomes⁴⁹ (FIG. 1).

Whether the pathophysiology of AE-RD-ILD is similar to that of acute exacerbation in other ILD types, and whether it proceeds via intrinsic (sudden) acceleration of the underlying fibrotic process, as characterized by enhanced epithelial injury and proliferation along with coagulation abnormalities, or in response to external events that result in acute lung injury and DAD, is not yet known⁵⁰. DAD is detected in the autopsies of individuals who die as a result of AE-IPF⁵⁰, and it is also found in autopsies of individuals with other ILDs, including RD-ILD⁵¹. In a study of patients with acute exacerbation with various underlying disorders, the histological

pattern of organizing pneumonia was associated with a higher survival rate than that of DAD, suggesting responsiveness to steroid and immunosuppressive treatment⁵².

Pulmonary infections can trigger and contribute to AE-ILD occurrence, and infection-associated AE-ILD should possibly be recognized as a distinct AE-ILD phenotype. Evidence of the role of infection includes the seasonal nature of AE-IPF, with most cases occurring during winter months^{53,54}, and the observation that respiratory tract infections confer a mortality risk similar to that seen with acute exacerbation⁵⁵. Furthermore, post-mortem examination in confirmed instances of infection frequently reveals DAD identical to that seen during AE-IPF, and, compared with placebo, immunosuppressive medication is associated with a higher rate of infections and, therefore, acute exacerbation⁵⁶.

In a study comparing the respiratory microbiota of patients with AE-IPF and matched patients with stable IPF, AE-IPF was associated with a greater bronchoalveolar lavage bacterial burden than stable IPF⁵⁷. Furthermore, the microbial species distribution was different in AE-IPF samples to that in stable IPF; for example, in AE-IPF, *Campylobacter* and *Stenotrophomonas* species were more abundant, and *Veillonella* species were less abundant than in stable IPF⁵⁷. This result suggests that bacteria might have a causative role, at least in some AE-IPF cases. In a study of patients with early RA, a form of distal airway dysbiosis was observed, with lower relative abundance in the bronchoalveolar lavage fluid of several bacterial taxa compared with healthy individuals, and a concomitant disease-specific over-representation of *Pseudonocardia* species, correlating with local and systemic autoimmune and inflammatory changes, which could be associated with RA initiation⁵⁸. In a study of intestinal microbiota, *Prevotella copri* was the dominant species in a subpopulation of patients in the preclinical stages of RA⁵⁹. Intestinal expansion of *Prevotella* species in association with preclinical RA suggests that intestinal dysbiosis is involved in the development of RA⁶⁰.

Microaspiration is a risk factor for acute exacerbation, as demonstrated by the detection of higher concentrations of pepsin (a marker of gastric-content aspiration) in bronchoalveolar lavage samples from patients with AE-IPF than in samples from individuals with stable IPF⁶¹, and it might have a relationship to the development of acute exacerbation in all ILDs⁶². In a post hoc analysis of three clinical trials involving patients with IPF, none of the patients who developed acute exacerbation received anti-acid treatment⁶³. Furthermore, in a cohort of individuals with SSC-associated ILD, reflux was associated with a decline in pulmonary function⁶⁴. Although a relationship between reflux and AE-SSc-ILD has not yet been demonstrated, gastroesophageal reflux disease affects $\geq 70\%$ of patients with SSC, suggesting that microaspiration has a role in this form of AE-RD-ILD⁶⁵.

Another line of evidence indicates that AE-IPF might result from exposure to ambient air pollution. In a retrospective study of a large, well-defined cohort of patients with IPF, the mean and maximum exposures to ozone and nitrogen dioxide were associated with the risk of AE-IPF⁶⁶. The frequency of exposure to pollution

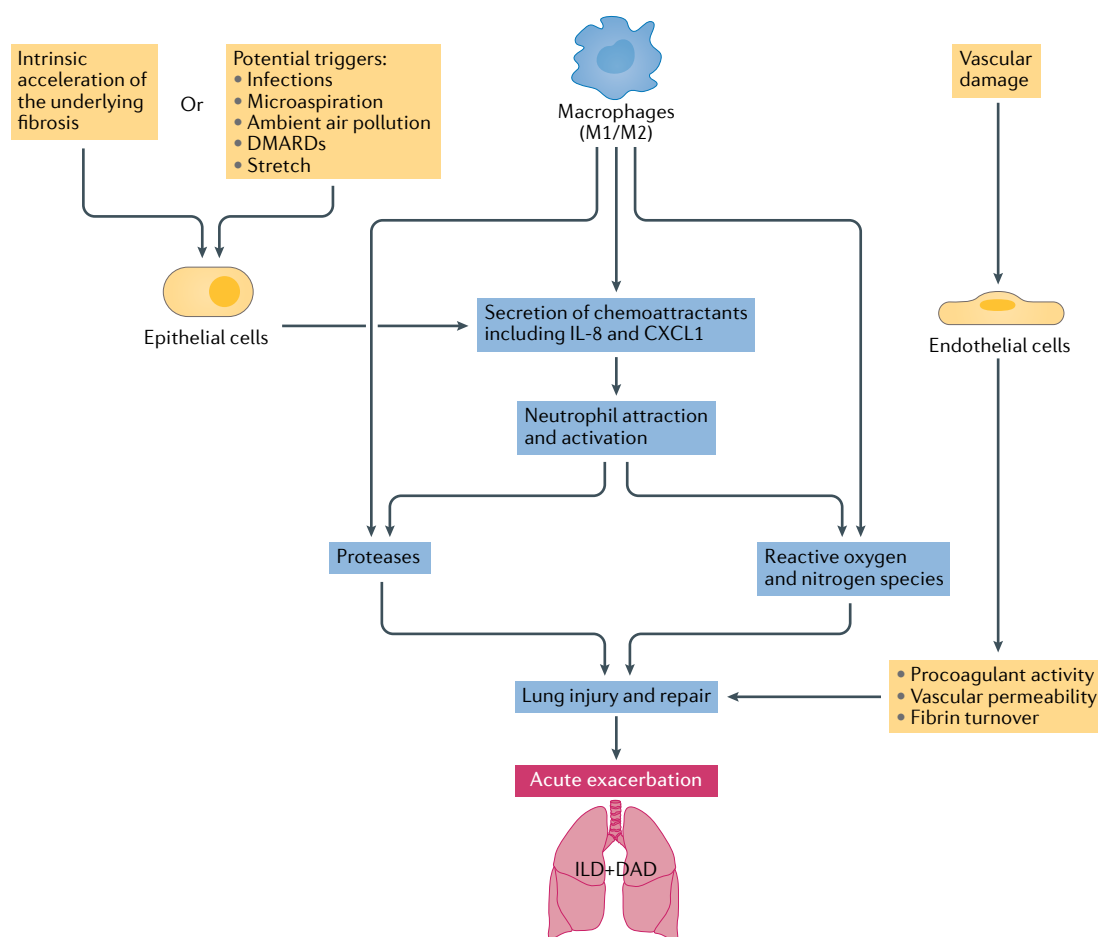


Fig. 1 | Pathogenesis of acute exacerbation of interstitial lung disease in rheumatic disease. During acute exacerbation of interstitial lung disease (ILD) in rheumatic disease, which is associated with a variety of risk factors and potential triggers, lung inflammation results from upregulation of macrophage, epithelial and endothelial activation pathways, leading to secretion of various chemoattractant molecules, including IL-8 and CXCL1, resulting in neutrophil chemoattraction and activation. Subsequently, activated M1 macrophages and neutrophils release various pro-inflammatory cytokines, reactive oxygen and nitrogen species and proteolytic enzymes, leading to lung damage, capillary–alveolar permeability and oxygen deficiency. M2-phenotype macrophages releasing anti-inflammatory molecules have also been detected, and have a pivotal role in repair of lung damage, and in counteracting M1 macrophage function. DAD, diffuse alveolar damage.

levels exceeding published air-quality standards was also related to the risk of AE–IPF. Although there is no evidence yet of such an association in AE–RD–ILD, a similar relationship seems likely.

Mechanical stress might be another contributing factor for the occurrence of AE–ILD. Surgery can lead to acute exacerbation, presumably as a result of mechanical stress to the lungs⁶². Notably, however, evidence suggests that the frequency of AE–ILD following pulmonary surgery is similar to that after non-pulmonary surgery⁶⁷. Nevertheless, prolonged mechanical ventilation, high tidal volume and high intraoperative concentration of supplemental oxygen have been proposed as potential causes of AE–ILD⁶⁸. Other factors that potentially increase the risk of AE–ILD following surgery include the presence of typical histological honeycombing, greater extent of radiological fibrosis, production of the mucin-like glycoprotein Krebs von den Lungen-6 (KL-6), the extent of surgical resection (lobe versus wedge resection), high intraoperative fluid balance and preoperative elevation of concentrations of C-reactive

protein³⁸. The risk of AE–ILD might also be higher in patients with poor lung function undergoing multiple bronchoalveolar lavage procedures than in those undergoing single lavage⁶⁹.

DMARDs are commonly used in the treatment of RA⁷⁰. Acute pneumonitis, although rare, is the most common lung complication related to the use of the conventional synthetic DMARD methotrexate: it usually occurs soon after methotrexate initiation, and its onset is dose independent^{30,71}. In a narrative review of the role of methotrexate in lung disease in patients with RA⁷², it was suggested that methotrexate-related pneumonitis is not associated with the development of RA–ILD. Results also indicate that methotrexate use is not associated with the occurrence of AE–RA–ILD⁷³. Leflunomide, an alternative to methotrexate, has been linked to AE–RA–ILD development and/or worsening⁷⁴, suggesting that this drug is a potential trigger of AE–RA–ILD. Notably, biologic DMARDs (including inhibitors of TNF, IL-1 and IL-6, anti-CD20 monoclonal antibody and selective T-cell co-stimulation modulators) and targeted synthetic

DMARDs can cause new-onset ILD or exacerbation of existing ILD in patients with RA⁷⁵. Differentiating between drug-induced acute ILD and AE-RD-ILD is difficult, and often relies on assessment of the temporal relationship between treatment initiation and the development of symptoms, and on improvement upon drug discontinuation^{76,77}.

Clinical, imaging and pathology findings

AE-RD-ILD can develop in different scenarios. It can be the first clinical manifestation of a rheumatic disease, prior to recognition of pulmonary and systemic features, suggesting the need for inclusion of rheumatic disease in the differential diagnosis of acute respiratory deterioration. AE-RD-ILD can also develop in the context of a well-characterized rheumatic disease, in which the underlying ILD remains unidentified. Another possibility is that both ILD and extrapulmonary involvement can be previously recognized, so that acute exacerbation occurs in the course of an established ILD and in the context of a rheumatic disease^{78,79}.

When acute exacerbation is the initial manifestation of a rheumatic disease, differential diagnosis between AE-RD-ILD and acute exacerbation secondary to IIP can be very challenging in the absence of extrapulmonary manifestations of the rheumatic disease. In around 10% of patients with RA-ILD, and in other rheumatic diseases such as dermatomyositis, antisynthetase syndrome and SSc, the systemic manifestations of disease can appear late in the clinical history or remain mild or underestimated^{78–83}. In some instances of antisynthetase syndrome that are positive for the presence of anti-PL-7 and anti-PL-12 antibodies, ILD is the only clinical manifestation that is observed⁸¹. In these situations, a differential diagnosis between idiopathic and secondary ILD can be difficult, and close collaboration between rheumatologist and pulmonologist is recommended, to correctly address patient management. Furthermore, antineutrophil cytoplasmic antibody (ANCA)-associated vasculitides, such as microscopic polyangiitis, can also be associated with ILD, and can exhibit acute exacerbation, further complicating diagnostic differentiation from AE-RD-ILD⁴².

The heterogeneity of lung involvement in rheumatic diseases in stable states and the complexity of clinical features of rheumatic diseases make diagnosis of acute exacerbation difficult in many cases. In addition, the multitude of systemic manifestations, the presence of autoantibodies and other autoimmune features, the risk of infection (including opportunistic infection) and the varied patterns of lung disease all complicate the management of these patients. Among rheumatic diseases, RA-ILD shows many similarities with IPF. In particular, in the presence of a UIP pattern, differential diagnosis between RA-ILD and IPF can be challenging when ILD precedes joint involvement. Autoantibodies, namely rheumatoid factor and anti-citrullinated protein antibodies (ACPAs), can be absent or only appear late in the course of disease, further complicating the RA-ILD diagnosis. However, particular features of AE-RA-ILD can help to distinguish it from acute exacerbation of ILD in other rheumatic disease and in IIP (including IPF).

Detection of ACPAs is very specific to RA. The role of autoimmunity and inflammation in RA-ILD pathogenesis and progression is unknown, but results have shown that, among patients with RA, the risks of ILD and acute exacerbation are positively associated with the presence of high-titre ACPAs and persistent active joint disease^{84,85}. Despite the unknown roles of ACPAs, rheumatoid factor and antinuclear antibodies (ANAs) in AE-RA-ILD, and more generally in AE-RD-ILD, their detection can help in the differential diagnosis between idiopathic and rheumatic disease-related AE-ILD. The role of DMARDs, both conventional synthetic and biologic, as possible triggers of AE-RA-ILD, is controversial and still under debate. In patients with RD-ILD, differential diagnosis between drug-induced pneumonia and acute exacerbation is not always feasible. The possible role of DMARDs in acute exacerbation also suggests the involvement of cytokines (in particular TNF) in the pathogenesis of rheumatic disease, RD-ILD and AE-RD-ILD⁸⁶. The risk of infection is higher in patients with RD-ILD than in patients with RD but without ILD. Infection by opportunistic pathogens can be difficult to detect, as it can manifest over days to weeks, with CT features that are difficult to differentiate from those associated with lung injury and ILD. The selective action of biologic DMARDs on some cytokines can favour specific pathogens, such as *Mycobacterium tuberculosis*, non-tuberculous mycobacteria, *Pneumocystis jirovecii*, fungal pathogens and cytomegalovirus⁸⁷.

In patients with AE-ILD, to determine whether rheumatic disease is involved, investigation of medical history should focus on family history of rheumatic disease, smoking habits, toxic exposure, prescribed drugs and signs and symptoms related to rheumatic disease, including sicca syndrome, inflammatory joint pain or stiffness, rashes, skeletal-muscle symptoms (such as proximal weakness and myalgia) and Raynaud phenomenon (especially recent onset)⁸⁸. Serological evaluation should also be performed for ANA, extractable nuclear antigen antibody, rheumatoid factor, ACPA, ANCA, myositis-specific antibodies and creatine kinase. Most patients with AE-RD-ILD experience dyspnoea and severe hypoxaemia, and fever, coughing and flu-like symptoms can also be noted.

Physical findings in patients with AE-RD-ILD include respiratory signs such as tachypnoea, cyanosis, digital clubbing and bilateral inspiratory crackles. Extrapulmonary findings depend on the specific rheumatic disease, and include synovitis, cutaneous signs (such as mechanic's hands, Gottron's papules and malar rash) and proximal muscle weakness⁸⁸. Great heterogeneity exists in the degree of lung functional impairment, time from RD-ILD diagnosis, need for supplemental oxygen, use of steroids or immunosuppressive drugs prior to the acute event and the degree of hypoxaemia at presentation⁸⁹.

Many patients with AE-RD-ILD have severe respiratory failure, warranting mechanical ventilation⁹⁰. On high-resolution CT (HRCT), the characteristic findings of AE-RD-ILD include new-onset ground-glass opacities and/or airspace consolidations superimposed on an underlying ILD^{19,37}. In IPF, the three main

Tachypnoea

Abnormally rapid breathing.

Cyanosis

A physical sign causing bluish discolouration of the skin and mucous membranes, caused by deoxygenated or reduced haemoglobin in the blood.

Ground-glass opacities

An area of increased attenuation in the lung on CT, with preserved bronchial and vascular markings, which is a non-specific sign with a wide aetiology, including infection, chronic interstitial disease and acute alveolar disease.

Hyaline membrane

Eosinophilic and proteinaceous material (derived from fibrin degradation) covering alveoli.

types of HRCT pattern that are seen are peripheral, multifocal and diffuse ground-glass opacities. Multifocal and diffuse types are associated with a histological pattern of DAD, and are associated with greater mortality and less response to therapy than peripheral opacities, likely reflecting disease extent rather than distinct pathogenic processes⁹¹ (FIG. 2). It remains to be seen whether similar patterns occur and have the same prognostic significance in AE–RD–ILD.

Lung histopathology in AE–RD–ILD is characterized by a combination of the underlying ILD pattern superimposed with acute lung injury features such as DAD (FIG. 3) and/or organizing pneumonia²². In the early phase, the pulmonary acute injury shows interstitial oedema and hyaline membranes. Moreover, type II pneumocyte hyperplasia and fibroblast foci, as well as squamous metaplasia and honeycombing with and without hyaline membranes, have been observed in tissues from both biopsy and autopsy procedures²⁷.

AE–ILD shows a combination of an underlying fibrotic interstitial pneumonia and a superimposed form of acute lung injury, either DAD or organizing pneumonia. The pattern of DAD is also observed in patients with ARDS, which is associated with various diagnoses, including sepsis, pneumonia, aspiration and trauma^{92,93}. Survivors of both ARDS and AE–RD–ILD usually have a good long-term prognosis, but can also experience relapses or progressive functional deterioration².

Diagnosis

Diagnosis of AE–RD–ILD relies on clinical suspicion, relevant symptom worsening and identification of potential individual or environmental triggers such as infection, microaspiration, gastro-oesophageal reflux, toxic drugs, thoracic or extrathoracic surgery, bronchoscopy or air pollution. Cardiac failure and fluid overload and diagnosis of competing diseases such as pulmonary embolism should be excluded (FIG. 4). Clinical investigations should include HRCT followed by contrast CT (if needed) to confirm or exclude pulmonary embolism. The order of CT imaging is important, because intravenous contrast enhancement can disrupt the interpretation of HRCT, resulting in unpredictable attenuation of the background lung parenchyma, which complicates evaluation of whether the lungs have abnormally high attenuation⁹⁴.

In addition to findings such as new ground-glass opacities and/or airspace consolidations on top of a fibrotic ILD pattern (most often UIP), HRCT can also rule out pneumothorax and pleural effusion as causes of respiratory deterioration. Previous HRCT results in patients with AE–RD–ILD might demonstrate a radiological pattern of UIP, or of NSIP or organizing pneumonia, or they could identify other, less specific fibrotic features. Although the presence of a UIP pattern is associated with a high risk of AE–RD–ILD, the other patterns should not be ignored, as they can help

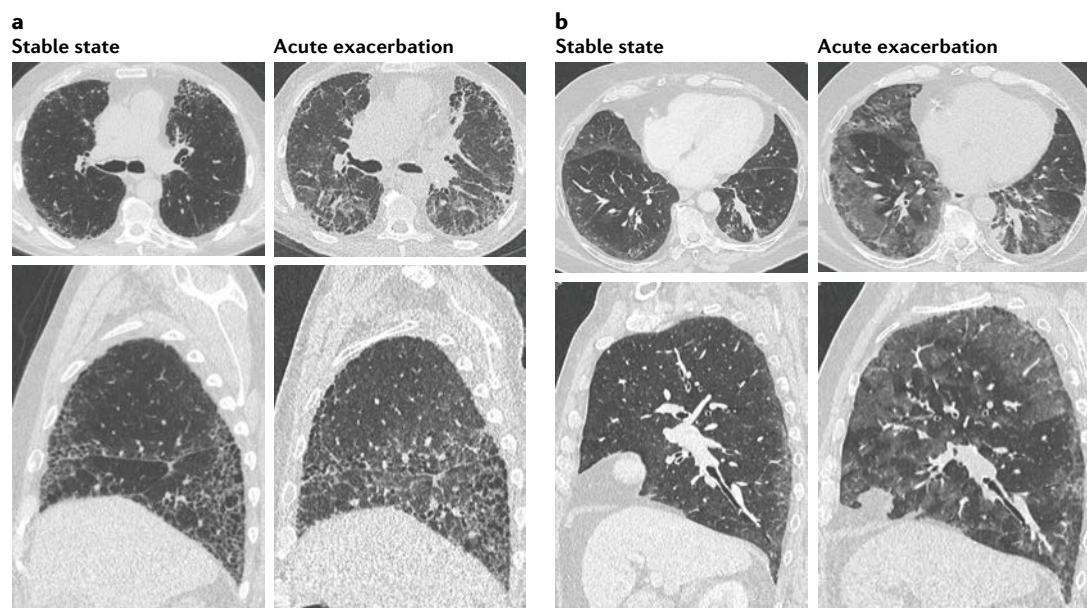


Fig. 2 | High-resolution chest CT in stable state and acute exacerbation of interstitial lung disease in rheumatic disease. a,b | Interstitial lung disease (ILD) with usual interstitial pneumonia (UIP) pattern in a 59-year-old patient with rheumatoid arthritis (RA). **a** | Baseline high-resolution CT (HRCT) in the stable state shows a typical UIP pattern with subpleural reticulation layered with propeller-blade distribution across lung zones, traction bronchiolectasis–bronchiectasis and further signs of distortion with volume loss. **b** | After 14 months, the patient experienced acute shortness of breath leading to respiratory failure, showing substantial morphological changes on HRCT: ground-glass opacities with extensive patchy distribution, increase in subpleural reticulation and of severity in traction bronchiectasis, and signs of volume loss. **c,d** | ILD with non-specific interstitial pneumonia (NSIP) pattern in a 53-year-old patient with systemic sclerosis. **c** | Baseline HRCT in the stable state shows NSIP pattern with ground-glass opacities with homogeneous distribution and sparing of subpleural parenchyma. **d** | After 3 months, the patient experienced acute shortness of breath leading to respiratory failure, showing substantial morphological changes on HRCT: increased extent of ground-glass opacities with diffuse involvement of all the lung parenchyma, with some areas of patchy sparing, without apparent signs of substantial volume loss. Images courtesy of Nicola Sverzellati and Mario Silva.

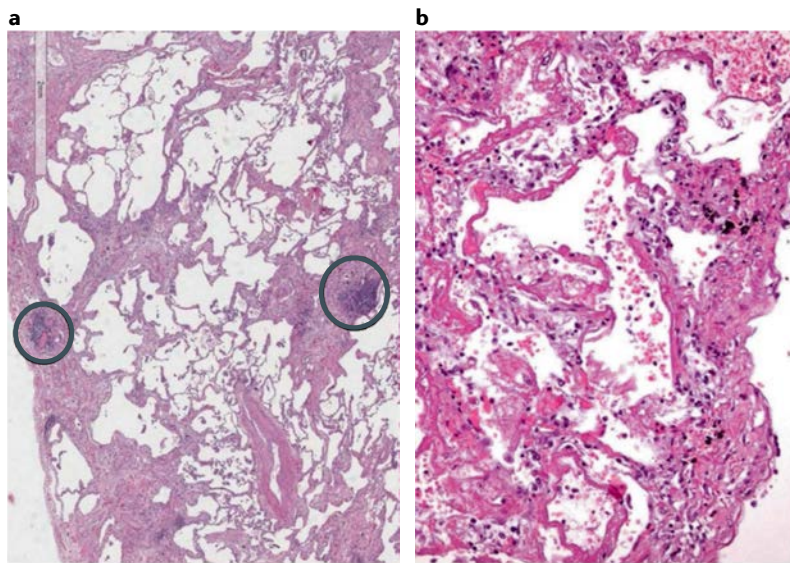


Fig. 3 | Pathological examination of patients with acute exacerbation of interstitial lung disease in rheumatic disease. a | Histological examination following video-assisted thoracoscopic surgery showing a usual interstitial pneumonia (UIP)-like pattern, characterized by heterogeneous spatial and temporal fibrosis, occasional fibroblastic foci and lymphoid follicular hyperplasia (circles) involving both parenchyma and pleura in a patient affected by acute exacerbation of interstitial lung disease associated with rheumatoid arthritis. Haematoxylin and eosin staining, 40× magnification, scale bar = 2 mm. **b** | Section of lung tissue from an autopsy of a patient who died following acute respiratory distress at the onset of an autoimmune disease (characterized by identification of anti-Jo1 antibody), showing an acute pattern, characterized by diffuse alveolar damage, with evidence of endoalveolar hyaline membranes, fibrin and debris, lymphocytes and polymorphonuclear cell infiltrates. Haematoxylin and eosin staining, 200× magnification. Images courtesy of Francesca Bono.

the clinician to identify the underlying lung disease, thereby raising the suspicion of AE-RD-ILD (TABLE 2). Specific diagnostic criteria have not been published for AE-RD-ILD; the clinical criteria indicated in TABLE 2 are presented here as a proposal, and have been derived by comparison with those that are available for AE-IPF. As part of the diagnostic work-up, electrocardiogram and echocardiography should be added when a concomitant cardiac disease is suspected.

In routine blood testing of patients with AE-ILD, concentrations of inflammatory biomarkers such as C-reactive protein and lactate dehydrogenase, erythrocyte sedimentation rate and leukocyte counts are generally elevated³⁷. In a study of RA-ILD, changes in KL-6 concentrations at RA-ILD diagnosis were associated with acute exacerbation⁹⁵, suggesting that KL-6, a blood biomarker of ILD, might have potential as a prognostic marker for AE-RD-ILD.

For diagnosis of AE-RD-ILD, blood, urine and sputum should be collected for culture; however, bronchoscopy for microbiological assays is controversial. In patients with AE-IPF, bronchoalveolar lavage fluid typically shows neutrophilia^{23,57} and, more rarely, lymphocytosis⁹⁶. Although RD-ILD and IPF are different diseases in terms of triggers and possibly disease severity, bronchoalveolar lavage has also been considered a useful tool in the differential diagnosis of AE-RD-ILD, in which an immunosuppressive state usually occurs, and therefore a precise microbiological diagnosis is needed.

Notably, however, in a study of 225 patients with ILD and with acute respiratory worsening, 106 patients (37 with RD-ILD) underwent bronchoscopy to exclude alveolar haemorrhage or infection (according to the 2007 definition of AE-IPF), and 16 (13%) had positive bronchoscopy findings, but these findings only resulted in a change in the initial management in 4 (3%) of the patients⁹⁷. Concurrently, many patients required new or prolonged intensive-care unit and ventilator treatment as a consequence of bronchoscopy. Thus, bronchoalveolar lavage in non-intubated patients with a high oxygen requirement poses a risk of worsening hypoxaemia, with a possible negative outcome for the patients, and therefore should be carefully considered and performed only in a limited number of instances of AE-RD-ILD. Similarly, lung pathology obtained either by bronchoscopy or surgical lung biopsy should be carefully considered and avoided as much as possible because it has a limited likelihood of providing a result that would change the diagnosis or management, and the mortality risk is considerably higher for patients with suspected RD-ILD and IPF than for other ILD diagnoses and non-elective procedures⁹⁸.

In the differential diagnosis of patients with suspected AE-RD-ILD, the possibility of infection-induced or drug-induced ILD should also be considered, because these complications are particularly frequent in patients with rheumatic disease, who can receive DMARDs, such as methotrexate, leflunomide and biological agents (including those that target TNF and IL-6) for rheumatic symptoms, which may cause AE-RD-ILD.

Prognosis

Limited epidemiological data exist for AE-RD-ILD⁹⁹, but prognostically it is associated with an in-hospital mortality of 50–100%, with >90% mortality in patients requiring ventilatory assistance^{19,37}. Although AE-RD-ILD is generally associated with better overall survival than AE-IPF^{21,100}, results from one study showed no significant difference between RD-ILD and IPF in the 3-month survival rate after acute exacerbation, even though prognosis tended to be worse in AE-RD-ILD¹⁰¹. Although the UIP pattern is also a risk factor for AE-RD-ILD occurrence, its prognostic role for long-term survival is inconsistent^{102,103}.

Patients with exacerbation of a progressive fibrosing phenotype, including patients with progressive RA-ILD and CTD-ILD, have worse prognoses and higher mortality than patients with ILDs without a fibrotic phenotype^{16,104}. Likewise, in patients with IPF, low lung function at baseline, compromised oxygenation and extension of the radiological findings on HRCT are linked to an increased risk of mortality in RD-ILD^{7,16,37}. Other prognostic factors of AE-RD-ILD are the period of time between ILD diagnosis and acute exacerbation occurrence, and a high neutrophil count in peripheral blood¹⁰¹.

In-hospital mortality following AE-RD-ILD varies widely between studies. In one study involving 93 patients with RD-ILD in South Korea, acute exacerbation was reported in four individuals, all of whom died³⁷. Similarly, in a group of 83 patients with RD-ILD in Japan, six developed acute exacerbation and five of

GAP

A clinical prediction model using commonly measured clinical (gender and age) and physiological (lung function) variables to predict mortality in patients with idiopathic pulmonary fibrosis.

them died¹⁹. By contrast, in a retrospective study of 155 patients with RD-ILD in Japan, only one death occurred among 10 individuals within 30 days of diagnosis of AE-RD-ILD¹⁰⁵. Among 105 consecutive patients with RD-ILD at a single centre in India, 15 developed AE-RD-ILD and five died¹⁰⁶. In a large, retrospective, case-control study from China, among 665 patients with idiopathic inflammatory myopathy, AE-RD-ILD occurred in 64, and its associated short-term mortality was 39%¹⁰⁷. Myositis disease activity at admission and the occurrence of bacterial infection were both associated with poor outcome, but the combined use of steroids and DMARDs resulted in reduction of short-term mortality. In another cohort of 60 patients with idiopathic inflammatory myopathies and AE-RD-ILD (26 of whom died during follow-up), the Gender-Age-lung Physiology (GAP) model enabled prediction of long-term prognosis¹⁰⁸. AE-RD-ILD has also been investigated in a prospective study in which, over 24 months, nine acute exacerbations were observed in 78 patients with RD-ILD, with five deaths²⁸. Among the four survivors of AE-RD-ILD, lung function recovered fully in three, but that of the fourth remained impaired²⁸.

A prospective study of the Danish population has demonstrated that acute exacerbation also affects the survival of patients with RA-ILD⁷⁸. In a comparison of 679 patients with RA-ILD and 11,722 individuals with RA but without ILD, a very high hazard ratio was identified for death within the first 30 days after ILD diagnosis, particularly among men and among the 65–74-years age group. The high mortality in the RA-ILD population was explained by the occurrence of acute exacerbation of previously undiagnosed ILD. In a retrospective study of 165 patients with RA-ILD, the UIP pattern on HRCT was associated with both AE-ILD occurrence and with mortality⁷³. The absence of methotrexate treatment was also associated with a poor prognosis.

Finally, patients surviving acute exacerbation have impaired quality of life and reduced long-term survival because of the resulting lung-function impairment and worsening of respiratory symptoms (mainly dyspnoea)¹⁰⁹.

Management

Current therapeutic strategies. The therapeutic approach for patients with AE-RD-ILD is mainly based on the management of AE-IPF. In the absence of evidence-based treatment, this approach involves supportive care and the use of drugs without proven benefits²⁷. Thus, the IPF guidelines weakly recommend the use of systemic steroids in patients with AE-IPF, with no recommendation on the most appropriate type, dose or duration of steroids to be used^{27,33}. However, results from a retrospective study of the treatment of patients with AE-IPF identified no evidence of improvement of outcomes with the use of glucocorticoids¹¹⁰. The majority of patients are already undergoing treatment with steroids, and/or conventional and/or biologic DMARDs when they are admitted for AE-RD-ILD¹¹¹. Withdrawal of DMARDs is often the first step of the therapeutic strategy for AE-RA-ILD. High-dose steroids, intravenous cyclophosphamide or rituximab have been proposed for patients with AE-RA-ILD, but evidence in support of these strategies is limited.

Although exclusion of an infectious trigger is not required to correctly diagnose AE-RD-ILD, detection of possible pathogens remains important to inform the appropriate choice of antibiotic treatment²⁷. Because of the difficulties in differentiation of AE-RD-ILD from bronchopulmonary infection occurring in the course of a rheumatic disease, and the potential overlap between the two conditions, broad-spectrum antibiotics are often administered in patients with acute worsening of dyspnoea during both AE-RD-ILD and bronchopulmonary infection occurring in the course of a rheumatic disease. In a randomized controlled trial evaluating interventions for AE-IPF, the use of procalcitonin as a biomarker of infection showed that procalcitonin-guided antibiotic treatment and clinician-determined antibiotic treatment were associated with similar mortality¹¹², suggesting that there are no helpful biomarkers to guide initiation of antibiotic treatment in AE-ILDs.

A number of treatments, including cyclosporine, rituximab combined with plasma exchange and

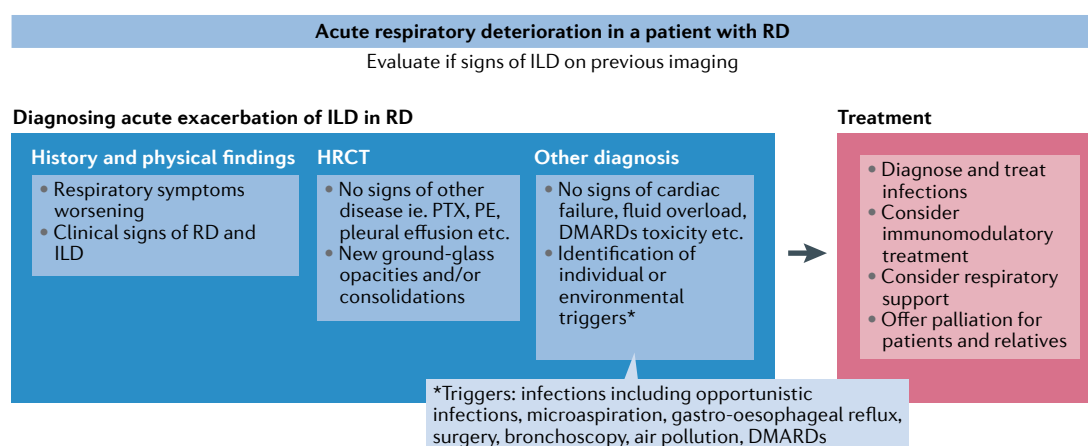


Fig. 4 | **Diagnosis and treatment of acute exacerbation of interstitial lung disease in rheumatic disease.** Acute exacerbation of interstitial lung disease (ILD) in patients with rheumatic disease (RD) is a clinical diagnosis based on worsening of respiratory symptoms in a patient with known or newly diagnosed RD, worsening or new radiological features, and the exclusion of other diseases. HRCT, high-resolution CT; PE, pulmonary embolism; PTX, pneumothorax.

intravenous immunoglobulin, oral tacrolimus and intravenous thrombomodulin, have no benefits in patients with AE–RD–ILD^{113–117}. In a retrospective study of 17 patients with AE–RA–ILD who were all treated with steroids, additional treatments with tacrolimus, cyclosporine and cyclophosphamide were used in three, four and five patients, respectively¹¹⁸. All of these treatment combinations resulted in improvement of pulmonary function and CT imaging, and the cyclophosphamide combination was particularly beneficial in terms of survival. Two patients in the cyclosporine group and one patient treated with steroids alone died from acute-exacerbation relapse. In another retrospective study, among 155 patients with RD–ILD, 10 developed AE–RD–ILD, including six patients with RA; all patients were treated with antimicrobial agents and high-dose steroids; cyclophosphamide or tacrolimus were added only when patients responded poorly to steroids. The median survival time after onset of acute exacerbation was significantly longer in patients who responded well to steroids alone than in those who responded poorly and therefore received secondary medications¹⁰⁵. The effectiveness and safety of cyclophosphamide in AE–RA–ILD has been investigated in a large, retrospective Japanese study, in which the addition of intravenous cyclophosphamide to steroid treatment was associated with a higher rate of adverse effects and no survival advantage compared with steroids alone¹¹⁹.

Medications for treatment of RA, such as inhibitors of TNF and IL-6, are associated with both progression of pre-existing ILD and the occurrence of acute exacerbation^{120–124}. Although little evidence is available, the British Society of Rheumatology has previously advised against the use of TNF inhibitors in patients with pre-existing ILD and suggested that their withdrawal should be considered in patients with worsening or new features of ILD¹²⁵. In their 2019 guidelines, ILD was not considered an absolute contraindication for TNF inhibitors, but close monitoring was suggested for patients with RA–ILD who are treated with biologic DMARDs¹²⁶. Similarly, controversies exist regarding methotrexate. In an investigation of the clinical features and risk factors of AE–ILD and mortality in RA–ILD, results suggested that methotrexate has a protective effect against AE–RA–ILD⁷³. In 2021, the ACR conditionally recommended the use of methotrexate in patients with RA–ILD, because of its efficacy and the lack of alternatives with long-term safety profiles⁷¹. However, patients with pre-existing lung disease should be informed of the risk of methotrexate pneumonitis prior to initiating this treatment.

Although most patients with AE–IPF develop acute respiratory failure, current treatment guidelines suggest that these patients should not receive mechanical ventilation, because of the lack of effectiveness of this intervention³³. However, results suggest that improvements might have occurred in the overall survival of some patients, possibly because of changes in factors such as diagnostic criteria, study design, baseline clinical risk and patient management⁹⁰. Possible predictive factors for mortality associated with mechanical ventilation

have been investigated, but further studies are required to facilitate selection of the appropriate subgroup of patients to be treated¹²⁷. Currently, the outcome after mechanical ventilatory support is very poor. Because the vast majority of patients with AE–ILD, including those with AE–RD–ILD, will die in the intensive-care unit or during the follow-up period⁸⁹, a decision not to intubate is generally taken, especially when infection and potential confusing factors have been ruled out. However, a small subset of patients can be discharged from the intensive-care unit, providing an opportunity to consider lung transplantation if eligible. Little experience is available regarding non-invasive mechanical ventilation using spontaneous-timed mode, or continuous positive airway pressure (CPAP) mode, which could be useful in selected patients⁹⁰.

End-of-life palliation in AE–RD–ILD. Studies of end-of-life care in patients with AE–RD–ILD are currently unavailable. However, palliation seems to be an important goal for these patients, considering that most of them show an unfavourable outcome when hospitalized, and generally are not sedated and intubated, so that they and their relatives are exposed to dramatic and painful symptoms and experiences¹²⁸. Palliation of dyspnoea and anxiety is generally achieved with opioids¹²⁹ and benzodiazepines¹³⁰. Respiratory depression is often wrongly feared as a major clinical problem associated with such treatment; nevertheless, an open discussion with patients and relatives is mandatory to explain the aims of palliation^{131,132}. Cough management, which is also important, can be achieved through the use of various types of drugs, including opioids¹³³. Although data relating to non-invasive mechanical ventilation using spontaneous-timed mode or CPAP mode are limited, this intervention might be useful to palliate shortness of breath⁹⁰.

Conclusions

AE–RD–ILD is a life-threatening event with high mortality during or immediately after its occurrence and with an extremely low 1-year survival rate. The current definition of AE–IPF considers both idiopathic and triggered acute exacerbation, although whether a triggered AE–RD–ILD has a worse prognosis than an idiopathic AE–RD–ILD remains unconfirmed. The clinical presentation associated with acute exacerbation is similar in rheumatic disease and in IPF. Nevertheless, compared with AE–IPF, AE–RD–ILD is probably less common, and is associated with lower mortality. However, knowledge relating to AE–RD–ILD remains incomplete, particularly regarding aetiology, pathogenesis and management. Signs of AE–RD–ILD must be detected early, and patients who have a high risk of developing AE–ILD should be identified, possibly by measuring specific biomarkers that can identify predisposed patients before the appearance of symptoms and HRCT features. Considering the lack of evidence-based therapy options, more studies in this field are urgently needed to determine effective treatments.

Published online 7 December 2021

1. Wallis, A. & Spinks, K. The diagnosis and management of interstitial lung diseases. *Br. Med. J.* **350**, h2072–h2072 (2015).
2. Travis, W. D. et al. An official American Thoracic Society/European Respiratory Society statement: update of the international multidisciplinary classification of the idiopathic interstitial pneumonias. *Am. J. Respir. Crit. Care Med.* **188**, 733–748 (2013).
3. Richeldi, L., Collard, H. R. & Jones, M. G. Idiopathic pulmonary fibrosis. *Lancet* **389**, 1941–1952 (2017).
4. Wells, A. U. & Denton, C. P. Interstitial lung disease in connective tissue disease — mechanisms and management. *Nat. Rev. Rheumatol.* **10**, 728–739 (2014).
5. Kim, E. J. et al. Usual interstitial pneumonia in rheumatoid arthritis-associated interstitial lung disease. *Eur. Respir. J.* **35**, 1322–1328 (2010).
6. Tsuchiya, Y. et al. Lung diseases directly associated with rheumatoid arthritis and their relationship to outcome. *Eur. Respir. J.* **37**, 1411–1417 (2011).
7. Park, J. H. et al. Prognosis of fibrotic interstitial pneumonia: idiopathic versus collagen vascular disease-related subtypes. *Am. J. Respir. Crit. Care Med.* **175**, 705–711 (2007).
8. Bours, D. et al. Histopathologic subsets of fibrosing alveolitis in patients with systemic sclerosis and their relationship to outcome. *Am. J. Respir. Crit. Care Med.* **165**, 1581–1586 (2002).
9. Douglas, W. W. et al. Polymyositis-dermatomyositis-associated interstitial lung disease. *Am. J. Respir. Crit. Care Med.* **164**, 1182–1185 (2001).
10. Luppi, F. et al. Lung complications of Sjogren syndrome. *Eur. Respir. Rev.* **29**, 200021 (2020).
11. Cottin, V. Idiopathic interstitial pneumonia with connective tissue diseases features: a review. *Respirology* **21**, 245–258 (2016).
12. Ley, B., Collard, H. R. & King, T. E. Clinical course and prediction of survival in idiopathic pulmonary fibrosis. *Am. J. Respir. Crit. Care Med.* **183**, 431–440 (2011).
13. Song, J. W., Hong, S.-B., Lim, C.-M., Koh, Y. & Kim, D. S. Acute exacerbation of idiopathic pulmonary fibrosis: incidence, risk factors and outcome. *Eur. Respir. J.* **37**, 356–363 (2011).
14. Kreuter, M. et al. Acute exacerbation of idiopathic pulmonary fibrosis: international survey and call for harmonisation. *Eur. Respir. J.* **55**, 1901760 (2020).
15. Arai, T. et al. Heterogeneity of incidence and outcome of acute exacerbation in idiopathic interstitial pneumonia. *Respirology* **21**, 1431–1437 (2016).
16. Moua, T. et al. Patients with fibrotic interstitial lung disease hospitalized for acute respiratory worsening. *Chest* **149**, 1205–1214 (2016).
17. Salonen, J., Purokivi, M., Bloig, R. & Kaarteenaho, R. Prognosis and causes of death of patients with acute exacerbation of fibrosing interstitial lung diseases. *BMJ Open Respir. Res.* **7**, e000563 (2020).
18. Suzuki, A. et al. Acute exacerbations of fibrotic interstitial lung diseases. *Respirology* **25**, 525–534 (2020).
19. Suda, T. et al. Acute exacerbation of interstitial pneumonia associated with collagen vascular diseases. *Respir. Med.* **103**, 846–853 (2009).
20. Kondoh, Y. et al. Acute exacerbation of interstitial pneumonia following surgical lung biopsy. *Respir. Med.* **100**, 1753–1759 (2006).
21. Miyashita, K. et al. Prognosis after acute exacerbation in patients with interstitial lung disease other than idiopathic pulmonary fibrosis. *Clin. Respir. J.* **15**, 336–344 (2021).
22. Churg, A., Muller, N. L., Silva, C. I. S. & Wright, J. L. Acute exacerbation (acute lung injury of unknown cause) in UIP and other forms of fibrotic interstitial pneumonias. *Am. J. Surg. Pathol.* **31**, 277–284 (2007).
23. Kondoh, Y. et al. Acute exacerbation in idiopathic pulmonary fibrosis. *Chest* **103**, 1808–1812 (1993).
24. Collard, H. R. et al. Acute exacerbations of idiopathic pulmonary fibrosis. *Am. J. Respir. Crit. Care Med.* **176**, 636–643 (2007).
25. Spagnolo, P. & Wuyts, W. Acute exacerbations of interstitial lung disease: lessons from idiopathic pulmonary fibrosis. *Curr. Opin. Pulm. Med.* **23**, 411–417 (2017).
26. Johansson, K. A. & Collard, H. R. Acute exacerbation of idiopathic pulmonary fibrosis: a proposal. *Curr. Respir. Care Rep.* **2**, 233–240 (2013).
27. Collard, H. R. et al. Acute exacerbation of idiopathic pulmonary fibrosis. An international working group report. *Am. J. Respir. Crit. Care Med.* **194**, 265–275 (2016).
28. Manfredi, A. et al. Acute exacerbation of interstitial lung diseases secondary to systemic rheumatic diseases: a prospective study and review of the literature. *J. Thorac. Dis.* **11**, 1621–1628 (2019).
29. Ryerson, C. J. & Collard, H. R. Acute exacerbations complicating interstitial lung disease. *Curr. Opin. Pulm. Med.* **20**, 436–441 (2014).
30. Roubille, C. & Haraoui, B. Interstitial lung diseases induced or exacerbated by DMARDs and biologic agents in rheumatoid arthritis: a systematic literature review. *Semin. Arthritis Rheum.* **43**, 613–626 (2014).
31. Singh, J. A. et al. Risk of serious infection in biological treatment of patients with rheumatoid arthritis: a systematic review and meta-analysis. *Lancet* **386**, 258–265 (2015).
32. Kreuter, M. et al. Exploring clinical and epidemiological characteristics of interstitial lung diseases: rationale, aims, and design of a nationwide prospective registry — the EXCITING-ILD Registry. *Biomed. Res. Int.* **2015**, 1–9 (2015).
33. Raghu, G. et al. An Official ATS/ERS/JRS/ALAT Statement: Idiopathic Pulmonary Fibrosis: Evidence-based Guidelines for Diagnosis and Management. *Am. J. Respir. Crit. Care Med.* **183**, 788–824 (2011).
34. Jegannathan, N. & Sathananthan, M. Connective tissue disease-related interstitial lung disease: prevalence, patterns, predictors, prognosis, and treatment. *Lung* **198**, 735–759 (2020).
35. Raimundo, K. et al. Rheumatoid arthritis–interstitial lung disease in the United States: prevalence, incidence, and healthcare costs and mortality. *J. Rheumatol.* **46**, 360–369 (2019).
36. Ryerson, C. J., Cottin, V., Brown, K. K. & Collard, H. R. Acute exacerbation of idiopathic pulmonary fibrosis: shifting the paradigm. *Eur. Respir. J.* **46**, 512–520 (2015).
37. Park, I.-N. et al. Acute exacerbation of interstitial pneumonia other than idiopathic pulmonary fibrosis. *Chest* **132**, 214–220 (2007).
38. Kolb, M. et al. Acute exacerbations of progressive-fibrosing interstitial lung diseases. *Eur. Respir. Rev.* **27**, 180071 (2018).
39. Ioannidis, J. P. A. et al. Mortality in systemic sclerosis: an international meta-analysis of individual patient data. *Am. J. Med.* **118**, 2–10 (2005).
40. Tomiyama, F. et al. High prevalence of acute exacerbation of interstitial lung disease in Japanese patients with systemic sclerosis. *Tohoku J. Exp. Med.* **239**, 297–305 (2016).
41. Peng, J.-M. et al. Dermatomyositis and polymyositis in the intensive care unit: a single-center retrospective cohort study of 102 patients. *PLoS One* **11**, e0154441 (2016).
42. Hozumi, H. et al. Clinical significance of interstitial lung disease and its acute exacerbation in microscopic polyangiitis. *Chest* **159**, 2334–2345 (2021).
43. Salonen, J. et al. Bronchoalveolar lavage differential cell count on prognostic assessment of patients with stable or acute interstitial lung disease: a retrospective real-life study. *Clin. Immunol.* **220**, 108594 (2020).
44. Laskin, D. L., Malaviya, R. & Laskin, J. D. Role of macrophages in acute lung injury and chronic fibrosis induced by pulmonary toxicants. *Toxicol. Sci.* **168**, 287–301 (2019).
45. Schupp, J. C. et al. Macrophage activation in acute exacerbation of idiopathic pulmonary fibrosis. *PLoS One* **10**, e0116775 (2015).
46. Lee, J.-W. et al. The role of macrophages in the development of acute and chronic inflammatory lung diseases. *Cells* **10**, 897 (2021).
47. Probst, C. K., Montes, S. B., Medoff, B. D., Shea, B. S. & Knipe, R. S. Vascular permeability in the fibrotic lung. *Eur. Respir. J.* **56**, 1900100 (2020).
48. Kao, K.-C. et al. Diffuse alveolar damage associated mortality in selected acute respiratory distress syndrome patients with open lung biopsy. *Crit. Care* **19**, 228 (2015).
49. Williams, A. E. & Chambers, R. C. The mercurial nature of neutrophils: still an enigma in ARDS? *Am. J. Physiol. Cell. Mol. Physiol.* **306**, L217–L230 (2014).
50. Oda, K. et al. Autopsy analyses in acute exacerbation of idiopathic pulmonary fibrosis. *Respir. Res.* **15**, 109 (2014).
51. Rice, A. J. et al. Terminal diffuse alveolar damage in relation to interstitial pneumonias: an autopsy study. *Am. J. Clin. Pathol.* **119**, 709–714 (2003).
52. Silva, C. I. S. et al. Acute exacerbation of chronic interstitial pneumonia: high-resolution computed tomography and pathologic findings. *J. Thorac. Imaging* **22**, 221–229 (2007).
53. Olson, A. L., Swigris, J. J., Raghu, G. & Brown, K. K. Seasonal variation. *Chest* **136**, 16–22 (2009).
54. Simon-Blancal, V. et al. Acute exacerbation of idiopathic pulmonary fibrosis: outcome and prognostic factors. *Respiration* **83**, 28–35 (2012).
55. Azadeh, N., Limper, A. H., Carmona, E. M. & Ryu, J. H. The role of infection in interstitial lung diseases. *Chest* **152**, 842–852 (2017).
56. Idiopathic Pulmonary Fibrosis Clinical Research Network. et al. Prednisone, azathioprine, and N-acetylcysteine for pulmonary fibrosis. *N. Engl. J. Med.* **366**, 1968–1977 (2012).
57. Molyneux, P. L. et al. Changes in the respiratory microbiome during acute exacerbations of idiopathic pulmonary fibrosis. *Respir. Res.* **18**, 29 (2017).
58. Scher, J. U. et al. The lung microbiota in early rheumatoid arthritis and autoimmunity. *Microbiome* **4**, 60 (2016).
59. Maeda, Y. et al. Dysbiosis contributes to arthritis development via activation of autoreactive T cells in the intestine. *Arthritis Rheumatol.* **68**, 2646–2661 (2016).
60. Alpariz-Rodriguez, D. et al. *Prevotella copri* in individuals at risk for rheumatoid arthritis. *Ann. Rheum. Dis.* **78**, 590–593 (2019).
61. Lee, J. S. et al. Bronchoalveolar lavage pepsin in acute exacerbation of idiopathic pulmonary fibrosis. *Eur. Respir. J.* **39**, 352–358 (2012).
62. Leuschner, G. & Behr, J. Acute exacerbation in interstitial lung disease. *Front. Med.* **4**, 176 (2017).
63. Lee, J. S. et al. Anti-acid treatment and disease progression in idiopathic pulmonary fibrosis: an analysis of data from three randomised controlled trials. *Lancet Respir. Med.* **1**, 369–376 (2013).
64. Hoffmann-Vold, A.-M. et al. Progressive interstitial lung disease in patients with systemic sclerosis-associated interstitial lung disease in the EUSTAR database. *Ann. Rheum. Dis.* **80**, 219–227 (2021).
65. Shreiner, A. B., Murray, C., Denton, C. & Khanna, D. Gastrointestinal manifestations of systemic sclerosis. *J. Scleroderma Relat. Disord.* **1**, 247–256 (2016).
66. Johansson, K. A. et al. Acute exacerbation of idiopathic pulmonary fibrosis associated with air pollution exposure. *Eur. Respir. J.* **43**, 1124–1131 (2014).
67. Miyamura, T. et al. Postoperative acute exacerbation of interstitial pneumonia in pulmonary and non-pulmonary surgery: a retrospective study. *Respir. Res.* **20**, 154 (2019).
68. Amundson, W. H. et al. Acute exacerbation of interstitial lung disease after procedures. *Respir. Med.* **150**, 30–37 (2019).
69. Sakamoto, K. et al. Acute exacerbation of IPF following diagnostic bronchoalveolar lavage procedures. *Respir. Med.* **106**, 436–442 (2012).
70. Cassone, G. et al. Treatment of rheumatoid arthritis-associated interstitial lung disease: lights and shadows. *J. Clin. Med.* **9**, 1082 (2020).
71. Fraenkel, L. et al. 2021 American College of Rheumatology Guideline for the treatment of rheumatoid arthritis. *Arthritis Care Res.* **73**, 924–939 (2021).
72. Fragoulis, G. E., Conway, R. & Nikiphorou, E. Methotrexate and interstitial lung disease: controversies and questions. A narrative review of the literature. *Rheumatology* **58**, 1900–1906 (2019).
73. Izuka, S., Yamashita, H., Iba, A., Takahashi, Y. & Kaneko, H. Acute exacerbation of rheumatoid arthritis-associated interstitial lung disease: clinical features and prognosis. *Rheumatology* **60**, 2348–2354 (2020).
74. Shaw, M., Collins, B. F., Ho, L. A. & Raghu, G. Rheumatoid arthritis-associated lung disease. *Eur. Respir. Rev.* **24**, 1–16 (2015).
75. Chen, J. et al. Biologics-induced interstitial lung diseases in rheumatic patients: facts and controversies. *Expert Opin. Biol. Ther.* **17**, 265–283 (2017).
76. Cottin, V. et al. The case of methotrexate and the lung: Dr Jekyll and Mr Hyde. *Eur. Respir. J.* **57**, 2100079 (2021).
77. Dias, O. M. et al. Adalimumab-induced acute interstitial lung disease in a patient with rheumatoid arthritis. *J. Bras. Pneumol.* **40**, 77–81 (2014).
78. Hyldegaard, C. et al. A population-based cohort study of rheumatoid arthritis-associated interstitial lung disease: comorbidity and mortality. *Ann. Rheum. Dis.* **76**, 1700–1706 (2017).
79. Manfredi, A. et al. Rheumatoid arthritis related interstitial lung disease. *Expert Rev. Clin. Immunol.* **17**, 485–497 (2021).
80. Manfredi, A. et al. Prevalence and characterization of non-sicca onset primary Sjögren syndrome with interstitial lung involvement. *Clin. Rheumatol.* **36**, 1261–1268 (2017).

81. Cavagna et al. Influence of antisynthetase antibodies specificities on antisynthetase syndrome clinical spectrum time course. *J. Clin. Med.* **8**, 2013 (2019).
82. Kuwana, M., Gil-Vila, A. & Selva-O'Callaghan, A. Role of autoantibodies in the diagnosis and prognosis of interstitial lung disease in autoimmune rheumatic disorders. *Ther. Adv. Musculoskelet. Dis.* **13**, 1759720–2110324 (2021).
83. van der Kamp, R., Tak, P. P., Jansen, H. M. & Bresser, P. Interstitial lung disease as the first manifestation of systemic sclerosis. *Neth. J. Med.* **65**, 390–394 (2007).
84. Furukawa, H. et al. Biomarkers for interstitial lung disease and acute-onset diffuse interstitial lung disease in rheumatoid arthritis. *Ther. Adv. Musculoskelet. Dis.* **13**, 1759720–2110225 (2021).
85. Kamiya, H. & Panlaku, O. M. Systematic review and meta-analysis of the risk of rheumatoid arthritis-associated interstitial lung disease related to anti-cyclic citrullinated peptide (CCP) antibody. *BMJ Open* **11**, e040465 (2021).
86. Perez-Alvarez, R. et al. Interstitial lung disease induced or exacerbated by TNF-targeted therapies: analysis of 122 cases. *Semin. Arthritis Rheum.* **41**, 256–264 (2011).
87. Winthrop, K. L. et al. Opportunistic infections and biologic therapies in immune-mediated inflammatory diseases: consensus recommendations for infection reporting during clinical trials and postmarketing surveillance. *Ann. Rheum. Dis.* **74**, 2107–2116 (2015).
88. Mathai, S. C. & Danoff, S. K. Management of interstitial lung disease associated with connective tissue disease. *Br. Med. J.* **352**, h6819 (2016).
89. Luppi, F., Cerri, S., Taddai, S., Ferrara, G. & Cottin, V. Acute exacerbation of idiopathic pulmonary fibrosis: a clinical review. *Intern. Emerg. Med.* **10**, 401–411 (2015).
90. Kondoh, Y., Cottin, V. & Brown, K. K. Recent lessons learned in the management of acute exacerbation of idiopathic pulmonary fibrosis. *Eur. Respir. Rev.* **26**, 170050 (2017).
91. Akira, M., Kozuka, T., Yamamoto, S. & Sakatani, M. Computed tomography findings in acute exacerbation of idiopathic pulmonary fibrosis. *Am. J. Respir. Crit. Care Med.* **178**, 372–378 (2008).
92. Rezoagli, E., Fumagalli, R. & Bellani, G. Definition and epidemiology of acute respiratory distress syndrome. *Ann. Transl. Med.* **5**, 282–282 (2017).
93. Marchioni, A. et al. Acute exacerbation of idiopathic pulmonary fibrosis: lessons learned from acute respiratory distress syndrome? *Crit. Care* **22**, 80 (2018).
94. Jacob, J. & Hansell, D. M. HRCT of fibrosing lung disease. *Respirology* **20**, 859–872 (2015).
95. Tanaka, N. et al. Annual variation rate of KL-6 for predicting acute exacerbation in patients with rheumatoid arthritis-associated interstitial lung disease. *Mod. Rheumatol.* **31**, 1100–1106 (2021).
96. Judge, E. P., Fabre, A., Adamali, H. I. & Egan, J. J. Acute exacerbations and pulmonary hypertension in advanced idiopathic pulmonary fibrosis. *Eur. Respir. J.* **40**, 93–100 (2012).
97. Arcadu, A. & Moua, T. Bronchoscopy assessment of acute respiratory failure in interstitial lung disease. *Respirology* **22**, 352–359 (2017).
98. Hutchinson, J. P., Fogarty, A. W., McKeever, T. M. & Hubbard, R. B. In-hospital mortality after surgical lung biopsy for interstitial lung disease in the United States, 2000 to 2011. *Am. J. Respir. Crit. Care Med.* **193**, 1161–1167 (2016).
99. Olson, A. L., Gifford, A. H., Inase, N., Fernández Pérez, E. R. & Suda, T. The epidemiology of idiopathic pulmonary fibrosis and interstitial lung diseases at risk of a progressive-fibrosing phenotype. *Eur. Respir. Rev.* **27**, 180077 (2018).
100. Cao, M. et al. Acute exacerbations of fibrosing interstitial lung disease associated with connective tissue diseases: a population-based study. *BMC Pulm. Med.* **19**, 215 (2019).
101. Enomoto, N. et al. Differences in clinical features of acute exacerbation between connective tissue disease-associated interstitial pneumonia and idiopathic pulmonary fibrosis. *Chron. Respir. Dis.* **16**, 147997231880947 (2019).
102. Hozumi, H. et al. Acute exacerbation in rheumatoid arthritis-associated interstitial lung disease: a retrospective case control study. *BMJ Open* **3**, e003132 (2013).
103. Zamora-Legoff, J. A., Krause, M. L., Crowson, C. S., Ryu, J. H. & Matteson, E. L. Patterns of interstitial lung disease and mortality in rheumatoid arthritis. *Rheumatology* **56**, 344–350 (2017).
104. Cottin, V. et al. Burden of idiopathic pulmonary fibrosis progression: a 5-year longitudinal follow-up study. *PLoS One* **12**, e0166462 (2017).
105. Toyoda, Y. et al. Clinical features and outcome of acute exacerbation of interstitial pneumonia associated with connective tissue disease. *J. Med. Investig.* **63**, 294–299 (2016).
106. Singh, P., Thakur, B., Mohapatra, A. K. & Padhan, P. Clinical features and outcome of acute exacerbation in connective tissue disease-associated interstitial lung disease: a single-center study from India. *Int. J. Rheum. Dis.* **22**, 1741–1745 (2019).
107. Liang, J. et al. Acute exacerbation of interstitial lung disease in adult patients with idiopathic inflammatory myopathies: a retrospective case-control study. *Front. Med.* **7**, 12 (2020).
108. Cao, H. et al. Predicting survival across acute exacerbation of interstitial lung disease in patients with idiopathic inflammatory myositis: the GAP-ILD model. *Rheumatol. Ther.* **7**, 967–978 (2020).
109. Koyama, K. et al. The activities of daily living after an acute exacerbation of idiopathic pulmonary fibrosis. *Intern. Med.* **56**, 2837–2843 (2017).
110. Farrand, E., Vittinghoff, E., Ley, B., Butte, A. J. & Collard, H. R. Corticosteroid use is not associated with improved outcomes in acute exacerbation of IPF. *Respirology* **25**, 629–635 (2020).
111. Wijsenbeek, M. et al. Progressive fibrosing interstitial lung diseases: current practice in diagnosis and management. *Curr. Med. Res. Opin.* **35**, 2015–2024 (2019).
112. Ding, J., Chen, Z. & Feng, K. Procalcitonin-guided antibiotic use in acute exacerbations of idiopathic pulmonary fibrosis. *Int. J. Med. Sci.* **10**, 903–907 (2013).
113. Inase, N. et al. Cyclosporin A followed by the treatment of acute exacerbation of idiopathic pulmonary fibrosis with corticosteroid. *Intern. Med.* **42**, 565–570 (2003).
114. Homma, S. et al. Cyclosporin treatment in steroid-resistant and acutely exacerbated interstitial pneumonia. *Intern. Med.* **44**, 1144–1150 (2005).
115. Sakamoto, S. et al. Cyclosporin A in the treatment of acute exacerbation of idiopathic pulmonary fibrosis. *Intern. Med.* **49**, 109–115 (2010).
116. Donahoe, M. et al. Autoantibody-targeted treatments for acute exacerbations of idiopathic pulmonary fibrosis. *PLoS ONE* **10**, e0127771 (2015).
117. Horita, N. et al. Tacrolimus and steroid treatment for acute exacerbation of idiopathic pulmonary fibrosis. *Intern. Med.* **50**, 189–195 (2011).
118. Ota, M. et al. Efficacy of intensive immunosuppression in exacerbated rheumatoid arthritis-associated interstitial lung disease. *Mod. Rheumatol.* **27**, 22–28 (2017).
119. Nakamura, K. et al. Intravenous cyclophosphamide in acute exacerbation of rheumatoid arthritis-related interstitial lung disease: a propensity-matched analysis using a nationwide inpatient database. *Semin. Arthritis Rheum.* **51**, 977–982 (2021).
120. Pearce, F., Johnson, S. R. & Courtney, P. Interstitial lung disease following certolizumab pegol. *Rheumatology* **51**, 578–580 (2012).
121. Migita, K. et al. Acute exacerbation of rheumatoid interstitial lung disease during the maintenance therapy with certolizumab pegol. *Mod. Rheumatol.* **27**, 1079–1082 (2017).
122. Savage, E. M., Millar, A. M. & Taggart, A. J. Comment on: a case of certolizumab-induced interstitial lung disease in a patient with rheumatoid arthritis. *Rheumatology* **53**, 1154–1155 (2014).
123. Kawashiri, S., Kawakami, A., Sakamoto, N., Ishimatsu, Y. & Eguchi, K. A fatal case of acute exacerbation of interstitial lung disease in a patient with rheumatoid arthritis during treatment with tocilizumab. *Rheumatol. Int.* **32**, 4023–4026 (2012).
124. Akiyama, M., Kaneko, Y., Yamaoka, K., Kondo, H. & Takeuchi, T. Association of disease activity with acute exacerbation of interstitial lung disease during tocilizumab treatment in patients with rheumatoid arthritis: a retrospective, case–control study. *Rheumatol. Int.* **36**, 881–889 (2016).
125. Ding, T. et al. BSR and BHRP rheumatoid arthritis guidelines on safety of anti-TNF therapies. *Rheumatology* **49**, 2217–2219 (2010).
126. Holroyd, C. R. et al. The British Society for Rheumatology biologic DMARD safety guidelines in inflammatory arthritis. *Rheumatology* **58**, e3–e42 (2019).
127. Martin, M. J. & Moua, T. Mechanical ventilation and predictors of in-hospital mortality in fibrotic interstitial lung disease with acute respiratory failure. *Crit. Care Med.* **48**, 993–1000 (2020).
128. Kreuter, M. et al. Palliative care in interstitial lung disease: living well. *Lancet Respir. Med.* **5**, 968–980 (2017).
129. Kohberg, C., Andersen, C. U. & Bendstrup, E. Opioids: an unexplored option for treatment of dyspnea in IPF. *Eur. Clin. Respir. J.* **3**, 30629 (2016).
130. Simon, S. T. et al. Benzodiazepines for the relief of breathlessness in advanced malignant and non-malignant diseases in adults. *Cochrane Database Syst. Rev.* **10**, CD007354 (2016).
131. Bajwah, S. et al. Safety of benzodiazepines and opioids in interstitial lung disease: a national prospective study. *Eur. Respir. J.* **52**, 1801278 (2018).
132. Kronborg-White, S., Andersen, C. U., Kohberg, C., Hilberg, O. & Bendstrup, E. Palliation of chronic breathlessness with morphine in patients with fibrotic interstitial lung disease — a randomised placebo-controlled trial. *Respir. Res.* **21**, 195 (2020).
133. Ferrara, G. et al. Best supportive care for idiopathic pulmonary fibrosis: current gaps and future directions. *Eur. Respir. Rev.* **27**, 170076 (2018).

Acknowledgements

The work of F.L. was partially supported by the Italian Ministry of University and Research — Department of Excellence project PREMIA (PRECision Medicine Approach: bringing biomarker research to clinic).

Author contributions

All authors contributed equally to all aspects of the article.

Competing interests

The authors declare no competing interests.

Peer review information

Nature Reviews Rheumatology thanks F. Bonella, A. Wells and the other, anonymous, reviewer(s) for their contribution to the peer review of this work.

Publisher's note

Springer Nature remains neutral with regard to jurisdictional claims in published maps and institutional affiliations.

© Springer Nature Limited 2021

Excess comorbidities in gout: the causal paradigm and pleiotropic approaches to care

Hyon K. Choi^{1,2,3,4}✉, Natalie McCormick^{1,2,3,4} and Chio Yokose^{1,2,3}

Abstract | Gout is a common hyperuricaemic metabolic condition that leads to painful inflammatory arthritis and a high comorbidity burden, especially cardiometabolic-renal (CMR) conditions, including hypertension, myocardial infarction, stroke, obesity, hyperlipidaemia, type 2 diabetes mellitus and chronic kidney disease. Substantial advances have been made in our understanding of the excess CMR burden in gout, ranging from pathogenesis underlying excess CMR comorbidities, inferring causal relationships from Mendelian randomization studies, and potentially discovering urate crystals in coronary arteries using advanced imaging, to clinical trials and observational studies. Despite many studies finding an independent association between blood urate levels and risk of incident CMR events, Mendelian randomization studies have largely found that serum urate is not causal for CMR end points or intermediate risk factors or outcomes (such as kidney function, adiposity, metabolic syndrome, glycaemic traits or blood lipid concentrations). Although limited, randomized controlled trials to date in adults without gout support this conclusion. If imaging studies suggesting that monosodium urate crystals are deposited in coronary plaques in patients with gout are confirmed, it is possible that these crystals might have a role in the inflammatory pathogenesis of increased cardiovascular risk in patients with gout; removing monosodium urate crystals or blocking the inflammatory pathway could reduce this excess risk. Accordingly, data for CMR outcomes with these urate-lowering or anti-inflammatory therapies in patients with gout are needed. In the meantime, highly pleiotropic CMR and urate-lowering benefits of sodium–glucose cotransporter 2 (SGLT2) inhibitors and key lifestyle measures could play an important role in comorbidity care, in conjunction with effective gout care based on target serum urate concentrations according to the latest guidelines.

¹Clinical Epidemiology Program, Division of Rheumatology, Allergy, and Immunology, Massachusetts General Hospital, Boston, MA, USA.

²Mongan Institute, Department of Medicine, Massachusetts General Hospital, Boston, MA, USA.

³Department of Medicine, Harvard Medical School, Boston, MA, USA.

⁴Arthritis Research Canada, Vancouver, British Columbia, Canada.

✉e-mail: hchoi@mgh.harvard.edu
<https://doi.org/10.1038/s41584-021-00725-9>

Gout is a common hyperuricaemic metabolic condition that leads to painful inflammatory arthritis and has a high comorbidity burden^{1–3}. Exacerbated by the rising prevalence of the ‘Western’ lifestyle and the obesity epidemic, the incidence^{4–7}, prevalence^{4,5,8–10} and disability burden of gout have risen worldwide for decades, as detailed in several Global Burden of Disease analyses of 195 countries and territories between 1990 and 2017 (REFS^{11,12}). Although inflammatory arthritis is the cardinal feature of gout, gout is a metabolic condition that is complicated by an increased burden of cardiometabolic-renal (CMR) comorbidities and sequelae^{13–15}. As 63% of patients with gout in the US population also have metabolic syndrome¹, gout is associated with increased prevalence of coexistent hypertension (74%), obesity (53%), type 2 diabetes mellitus (T2DM; 26%), chronic kidney disease (CKD; stage ≥3; 20%), myocardial infarction (MI; 14%) and stroke

(10%)¹⁵ (FIG. 1), all of which are ≥2-fold more prevalent than in individuals without gout, after adjusting for age and sex. In the UK population, gout is independently associated with higher prevalence of CKD, T2DM, ischaemic heart disease and hyperlipidaemia, even after adjusting for serum (that is, soluble) urate concentration, age and sex¹⁶. This remarkable CMR burden also seems to exceed that of many other rheumatic diseases^{17,18} as, in a Swedish study, age-standardized prevalence of obesity, hypertension, T2DM and hyperlipidaemia were higher in gout than in psoriatic arthritis, rheumatoid arthritis or ankylosing spondylitis¹⁷. Furthermore, this comorbidity burden seems to be worsening over time: a comparison of the presenting characteristics of patients with incident gout diagnosed in the same US practice setting 20 years apart (2009–2010 and 1989–1990) revealed that the average BMI was higher and nearly all CMR comorbidities were more prevalent in the later cohort,

Key points

- Exacerbated by the 'Western' lifestyle and obesity epidemics, the frequency and burden of gout, a hyperuricaemic metabolic condition complicated by excess cardiometabolic-renal (CMR) comorbidities and sequelae, have risen worldwide for decades.
- Many prospective studies have associated blood urate levels with the development of incident CMR events, but evidence from Mendelian randomization studies and randomized controlled trials does not support a causal effect for serum (soluble) urate.
- In addition to activating inflammasome pathways and inducing gout flares in joints, monosodium urate crystals might also deposit in coronary plaques and have pro-inflammatory roles in the pathogenesis of excess cardiovascular risk associated with gout, analogous to cholesterol crystals.
- Sodium-glucose cotransporter 2 (SGLT2) inhibitors, with their highly pleiotropic CMR and urate-lowering benefits, are an attractive alternative or adjunct therapy for patients with gout, although more evidence of their effects in gout populations is needed.
- The downstream effects of weight loss and lifestyle modification, including adherence to healthy cardiometabolic diets, should simultaneously reduce CMR risk and serum urate concentrations and the risk of incident gout.
- Pharmacotherapy and diet and lifestyle recommendations for gout prevention and management can be guided by concurrent CMR comorbidities and shared decision-making that reflects patient preferences.

whereas age and sex distributions were unchanged^{7,19} (FIG. 1). In a general population study in the UK, the increased prevalence of these comorbidities is reflected in a premature mortality gap in patients with gout, which did not improve between 1999 and 2014 (REF.²⁰), whereas that in patients with rheumatoid arthritis showed a clear improvement over the same period²¹ (Supplementary Figure 1). Collectively, these concerning trends represent a life-threatening component of the disease burden of gout, with clear unmet needs for improved approaches to prevention, early recognition and effective management of gout CMR comorbidities.

Nevertheless, understanding of these CMR comorbidities of gout is improving, with advanced imaging to explore their pathogenesis, Mendelian randomization studies, as well as randomized controlled trials and observational studies to investigate the pleiotropic benefits of drug therapies for gout CMR comorbidities (Supplementary Box 1). In this Review, we provide an overview of these developments to establish clinical relevance and identify future research needs.

Gout and risk of CMR events

In addition to the frequent coexistence of comorbidities in patients with gout, many original studies, systematic reviews and meta-analyses have found an independent association between serum urate concentrations and risk of incident CMR events^{22–25}. Furthermore, gout has been linked to an increased risk of CMR sequelae and premature death. For example, the Framingham Heart Study found that gout was associated with a 60% increased risk of coronary heart disease (CHD) in men²⁶. In the Multiple Risk Factor Intervention Trial, gout was associated with a 26% increased risk of MI²⁷, a 33% increased risk of peripheral arterial disease²⁸ and a 35% increased risk of CHD mortality³. Similarly, a large cohort study found a 60% increased risk of non-fatal MI and 55% increased risk of fatal MI among men with gout². Another prospective cohort study of men with gout

demonstrated a 28% higher risk of death from all causes, a 38% higher risk of death from cardiovascular disease (CVD) and a 55% higher risk of death from CHD². A temporal trend analysis of the UK general population showed that the level of premature mortality among patients with gout did not improve over the 16-year period between 1999 and 2014 (REF.²⁰), unlike with rheumatoid arthritis, for which premature mortality reduced significantly during that time²¹ (Supplemental Fig. 1). Moreover, men with gout had a 41% increased risk of incident T2DM²⁹, whereas this risk was even higher among women³⁰. Finally, incident gout is associated with a 78% higher risk of CKD stage ≥ 3 (REF.³¹). However, as these associations do not necessarily equate to causation, below we examine studies that allow causality to be inferred and illuminate the potential underlying pathogenesis of these CMR comorbidities.

Association versus causation

Although gout is clearly associated with an elevated risk of CMR comorbidities, the nature and direction of any causal relationship between the development of gout and these diseases is still unclear. For example, longitudinal analysis of a representative sample of the UK general population (captured in the Clinical Practice Research Datalink) showed that not only are people with underlying renal disease or CVD (including MI, heart failure, stroke and hypertension) more likely to develop incident gout than age- and sex-matched individuals but that incident gout was subsequently associated with an increased risk of developing these incident CMR comorbidities³². As such, despite the reported independent associations of hyperuricaemia and gout with increased risk of CMR comorbidities^{30,33,34}, these findings could still reflect reverse causality or residual confounding from shared risk factors such as obesity^{35–37}, consumption of sugar-sweetened beverages^{38–40} or unmeasured factors. Moreover, observational studies examining the impact of urate-lowering therapies (ULTs) on risk or progression of CMR comorbidities or on mortality^{41–43}, although larger and more generalizable than randomized clinical trials, are still subject to confounding by indication and critical time-related biases that can severely mislead inferences about treatment effects^{44,45}.

Mendelian randomization data for urate

By contrast, Mendelian randomization enables unconfounded estimates of potential causal effects to be obtained by using genetic variants as instrumental variables for genetically determined exposures at conception^{46,47} and thus is free of confounding or reverse causation by all factors after birth (that is, non-genetic risk factors). Mendelian randomization is well-suited for investigating the causal effects of serum urate, as genetic variants explain a substantial proportion (>7%) of total phenotypic variance in serum urate concentrations⁴⁸, driven mostly by prominent non-pleiotropic variants in the prominent gene *SLC2A9* (which encodes GLUT9). The vast majority of Mendelian randomization studies have found that serum urate is not causal for hard clinical CMR end points, including CHD, stroke and T2DM, or intermediate risk factor traits (including kidney function,

Instrumental variables

Variables (for example, single or multiple genetic variants) that function as a proxy for the exposure of interest and must be associated with the exposure but cannot be independently associated with the outcome of interest (that is, outside its association with the exposure itself).

Non-pleiotropic variants

A genetic variant associated only with the exposure of interest (for example, serum urate levels) and not directly associated with the outcome of interest (for example, fasting insulin levels) or other traits that could be causal for the outcome of interest through a different pathway (for example, triglycerides).

Horizontal pleiotropy

When genetic variants can affect the outcome of interest through more than one biological pathway, including those that are independent of the exposure of interest.

Pleiotropic variants

Genetic variants associated with the exposure of interest (for example, serum urate levels) but also directly associated with additional traits (for example, triglyceride levels) that could affect the outcome of interest (for example, fasting insulin levels) independently of the main exposure.

adiposity, insulin resistance, glycaemic traits and blood lipid concentrations)^{49–51} (TABLE 1). Indeed, many studies have produced both observational and Mendelian randomization estimates from the same dataset and reached different inferences about the effect of serum urate. For example, one study⁵² reported an odds ratio (OR) for T2DM of 1.10 (95% confidence interval (CI) 1.02–1.17; $P = 0.007$) and 1.01 (95% CI 0.96–1.06; $P = 0.75$) per standard deviation (s.d.) change in serum urate concentration in the traditional observational analysis and for the serum urate genetic risk score (that is, the causal estimate from Mendelian randomization), respectively. Blood pressure is one CMR trait for which the Mendelian randomization evidence has been rather inconsistent, as seven studies reported no association^{53–59}, four reported a positive association^{60–63} and one reported a negative association⁶⁴ between serum urate and systolic blood

pressure or hypertension. Heterogeneity in the choice of antihypertensive treatment in the study population, particularly diuretic use⁶⁴, might explain some of these inconsistencies, whereas horizontal pleiotropy might not have been fully addressed in the two positive studies that used a polygenic instrument^{61,62}. These conflicting results belie the importance of sensitivity analyses, including single-variant analyses with *SLC2A9* alone (given that it is non-pleiotropic), to help confirm whether any apparent causal effects are specific to changes in serum urate and are otherwise free of genetic confounding.

Serum urate concentration has most frequently been the exposure of interest (as opposed to the outcome) in these Mendelian randomization studies. However, in addition to residual confounding, the coexistence of hyperuricaemia or gout and CMR comorbidities might also be due to reverse causation, with CMR events or conditions actually leading to hyperuricaemia. This relationship has been assessed in bidirectional Mendelian randomization studies (TABLE 1), including two studies^{57,65} in which genetically determined hyperuricaemia had no causal effect on body fat mass, whereas genetically determined fat mass was positively associated with hyperuricaemia (for example, an increase in serum urate levels of 0.31 mg/dl per s.d. change in fat mass⁶⁵) (FIG. 2), and two other studies^{66,67} in which hyperuricaemia was not associated with triglyceride concentrations, whereas genetically determined triglyceride levels were positively associated with serum urate levels. Another bidirectional Mendelian randomization analysis examined the relationship between insulin resistance (as measured by fasting insulin concentrations) and serum urate⁶⁸, using summary-level data from the largest, most recent multi-cohort genome-wide association studies for these exposures^{48,69}. In this study, genetically determined serum urate concentration, whether inferred from the polygenic instrument or the *SLC2A9* or *ABCG2* variants alone (the two strongest genetic variants), was not associated with fasting insulin concentration, despite the analysis having >99% power to detect such an association. By contrast, genetically determined fasting insulin concentration was positively associated with serum urate concentration, with effect estimates ranging from 0.63 mg/dl per s.d. change in fasting insulin concentration, to 1.18 mg/dl per s.d. change after removal of pleiotropic variants (including one that mapped to *GCKR*, a highly pleiotropic gene that is associated with multiple cardiometabolic traits, such as triglycerides, which could affect fasting insulin concentrations independently of serum urate) and conditioning on genetically determined BMI. These associations were subsequently replicated using individual-level data from the UK Biobank⁶⁸. These findings reinforce the presence of a causal effect of fasting insulin inferred from human physiological studies, in which intravenous insulin induced hyperuricaemia^{70,71}, and suggest that pathophysiological changes in the earliest stages of insulin resistance might actually lead to an increase in serum urate concentration before dysglycaemia becomes clinically apparent (FIG. 2). Altogether, data from these bidirectional Mendelian randomization analyses strengthen the notion that interventions to reduce insulin resistance

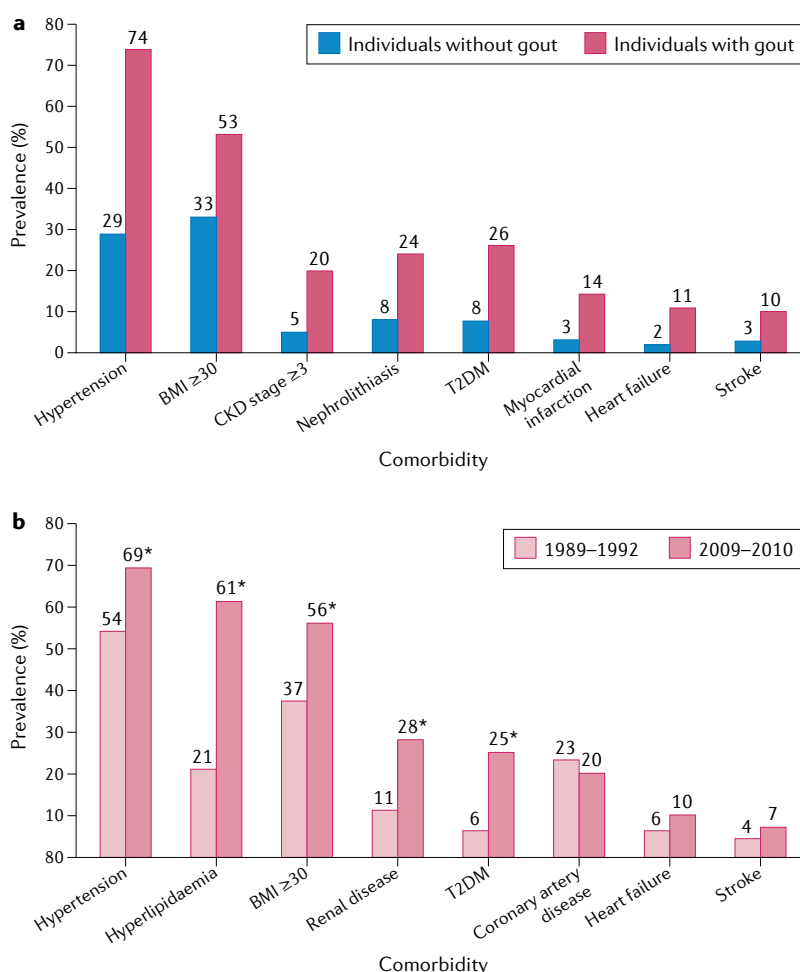


Fig. 1 | Contemporary prevalence and trends of cardiometabolic-renal conditions in gout populations. a | Contemporary prevalence of comorbidities in the US general population during the period 2007–2008. The graph illustrates the sex- and age-adjusted prevalence of cardiometabolic-renal comorbidities among adults without or with gout, according to the 2007–2008 National Health and Nutrition Examination Survey¹⁵. **b** | Worsening prevalence of comorbidities in patients with gout. The graph illustrates the higher frequency of comorbidities among patients with incident gout diagnosed in the same US practice setting (Olmsted County, Minnesota) during two time periods: 1989–1992 and 2009–2010 (mean age 59.3 and 60.3 years, respectively)^{7,19}. Asterisk indicates $P < 0.01$. BMI, body mass index; CKD, chronic kidney disease; T2DM, type 2 diabetes mellitus.

Table 1 | Mendelian randomization studies assessing causal relationships between serum urate and CMR outcomes

Outcome or exposure ^a	Significant studies (n)/total studies (n) ^b	Key studies		Refs
		Genetic instrument	Effect estimate or change in serum urate concentration ^c	
Serum urate as exposure				
Coronary artery disease	2(+)/13	7 non-pleiotropic variants ⁵³	OR 1.04; 95% CI 0.97–1.11; <i>P</i> = 0.29	53–58,61, 182–188
Chronic kidney disease	1(–)/5	22 variants (outliers excluded) ¹⁸⁹	OR 0.99; 95% CI 0.91–1.07; <i>P</i> = 0.74	54,57, 189–191
Glycaemic traits (fasting glucose, HbA _{1c})	0/4	16 non-pleiotropic variants ¹⁹²	FG: β = 0.000; 95% CI –0.021–0.021; <i>P</i> > 0.99	54,59, 62,192
		17 non-pleiotropic variants ¹⁹²	HbA _{1c} : β = 0.002; 95% CI –0.012–0.016; <i>P</i> = 0.79	
Type 2 diabetes mellitus	0/6	14 non-pleiotropic variants ¹⁸³	OR 0.95; 95% CI 0.86–1.05; <i>P</i> = 0.28	52,57,183, 192–194
Lipids	1(+)/7	SLC2A9 variant ⁶⁷	TG: β = 0.000; 95% CI –0.001–0.001; <i>P</i> = 0.99 HDL: β = –0.011; 95% CI –0.011–0.009; <i>P</i> = 0.72	55–57,59, 62,66,67
Insulin resistance or metabolic syndrome	0/7	29 variants (outliers excluded) ⁶⁸	FI: β = 0.026; 95% CI –0.011–0.062; <i>P</i> = 0.17	54,59, 68,192, 195–197
		SLC2A9 variant ⁶⁸	FI: β = –0.005; 95% CI –0.021–0.010; <i>P</i> = 0.49	
Adiposity	0/5	SLC2A9 variant ⁵⁸	BMI: β = –0.04; 95% CI –0.25–0.16	57–59, 62,65
Blood pressure or hypertension	5(4+; 1–)/12	SLC2A9 variant ⁵⁴	SBP: β = 0.061; –0.053–0.597; <i>P</i> = 0.10 DBP: β = 0.092; 95% CI –0.110–0.294; <i>P</i> = 0.37	53–64
Ischaemic stroke	1/5	14 non-pleiotropic variants ¹⁸³	OR 0.99; 95% CI 0.88–1.12; <i>P</i> = 0.93	53,56,57, 61,183
Serum urate as outcome				
Lipids	2/2	49 variants ⁶⁷	TG: 0.10; 95% CI 0.06–0.14; <i>P</i> < 0.001	66,67
		87 variants ⁶⁷	HDL: –0.09; 95% CI –0.012–0.05; <i>P</i> < 0.001	
Insulin resistance or metabolic syndrome	2/2	71 variants (outliers excluded) ⁶⁸	FI: 0.56; 95% CI 0.45–0.67; <i>P</i> < 0.001 per s.d.	68,192
Adiposity	4/4	3 variants: mapped to <i>FTO</i> , <i>MC4R</i> , <i>TMEM18</i> (REF. ³)	BMI: 0.51; 95% CI 0.34–0.67; per s.d.	57,58, 65,198

BMI, body mass index; CI, confidence interval; DBP, diastolic blood pressure; FG, fasting blood glucose; FI, fasting insulin; HbA_{1c}, glycated haemoglobin; HDL, high-density lipoprotein cholesterol; OR, odds ratio; SBP, systolic blood pressure; s.d., standard deviation; TG, triglycerides. ^aOutcomes are listed for studies of serum urate as exposure, and exposures are listed for studies of serum urate as outcome. ^bNumbers in parentheses indicate the studies in which the association was positive (+) or negative (–). ^cEffect estimate (odds ratio) per standard deviation of serum urate, or change in serum urate concentration (mg/dl) per standard deviation exposure, are indicated.

and adiposity might lower serum urate concentration, whereas ULT is unlikely to lower the risk of metabolic syndrome or CMR events (FIG. 2).

To date, no Mendelian randomization studies have been performed to assess a potential causal effect of gout specifically (above and beyond serum urate concentrations) on CMR events, largely owing to a lack of robust genetic instruments, which calls for future studies on this topic (BOX 1).

Preclinical mechanistic urate data

Potential mechanisms underlying a link between hyperuricaemia and development of hypertension include the nitric oxide and renin–angiotensin pathways, based on

studies in a rat model of mild hyperuricaemia through the use of a uricase inhibitor (for example, oxonic acid)^{72,73}. In this model, mild hyperuricaemia induced by administration of a uricase inhibitor led to endothelial cell dysfunction resulting from decreased production of nitric oxide synthase^{74–76} and to vascular smooth muscle cell proliferation^{77,78}. Furthermore, elevated serum urate stimulated the renin–angiotensin system⁷⁹ and led to renal afferent arteriopathy and tubulointerstitial disease, resulting in hypertension⁸⁰. Administration of the xanthine oxidase inhibitor (XOI) allopurinol or the uricosuric agent benzbodaron prevented the development of renal lesions and hypertension, and the angiotensin-converting enzyme inhibitor enalapril

reversed both the renal lesions and the hypertension⁸⁰. Although observations with the rat model of induced mild hyperuricaemia suggest a causal role of hyperuricaemia in hypertension in rodents, physiological differences between humans and rodents (that is, the constitutive presence of uricase in rodents but not humans) has been a major hurdle in translating these findings to humans.

CMR effects of ULT in a non-gout context

To translate these data from rodent models, human clinical trials are essential. To date, demonstration of the CMR benefits of ULT has been limited to blood pressure-lowering in adolescents but not in adults (TABLE 2). For example, two randomized controlled trials of ULTs (allopurinol or probenecid) in adolescents without gout who have hyperuricaemic pre-hypertension ($n = 30$) or stage 1 hypertension ($n = 60$) found that ULTs lowered blood pressure compared with placebo^{81,82}. However, a similarly designed trial in adults ($n = 149$) showed no blood pressure benefit⁸³ and another randomized control trial ($n = 99$ adults) found no improvement in blood pressure or hsCRP levels with ULTs⁸⁴. If hyperuricaemia has an acute effect on blood pressure by activating the renin–angiotensin system and reducing

endothelial nitric oxide synthase during the early stages of hypertension but not the later stages associated with microvascular damage (as suggested from the rat model of induced mild hyperuricaemia^{78,80,85}), then lowering serum urate in adults ('late stage') may not result in the same blood pressure reduction as in adolescents. In addition, two independent placebo-controlled, double-blind, randomized controlled trials reported no benefits of ULT with escalating doses of allopurinol on the progression of CKD over 3-year⁸⁶ or 2-year⁸⁷ follow-up among patients with CKD stage 1–4. No blood pressure or other cardiometabolic benefits were observed in these trials^{86,87}, which specifically excluded people with gout^{83,86,87}.

However, allopurinol does have some cardiovascular (CV) benefits in non-gout populations, although these effects may be mediated through separate, non-urate-lowering pathways. For example, two placebo-controlled randomized controlled trials documented benefits of ULT on endothelial function, although only with xanthine oxidase inhibition (using allopurinol) and not by lowering serum urate with the uricosuric agent probenecid⁸⁸. These findings suggest that allopurinol might reduce cardiac afterload by improving arterial compliance through improved

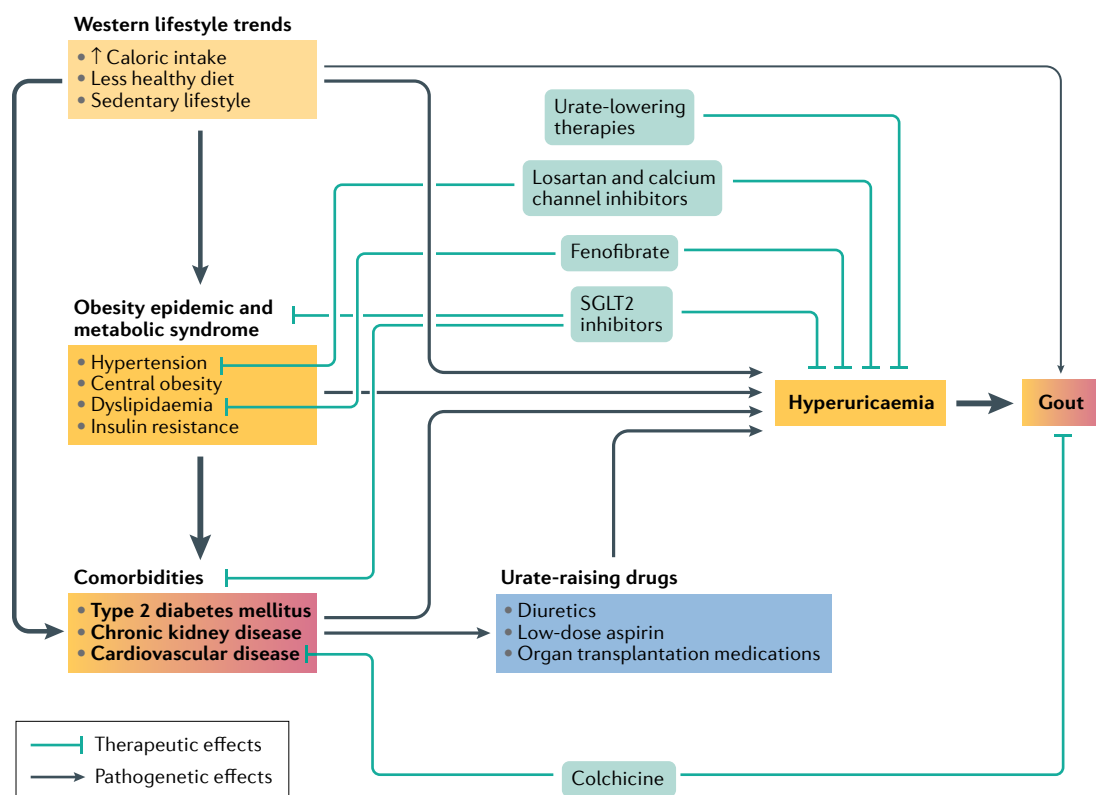


Fig. 2 | **Causal pathways of gout, CMR comorbidities and pleiotropic effects of CMR pharmacotherapies.**

Increasingly 'Westernized' lifestyles (risk factors) have contributed to obesity and metabolic syndrome (intermediates) and driven the development of cardiometabolic–renal (CMR) comorbidity conditions (clinical end points). Each factor can also increase the risk of incident gout (clinical end point) directly or indirectly by promoting hyperuricaemia (intermediate). Although some pharmacotherapies for these comorbidities have urate-raising effects, others lower serum urate levels and thus have pleiotropic benefits, by simultaneously addressing one or more CMR comorbidities and hyperuricaemia. Urate-lowering therapies are an exception, as randomized controlled trials to date have not found any consistent or apparent improvement in intermediate CMR outcomes in adults (with or without gout). GFR, glomerular filtration rate; SGLT2, sodium–glucose cotransporter 2.

endothelial function and reduced wave reflection. In a crossover randomized controlled trial of 65 patients with angina and angiographically documented coronary artery disease (CAD), allopurinol (600 mg daily) showed anti-ischaemic activity, in that it increased exercise time and reduced chest pain⁸⁹, potentially through its ability to lower oxidative stress by reducing superoxide anions and other free radicals (xanthine oxidase is a major source of reactive oxygen species)⁹⁰. Reduced oxidative stress would, in turn, reduce cardiac hypertrophy, increase tissue oxygenation and reduce the atherosclerotic plaque rupture involved in MI^{88,91–93}. Furthermore, raised levels of hypoxanthine, a downstream effect of xanthine oxidase inhibition, might also contribute to allopurinol's effects by increasing ATP levels and thereby the amount of energy available to tissues, and subsequently prevent

ischaemic cardiomyocytes from infarcting during an ischaemic insult such as acute coronary syndrome^{94,95}. Based on these findings, the ALL-HEART study, a multi-centre, controlled, prospective, randomized, open-label blinded end-point (PROBE) trial, is currently underway to assess the potential CV end-point and mortality benefits of allopurinol (600 mg daily, a dose that reduces oxidative stress) among patients with ischaemic heart disease but without gout⁹⁶ (TABLE 2).

CMR drugs that also lower serum urate

Some drugs used for the treatment of frequent CMR comorbidities of gout, such as diuretics and low-dose aspirin, raise serum urate concentration (Supplementary Box 1), thereby contributing to the risk of gout flares, whereas others are neutral or lower serum urate, reducing the risk while improving diabetes, hypertension, dyslipidaemia, CVD and CKD (FIG. 2; FIG. 3). Consequently, strategic adoption of these agents could help to achieve treatment of gout and CMR simultaneously while reducing polypharmacy. These drugs include losartan and calcium channel inhibitors (for hypertension), fenofibrate (for dyslipidaemias) and sodium–glucose cotransporter 2 (SGLT2) inhibitors (for T2DM). SGLT2 inhibitors reduce the risk of CKD worsening, major CV events and premature mortality⁹⁷, making them highly relevant to gout care, as do their urate-lowering ability^{98–100}. SGLT2 inhibitors (such as dapagliflozin, empagliflozin and canagliflozin) reduce serum urate concentration by increasing glycosuria; glucose in the urine competes with soluble urate for GLUT9-mediated reabsorption in the proximal tubule⁹⁸. With regard to gout end points, SGLT2 inhibitors reduce the risk of incident gout among patients with T2DM by 36% compared with glucose-lowering glucagon-like peptide 1 receptor (GLP1R) agonists⁹⁹. Furthermore, although initially documented in patients with diabetes, these pleiotropic CMR benefits of SGLT2 inhibitors were demonstrated in individuals without diabetes. Although all SGLT2 inhibitors are uricosurics, dapagliflozin and empagliflozin are the SGLT2 inhibitors that show benefits in trials with hard CV end points to date, including significant reductions in the risk of heart failure hospitalization and CV death, irrespective of diabetes status^{101,102}; these SGLT2 inhibitors also provide renoprotective effects as well as survival benefits in patients with CKD, regardless of diabetes status^{101,103} (FIG. 3). Given the high prevalence and risk of these CMR conditions in patients with gout (FIG. 1), SGLT2 inhibitors are already indicated in many of these patients. The serum urate-lowering effects of these SGLT2 inhibitors would likely be more relevant to patients with less advanced gout, typically those in primary care (as opposed to patients with advanced gout who are typically seen in rheumatology practice), although further research is needed (BOX 1). However, even among patients with advanced gout, supplementation of conventional ULT with SGLT inhibitors or other urate-lowering CMR drugs might be a promising strategy for achieving a treat-to-target serum urate approach, particularly among those who do not respond sufficiently to monotherapy with first-line ULTs (BOX 1).

Box 1 | Future directions in gout comorbidity research and treatment

Impact of a treat-to-target serum urate approach on CMR comorbidities in patients with gout

Although the evidence among non-gout adults has been largely negative to date, the impact of the treat-to-target serum urate approach on cardiometabolic-renal (CMR) outcomes in patients with gout is unknown. If benefits beyond reduced gout morbidity can be demonstrated, then the justification for a treat-to-target serum urate approach in gout care will be further strengthened, as recognized in multiple gout guidelines^{200,201}.

Urate-lowering benefits of SGLT2 inhibitors in patients with gout

The pleiotropic CMR benefits of sodium–glucose cotransporter 2 (SGLT2) inhibitors are highly relevant to gout care but have not been evaluated specifically in individuals with gout. Such data would inform how SGLT2 inhibitors can be integrated into the current pharmacological management of gout, as an adjunct or replacement for urate-lowering therapies.

Confirming the presence of MSU crystals in coronary arteries

Several studies suggest that monosodium urate (MSU) crystals form deposits in coronary arteries and large blood vessels^{121,122}. However, potential beam-hardening artefacts from calcified atheromas and partial volume effects, both of which are known sources of artefacts in the two-material decomposition algorithm of dual-energy computed tomography, confound interpretation of these findings¹¹⁵. Appropriate screening of those artefacts in future studies, ideally involving multiple readers from multiple centres, would enhance the credence of these data, with important implications on the topic. Furthermore, imaging–pathology–polarization-sensitive micro-optical coherence tomography^{125,202} correlation of specific MSU deposit locations would eliminate the potential of imaging artefacts.

Confirming the presence of MSU crystals in the renal medulla

Cross-sectional studies suggest that MSU crystals can deposit in the renal medulla of patients with severe gout^{128,203}, which is consistent with gouty nephropathy, an entity that was previously proposed but largely dismissed. Although compelling, these findings require replication in other populations, ideally in the form of a blinded multi-site study with standardized reading by multiple radiologists.

Mendelian randomization studies of the potential impact of gout on CMR risk

Largely owing to a lack of genome-wide association study (GWAS) data for gout specifically, most of the known 'gout' genetic variants^{48,204} have only been identified through their associations with serum urate, which is necessary but not sufficient to cause gout. Emerging large-scale GWAS data for patients with gout should enhance our understanding of the genetic architecture of gout and facilitate comprehensive Mendelian randomization analyses of the potential causal effects of gout on CMR comorbidities, independent of hyperuricaemia.

Omics profiling

Omics approaches such as metabolomics can enhance prediction of incident cardiovascular events in people with rheumatic conditions^{205,206}. Similar metabolomic profiling and integration with the forthcoming Global Gout GWAS data (multi-omics)²⁰⁵ could help to clarify the mechanisms and prognosticate the risk of CMR comorbidities among patients with gout.

Table 2 | Key randomized trials of urate-lowering drugs for CMR outcomes

Trial (design)	Population (n)	Interventions	Results (CMR outcomes)	Comments	Ref.
Trials in patients without gout					
CKD-FIX (double-blind)	Adults with stage 3–4 CKD (369)	Allopurinol versus placebo (2 years)	Primary: no renal progression difference Secondary: deaths with allopurinol versus placebo HR 1.9 (95% CI 0.7–5.1)	Serum urate reduction difference = 2.7 mg/dl	87
PERL (double-blind)	Adults with T1DM with GFR of 40.0 to 99.9, serum urate >4.5 mg/dl (530)	Allopurinol versus placebo (3 years, plus 2-month washout)	Primary: no renal progression difference Secondary: fatal or non-fatal CV events HR 1.9 (95% CI 0.8–4.5) for allopurinol versus placebo	Serum urate reduction difference = 2.4 mg/dl	86
MODERATE (double-blind)	Overweight or obese adults with serum urate ≥5 mg/dl (149)	Allopurinol versus probenecid versus placebo (8 weeks)	Primary: no improvement in renin–angiotensin activities (unlike animal studies) Secondary: no improvement in mean 24-h blood pressure or mean blood pressure	Serum urate reduction difference = 3.2 mg/dl (allopurinol group)	83
Noman et al. (2010) (double-blind, crossover)	Adults with coronary artery disease (65)	Allopurinol (600 mg daily) versus placebo for 6 weeks × 2 (crossover)	Primary: allopurinol improved time to ST depression Secondary: allopurinol improved total exercise time and time to chest pain	Serum urate reduction difference = 3.7 mg/dl (allopurinol group)	89
SURPHER (double-blind, crossover)	Young adults (18–40 years of age) with hypertension; serum urate ≥5.0 mg/dl for men or ≥4.0 mg/dl for women; no diabetes mellitus (99)	Allopurinol (300 mg daily) versus placebo for 4 weeks × 2 (crossover)	No change in SBP or hsCRP levels	Serum urate reduction difference = 1.3 mg/dl (allopurinol phase)	84
ALL-HEARTS (PROBE design)	Adults ≥60 years of age with ischaemic heart disease (5,938)	Allopurinol (up to 600 mg daily)	Data collection completed and results pending	Results pending	96
Soletsky et al. (2012) (double-blind)	Prehypertensive adolescents with obesity (60)	Allopurinol versus probenecid versus placebo (8 weeks)	Primary: both drugs improved blood pressure Secondary: both drugs improved systemic vascular resistance	Serum urate reduction difference = 2.8 mg/dl (allopurinol group)	82
Feig et al. (2008) (double-blind, crossover)	Adolescents with stage 1 hypertension and serum urate ≥6 mg/dl (30)	Allopurinol (400 mg daily) versus placebo for 4 weeks × 2 (crossover)	Primary: allopurinol improved casual blood pressure Secondary: allopurinol led to a higher rate of blood pressure normalization	Serum urate reduction difference = 2.8 mg/dl (allopurinol phase)	81
Trials in patients with gout					
CARES (double-blind)	Patients with gout and a history of major CVD (6,190)	Febuxostat TTT versus allopurinol TTT (32 months)	Primary: no change in MACE risk (HR 1.03) Secondary: ↑ risk of CV mortality (HR 1.34) and all-cause mortality (HR 1.22)	45% loss to follow up	130
FAST (PROBE design)	Patients with gout and a cardiovascular risk factor (6,128)	Febuxostat TTT versus allopurinol TTT (48 months)	Primary: no change in MACE risk (HR 0.85) Secondary: no change in CV mortality (HR 0.75) and all-cause mortality (HR 0.91)	6% loss to follow up; mean follow up serum urate level 3.6 mg/dl in febuxostat group and 5.0 mg/dl in allopurinol group	133
Nurse-led TTT (open-label)	Patients with gout and a recent flare (517)	Nurse-led TTT versus usual care (24 months)	Additional: no difference in renal function or BMI	15% loss to follow up; serum urate reduction difference = 3.2 mg/dl (TTT group)	138
VA CSP trial (double-blind)	Patients with gout and a recent flare (940)	Febuxostat TTT versus allopurinol TTT (18 months)	Additional: no evidence of increased cardiovascular toxicity with febuxostat compared with allopurinol	21% loss to follow up	199

BMI, body mass index; CKD, chronic kidney disease; CMR, cardiometabolic–renal; CV, cardiovascular; CVD, cardiovascular disease; GFR, glomerular filtration rate; HR, hazard ratio; hsCRP, high-sensitivity C-reactive protein; MACE, major adverse cardiovascular event; PROBE, prospective, randomized, open-label, blinded end point; SBP, systolic blood pressure; SU, serum urate; T1DM, type 1 diabetes mellitus; TTT, treat-to-target.

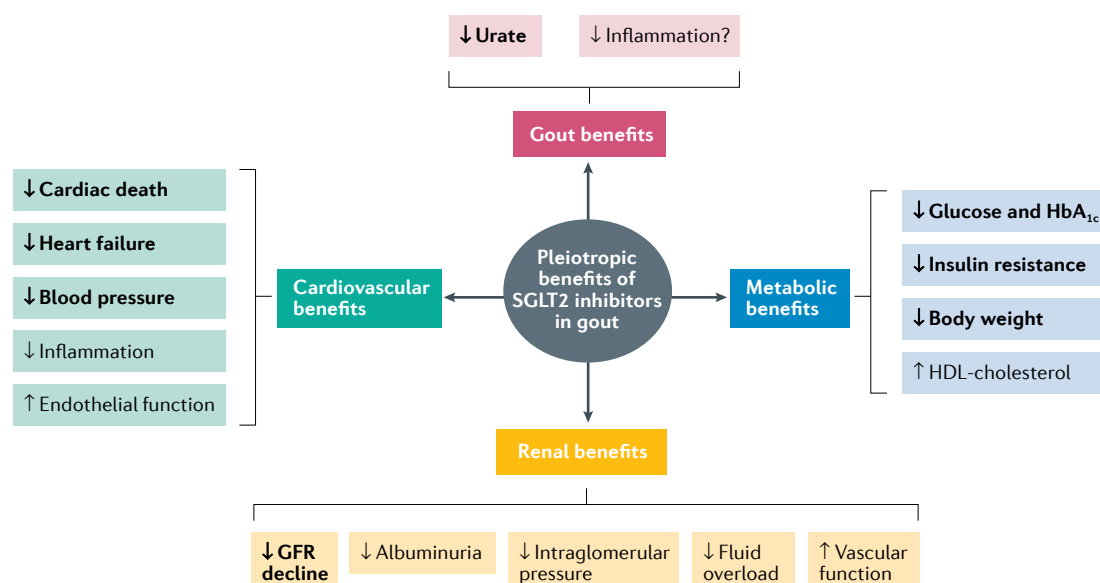


Fig. 3 | Pleiotropic benefits of SGLT2 inhibitors in gout and CMR comorbidities. The pleiotropic cardiometabolic-renal (CMR) benefits of sodium–glucose cotransporter 2 (SGLT2) inhibitors, which have been demonstrated in people with and without type 2 diabetes mellitus^{101,103}, include improvements in metabolic parameters (blue), and reduction in the risk of chronic kidney disease progression (yellow), major cardiovascular events (green) and premature mortality⁹⁷. These multiple benefits are highly relevant to comprehensive gout comorbidity care, as is the urate-lowering property of SGLT2 inhibitors^{98–100} and their apparent ability to reduce the risk of incident gout⁹⁹ (red). Key comorbidities in gout are indicated in bold. GFR, glomerular filtration rate; HbA_{1c}, glycated haemoglobin; HDL, high-density lipoprotein.

The most frequent comorbidity of gout is hypertension (74%)¹⁵, for which medication selection may therefore be of particular importance (FIG. 1). Although thiazide diuretics (such as hydrochlorothiazide and bendroflumethiazide) and beta blockers (such as propranolol) have been shown to increase serum urate concentrations in short-term studies^{104,105}, calcium channel blockers (amlodipine, nifedipine and diltiazem) and losartan (which has uricosuric effects through inhibition of URAT1) have demonstrated urate-lowering effects^{106–112} (Supplementary Box 1). Indeed, several population-based studies have confirmed a lower risk of incident gout associated with prior use of calcium channel blockers or losartan among patients with hypertension, whereas diuretics, beta blockers, angiotensin-converting enzyme inhibitors and non-losartan angiotensin II receptor antagonists were associated with an increased risk of gout^{113,114}. Thus, strategic choice of antihypertensive agents could provide additional benefits by simultaneously treating both hypertension and hyperuricaemia or gout.

Similarly, in a randomized controlled trial, fenofibrate lowered serum urate concentrations by 20% through inhibition of URAT1 (Supplementary Box 1) and almost halved the risk of incident gout over 5 years of treatment¹¹⁵. Fenofibrate could also be a useful adjunct treatment for preventing gout, particularly in patients with hypertriglyceridaemia and/or T2DM¹¹⁵.

MSU crystals in gout CMR pathogenesis

Beyond the potential effects of serum urate in gout CMR comorbidity pathogenesis discussed above, gout is also characterized by the presence of monosodium

urate (MSU) crystals that directly activate the NLRP3 inflammasome, which induces the release of potent pro-inflammatory cytokines such as interleukin-1 β (IL-1 β) and other inflammatory factors^{116–119} (FIG. 4). The NLRP3 inflammasome is also the link in CHD pathogenesis between vascular deposition of lipids and lipoproteins such as cholesterol crystals and the inflammatory responses driving the atherosclerotic process, a self-feeding cycle of cholesterol crystal formation and NLRP3 activation that contributes to chronic vascular inflammation¹²⁰. Phagocytosis of extracellular cholesterol crystals, as well as intracellular cholesterol crystal formation, causes lysosomal damage, which triggers NLRP3 inflammasome activation. Cholesterol crystals also activate the complement system, which promotes macrophage priming as well as cholesterol crystal phagocytosis and thereby NLRP3 activation. Secreted IL-1 β and IL-18 also promote macrophage priming via IL-1R signalling, contributing to the self-feeding cycle.

Interestingly, several dual-energy computed tomography studies of coronary arteries suggest that MSU crystals are deposited in the coronary arteries^{121–123}, with one study obtaining potential corroboration of this result in cadavers by detection of negatively birefringent, needle-like crystals diagnostic of MSU crystals by polarized light microscopy¹²¹. These MSU crystal deposits were detected in 86% of patients with gout (86%) but in only 15% of individuals without gout or other inflammatory rheumatic conditions (15%) and were associated with higher CT coronary calcium scores¹²¹ (a measure of arterial calcification). Although exciting, and with critical implications for the understanding of excess CHD risk in gout, these findings must be interpreted with caution

Beam-hardening artefacts

Phenomena that occur when lower energy photons are selectively attenuated as they pass through a dense object.

Partial volume effects

Phenomena that occur when tissues of widely different absorption are included in the same CT voxel, producing a beam attenuation that is proportional to the average value of the tissues within the voxel.

owing to potential beam-hardening artefacts (owing to adjacent calcified atheromas) and partial volume effects (owing to the averaging of attenuation properties of different materials)¹²⁴. Thus, these findings require confirmation in future studies involving robustly screened readings by multiple readers, ideally in a multi-centre study (BOX 1). Nevertheless, a post-mortem study compared the prevalence of coronary artery MSU crystals using cadaveric hearts from patients with gout and control individuals with a history of atherosclerotic cardiovascular disease (ASCVD) using polarization-sensitive micro-optical coherence tomography¹²⁵, a type of optical coherence tomography that can detect polarization changes in the light returning from the tissue sample¹²⁶. This study showed that the polarization-sensitive micro-optical coherence tomography-identified MSU crystals demonstrated negative birefringence by conventional polarized light microscopy, dissolved with uricase immersion and were significantly more abundant in patients with gout than in control individuals (12.4 versus 0.6 crystals/mm, $P < 0.05$)¹²⁵.

If the presence of MSU crystals in coronary plaques can be confirmed in future studies (BOX 1), it is possible that these crystals could play a self-feeding pro-inflammatory role in the pathogenesis of excess CHD

risk in gout, similar to that of cholesterol crystals in CHD (FIG. 4); targeting these inflammatory foci by removing MSU crystals (analogous to lowering cholesterol to remove cholesterol crystals) or blocking the inflammatory pathway could reduce CVD risk in gout¹¹⁹. The Canakinumab Anti-inflammatory Thrombosis Outcome Study (CANTOS) demonstrated that selective inhibition of IL-1 β lowered the risk of recurrent CV events¹²⁷, supporting this hypothesis. In addition, a parallel process may be occurring in the renal medulla, with a cross-sectional study of patients with untreated, severe gout reporting increased renal medullary echogenicity on renal ultrasonography suggestive of MSU deposits in 36% of 503 consecutive patients seen in a gout clinic in Vietnam¹²⁸. Similar findings were reported in 4 of 10 French patients with severe gout and thus these results, if replicated in future studies, might suggest the existence of gouty nephropathy, with implications for the management of CKD in patients with gout. In addition, reducing ongoing low-grade inflammation generated by MSU crystals in patients with gout could ameliorate the thrombotic or diabetogenic process^{29,129}. Finally, a reduced need for NSAIDs and glucocorticoids used for the prevention of gout flares associated with ULT could translate to CMR benefits.

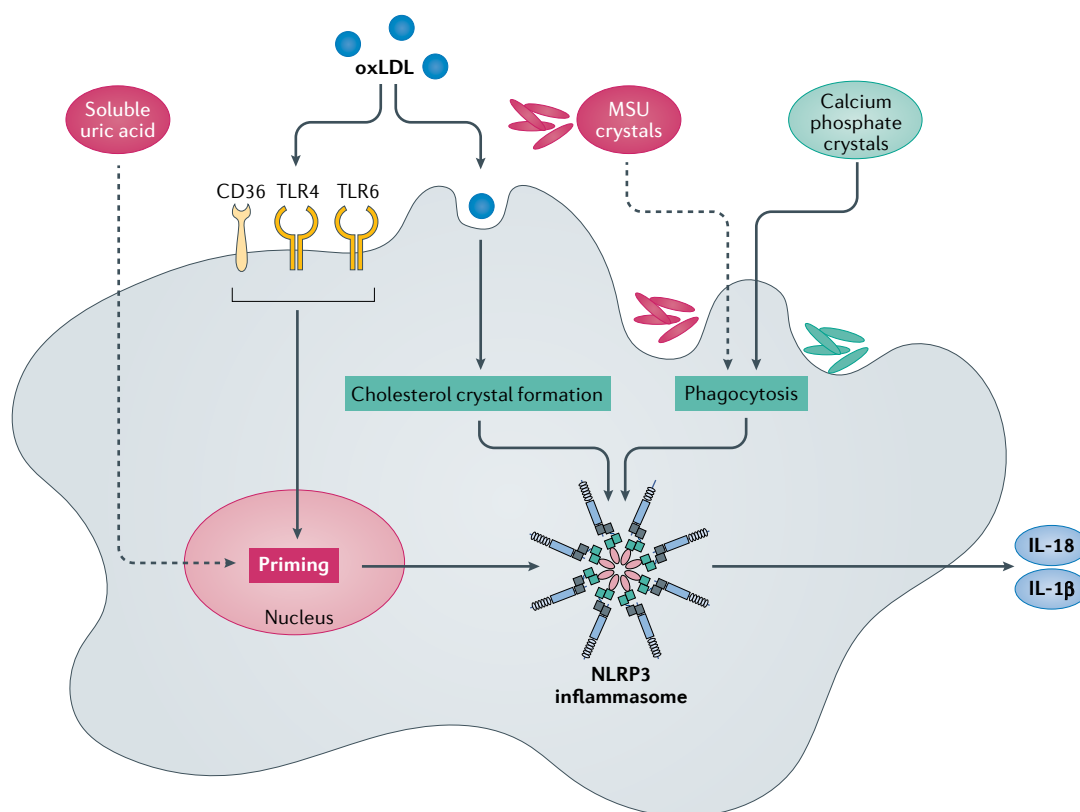


Fig. 4 | Shared inflammasome-pathway hypothesis: inflammation in gout and cardiovascular disease. In coronary heart disease (CHD), cholesterol crystals deposited in the vasculature activate the NLRP3 inflammasome, initiating inflammatory responses that drive the atherosclerotic process¹²⁰. This self-feeding cycle of cholesterol crystal formation and activation of inflammation contributes to chronic vascular inflammation. Similarly, in gout, monosodium urate (MSU) crystals have been proposed to form deposits in coronary plaques^{121–123}, where they could directly activate the NLRP3 inflammasome, which induces the release of potent pro-inflammatory cytokines including IL-1 β . In this way, MSU crystals could potentially play an analogous self-feeding pro-inflammatory role in the pathogenesis of excess CHD risk in gout as cholesterol crystals do in CHD. oxLDL, oxidized low-density lipoprotein.

CMR impact of ULT in gout

Several large-scale CV end-point trials have been conducted in patients with gout as part of a post-marketing safety requirement following FDA and EMA approval of the XO1 febuxostat (TABLE 2). The FDA-mandated Cardiovascular Safety of Febuxostat and Allopurinol in Patients With Gout and Cardiovascular Morbidities (CARES) trial, published in 2018, reported increased all-cause and CV-related mortality in participants receiving febuxostat compared with those receiving allopurinol^{130,131}, leading to a subsequent FDA black box warning for febuxostat use¹³². Conversely, the EMA-mandated Febuxostat versus Allopurinol Streamlined Trial (FAST)¹³³, published in 2020, found no increased risk of composite CV events or of CV or all-cause mortality for febuxostat compared with allopurinol¹³⁴. The two trials found that these two XOIs had comparable efficacy in lowering serum urate levels and gout flares.

Despite many differences between the CARES trial and FAST, the most critical distinction directly affecting validity is the difference in the loss to follow-up (45% in the CARES trial compared with 6% in FAST), leaving the CARES trial open to substantial selection bias¹³⁴ (extensively discussed elsewhere^{131,134,135}). This shortcoming of the CARES trial is also supported by its own post hoc ascertainment efforts nullifying the increased mortality risk associated with febuxostat¹³⁴. Finally, several large-scale pharmaco-epidemiological studies also support the FAST findings but not those of CARES^{136,137}. Consequently, FAST should be considered to have superior internal validity compared with the CARES trial, regardless of other differences, and the collective verdict on the CV safety of febuxostat should rely more on the results of FAST than of the CARES trial (that is, there is no difference in CV risk between the two XOIs)¹³⁴. In light of these considerations, the suggestion that regulatory agencies should update their guidance on the CV risk of febuxostat accordingly¹³³ seems reasonable.

Finally, trials with serum urate reduction as the primary end point in patients with gout^{138,139} did not find any consistent or apparent improvement in routine CMR outcomes, such as blood pressure, BMI and renal function, including a nurse-led treat-to-target intervention trial¹³⁸ (TABLE 2). Nevertheless, given the potential role of MSU crystals in the inflammatory pathogenesis of CMR comorbidities in gout, the potential impact of a treat-to-target serum urate approach on CMR end points is important to clarify in future trials, by rigorously choosing CMR end points with proper adjudication in correctly targeted gout populations (BOX 1).

CVD benefits of colchicine

To directly evaluate the inflammation pathway hypothesis in CVD pathogenesis, a series of randomized controlled trials of drugs that reduce relevant inflammatory steps have been conducted in patients with CVD. Although the CANTOS trial showed that interleukin-1 β inhibition with canakinumab lowers the risk of major CV events (by 12%)¹²⁷, four randomized controlled trials (COPS, COLCOT, LoDoCo and LoDoCo2) tested

the effect of colchicine (dosed at 0.5 mg daily except for COPS, in which it was dosed at 0.5 mg twice daily for 1 month and then 0.5 mg daily thereafter) in patients with various presentations of CVD (for example, COLCOT involved patients with CHD within 30 days of an MI, whereas LoDoCo2 involved those with chronic coronary disease). The central mechanism of colchicine's anti-inflammatory action is the inhibition of microtubule function leading to the inhibition of granulocyte function, interference with selectin expression and neutrophil-platelet interactions, and non-specific inhibition of the assembly of the inflammasome in cells of the innate immune system, including neutrophils, macrophages, monocytes and dendritic cells. These trials found that colchicine reduced the risk of a composite of major CV events by 23–35% compared with controls^{140–143}. Among participants with gout at baseline in CANTOS¹²⁷ and LoDoCo2¹⁴² (~8% in both trials), risk of gout flares during the trial was reduced by 50% and 60%, respectively. However, risk of fatal infection in participants receiving canakinumab was 72% higher than for placebo in the CANTOS trial¹²⁷, whereas colchicine treatment was associated with a small, statistically significant increased risk of pneumonia and non-CV deaths in LoDoCo2¹⁴² and COPS¹⁴⁰, respectively.

These data might be relevant for management of CVD in patients with gout. Given the dual benefits of colchicine (or canakinumab) in patients with gout who have CAD, we expect a more favourable risk/benefit ratio than in those without gout; however, potential long-term adverse effects of colchicine should be clarified and scrutinized further, particularly infection and potential tophus development (when colchicine is used alone, without effective control of serum urate).

Diagnosis of CMR comorbidities in gout

As gout and metabolic syndrome frequently coexist in patients with gout (63%), this is an important patient population to screen for prediabetes (that is, impaired glucose intolerance) and CV risk factors, including obesity, dyslipidaemia and hypertension^{144–148}. Indeed, hyperuricaemia might serve as a surrogate marker of metabolic syndrome, even in those without gout^{144–148}. Individuals deemed at a higher risk of metabolic syndrome or its sequelae should be encouraged to make lifestyle modifications that reduce harmful visceral adipose, intrahepatic and deep subcutaneous abdominal fat volume, and improve blood lipid profiles and insulin concentrations and resistance. These modifications should encompass physical activity^{149,150} and a healthy cardiometabolic diet, potentially even a 'green' Mediterranean diet emphasizing consumption of plant protein over red or processed meats and other animal proteins^{151,152}. If there is substantial impairment of glucose tolerance, management should also encompass the use of drugs to increase insulin sensitivity, including metformin or SGLT2 inhibitors, as discussed below.

In addition to screening for CMR comorbidities based on the usual clinical history and laboratory parameters, there might be an added benefit of incorporating non-invasive ASCVD screening modalities in a subset

of patients with hyperuricaemia and/or gout and CMR risk factors. Owing to the increasing recognition of ASCVD as an inflammatory disease¹⁵³, there have been concerns regarding the underestimation of ASCVD risk among patients with rheumatic conditions using traditional, general population-derived ASCVD risk estimators^{154–157}. Indeed, addition of a carotid plaque score (measured by carotid ultrasonography) as a risk stratification tool among patients with gout at intermediate risk of ASCVD resulted in the risk being upgraded in 56% of these patients¹⁵⁸. The American College of Cardiology and American Heart Association guidelines for the primary prevention of ASCVD endorse the addition of coronary artery calcium (CAC) scores (measured by coronary CT) among patients with borderline to intermediate ASCVD risk in whom treatment decisions regarding statins remain uncertain¹⁵⁹. CAC is a highly specific feature of coronary atherosclerosis, with the CAC score demonstrating sensitivities of 88–100% and negative predictive value of nearly 100% for obstructive CAD¹⁶⁰. The CAC score is a widely available, validated and reproducible measure for improving ASCVD risk stratification^{161–163} and consistently outperforms other measures, such as the carotid ultrasonography^{164,165}. However, additional studies are needed to determine the utility of CAC scoring for risk re-stratification among patients with gout; consequently, this remains an area of future investigation.

Lifestyle for gout CMR comorbidities

By helping to address obesity, metabolic syndrome and hyperuricaemia, the adoption of healthier lifestyle practices offers many downstream benefits relevant to gout and its CMR comorbidities (FIG. 2), analogous to the pleiotropic benefits of CMR drugs, such as SGLT2 inhibitors. Although many patients with gout require the substantial urate-lowering effects of XOIs to reduce serum urate concentrations below the urate saturation threshold and prevent recurrent flares, non-pharmacological approaches should form a cornerstone of comorbidity care for patients with or at risk of gout, even those on ULTs. The randomized controlled trials^{86,130,138,139} and Mendelian randomization studies (TABLE 1, TABLE 2) published to date show no evidence that lowering serum urate provides the CMR benefits^{86,130,138,139} that can be achieved through weight loss, increased physical activity and concordant improvements in dietary quality.

Although the traditional, low-purine dietary approach to gout management has focused on limiting protein intake to reduce purine loading¹³, this diet has limited palatability and sustainability, and leads to increased consumption of refined carbohydrates (including fructose, an established risk factor for hyperuricaemia, gout^{38–40,166}, obesity and multiple CMR conditions) and unhealthy saturated and trans fats^{13,167}. These nutrients could worsen insulin resistance, leading to elevated plasma concentrations of insulin, glucose, triglycerides and LDL cholesterol and decreased concentrations of HDL cholesterol, enhancing the risk of metabolic syndrome and CMR events^{13,167}. Furthermore, there is a growing body of evidence, including from secondary analyses of randomized controlled trials, that

healthy cardiometabolic diets demonstrated to reduce hypertension, obesity and CVD risk factors, including the Mediterranean^{168–170} and Dietary Approaches to Stop Hypertension (DASH)^{170–173} diets, can simultaneously reduce serum urate, risk of incident gout and potentially even the frequency of recurrent gout flares¹⁶⁷, by lowering insulin resistance and adiposity.

Personalized gout comorbidity care

To optimize long-term adherence to a healthy lifestyle and improve CMR risk profiles, the particular healthy dietary pattern adopted by a person with gout can be guided by their concurrent comorbidities and personal preferences and culinary traditions. Efforts to identify phenotypically distinct comorbidity clusters or subtypes in gout can inform this approach. A cluster analysis among a cohort of patients with gout in France¹⁷⁴ revealed five distinct comorbidity clusters: gout with few comorbidities or gout with obesity and hypertension; T2DM; dyslipidaemia; or cardiorenal disease. Similar analyses have been performed with the nationally representative NHANES data in the United States¹⁷⁵, and a prospective gout cohort in the UK¹⁷⁶, revealing that the types of incident comorbidities that participants developed over the following 5 years were related to their baseline cluster membership¹⁷⁷. FIGURE 5 illustrates a proposed personalized medicine framework based on these subtypes. For example, the DASH diet might be ideal for patients with hypertension. This diet can be implemented with caloric restriction for those hypertensive patients who are overweight or obese, whereas a protein-enriched version (used in the OmniHeart trial¹⁷⁸) is also available, and might lead to improved long-term adherence for some individuals. Those individuals who require improved lipid or glycaemic control could choose the Mediterranean diet, which improves HDL, triglycerides and markers of insulin resistance¹⁷⁹, whereas those with isolated gout could choose the DASH or Mediterranean diets, or base their food choices on the Alternative Healthy Eating Index¹⁸⁰, which emphasizes foods and nutrients consistently associated with a lower risk of chronic disease.

Just as the personalization of lifestyle recommendations to simultaneously target hyperuricaemia or gout and its CMR comorbidities is encouraged, a similar approach can be taken among patients whose CMR comorbidities are severe enough to require pharmacological management. Many existing treatment guidelines for CMR conditions already acknowledge the fact that some medications for a primary CMR indication might have pleiotropic benefits for a number of associated CMR conditions (Supplementary Box 1) and offer options for personalizing the treatment algorithm to fit the individual patient. The most notable example of this extended benefit can be seen with diabetes treatment guidelines as they pertain to SGLT2 inhibitors, given the multitude of CMR benefits as discussed above (FIG. 2, FIG. 3). Accordingly, multiple diabetes treatment guidelines, including the 2018 American Diabetes Association and European Association for the Study of Diabetes consensus report, 2019 ACR/American Heart Association practical guidelines, and 2019

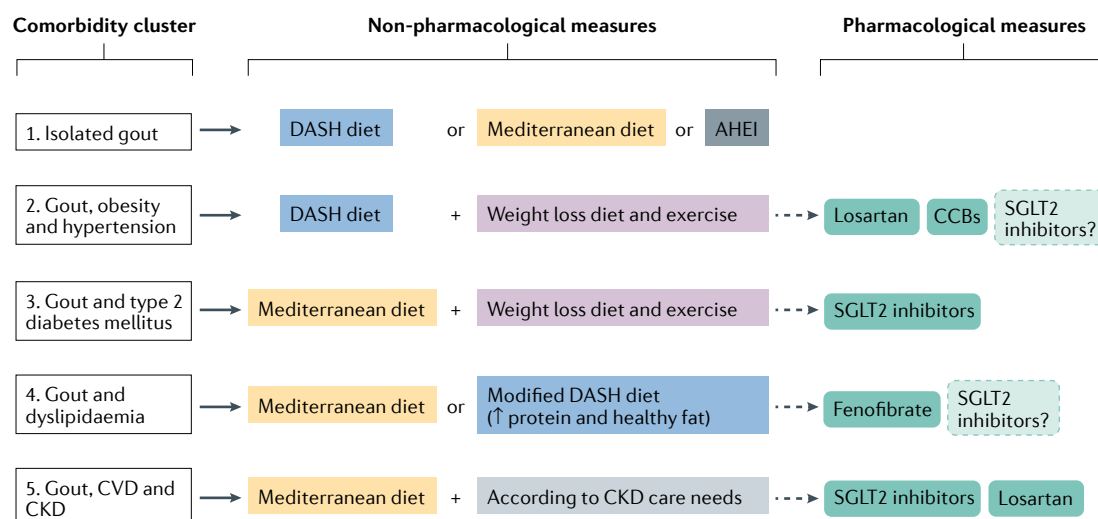


Fig. 5 | Proposed personalized medicine framework for comorbidity care in gout. The comorbidity care approach can be personalized based on the cluster of comorbidities in the patient, of which five have been recognized in one study¹⁷⁴. Non-pharmacological measures, such as dietary and lifestyle changes, and pharmacological measures, such as urate-lowering therapy (not shown), fenofibrate, sodium–glucose cotransporter 2 (SGLT2) inhibitors (glucosuric antidiabetic drugs such as canagliflozin, dapagliflozin and empagliflozin) and antihypertensive drugs (such as calcium channel blockers (CCBs) and losartan), can be combined to optimize care. Dietary approaches include the Mediterranean diet, the conventional Dietary Approaches to Stop Hypertension (DASH) diet^{171,172} or a modified version of the DASH diet enriched with protein or monounsaturated fat¹⁷⁸, as well as diets with a high Alternative Healthy Eating Index (AHEI) score. The question mark indicates conditions for which evidence of the clinical efficacy of SGLT2 inhibitors is limited. CKD, chronic kidney disease; CVD, cardiovascular disease.

European Society of Cardiology guidelines, all recommend the preferential use of SGLT2 inhibitors with or without metformin among patients with select CMR comorbidities or risk factors¹⁸¹. SGLT2 inhibitors have been approved by the FDA since 2013 and the EMA since 2016 for diabetes care, whereas the indication for heart failure and CKD (regardless of diabetes) has been approved by the US FDA starting in 2020 (dapagliflozin for heart failure and CKD and empagliflozin for heart failure) based on landmark trial results^{101–103}; it is anticipated that other countries will similarly approve these SGLT2 inhibitors for other indications in due course.

Other management approaches for CMR comorbidities and risk factors (for example, smoking cessation) should similarly be pursued in an evidence-based manner, but with particular attention to medications that might simultaneously address or benefit two or more comorbidities.

Conclusions

Although the frequency and burden of gout have been rising globally, evidence has also been building that is improving our understanding of the pathogenetic mechanisms underlying the excess CMR comorbidity burden in gout, as well as providing innovative, potentially more effective treatment options. Indeed, the pleiotropic CMR and urate-lowering benefits of various CMR agents, such as SGLT2 inhibitors, calcium channel blockers, losartan and fenofibrate, could play an important role in the management of gout CMR comorbidities and facilitate the provision of comprehensive gout care. The combination of these CMR drugs with conventional ULT, adherence to healthy cardiometabolic diets and adoption of other evidence-based, personalized lifestyle measures would enable the simultaneous management of serum urate concentrations, adiposity and CMR risk factors.

Published online 17 December 2021

- Choi, H. K., Ford, E. S., Li, C. & Curhan, G. Prevalence of the metabolic syndrome in patients with gout: the Third National Health and Nutrition Examination Survey. *Arthritis Rheum.* **57**, 109–115 (2007).
- Choi, H. K. & Curhan, G. Independent impact of gout on mortality and risk for coronary heart disease. *Circulation* **116**, 894–900 (2007).
- Krishnan, E., Svendsen, K., Neaton, J. D., Grandits, G. & Kuller, L. H. Long-term cardiovascular mortality among middle-aged men with gout. *Arch. Intern. Med.* **168**, 1104–1110 (2008).
- Kuo, C. F., Grainger, M. J., Mallen, C., Zhang, W. & Doherty, M. Rising burden of gout in the UK but continuing suboptimal management: a nationwide population study. *Ann. Rheum. Dis.* **74**, 661–667 (2015).
- Rai, S. K. et al. Rising incidence and prevalence of gout in the Canadian general population. *Arthritis Rheumatol.* **67**, 292–294 (2015).
- Arromdee, E., Michet, C. J., Crowson, C. S., O'Fallon, W. M. & Gabriel, S. E. Epidemiology of gout: is the incidence rising? *J. Rheumatol.* **29**, 2403–2406 (2002).
- Elfishawi, M. M. et al. The rising incidence of gout and the increasing burden of comorbidities: a population-based study over 20 Years. *J. Rheumatol.* **45**, 574–579 (2018).
- Klemp, P., Stansfield, S. A., Castle, B. & Robertson, M. C. Gout is on the increase in New Zealand. *Ann. Rheum. Dis.* **56**, 22–26 (1997).
- Miao, Z. et al. Dietary and lifestyle changes associated with high prevalence of hyperuricemia and gout in the Shandong coastal cities of Eastern China. *J. Rheumatol.* **35**, 1859–1864 (2008).
- Cassim, B., Mody, G. M., Deenadayalu, V. K. & Hammond, M. G. Gout in black South Africans: a clinical and genetic study. *Ann. Rheum. Dis.* **53**, 759–762 (1994).
- Xia, Y. et al. Global, regional and national burden of gout, 1990–2017: a systematic analysis of the global burden of disease study. *Rheumatology* **59**, 1529–1538 (2020).
- Safiri, S. et al. Prevalence, incidence, and years lived with disability due to gout and its attributable risk factors for 195 countries and territories 1990–2017: a systematic analysis of the global burden of disease study 2017. *Arthritis Rheumatol.* **72**, 1916–1927 (2020).
- Fam, A. G. Gout, diet, and the insulin resistance syndrome. *J. Rheumatol.* **29**, 1350–1355 (2002).
- Choi, H. K., Mount, D. B. & Reginato, A. M. Pathogenesis of gout. *Ann. Intern. Med.* **143**, 499–516 (2005).
- Zhu, Y., Pandya, B. J. & Choi, H. K. Comorbidities of gout and hyperuricemia in the US general population: NHANES 2007–2008. *Am. J. Med.* **125**, 679–687 e671 (2012).

16. Sandoval-Plata, G., Nakafero, G., Chakravorty, M., Morgan, K. & Abhishek, A. Association between serum urate, gout and comorbidities: a case-control study using data from the UK biobank. *Rheumatology* **60**, 3243–3251 (2021).
17. Landgren, A. J., Dehlin, M., Jacobsson, L., Bergsten, U. & Klingberg, E. Cardiovascular risk factors in gout, psoriatic arthritis, rheumatoid arthritis and ankylosing spondylitis: a cross-sectional survey of patients in Western Sweden. *RMD Open* **7**, e001568 (2021).
18. England, B. et al. Multimorbidity in rheumatoid arthritis, psoriatic arthritis, gout, and osteoarthritis within the rheumatology informatics system for effectiveness (RISE) registry [abstract]. *Arthritis Rheum.* **72**, 111 (2020).
19. Elfshawi, M. M. et al. Changes in the presentation of incident gout and the risk of subsequent flares: a population-based study over 20 years. *J. Rheumatol.* **47**, 613–618 (2020).
20. Fisher, M. C., Rai, S. K., Lu, N., Zhang, Y. & Choi, H. K. The unclosing premature mortality gap in gout: a general population-based study. *Ann. Rheum. Dis.* **76**, 1289–1294 (2017).
21. Zhang, Y. et al. Improved survival in rheumatoid arthritis: a general population-based cohort study. *Ann. Rheum. Dis.* **76**, 408–413 (2017).
22. Richette, P. et al. Improving cardiovascular and renal outcomes in gout: what should we target? *Nat. Rev. Rheumatol.* **10**, 654–661 (2014).
23. Kim, S. Y. et al. Hyperuricemia and coronary heart disease: a systematic review and meta-analysis. *Arthritis Care Res.* **62**, 170–180 (2010).
24. Kim, S. Y. et al. Hyperuricemia and risk of stroke: a systematic review and meta-analysis. *Arthritis Rheum.* **61**, 885–892 (2009).
25. Grayson, P. C., Kim, S. Y., LaValley, M. & Choi, H. K. Hyperuricemia and incident hypertension: a systematic review and meta-analysis. *Arthritis Care Res.* **63**, 102–110 (2011).
26. Abbott, R. D., Brand, F. N., Kannel, W. B. & Castelli, W. P. Gout and coronary heart disease: the Framingham study. *J. Clin. Epidemiol.* **41**, 237–242 (1988).
27. Krishnan, E., Baker, J. F., Furst, D. E. & Schumacher, H. R. Gout and the risk of acute myocardial infarction. *Arthritis Rheum.* **54**, 2688–2696 (2006).
28. Baker, J. F., Schumacher, H. R. & Krishnan, E. Serum uric acid level and risk for peripheral arterial disease: analysis of data from the multiple risk factor intervention trial. *Angiology* **58**, 450–457 (2007).
29. Choi, H. K., De Vera, M. A. & Krishnan, E. Gout and the risk of type 2 diabetes among men with a high cardiovascular risk profile. *Rheumatology* **47**, 1567–1570 (2008).
30. Rho, Y. H. et al. Independent impact of gout on the risk of diabetes mellitus among women and men: a population-based, BMI-matched cohort study. *Ann. Rheum. Dis.* **75**, 91–95 (2016).
31. Roughley, M. et al. Risk of chronic kidney disease in patients with gout and the impact of urate lowering therapy: a population-based cohort study. *Arthritis Res. Ther.* **20**, 243 (2018).
32. Kuo, C. F., Grainger, M. J., Mallen, C., Zhang, W. & Doherty, M. Comorbidities in patients with gout prior to and following diagnosis: case-control study. *Ann. Rheum. Dis.* **75**, 210–217 (2016).
33. De Vera, M. A., Rahman, M. M., Bhole, V., Kopec, J. A. & Choi, H. K. Independent impact of gout on the risk of acute myocardial infarction among elderly women: a population-based study. *Ann. Rheum. Dis.* **69**, 1162–1164 (2010).
34. Krishnan, E., Pandya, B. J., Chung, L., Hariri, A. & Dabbous, O. Hyperuricemia in young adults and risk of insulin resistance, prediabetes, and diabetes: a 15-year follow-up study. *Am. J. Epidemiol.* **176**, 108–116 (2012).
35. Choi, H. K., Atkinson, K., Karlson, E. W. & Curhan, G. Obesity, weight change, hypertension, diuretic use, and risk of gout in men: the health professionals follow-up study. *Arch. Intern. Med.* **165**, 742–748 (2005).
36. Choi, H. K. et al. Population impact attributable to modifiable risk factors for hyperuricemia. *Arthritis Rheumatol.* **72**, 157–165 (2020).
37. McCormick, N. et al. Estimation of primary prevention of gout in men through modification of obesity and other key lifestyle factors. *JAMA Netw. Open* **3**, e2027421 (2020).
38. Choi, H. K. & Curhan, G. Soft drinks, fructose consumption, and the risk of gout in men: prospective cohort study. *BMJ* **336**, 309–312 (2008).
39. Choi, H. K., Willett, W. & Curhan, G. Fructose-rich beverages and risk of gout in women. *JAMA* **304**, 2270–2278 (2010).
40. Gao, X. et al. Intake of added sugar and sugar-sweetened drink and serum uric acid concentration in US men and women. *Hypertension* **50**, 306–312 (2007).
41. Kim, S. C. et al. Cardiovascular risks of probenecid versus allopurinol in older patients with gout. *J. Am. Coll. Cardiol.* **71**, 994–1004 (2018).
42. Hay, C. A., Prior, J. A., Belcher, J., Mallen, C. D. & Roddy, E. Mortality in patients with gout treated with allopurinol: a systematic review and meta-analysis. *Arthritis Care Res.* **73**, 1049–1054 (2021).
43. Weisman, A. et al. Allopurinol and renal outcomes in adults with and without type 2 diabetes: a retrospective, population-based cohort study and propensity score analysis. *Can. J. Diabetes* **45**, 641–649.e4 (2021).
44. Suissa, S., Suissa, K. & Hudson, M. Effectiveness of allopurinol on reducing mortality: time-related biases in observational studies. *Arthritis Rheumatol.* **73**, 1749–1757 (2021).
45. Suissa, S., Suissa, K. & Hudson, M. Allopurinol and cardiovascular events: time-related biases in observational studies. *Arthritis Care Res.* <https://doi.org/10.1002/acr.24713> (2021).
46. Pierce, B. L. & Burgess, S. Efficient design for Mendelian randomization studies: subsample and 2-sample instrumental variable estimators. *Am. J. Epidemiol.* **178**, 1177–1184 (2013).
47. Davies, N. M., Holmes, M. V. & Davey Smith, G. Reading Mendelian randomisation studies: a guide, glossary, and checklist for clinicians. *BMJ* **362**, k601 (2018).
48. Tin, A. et al. Target genes, variants, tissues and transcriptional pathways influencing human serum urate levels. *Nat. Genet.* **51**, 1459–1474 (2019).
49. Choi, J. W., McCormick, N., Marozoff, S., De Vera, M. & Choi, H. K. The impact of genetically determined serum urate levels on the development of cardiovascular diseases: a systematic review and meta-analysis of Mendelian randomization studies [abstract]. *Ann. Rheum. Dis.* <https://doi.org/10.1136/annrheumdis-2020-eular.6191> (2020).
50. Sumpter, N. A., Saag, K. G., Reynolds, R. J. & Merriman, T. R. Comorbidities in gout and hyperuricemia: causality or epiphenomena? *Curr. Opin. Rheumatol.* **32**, 126–133 (2020).
51. Li, X. et al. Serum uric acid levels and multiple health outcomes: umbrella review of evidence from observational studies, randomised controlled trials, and Mendelian randomisation studies. *BMJ* **357**, j2576 (2017).
52. Keerman, M. et al. Mendelian randomization study of serum uric acid levels and diabetes risk: evidence from the Dongfeng-Tongji cohort. *BMJ Open Diabetes Res. Care* **8**, e000834 (2020).
53. Elfstathiadou, A., Gill, D., McGrane, F., Quinn, T. & Dawson, J. Genetically determined uric acid and the risk of cardiovascular and neurovascular diseases: a Mendelian randomization study of outcomes investigated in randomized trials. *J. Am. Heart Assoc.* **8**, e012738 (2019).
54. Yang, Q. et al. Multiple genetic loci influence serum urate levels and their relationship with gout and cardiovascular disease risk factors. *Circ. Cardiovasc. Genet.* **3**, 523–530 (2010).
55. Li, X. et al. MR-PheWAS: exploring the causal effect of SUA level on multiple disease outcomes by using genetic instruments in UK Biobank. *Ann. Rheum. Dis.* **77**, 1039–1047 (2018).
56. Li, X. et al. Genetically determined serum urate levels and cardiovascular and other diseases in UK Biobank cohort: a phenotype-wide mendelian randomization study. *PLoS Med.* **16**, e1002937 (2019).
57. Si, S. et al. Causal pathways from body components and regional fat to extensive metabolic phenotypes: a Mendelian randomization study. *Obesity* **28**, 1536–1549 (2020).
58. Palmer, T. M. et al. Association of plasma uric acid with ischaemic heart disease and blood pressure: Mendelian randomisation analysis of two large cohorts. *BMJ* **347**, f4262 (2013).
59. Wang, L., Zhang, T., Liu, Y., Tang, F. & Xue, F. Association of serum uric acid with metabolic syndrome and its components: a Mendelian randomization analysis. *Biomed. Res. Int.* **2020**, 6238693 (2020).
60. Parsa, A. et al. Genotype-based changes in serum uric acid affect blood pressure. *Kidney Int.* **81**, 502–507 (2012).
61. Gill, D. et al. Urate, blood pressure, and cardiovascular disease: evidence from Mendelian randomization and meta-analysis of clinical trials. *Hypertension* **77**, 383–392 (2021).
62. Biradar, M. I., Chiang, K. M., Yang, H. C., Huang, Y. T. & Pan, W. H. The causal role of elevated uric acid and waist circumference on the risk of metabolic syndrome components. *Int. J. Obes.* **44**, 865–874 (2020).
63. Mallamaci, F. et al. A polymorphism in the major gene regulating serum uric acid associates with clinic SBP and the white-coat effect in a family-based study. *J. Hypertens.* **32**, 1621–1628 (2014). discussion 1628.
64. Sedaghat, S. et al. Association of uric acid genetic risk score with blood pressure: the Rotterdam study. *Hypertension* **64**, 1061–1066 (2014).
65. Lyngdoh, T. et al. Serum uric acid and adiposity: deciphering causality using a bidirectional Mendelian randomization approach. *PLoS One* **7**, e39321 (2012).
66. Rasheed, H., Hughes, K., Flynn, T. J. & Merriman, T. R. Mendelian randomization provides no evidence for a causal role of serum urate in increasing serum triglyceride levels. *Circ. Cardiovasc. Genet.* **7**, 830–837 (2014).
67. Yu, X., Wang, T., Huang, S. & Zeng, P. Evaluation of the causal effects of blood lipid levels on gout with summary level GWAS data: two-sample Mendelian randomization and mediation analysis. *J. Hum. Genet.* **66**, 465–473 (2021).
68. McCormick, N. et al. Assessing the causal relationships between insulin resistance and hyperuricemia and gout using bidirectional Mendelian randomization. *Arthritis Rheumatol.* **73**, 2096–2104 (2021).
69. Chen, J. et al. The trans-ancestral genomic architecture of glycemic traits. *Nat. Genet.* **53**, 840–860 (2021).
70. Ter Maaten, J. C. et al. Renal handling of urate and sodium during acute physiological hyperinsulinaemia in healthy subjects. *Clin. Sci.* **92**, 51–58 (1997).
71. Muscelli, E. et al. Effect of insulin on renal sodium and uric acid handling in essential hypertension. *Am. J. Hypertens.* **9**, 746–752 (1996).
72. Johnson, R. J. et al. Is there a pathogenetic role for uric acid in hypertension and cardiovascular and renal disease? *Hypertension* **41**, 1183–1190 (2003).
73. Mene, P. & Punzo, G. Uric acid: bystander or culprit in hypertension and progressive renal disease? *J. Hypertens.* **26**, 2085–2092 (2008).
74. Khosla, U. M. et al. Hyperuricemia induces endothelial dysfunction. *Kidney Int.* **67**, 1739–1742 (2005).
75. Farquharson, C. A., Butler, R., Hill, A., Belch, J. J. & Struthers, A. D. Allopurinol improves endothelial dysfunction in chronic heart failure. *Circulation* **106**, 221–226 (2002).
76. Doehner, W. et al. Effects of xanthine oxidase inhibition with allopurinol on endothelial function and peripheral blood flow in hyperuricemic patients with chronic heart failure: results from 2 placebo-controlled studies. *Circulation* **105**, 2619–2624 (2002).
77. Rao, G. N., Corson, M. A. & Berk, B. C. Uric acid stimulates vascular smooth muscle cell proliferation by increasing platelet-derived growth factor A-chain expression. *J. Biol. Chem.* **266**, 8604–8608 (1991).
78. Mazzali, M. et al. Hyperuricemia induces a primary renal arteriopathy in rats by a blood pressure-independent mechanism. *Am. J. Physiol. Renal Physiol.* **282**, F991–F997 (2002).
79. Toma, I., Kan, J., Meer, E. & Pet-Peterdi, J. Uric acid triggers renin release via a macula densa-dependent pathway. *J. Am. Soc. Nephrol.* **18**, 156A (2007).
80. Mazzali, M. et al. Elevated uric acid increases blood pressure in the rat by a novel crystal-independent mechanism. *Hypertension* **38**, 1101–1106 (2001).
81. Feig, D. I., Soletsky, B. & Johnson, R. J. Effect of allopurinol on blood pressure of adolescents with newly diagnosed essential hypertension: a randomized trial. *JAMA* **300**, 924–932 (2008).
82. Soletsky, B. & Feig, D. I. Uric acid reduction rectifies prehypertension in obese adolescents. *Hypertension* **60**, 1148–1156 (2012).
83. McMullan, C. J., Borgi, L., Fisher, N., Curhan, G. & Forman, J. Effect of uric acid lowering on renin-angiotensin-system activation and ambulatory BP: a randomized controlled trial. *Clin. J. Am. Soc. Nephrol.* **12**, 807–816 (2017).
84. Gaffo, A. L. et al. Effect of serum urate lowering with allopurinol on blood pressure in young adults: a randomized, controlled, crossover trial. *Arthritis Rheumatol.* **73**, 1514–1522 (2021).

85. Johnson, R. J. et al. Essential hypertension, progressive renal disease, and uric acid: a pathogenetic link? *J. Am. Soc. Nephrol.* **16**, 1909–1919 (2005).
86. Doria, A. et al. Serum urate lowering with allopurinol and kidney function in type 1 diabetes. *N. Engl. J. Med.* **382**, 2493–2503 (2020).
87. Badve, S. V. et al. Effects of allopurinol on the progression of chronic kidney disease. *N. Engl. J. Med.* **382**, 2504–2513 (2020).
88. George, J., Carr, E., Davies, J., Belch, J. J. & Struthers, A. High-dose allopurinol improves endothelial function by profoundly reducing vascular oxidative stress and not by lowering uric acid. *Circulation* **114**, 2508–2516 (2006).
89. Noman, A., Ang, D. S., Ogston, S., Lang, C. C. & Struthers, A. D. Effect of high-dose allopurinol on exercise in patients with chronic stable angina: a randomised, placebo controlled crossover trial. *Lancet* **375**, 2161–2167 (2010).
90. Berry, C. E. & Hare, J. M. Xanthine oxidoreductase and cardiovascular disease: molecular mechanisms and pathophysiological implications. *J. Physiol.* **555**, 589–606 (2004).
91. Rajagopalan, S., Meng, X. P., Ramasamy, S., Harrison, D. G. & Galis, Z. S. Reactive oxygen species produced by macrophage-derived foam cells regulate the activity of vascular matrix metalloproteinases in vitro. Implications for atherosclerotic plaque stability. *J. Clin. Invest.* **98**, 2572–2579 (1996).
92. Takimoto, E. & Kass, D. A. Role of oxidative stress in cardiac hypertrophy and remodeling. *Hypertension* **49**, 241–248 (2007).
93. Rajendra, N. S. et al. Mechanistic insights into the therapeutic use of high-dose allopurinol in angina pectoris. *J. Am. Coll. Cardiol.* **58**, 820–828 (2011).
94. Khatib, S. Y., Farah, H. & El-Migdadi, F. Allopurinol enhances adenine nucleotide levels and improves myocardial function in isolated hypoxic rat heart. *Biochemistry* **66**, 328–333 (2001).
95. Hirsch, G. A., Bottomley, P. A., Gerstenblith, G. & Weiss, R. G. Allopurinol acutely increases adenosine triphosphate energy delivery in failing human hearts. *J. Am. Coll. Cardiol.* **59**, 802–808 (2012).
96. Mackenzie, I. S. et al. Multicentre, prospective, randomised, open-label, blinded end point trial of the efficacy of allopurinol therapy in improving cardiovascular outcomes in patients with ischaemic heart disease: protocol of the ALL-HEART study. *BMJ Open* **6**, e013774 (2016).
97. Khunti, K. SGLT2 inhibitors in people with and without T2DM. *Nat. Rev. Endocrinol.* **17**, 75–76 (2021).
98. Bailey, C. J. Uric acid and the cardio-renal effects of SGLT2 inhibitors. *Diabetes Obes. Metab.* **21**, 1291–1298 (2019).
99. Fralick, M., Chen, S. K., Paterno, E. & Kim, S. C. Assessing the risk for gout with sodium-glucose cotransporter-2 inhibitors in patients with type 2 diabetes: a population-based cohort study. *Ann. Intern. Med.* **172**, 186–194 (2020).
100. Zhao, Y. et al. Effects of sodium-glucose co-transporter 2 (SGLT2) inhibitors on serum uric acid level: a meta-analysis of randomized controlled trials. *Diabetes Obes. Metab.* **20**, 458–462 (2018).
101. Packer, M. et al. Cardiovascular and renal outcomes with empagliflozin in heart failure. *N. Engl. J. Med.* **383**, 1413–1424 (2020).
102. McMurray, J. J. V. et al. Dapagliflozin in patients with heart failure and reduced ejection fraction. *N. Engl. J. Med.* **381**, 1995–2008 (2019).
103. Heerspink, H. J. L. et al. Dapagliflozin in patients with chronic kidney disease. *N. Engl. J. Med.* **383**, 1436–1446 (2020).
104. Reyes, A. J. Cardiovascular drugs and serum uric acid. *Cardiovasc. Drugs Ther.* **17**, 397–414 (2003).
105. No authors listed. Adverse reactions to benidrofualazine and propranolol for the treatment of mild hypertension. Report of medical research council working party on mild to moderate hypertension. *Lancet* **2**, 539–543 (1981).
106. Burnier, M., Waeber, B. & Brunner, H. R. Clinical pharmacology of the angiotensin II receptor antagonist losartan potassium in healthy subjects. *J. Hypertens. Suppl.* **13**, S23–S28 (1995).
107. Burnier, M., Roch-Ramel, F. & Brunner, H. R. Renal effects of angiotensin II receptor blockade in normotensive subjects. *Kidney Int.* **49**, 1787–1790 (1996).
108. Wurzner, G. et al. Comparative effects of losartan and irbesartan on serum uric acid in hypertensive patients with hyperuricaemia and gout. *J. Hypertens.* **19**, 1855–1860 (2001).
109. Minghelli, G., Seydoux, C., Goy, J. J. & Burnier, M. Uricosuric effect of the angiotensin II receptor antagonist losartan in heart transplant recipients. *Transplantation* **66**, 268–271 (1998).
110. Hamada, T. et al. Effect of the angiotensin II receptor antagonist losartan on uric acid and oxypurine metabolism in healthy subjects. *Intern. Med.* **41**, 793–797 (2002).
111. Hoiegggen, A. et al. The impact of serum uric acid on cardiovascular outcomes in the LIFE study. *Kidney Int.* **65**, 1041–1049 (2004).
112. Alderman, M. & Aiyer, K. J. Uric acid: role in cardiovascular disease and effects of losartan. *Curr. Med. Res. Opin.* **20**, 369–379 (2004).
113. Choi, H. K., Soriano, L. C., Zhang, Y. & Rodriguez, L. A. Antihypertensive drugs and risk of incident gout among patients with hypertension: population based case-control study. *BMJ* **344**, d8190 (2012).
114. Bruderer, S., Bodmer, M., Jick, S. S. & Meier, C. R. Use of diuretics and risk of incident gout: a population-based case-control study. *Arthritis Rheumatol.* **66**, 185–196 (2014).
115. Waldman, B. et al. Effect of fenofibrate on uric acid and gout in type 2 diabetes: a post-hoc analysis of the randomised, controlled FIELD study. *Lancet Diabetes Endocrinol.* **6**, 310–318 (2018).
116. Martinon, F., Pettrilli, V., Mayor, A., Tardivel, A. & Tschopp, J. Gout-associated uric acid crystals activate the NALP3 inflammasome. *Nature* **440**, 237–241 (2006).
117. Dalbeth, N. et al. Gout. *Nat. Rev. Dis. Prim.* **5**, 69 (2019).
118. So, A. K. & Martinon, F. Inflammation in gout: mechanisms and therapeutic targets. *Nat. Rev. Rheumatol.* **13**, 639–647 (2017).
119. Strandberg, T. E. & Kovanen, P. T. Coronary artery disease: 'gout' in the artery? *Eur. Heart J.* **42**, 2761–2764 (2021).
120. Grebe, A., Hoss, F. & Latz, E. NLRP3 inflammasome and the IL-1 pathway in atherosclerosis. *Circ. Res.* **122**, 1722–1740 (2018).
121. Klausner, A. S. et al. Dual-energy computed tomography detection of cardiovascular monosodium urate deposits in patients with gout. *JAMA Cardiol.* **4**, 1019–1028 (2019).
122. Barazani, S. H. et al. Quantification of uric acid in vasculature of patients with gout using dual-energy computed tomography. *World J. Radiol.* **12**, 184–194 (2020).
123. Feuchtnner, G. M. et al. Monosodium urate crystal deposition in coronary artery plaque by 128-slice dual-energy computed tomography: an ex vivo phantom and in vivo study. *J. Comput. Assist. Tomogr.* **45**, 856–862 (2021).
124. Becce, F., Ghoshhajra, B. & Choi, H. K. Identification of cardiovascular monosodium urate crystal deposition in patients with gout using dual-energy computed tomography. *JAMA Cardiol.* **5**, 486 (2020).
125. Nishimiya, K. et al. A novel approach for uric acid crystal detection in human coronary arteries with polarization-sensitive micro-OCT [abstract]. *Eur. Heart J.* <https://doi.org/10.1093/eurheartj/ehy565.P2772> (2018).
126. Oh, W. Y. et al. High-speed polarization sensitive optical frequency domain imaging with frequency multiplexing. *Opt. Express* **16**, 1096–1103 (2008).
127. Ridker, P. M. et al. Antiinflammatory therapy with canakinumab for atherosclerotic disease. *N. Engl. J. Med.* **377**, 1119–1131 (2017).
128. Bardin, T. et al. A cross-sectional study of 502 patients found a diffuse hypercholechoic kidney medulla pattern in patients with severe gout. *Kidney Int.* **99**, 218–226 (2021).
129. Pascual, E. Persistence of monosodium urate crystals and low-grade inflammation in the synovial fluid of patients with untreated gout. *Arthritis Rheum.* **34**, 141–145 (1991).
130. White, W. B. et al. Cardiovascular safety of febuxostat or allopurinol in patients with gout. *N. Engl. J. Med.* **378**, 1200–1210 (2018).
131. Choi, H., Neogi, T., Stamp, L., Dalbeth, N. & Terkeltaub, R. New perspectives in rheumatology: implications of the cardiovascular safety of febuxostat and allopurinol in patients with gout and cardiovascular morbidities trial and the associated food and drug administration public safety alert. *Arthritis Rheumatol.* **70**, 1702–1709 (2018).
132. FDA. FDA adds Boxed Warning for increased risk of death with gout medicine Uloric (febuxostat). <https://www.fda.gov/drugs/drug-safety-and-availability/fda-adds-boxed-warning-increased-risk-death-gout-medicine-uloric-febuxostat> (2019).
133. Mackenzie, I. S. et al. Long-term cardiovascular safety of febuxostat compared with allopurinol in patients with gout (FAST): a multicentre, prospective, randomised, open-label, non-inferiority trial. *Lancet* **396**, 1745–1757 (2020).
134. Choi, H. K., Neogi, T., Stamp, L. K., Terkeltaub, R. & Dalbeth, N. Reassessing the cardiovascular safety of febuxostat: implications of the febuxostat versus allopurinol streamlined trial. *Arthritis Rheumatol.* **73**, 721–724 (2021).
135. Bardin, T. & Richette, P. FAST: new look at the febuxostat safety profile. *Lancet* **396**, 1704–1705 (2020).
136. Zhang, M. et al. Assessment of cardiovascular risk in older patients with gout initiating febuxostat versus allopurinol: population-based cohort study. *Circulation* **138**, 1116–1126 (2018).
137. Kang, E. H. & Kim, S. C. Cardiovascular safety of urate lowering therapies. *Curr. Rheumatol. Rep.* **21**, 48 (2019).
138. Doherty, M. et al. Efficacy and cost-effectiveness of nurse-led care involving education and engagement of patients and a treat-to-target urate-lowering strategy versus usual care for gout: a randomised controlled trial. *Lancet* **392**, 1403–1412 (2018).
139. Becker, M. A. et al. Febuxostat compared with allopurinol in patients with hyperuricemia and gout. *N. Engl. J. Med.* **353**, 2450–2461 (2005).
140. Tong, D. C. et al. Colchicine in patients with acute coronary syndrome: the Australian COPS randomized clinical trial. *Circulation* **142**, 1890–1900 (2020).
141. Tardif, J. C. et al. Efficacy and safety of low-dose colchicine after myocardial infarction. *N. Engl. J. Med.* **381**, 2497–2505 (2019).
142. Nidorf, S. M. et al. Colchicine in patients with chronic coronary disease. *N. Engl. J. Med.* **383**, 1838–1847 (2020).
143. Nidorf, S. M., Eikelboom, J. W., Budgeon, C. A. & Thompson, P. L. Low-dose colchicine for secondary prevention of cardiovascular disease. *J. Am. Coll. Cardiol.* **61**, 404–410 (2013).
144. McGill, N. W. Gout and other crystal-associated arthropathies. *Best. Pract. Res. Clin. Rheumatol.* **14**, 445–460 (2000).
145. Emmerson, B. Hyperlipidaemia in hyperuricaemia and gout. *Ann. Rheum. Dis.* **57**, 509–510 (1998).
146. Vuorinen-Markkola, H. & Yki-Jarvinen, H. Hyperuricemia and insulin resistance. *J. Clin. Endocrinol. Metab.* **78**, 25–29 (1994).
147. Lee, J., Sparrow, D., Vokonas, P. S., Landsberg, L. & Weiss, S. T. Uric acid and coronary heart disease risk: evidence for a role of uric acid in the obesity-insulin resistance syndrome. The normative aging study. *Am. J. Epidemiol.* **142**, 288–294 (1995).
148. Puig, J. G. & Ruilope, L. M. Uric acid as a cardiovascular risk factor in arterial hypertension. *J. Hypertens.* **17**, 869–872 (1999).
149. Gepner, Y. et al. Effect of distinct lifestyle interventions on mobilization of fat storage pools: CENTRAL magnetic resonance imaging randomized controlled trial. *Circulation* **137**, 1143–1157 (2018).
150. Duncan, G. E. et al. Exercise training, without weight loss, increases insulin sensitivity and postheparin plasma lipase activity in previously sedentary adults. *Diabetes Care* **26**, 557–562 (2003).
151. Tsaban, G. et al. The effect of green Mediterranean diet on cardiometabolic risk: a randomised controlled trial. *Heart* <https://doi.org/10.1136/heartjnl-2020-317802> (2020).
152. Yaskolka Meir, A. et al. Effect of green-Mediterranean diet on intrahepatic fat: the DIRECT PLUS randomised controlled trial. *Gut* **70**, 2085–2095 (2021).
153. Libby, P. Inflammation in atherosclerosis — no longer a theory. *Clin. Chem.* **67**, 131–142 (2021).
154. Arts, E. E. et al. Performance of four current risk algorithms in predicting cardiovascular events in patients with early rheumatoid arthritis. *Ann. Rheum. Dis.* **74**, 668–674 (2015).
155. Arts, E. E. et al. Prediction of cardiovascular risk in rheumatoid arthritis: performance of original and adapted SCORE algorithms. *Ann. Rheum. Dis.* **75**, 674–680 (2016).
156. Crowson, C. S., Matteson, E. L., Roger, V. L., Thorneau, T. M. & Gabriel, S. E. Usefulness of risk scores to estimate the risk of cardiovascular disease in patients with rheumatoid arthritis. *Am. J. Cardiol.* **110**, 420–424 (2012).
157. Kawai, V. K. et al. The ability of the 2013 American College of Cardiology/American Heart Association cardiovascular risk score to identify rheumatoid arthritis patients with high coronary artery

- calcification scores. *Arthritis Rheumatol.* **67**, 381–385 (2015).
158. Andres, M. et al. Cardiovascular risk of patients with gout seen at rheumatology clinics following a structured assessment. *Ann. Rheum. Dis.* **76**, 1263–1268 (2017).
159. Arnett, D. K. et al. 2019 ACC/AHA guideline on the primary prevention of cardiovascular disease: a report of the American College of Cardiology/American Heart Association Task Force on Clinical Practice Guidelines. *J. Am. Coll. Cardiol.* **74**, e177–e232 (2019).
160. Greenland, P., Yano, Y. & Lloyd-Jones, D. M. Coronary calcium score and cardiovascular risk in elderly populations — reply. *JAMA Cardiol.* **3**, 180–181 (2018).
161. Erbel, R. et al. Coronary risk stratification, discrimination, and reclassification improvement based on quantification of subclinical coronary atherosclerosis: the Heinz Nixdorf recall study. *J. Am. Coll. Cardiol.* **56**, 1397–1406 (2010).
162. Polonsky, T. S. et al. Coronary artery calcium score and risk classification for coronary heart disease prediction. *JAMA* **303**, 1610–1616 (2010).
163. Hoffmann, U. et al. Cardiovascular event prediction and risk reclassification by coronary, aortic, and valvular calcification in the Framingham Heart Study. *J. Am. Heart Assoc.* **5**, e003144 (2016).
164. Gepner, A. D. et al. Comparison of carotid plaque score and coronary artery calcium score for predicting cardiovascular disease events: the multi-ethnic study of atherosclerosis. *J. Am. Heart Assoc.* **6**, e005179 (2017).
165. Gepner, A. D. et al. Comparison of coronary artery calcium presence, carotid plaque presence, and carotid intima-media thickness for cardiovascular disease prediction in the multi-ethnic study of atherosclerosis. *Circ. Cardiovasc. Imaging* **8**, e002262 (2015).
166. Choi, J. W., Ford, E. S., Gao, X. & Choi, H. K. Sugar-sweetened soft drinks, diet soft drinks, and serum uric acid level: the Third National Health and Nutrition Examination Survey. *Arthritis Rheum.* **59**, 109–116 (2008).
167. Dessein, P. H., Shipton, E. A., Stanwix, A. E., Joffe, B. I. & Ramokgadi, J. Beneficial effects of weight loss associated with moderate calorie/carbohydrate restriction, and increased proportional intake of protein and unsaturated fat on serum urate and lipoprotein levels in gout: a pilot study. *Ann. Rheum. Dis.* **59**, 539–543 (2000).
168. Guasch-Ferre, M. et al. Mediterranean diet and risk of hyperuricemia in elderly participants at high cardiovascular risk. *J. Gerontol. A Biol. Sci. Med. Sci.* **68**, 1263–1270 (2013).
169. Yokose, C. et al. Effects of low-fat, Mediterranean, or low-carbohydrate weight loss diets on serum urate and cardiometabolic risk factors: a secondary analysis of the dietary intervention randomized controlled trial (DIRECT). *Diabetes Care* **43**, 2812–2820 (2020).
170. Yokose, C. et al. Adherence to 2020–2025 dietary guidelines for Americans and the risk of new onset female gout. *JAMA Int. Med.* In press (2021).
171. Juraschek, S. P., Gelber, A. C., Choi, H. K., Appel, L. J. & Miller, E. R. 3rd Effects of the dietary approaches to stop hypertension (DASH) diet and sodium intake on serum uric acid. *Arthritis Rheumatol.* **68**, 3002–3009 (2016).
172. Juraschek, S. P. et al. Effects of dietary patterns on serum urate: results from a randomized trial of the effects of diet on hypertension. *Arthritis Rheumatol.* **73**, 1014–1020 (2021).
173. Rai, S. K. et al. The dietary approaches to stop hypertension (DASH) diet, Western diet, and risk of gout in men: prospective cohort study. *BMJ* **357**, j1794 (2017).
174. Richette, P., Clerson, P., Perissin, L., Flipo, R. M. & Bardin, T. Revisiting comorbidities in gout: a cluster analysis. *Ann. Rheum. Dis.* **74**, 142–147 (2015).
175. Yokose, C., Lu, L., Chen-Xu, M., Zhang, Y. & Choi, H. K. Comorbidity patterns in gout using the US general population: cluster analysis of the National Health and Nutrition Examination Survey. *Ann. Rheum. Dis.* **78**, A1294 (2019).
176. Bevis, M., Blagojevic-Bucknall, M., Mallen, C., Hider, S. & Roddy, E. Comorbidity clusters in people with gout: an observational cohort study with linked medical record review. *Rheumatology* **57**, 1358–1363 (2018).
177. Bajpai, R. et al. Onset of comorbidities and flare patterns within pre-existing morbidity clusters in people with gout: 5-year primary care cohort study. *Rheumatology* <https://doi.org/10.1093/rheumatology/keab283> (2021).
178. Appel, L. J. et al. Effects of protein, monounsaturated fat, and carbohydrate intake on blood pressure and serum lipids: results of the OmniHeart randomized trial. *JAMA* **294**, 2455–2464 (2005).
179. Shai, I. et al. Weight loss with a low-carbohydrate, Mediterranean, or low-fat diet. *N. Engl. J. Med.* **359**, 229–241 (2008).
180. Chiuev, S. E. et al. Alternative dietary indices both strongly predict risk of chronic disease. *J. Nutr.* **142**, 1009–1018 (2012).
181. Scheen, A. J. Sodium-glucose cotransporter type 2 inhibitors for the treatment of type 2 diabetes mellitus. *Nat. Rev. Endocrinol.* **16**, 556–577 (2020).
182. White, J. et al. Plasma urate concentration and risk of coronary heart disease: a Mendelian randomisation analysis. *Lancet Diabetes Endocrinol.* **4**, 327–336 (2016).
183. Keenan, T. et al. Causal assessment of serum urate levels in cardiometabolic diseases through a Mendelian randomization study. *J. Am. Coll. Cardiol.* **67**, 407–416 (2016).
184. Kleber, M. E. et al. Uric acid and cardiovascular events: a Mendelian randomization study. *J. Am. Soc. Nephrol.* **26**, 2831–2838 (2015).
185. Stark, K. et al. Common polymorphisms influencing serum uric acid levels contribute to susceptibility to gout, but not to coronary artery disease. *PLoS One* **4**, e7729 (2009).
186. Han, X. et al. Associations of the uric acid related genetic variants in SLC2A9 and ABCG2 loci with coronary heart disease risk. *BMC Genet.* **16**, 4 (2015).
187. Chiang, K. M. et al. Is hyperuricemia, an early-onset metabolic disorder, causally associated with cardiovascular disease events in Han Chinese? *J. Clin. Med.* **8**, 1202 (2019).
188. Macias-Kaufner, L. R. et al. Genetic contributors to serum uric acid levels in Mexicans and their effect on premature coronary artery disease. *Int. J. Cardiol.* **279**, 168–173 (2019).
189. Jordan, D. M. et al. No causal effects of serum urate levels on the risk of chronic kidney disease: a Mendelian randomization study. *PLoS Med.* **16**, e1002725 (2019).
190. Hughes, K., Flynn, T., de Zoysa, J., Dalbeth, N. & Merriman, T. R. Mendelian randomization analysis associates increased serum urate, due to genetic variation in uric acid transporters, with improved renal function. *Kidney Int.* **85**, 344–351 (2014).
191. Greenberg, K. I. et al. Plasma urate and risk of a hospital stay with AKI: the atherosclerosis risk in communities study. *Clin. J. Am. Soc. Nephrol.* **10**, 776–783 (2015).
192. Zhu, J. et al. Genetic predisposition to type 2 diabetes and insulin levels is positively associated with serum urate levels. *J. Clin. Endocrinol. Metab.* **106**, e2547–e2556 (2021).
193. Pfister, R. et al. No evidence for a causal link between uric acid and type 2 diabetes: a Mendelian randomisation approach. *Diabetologia* **54**, 2561–2569 (2011).
194. Sluijs, I. et al. A Mendelian randomization study of circulating uric acid and type 2 diabetes. *Diabetes* **64**, 3028–3036 (2015).
195. McKeigue, P. M. et al. Bayesian methods for instrumental variable analysis with genetic instruments (‘Mendelian randomization’): example with urate transporter SLC2A9 as an instrumental variable for effect of urate levels on metabolic syndrome. *Int. J. Epidemiol.* **39**, 907–918 (2010).
196. Dai, X. et al. Association between serum uric acid and the metabolic syndrome among a middle- and old-age Chinese population. *Eur. J. Epidemiol.* **28**, 669–676 (2013).
197. Hu, X. et al. Association between plasma uric acid and insulin resistance in type 2 diabetes: a Mendelian randomization analysis. *Diabetes Res. Clin. Pract.* **171**, 108542 (2021).
198. Larsson, S. C., Burgess, S. & Michaëlsson, K. Genetic association between adiposity and gout: a Mendelian randomization study. *Rheumatology* **57**, 2145–2148 (2018).
199. O’Dell, J. et al. Urate lowering therapy in the treatment of gout. A multicenter, randomized, double-blind comparison of allopurinol and febuxostat using a treat-to-target strategy [Abstract]. *Arthritis Rheum.* **73**, 3968–3970 (2021).
200. Qaseem, A., Harris, R. P. & Forciea, M. A. Management of acute and recurrent gout: a clinical practice guideline from the American College of Physicians. *Ann. Intern. Med.* **166**, 58–68 (2017).
201. Khanna, D. et al. 2012 American College of Rheumatology guidelines for management of gout. Part 1: systematic nonpharmacologic and pharmacologic therapeutic approaches to hyperuricemia. *Arthritis Care Res.* **64**, 1431–1446 (2012).
202. Liu, L. et al. Imaging the subcellular structure of human coronary atherosclerosis using micro-optical coherence tomography. *Nat. Med.* **17**, 1010–1014 (2011).
203. Bardin, T. et al. Renal medulla in severe gout: typical findings on ultrasonography and dual-energy CT study in two patients. *Ann. Rheum. Dis.* **78**, 433–434 (2019).
204. Kottgen, A. et al. Genome-wide association analyses identify 18 new loci associated with serum urate concentrations. *Nat. Genet.* **45**, 145–154 (2013).
205. Menni, C., Zierler, J., Valdes, A. M. & Spector, T. D. Mixing omics: combining genetics and metabolomics to study rheumatic diseases. *Nat. Rev. Rheumatol.* **13**, 174–181 (2017).
206. Colaco, K. et al. Targeted metabolomic profiling and prediction of cardiovascular events: a prospective study of patients with psoriatic arthritis and psoriasis. *Ann. Rheum. Dis.* **80**, 1429–1435 (2021).

Acknowledgements

H.K.C. is supported by National Institutes of Health grants R01-AR065944 and P50-AR060772. N.M. is supported by a Fellowship Award from the Canadian Institutes of Health Research. C.Y. is supported by a Scientist Development Award from the Rheumatology Research Foundation.

Author contributions

All authors researched data for the article. H.K.C. contributed substantially to discussion of the content. All authors wrote the article and reviewed and/or edited the manuscript before submission.

Competing interests

H.K.C. reports research support from Ironwood and Horizon, and consulting fees from Ironwood, Selecta, Horizon, Takeda, Kowa and Vaxart. N.M. and C.Y. declare no competing interests.

Peer review information

Nature Reviews Rheumatology thanks M. Dehlin, F. Liote and the other, anonymous, reviewer(s) for their contribution to the peer review of this work.

Publisher’s note

Springer Nature remains neutral with regard to jurisdictional claims in published maps and institutional affiliations.

Supplementary information

The online version contains supplementary material available at <https://doi.org/10.1038/s41584-021-00725-9>.

© Springer Nature Limited 2021

Studying osteoarthritis with artificial intelligence applied to magnetic resonance imaging

Francesco Calivà^{1,3}, Nikan K. Namiri^{1,3}, Maureen Dubreuil², Valentina Padoia¹, Eugene Ozhinsky¹ and Sharmila Majumdar¹✉

Abstract | The 3D nature and soft-tissue contrast of MRI makes it an invaluable tool for osteoarthritis research, by facilitating the elucidation of disease pathogenesis and progression. The recent increasing employment of MRI has certainly been stimulated by major advances that are due to considerable investment in research, particularly related to artificial intelligence (AI). These AI-related advances are revolutionizing the use of MRI in clinical research by augmenting activities ranging from image acquisition to post-processing. Automation is key to reducing the long acquisition times of MRI, conducting large-scale longitudinal studies and quantitatively defining morphometric and other important clinical features of both soft and hard tissues in various anatomical joints. Deep learning methods have been used recently for multiple applications in the musculoskeletal field to improve understanding of osteoarthritis. Compared with labour-intensive human efforts, AI-based methods have advantages and potential in all stages of imaging, as well as post-processing steps, including aiding diagnosis and prognosis. However, AI-based methods also have limitations, including the arguably limited interpretability of AI models. Given that the AI community is highly invested in uncovering uncertainties associated with model predictions and improving their interpretability, we envision future clinical translation and progressive increase in the use of AI algorithms to support clinicians in optimizing patient care.

Machine learning

Computer programmes that learn how to perform tasks with some degree of automation and are based in statistics and algorithms.

¹Department of Radiology and Biomedical Imaging and Center for Intelligent Imaging, University of California, San Francisco, San Francisco, CA, USA.

²Section of Rheumatology, Department of Medicine, Boston University School of Medicine, Boston, MA, USA.

³These authors contributed equally: Francesco Calivà, Nikan K. Namiri.

✉e-mail:

Sharmila.Majumdar@ucsf.edu

<https://doi.org/10.1038/s41584-021-00719-7>

Active multidisciplinary research is ongoing to discover quantitative biomarkers for early diagnosis and for monitoring and assessment of joint degeneration. Medical imaging has played a substantial role in this area; for example, radiographs can detect structural alterations in bone, but these scans have low sensitivity for detecting tissues that are thought to be important in joint degeneration in osteoarthritis (OA) (such as cartilage, menisci and other soft tissues) and cannot capture changes in bone marrow (that is, bone marrow lesions). Conversely, MRI has higher sensitivity than radiography in detecting soft-tissue changes, bone marrow oedema and early osteophytic changes. Advanced quantitative imaging techniques, novel computerized image post-processing and more recent machine learning (ML) techniques have made possible further advances towards quantitative characterization of early joint degeneration and identification of imaging biomarkers associated with OA¹.

Artificial intelligence (AI)-based methods are finding ever greater use in musculoskeletal imaging. Broadly, AI refers to a wide body of research that includes the theory and development of computerized systems that are

capable of performing tasks that usually require human involvement and can be quite labour intensive. ML is a branch of AI that is aimed at developing algorithms that are capable of learning patterns or performing tasks directly from data without the need for explicit instructions. Supported by an ever-increasing availability of data, research related to ML and emerging subfields such as deep learning (DL) have made possible the latest advances in medical image processing and analysis. The role of AI in medical imaging extends beyond automated image pre-processing and post-processing (FIG. 1), to include image generation (for example, DL-aided image acquisition). AI has further potential to facilitate imaging-based extraction of OA biomarkers by way of discovering patterns in the data that might otherwise be missed during human assessment.

In this Review, we explore how recent applications of DL have improved imaging-based understanding of OA (TABLE 1). We illustrate how DL techniques are applied at all stages of imaging to enable automation of acquisition and analysis. We focus primarily on MRI, although we briefly discuss X-ray imaging and other imaging

Key points

- Applications of deep learning to accelerate MRI acquisition and reconstruction show exciting results; nevertheless, fundamental questions remain regarding the most appropriate metrics for evaluating the quality of reconstructed images.
- Image segmentation errors from artificial intelligence (AI) models lie within the intra-reader variability range. Nonetheless, deployment in clinical practice still requires some form of quality assurance, which might include visual inspection of segmentation outputs.
- The role of AI in osteoarthritis lesion detection is not to provide a final diagnosis but rather to serve as an additional input for decision-making.
- AI has been tasked with searching for novel image features indicative of short-term and long-term progression of osteoarthritis to predict disease course on a patient-specific basis.
- Future research will likely be devoted to the interpretability and estimation of the uncertainty of deep learning models, with the aim of improving clinician trust in AI for supporting patient care.

Deep learning

A type of machine learning that performs multiple layers of mathematical algorithms (analogous to artificial neurons) on input data to execute a pre-defined task as output.

Classification

Predicting an observation based on a training dataset that includes observations about the predicted variable. The prediction assumes categorical values. In osteoarthritis, an example is predicting the presence or absence of a knee meniscus tear.

Regression

Predicting an observation based on a training dataset that includes observations about the predicted variable that assumes a continuous value (that is, not categorical); for example, the task of prescribing the imaging acquisition plane in MRI.

Segmentation

A form of classification at the pixel level of an image to identify a region of interest (ROI). The goal of segmentation is to assign each pixel to a label that describes the category to which the pixels belongs.

Raw data

Refers to the data stored during the acquisition of an MRI sequence as a function of time. Also known as *k*-space in MRI.

Supervised learning

The process of learning the relationship between input data and their labels, where all the samples in the training dataset have been labelled.

modalities where DL seems to possess great potential for future clinical translation.

Introduction to machine learning

Machine learning is the science that is aimed at automatically modelling patterns in data. Such patterns are commonly referred to as features and are characteristics that are used to describe the data and make informed decisions². ML is typically used to solve two types of problems, namely *classification* and *regression*. Classification consists of categorizing input data; for example, assigning an image to a particular class according to the presence or absence of a specific feature in the image, such as classification of decreased cartilage thickness in OA. The output of classification is a categorical, discrete value; conversely, regression problems map an input to a continuous value. This continuous value could be the staging of OA, prediction of cartilage thickness over time, or a score for OA-related pain.

Segmentation is a special case of classification and is the process of delineating regions of interest within an image. Segmentation can be considered to be classification at a pixel level, as every pixel is classified as being part of a specific tissue structure. Segmentation is an important task³ and is considered a pre-requisite in many clinical applications, such as therapeutic planning⁴ and quantifying treatment response⁵. In OA research, segmentation is an invaluable tool for improving understanding of disease-related structural change such as alteration of T2 values and cartilage thickness in patients^{6–8}. Image reconstruction is a problem of regression at a pixel level, as it outputs a pixel array of continuous values to obtain a clinical image from MRI raw data.

Both regression and classification can be achieved by following two main approaches. A supervised learning approach requires the presence of data coupled with target labels, which are often referred to as ground truth, whereas an approach that does not involve ground truth data is termed *unsupervised learning*⁹. DL is a type of ML that uses artificial neurons as functional units to mimic human cognitive reasoning and in so doing can extract complex patterns in data. DL methods can automatically identify useful features in the data; owing to tuning

of the parameters of DL models to maximize their performance in the task they are designed to solve¹⁰.

The model's parameters are tuned using a training dataset, which is a portion of the complete available dataset. The process of learning to perform a task is known as *model training*, and the ultimate goal of training is to minimize the error between the model's prediction and ground truth (that is, between the predicted labels and the target labels). This error is known as a *loss function* and serves as a proxy of how well the algorithm is modelling the data. The ability of the model to perform the same task on unseen data is investigated on a different portion of the dataset that is known as the development or validation dataset. This dataset is used for selection of the best-performing model and as a proxy for how well the model will perform when deployed in real-world scenarios.

Once the best-performing model has been selected, it is tested on a final held-back portion of the dataset termed the test dataset, which is used to infer the model's performance on never-seen data. It is imperative to keep the model blind to the test dataset until the moment in which the final model has been selected, to prevent access of the model to any information about the real-world data that will be used in the future, and thus avoid seemingly overly-optimistic model performance. Typical dataset splits involve 70% of the dataset assigned to the training set and the remaining 30% of the dataset equally split between the validation and test datasets. However, the proportions of the splits vary depending on various factors, including total sample size and individual preference. It is considered good practice to organize the data in such a way that data from a participant are included in only one of the datasets, to avoid data leakage across splits, which could be another cause of overly-optimistic performance. Each portion of the dataset should also contain an equal proportion of the disease samples under study.

Image acquisition

Deep learning for accelerated MRI and image super-resolution. A primary limitation of MRI is the long scan acquisition time, typically 20–40 min per imaged region. This scan duration is inherent to the acquisition process, which is performed in the frequency domain, and allows for storage of the MRI raw data (also known as *k*-space data). The *k*-space data hold all of the information that is required to create an interpretable MR image. Image reconstruction, the processing steps required to construct images that are interpretable by radiologists, is achieved using the Fourier transform (a mathematical operation) on the *k*-space data¹¹. Fourier transform and its inverse, the inverse Fourier transform, permit navigation from image to *k*-space domains and vice versa.

Besides a financial cost, the long duration of MRI scans can be a cause of patient discomfort and decreased compliance, resulting in imaging artefacts from patient motion. For example, in the largest OA observational study to date, the Osteoarthritis Initiative (OAI), imaging a pair of knees with the same sequence required 1 h of MRI scanner time, demonstrating the need for more efficient image acquisition and reconstruction techniques¹².

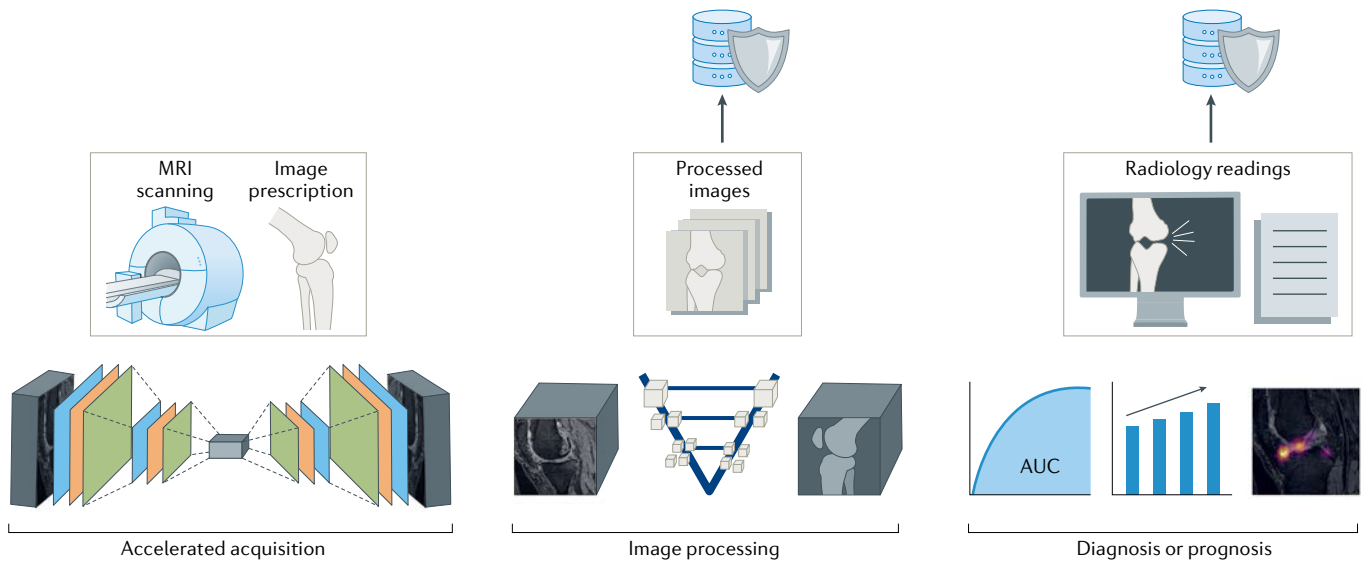


Fig. 1 | The role of artificial intelligence in stages of imaging. Artificial intelligence can contribute to several aspects of imaging-based patient management, from the selection of the most appropriate imaging examination method, including accelerating acquisition time, automation of image processing and extraction of quantitative biomarkers. Artificial intelligence can also provide radiologists with assistance in structuring clinical reports. MR images are reprinted from REF.¹¹⁶, CC BY 4.0 (<https://creativecommons.org/licenses/by/4.0/>).

Multiple ways exist to ‘accelerate MRI’, the process of decreasing reconstruction time while also limiting artefacts. A standard approach is parallel imaging^{13,14}, which uses complementary information collected with multiple coils to obtain high-quality MR images from limited k -space data. Another algorithm that is used to accelerate MRI acquisition and reconstruction is compressed sensing (CS)¹⁵, which is able to iteratively recover missing information in the signal by leveraging the sparsity in the signal itself. Other methods, such as low-rankness methods, explore linear correlations among MR images to generate high-quality MR images from reduced k -space data¹⁶. These conventional methods for image reconstruction require long reconstruction times or result in inadequate image quality, which have hampered their translation to clinical practice.

DL-based image reconstruction approaches offer the benefit of decreased overall time to completion (that is, the sum of acquisition and processing time), which has led to their use in accelerating MRI. Furthermore, these reconstruction approaches can separate image from artefacts by training the DL algorithms to output fully sampled MR images from undersampled MRI raw data^{17–20}. Images produced in this way can substitute for traditional clinical MRI scans, with image acquisition accelerated by up to sixfold^{21,22}, resulting in acquisition times as low as 10 min (BOX 1). Four groups of algorithms are used, namely image-domain learning, k -space-domain learning, hybrid or cascade of image-domain and k -space-domain learning, and domain mapping.

Image-domain learning relies on direct mapping between an aliased image (that is, multiple copies of the imaged anatomy are superimposed owing to some measurements being skipped to accelerate the MRI scan) and an output aliasing-free reference image. The input is an already processed image, as zero values can be

introduced in place of the missing raw data, producing an image referred to as a reconstructed zero-filled image. As a result, important anatomical structures might not be displayed or might be distorted. This is an implicit limitation of this family of approaches, as, in addition to recovering the missing pieces of information, they need to identify and correct potential data distortion^{23–31}.

In k -space-domain learning, the input is the k -space acquired at the MRI scanner, with no steps of post-processing involved, which prevents the introduction of distortion to the input data. As a result, the full potential of the raw data can be exploited, producing higher quality images^{32,33}. Hybrid approaches take advantage of the benefits of both image domain and k -space-domain learning^{18,23,34}. Ultimately, domain mapping approaches, such as automated transform by manifold approximation³⁵, can automatically map k -space to image-space by learning the transformation (that is, the Fourier transform) directly from the data.

The results from seminal studies applying DL to accelerate MRI acquisition and reconstruction are exciting for both clinical and technical scientists; however, fundamental questions remain regarding the most appropriate metrics for evaluating the quality of DL-based reconstructed MR images^{36–39}. A mere estimation of the reconstruction error might not be representative of the diagnostic value of the reconstructed images¹⁷. In fact, evaluation metrics must provide a quantitative assessment of DL-generated MR image quality, with high fidelity. Typically, metrics to assess image reconstruction quality are calculated at the pixel level, but these metrics correlate poorly with human perception^{38,40} and are insensitive to several types of visual distortions⁴¹. Perceptual similarity metrics better replicate human perception, as they estimate image statistics, often at various resolutions, and have been adopted in collaborative

Ground truth

Information provided by empirical evidence rather than by the inference of a machine learning model; for example, the pixel-by-pixel annotation of a particular region of interest in a segmentation task, or the fully sampled image in accelerated MRI reconstruction.

Unsupervised learning

The process of learning the relationship between input data and their labels, where the data have no labels and the role of the algorithm is to find the underlying structure of the data to use it on the task at hand.

Model training

The stage in machine learning in which an algorithm (regression or classification) is instructed to perform a task. Training can be supervised, semi-supervised or unsupervised. Also known as learning.

Table 1 | Advantages and challenges of AI in imaging acquisition, processing and interpretation for OA

Imaging step	Contribution	Advantages	Challenges
Acquisition	Acceleration	Decreased overall time to completion; separate image from artefacts	Need for reliable metrics for evaluating quality of reconstructed images; difficulty in reconstructing subtle abnormalities
Processing	Tissue segmentation	Automation of complex measurements (that is, cartilage thickness mapping); error lies within intra-reader variability of human readers	High segmentation accuracy does not necessarily correlate with accurate delineation of relevant structures; requires some form of final quality assurance (that is, visual inspection)
	Epidemiological studies	Better utilize full potential of large research studies (such as the Osteoarthritis Initiative); understand the relationship between relaxometry maps and osteoarthritis	Generalizability to data from multiple institutions
Interpretation	Anomaly detection	Predictions and saliency maps can improve inter-reader reliability of human readers; transfer learning can improve detection of less common lesions	Models cannot overcome limitations in inter- and intra-reader variability if trained with human grading as the ground truth (that is, in the absence of a gold standard ground truth); limited training dataset size leads to overfitting
	Prognosis and biomarker discovery	Rapid, automated stratification of patients at higher risk of developing OA or with accelerated progression for use in clinical trial inclusion; establish imaging biomarkers indicative of early osteoarthritis; versatile model development techniques, including multitask learning and gradient boosting	Current performance metrics are suboptimal for clinical application; multi-modal deep learning using imaging and clinical data remains a challenge; overall paucity of studies using MRI; AI predictions are not intuitive owing to 'black box' nature of deep learning algorithms

AI, artificial intelligence; OA, osteoarthritis.

Loss function

A mathematical entity for quantifying how well a machine learning algorithm models the data. Higher values indicate poorer modelling ability. During training, the loss function is coupled with an optimizer, which is used to tune the parameters of the machine learning or deep learning algorithm to minimize the loss function and ultimately maximize algorithm performance.

k-space

The *k*-space represents the spatial frequency information in two or three dimensions of an object, and each point in the *k*-space data matrix contains a portion of the information for the complete image. Also known as raw data in MRI.

Fourier transform

A mathematical transform utilized in image processing to decompose an image into its sine and cosine components, which allows mapping from the spatial domain of an image to its frequency domain. In MRI, the Fourier transform and its inverse maps raw data to image space and vice versa, respectively.

Image-domain learning

The procedure in which an algorithm learns to reconstruct a fully sampled MR image starting from an undersampled MR image.

research projects such as [FastMRI](#) and challenges such as the Multi-channel MR Reconstruction ([MC-MRRec](#)) challenge^{38,42,43}.

Failing to reconstruct clinically relevant features can lead to imprecise image interpretation, and even top-performing DL models can fail to reconstruct relatively small, though diagnostically valuable, abnormalities such as meniscal tears and subchondral osteophytes. This reconstruction failure⁴⁴, might be driven by a training dataset that underrepresents rare, yet salient, features or by an acceleration method that reduces the amount of input MRI data. Tools exist to identify difficult-to-reconstruct features⁴⁵, so that model training is robust and customized to improve the reconstruction⁴⁴. Benefits of customized and robust training include better preservation of abnormal signal changes in cartilage and sustained visibility of bone marrow oedema and cartilage lesions⁴⁴, which, besides being clinically relevant for grading the severity of lesions, are crucial in deciding a course of treatment⁴⁶.

In addition to DL-based reconstruction, faster MRI scanning can be achieved through the acquisition of images at lower spatial resolutions that are later enhanced using a technique known as image super-resolution. This technique enables the recovery of high-resolution images from low-resolution images⁴⁷, without sacrificing the signal-to-noise ratio or the diagnostic capability of the imaging modality. Recently, DL has made it possible to achieve super-resolution musculoskeletal MRI. In one of the earliest works on this topic, DL was used to enhance low-resolution MRI scans of the knee⁴⁸. A follow-up study showed further potential of DL-based super-resolution MRI approaches, demonstrating accelerated extraction of quantitative biomarkers with minimal systematic errors¹². With regard to these quantitative biomarkers, relaxometry maps have been predicted while reconstructing MRI using undersampled *k*-space⁴⁹.

Image processing

Deep learning for automated tissue segmentation. The process of characterizing OA by extracting relevant imaging biomarkers (such as cartilage thickness^{7,8,50,51} or bone surface shape^{52,53}) or compositional quantitative biomarkers (such as T_2 relaxation times)^{6,54–56} often involves image segmentation, which is the process of classifying each pixel of an image as belonging to a particular tissue type (BOX 2).

Manual segmentation, in which an annotator classifies tissue types, is considered the gold standard, although it requires expertise, takes a great amount of time and can be subject to intra-operator variability, making the automation of this task highly valuable. Consensus among annotators is particularly important for accurate disease diagnosis, patient care and avoiding inadvertent medical errors⁵⁷, which have been widely documented in the research literature^{39,58–61}. In addition, many algorithms that perform lesion detection or estimate prognosis require a robust initial segmentation step to isolate the region of interest (discussed below).

Extensive and active research is ongoing in the domain of automated knee MRI-based multi-tissue segmentation with AI^{62–64}. Recently, processing entire MRI volumes has become less of a problem, and 3D architecture alternatives are now standard^{65,66}. The available segmentation methods are highly accurate, irrespective of their different underlying theoretical assumptions. Statistical shape modelling^{67,68}, 3D active appearance models⁵¹, 2D and 3D convolutional neural networks (CNNs)^{69–71}, and more sophisticated combinations^{72,73} or variants of these models^{69,74} have been used. A report from the OAI cartilage segmentation challenge confirmed that, based on the number of entries, encoder-decoder style architectures are the most popular in the field^{75–77}. In their simplest form, these architectures consist of an encoder, which produces a compressed yet meaningful and descriptive representation of the input

***k*-space-domain learning**

The procedure in MRI reconstruction in which an algorithm learns to fill in the missing information in an undersampled *k*-space to ultimately obtain a fully sampled *k*-space.

Domain mapping

In image reconstruction, this term refers to the procedure where an algorithm learns the mapping from undersampled *k*-space to fully sampled image.

Aliased image

Aliasing is a signal processing term referring to effects that cause different signals to be indistinguishable. Aliasing can also describe artefacts or distortions in a signal reconstructed from a limited number of samples, which cause the output signal to differ from the original signal.

Relaxometry maps

Quantitative maps reporting measurements of relaxation times from MR images. T_1 , T_2 and T_2^* are common relaxometry maps that all require appropriate pulse sequence and parameters.

data (for example, MRI data), and a decoder, which re-expands the compressed representation to the output spatial size, while mapping it to the desired output task (that is, a segmentation map). Accurate cartilage segmentation does not necessarily require fully sampled MR images and has been obtained directly with 24-fold undersampled data as input, by bridging image reconstruction with image analysis⁷⁸. DL-based segmentation to delineate other musculoskeletal joints, including wrist⁷⁹, hip^{80,81} and scapula^{82–85}, are less well explored but active fields of research. Upper extremity compartments such as the shoulder joint are particularly difficult to segment, owing mostly to their intricate shapes. However, by first training the model to follow global anatomical properties of shape and location, high-quality segmentation of very complicated structures can be achieved⁸³.

Alternatively, acquired knowledge can be transferred across multiple datasets and tasks, using a technique termed transfer learning (also known as domain adaptation). With transfer learning, previously acquired knowledge can be transferred to a new problem: for example, the ability of a neural network to segment healthy shoulders can be leveraged and adapted to segment pathological shoulders on a different dataset⁸⁴. Transfer learning can also aid in the creation of effective 3D MRI models using a dataset with a limited number of datapoints⁸⁵. For example, such a model has been used to perform a quick and reliable quantification of glenoid bone loss, which is important for patient management, as it defines whether a patient should undergo arthroscopic repair or bone augmentation surgery⁸⁶.

Current metrics for evaluating segmentation performance, such as the Dice similarity coefficient (DSC; also known as the Sørensen–Dice coefficient), volumetric overlap error, root-mean-squared, coefficient of

variation and average symmetric surface distance, certainly can help in discarding underperforming DL segmentation methods in OA. However, it is very difficult to interpret these metrics when comparing methods that perform very similarly — we are at the point where almost all proposed OA segmentation methods perform comparably with human annotators.

In general, current metrics give a global evaluation of segmentation performance, making it difficult to validate the actual output quality. Alternatively, as provision of clinical support is the final goal of DL-based segmentation, aside from traditional metrics, biomarker extraction (such as cartilage thickness⁸⁷) could be used as the figure of merit. Segmentation performance in estimating cartilage thickness has been investigated by comparing the values obtained with segmentation with reference values to calculate the average error in thickness estimation⁵³. Interestingly, in the OA imaging knee MRI segmentation challenge, methods that performed at a comparable level in terms of DSC showed only weak correlation in extracted cartilage thickness values⁸. The reasons for such discrepancies are not well understood. In clinical practice, the most relevant aspect of segmentation is to depict true changes in tissue parameters, such as cartilage thickness, over time, and to correctly discern these from noise or measurement error. This weak correlation between DSC and tissue parameters suggests that DSC might not be a valid and easily interpretable metric because it is not sufficiently sensitive to detect the typically minute changes in tissue parameters, such as those seen in cartilage thickness.

Although progress in OA image segmentation has reached a point where algorithm errors lie within the intra-reader variability range, deployment in clinical practice still requires some form of supervision, including visual inspection of segmentation outputs and error maps when a ground truth is available. We envision that future DL research will focus heavily on improving the explainability and interpretability of DL models, which thus far have often been treated as ‘black boxes’⁸⁸. The hope is that by providing tools capable of explaining their predictions, clinicians will be more amenable to accepting suggestions provided by AI-powered systems.

Deep learning for large-scale epidemiological studies.

OA imaging studies have further utilized automated segmentation algorithms for high-throughput analysis of large epidemiological studies, such as OAI, with the aim of extracting OA biomarkers. T_2 relaxation time, a type of MR-derived compositional imaging, is sensitive to collagen organization and thus suitable for morphological measurements such as cartilage volume and thickness. Relaxation time maps may thus distinguish these OA biomarkers from cartilage composition determined using MRI. For example, in an automated knee cartilage segmentation study, T_2 relaxation time was analysed in 4,796 patients from over 25,000 MRI studies. T_2 values were subsequently found to have predictive power for OA incidence and need for total knee replacement (TKR)⁶. T_2 relaxometry maps have also improved prediction of radiographic OA⁵⁴. Segmented cartilage volumes have also been used to estimate

Box 1 | Do we need to accelerate MRI?

MRI is acquired by sampling data through a frequency domain, namely the *k*-space¹²⁰. Diagnostic and visually interpretable MR images are obtained when the *k*-space is completely covered. In principle, achieving a reduction of the trajectory time is possible but has its own impediments that cannot be controlled by the scanner, such as relaxation time required for nuclear spins to reach thermal equilibrium. Common MRI acceleration techniques include parallel imaging and compressed sensing (CS). Accelerating MRI has the potential to reduce health-care costs per scan (owing to less demand on technician time and less time in the medical facility) and enhance the availability of MRI (through increased flexibility in scheduling).

Why machine learning?

In parallel imaging, more sparsely acquired data are used^{13,14,121–124}. Multiple receiver coils with known sensitivities are utilized and they provide all the prior information needed, which makes faster reconstruction possible. Since its introduction, CS has proved to be a valuable algorithm for reconstructing images from limited samples¹²². CS is an optimization-based approach highly sensitive to the selection of hyperparameters and treats every processed data sample independently¹⁷. CS is inherently slow and does not apply any knowledge about previously processed data. This is inconsistent with the clinician’s way of reasoning, as throughout their career they consolidate their capability to quickly recognize diagnostic patterns. Instead, data-driven DL approaches can acquire prior knowledge through model training, which optimally tunes the parameters of the model for the reconstruction task at hand. After the initial training is complete, reconstructions can be provided extremely quickly, which is highly desirable for clinical applications. In general, reducing this overall acquisition time remains a topic of study.

Box 2 | Image-to-image translation with deep learning

Image reconstruction, segmentation and super-resolution with deep learning tools can essentially be thought of as an image-to-image translation problem. In simple terms, given an image as input to a deep neural network, the network tunes its internal parameters — by means of a guided optimization procedure — and uses them to extract meaningful features from the data. The model returns an image that reflects the task at hand: for image reconstruction, the output is the alias-free version of the input image; for segmentation the output is a probability map of each pixel's assignment to a certain class; for super-resolution the output is a higher resolution version of the input. Although variants exist, the solutions most commonly adopted for image-to-image translation problems comprise two fundamental components: an encoder, which compresses the input to a meaningful and descriptive encoded representation; and a decoder, which re-expands the encoded representation up to the desired output spatial size that often coincides with the input size. Omnipresent elements in encoder-decoder networks are the so-called skip connections, which are simple ways of facilitating information flow between the two blocks. Very popular (and effective) architectures with these structural characteristics include UNet¹²⁵ and VNet⁵⁶ and variants thereof. Generative adversarial networks (GANs) are another popular model type^{125,126}. GANs include two components: a generator and a discriminator. Both have specific roles: the generator produces images that match the statistical properties of real data (that is, the data to be generated), whereas the discriminator determines whether the image it sees was sampled from the training set or was outputted by the generator. GANs are trained in an adversarial fashion and play a minimum-maximum game where the generator tries to fool the discriminator.

T₂ relaxation time

A metric to quantify the T₂ relaxation rate in a region of interest. The relaxation time is described by a combination of exponential decay curves, in part owing to different compartments of water in tissues.

Encoder-decoder

A machine-learning algorithm comprising an encoder, which is used to condense the input into a smaller (encoded), meaningful and descriptive representation, and a decoder, which re-expands the encoded representation until the original input is reconstructed.

Domain adaptation

A set of techniques that are used to apply an algorithm trained on a source domain to a different related domain termed the target domain, with the aim of minimizing performance drop.

Neural network

A mathematical system comprising artificial neurons that mimic human neural networks and that are used to identify relationships in datasets. In AI, neural networks are considered building blocks of the most powerful machine learning algorithms. Multiple layers of neurons are concatenated to produce the popular deep neural networks.

cartilage thickness in an 8-year longitudinal study of 1,453 healthy knees, identifying subgroups with stable thickness and those characterized by accelerated or plateaued thinning or thickening of cartilage tissue⁷. This study is exemplary in showing that accurate segmentation can help to uncover associations between biomarker variations and pathological dynamics, and more importantly it represents progress towards understanding the associations between incidence of OA and dynamics of cartilage change. Hip cartilage segmentation may also aid in assessing post-operative outcomes consequent to femoro-acetabular impingement, hip dysplasia or avascular necrosis⁸¹.

Image interpretation

Deep learning for automated anomaly detection. An important step after processing a medical image is assessment by a clinician for the presence of pathological changes. However, the outcome assessment might vary depending on several factors, including the clinician's expertise. In efforts to reduce variability among readers, semi-quantitative scoring systems have been developed for standardizing severity assessment of joint abnormalities^{89–92}. Semi-quantitative scales transform qualitative observations into numerical values, enabling more meaningful comparisons. Despite the introduction of these grading systems, high inter-reader variability is not uncommon in assessments of OA changes from imaging.

Constructing robust AI for joint abnormality detection depends on several characteristics of the training dataset, particularly the type of image annotation, standards for ground truth, overall sample size and the breadth of pathology represented. The detail of image annotation (also known as supervision) determines the granularity at which the model can correlate input images to the diagnosis. A strongly supervised model is one that is trained with images that have diagnostic

labels assigned at the pixel level⁹³. Conversely, weakly supervised models, which typically use a single or multiple labels for an entire image, require less human annotation of images and might be a more reasonable choice for large datasets that are impractical to annotate at the pixel level. In cartilage assessment, weak supervision can involve labelling MRI using a semi-quantitative grading scale, such as the MRI Osteoarthritis Knee Score⁹¹ (MOAKS) or Whole Organ Magnetic Resonance Score (WORMS)^{89,94}. MOAKS is more widely utilized than WORMS for image assessment, including in large clinical studies such as the OAI. However, the majority of DL studies have utilized WORMS for establishing ground truth. WORMS stages knee OA according to 14 features within the subchondral bone, cartilage, meniscus and ligaments. MOAKS was developed in part based on WORMS and evaluates similar articular features with the added benefit of increased intra-reader reliability.

Knee meniscus lesions have similarly been detected with weak supervision in three classes of damage: normal (WORMS grade 0–1), mild to moderate (WORMS grade 2–3) and severe (WORMS grade 4)⁹⁴. Weak supervision is appropriate for these classification tasks, as the gold standard human annotation is based on a semi-quantitative scale. DL analysis of the meniscus has further included directionality of meniscus tears⁹⁵, specifically whether these are horizontal or vertical. Multiple CNNs have been employed to locate and classify tears in a two-step approach, motivated by the fact that the localization task is independent of the classification task⁹⁶. Similarly, multiple CNNs have been adopted for meniscus tear detection and anterior cruciate ligament tear detection^{97,98}, in addition to one CNN that was generalizable to external MRI datasets in classifying meniscus tears, anterior cruciate ligament tears and general OA abnormalities⁹⁹. Another single study trained a model with simplified semi-quantitative grading to detect cartilage, bone marrow, meniscus and ligament injury¹⁰⁰. However, even with a simplified grading scale, the model fell short of radiologist performance. Moreover, no AI has yet demonstrated comparable performance with expert graders in a head-to-head comparison of full semi-quantitative assessment of all joint features.

In addition to the knee, the hip joint is often burdened by OA, as ~9.2% of adults over 45 years of age experience symptomatic hip OA¹⁰¹. Researchers hope that AI can detect the granular structural changes caused by OA in complex intra-articular hip structures, such as the labrum, by leveraging the sensitivity of MRI. Current AI models base their assessment of MR images on Scoring Hip Osteoarthritis with MRI (SHOMRI), a validated semi-quantitative grading system for the hip joint⁹². Although AI algorithms are less prevalent for hip OA detection than for knee OA detection, AI models have successfully classified bone marrow oedema lesions, cysts and cartilage lesions within the hip⁵⁸. These three detection models were able to identify normal (SHOMRI grade 0) from damaged (SHOMRI grade ≥1) hip joints in each lesion group. The study went on to provide saliency maps, which are pixel weightings that the model utilizes for its predictions, through an interactive

Dice similarity coefficient

A statistic that is used to quantify the similarity between two samples; in image segmentation, it measures the overlap between the ground truth and the model-produced segmentation.

Volumetric overlap error

A metric for quantifying the dissimilarity between two datasets. In segmentation, it is computed as the overlap between ground truth and a model-produced segmentation, divided by the union of the two segmentations, subtracted from 1.

Root-mean-squared

A statistic for quantifying the difference between values predicted by a model and the observed values (ground truth). It is computed as the square root of the average of squared errors between predicted and expected values.

Coefficient of variation

A statistical measure of the dispersion of a probability distribution, which is calculated as the ratio between the standard deviation and the average.

Average symmetric surface distance

(ASSD). A metric for evaluating segmentation performance, which is computed by averaging all the distances from points on the boundary of the region segmented by a model to the boundary of the ground truth, and vice versa.

Figure of merit

A quantity utilized to characterize the performance of an algorithm. Sometimes, it is used interchangeably with the term loss function.

Interpretability

A model is interpretable when the relationship between input and predicted output is clear to the user.

Annotation

Labelling the data so that it can be utilized for training and testing machine learning algorithms. In MRI, annotation can be done at different levels of granularity depending on the type of task, such as classification tasks, segmentation or regression.

interface for clinical users. Providing these saliency maps substantially increased the inter-reader reliability and overall accuracy of radiologists in detecting hip lesions, which is the ultimate goal of building lesion-detection algorithms with DL⁵⁸.

Despite the growing application of DL in OA lesion detection, models are limited to the accuracy of ground truth used in training. Gratings from a single radiologist are typically used as ground truth and are likely to have some form of variability depending on the specific radiologist's judgement. Thus, clinician bias is inherently embedded in the AI training process. The role of AI in lesion detection is therefore not to provide a final diagnosis but rather to serve as an additional input for clinical decision-making. Furthermore, AI requires a large training dataset to ensure high-quality performance. Limited training data can lead to over-fitting of the data, a common problem for many supervised ML methods. Overfitting is also related to poor generalization to unseen data and can be mitigated by regularizing (implementation of algorithms to avoid over-fitting) the network¹⁰². In practice, ML algorithms can tend to memorize the training dataset, leading to poor modelling of the data and, consequently, weak performance.

Many of the studies we have highlighted required thousands of images to reach acceptable values for performance metrics. However, rare lesions are disproportionately under-represented in MRI datasets regardless of dataset size. Until comprehensive and balanced datasets are compiled and annotated, diagnosing rare lesions will remain a considerable challenge. To mitigate this problem, some groups^{97,103} have employed transfer learning, involving first training a model using a large, public dataset on common classification tasks (such as ImageNet¹⁰⁴), followed by additional training on a smaller dataset for the task of interest (for example, meniscus tear detection). Potential alternative approaches include weakly supervised training with labels for image noise, which enable models to focus on only pertinent image features. More accurate diagnoses might also be obtained from combining MRI classifiers with classifiers for radiographic imaging modalities^{105–109}. Predictions from AI algorithms might also yield more accurate classification when combined with other ML systems such as gradient boosting¹¹⁰. These hybrid models can utilize the strictly data-driven predictions from AI as one component of an overall classification pipeline that includes leveraging non-imaging data such as demographics and clinical evaluation.

Deep learning for prognosis and disease trajectory modelling. Although point-of-care detection of OA anomalies is crucial for making a diagnosis, there are no disease-modifying treatments to date that halt structural progression of OA¹¹¹. Identifying biomarkers that predict future disease progression has become an active area of research, as early interventions can limit future disease burden. However, establishing such biomarkers is not straightforward, as OA has a heterogeneous pathophysiology and can have multiple aetiologies¹¹². As a result, AI has been tasked with searching for novel image features that are indicative of short-term and

long-term progression of OA to predict disease course on a patient-specific basis.

The joint margin has been given considerable attention in the search for OA biomarkers, as shape changes in bone may indicate future OA symptoms^{52,113}. Bone shape with MRI has conventionally been studied by transforming 3D shape into vectors with reduced dimensionality⁵³. DL models have recently been trained on these vector maps to predict OA disease trajectory. Bone shape of femur, tibia and patella have been estimated from a cohort of patients who were studied annually for up to 8 years⁵³. From these bone shape maps, AI was used to accurately predict future OA incidence, defined as an increase in Kellgren–Lawrence (KL) grade from KL ≤ 1 to KL ≥ 2 (REF.¹¹⁴). Although such predictions from AI are not patently intuitive owing to its 'black box' nature, they may still hold value in identifying OA in its earlier stages and enable interventions to slow future disease progression. For example, bone shape calculations with ML models can be used as a relative metric in the population, similar to the T-score in osteoporosis, to categorize patients based on the number of standard deviations from an average bone shape score and in doing so determine risk of future pain, function and need for TKR¹¹⁵.

Efforts to increase the transparency of the AI decision-making process for disease trajectory predictions includes the use of DL to identify early changes on knee MR images that are predictive of needing a TKR within 5 years¹¹⁶. The model displayed knee areas that contributed most to its decision for predicting future TKR; areas of importance for the model were directly visualized using occlusion maps of the knee MRI (FIG. 2). Occlusion maps represent the magnitude of change in the AI's output when the highlighted MRI region is removed from the model's learning. The results might improve candidate selection for early OA treatment and prevent invasive operations such as TKR, while also ensuring the selection of algorithms that incorporate clinically relevant MRI regions in generating predictions. Another study utilized DL to classify morphological rapid osteoarthritis MRI eligibility score phenotypes¹¹⁷, which are structural groups representative of underlying OA-specific pathophysiological knee changes¹¹⁸. The study found that bone, inflammatory and hypertrophy phenotypes at baseline portended increased odds of needing TKR within 8 years. Although MRI is not typically ordered as part of an OA clinical assessment, morphological phenotypes in MRI can characterize progression of knee OA and may guide criteria for inclusion in trials of disease-modifying OA drugs. More broadly, establishing such phenotypes may help to establish the first ever disease-modifying OA drug.

Despite advances in MRI research, clinicians consider X-ray imaging the gold standard for the diagnosis of OA. Moreover, decisions about therapy are based on patient symptoms and not necessarily on imaging appearance. A provider might not perform TKR if a patient is unwilling to undergo surgery because their level of pain does not warrant it, even if the patient has full-thickness cartilage loss. Conversely, a patient might have severe knee pain and desire surgery but their imaging might show only mild degenerative changes. Patients do not

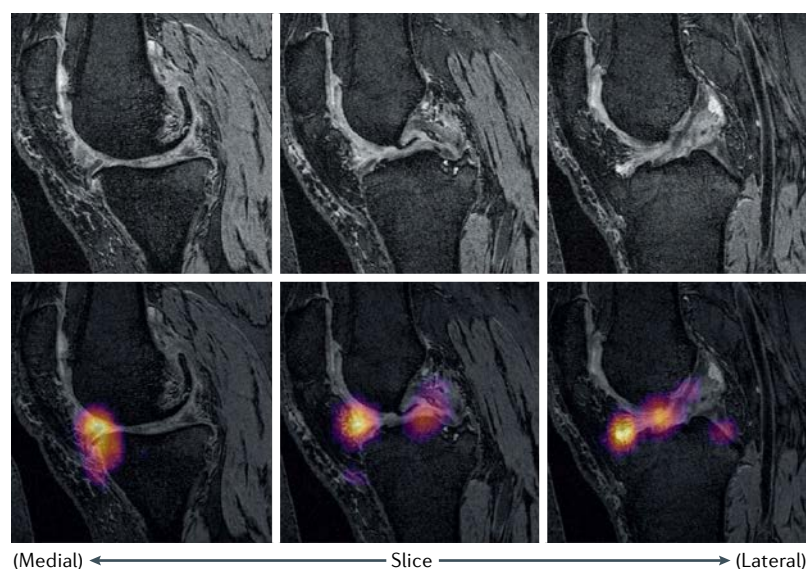


Fig. 2 | Anatomical structures on MRI scans influencing artificial intelligence model prediction of total knee replacement within 5 years. MRI slices (top row) and corresponding occlusion map slices (bottom row) of a knee classified by artificial intelligence as a true positive for undergoing future total knee replacement (TKR) within 5 years of initial MRI assessment¹¹⁶. Hotspots in occlusion maps for 124 true-positive knees were used to anatomically identify tissue types that corresponded with undergoing TKR within 5 years. Compared with true-negative controls, knees with hotspots in the medial patellar retinaculum, gastrocnemius tendon and plantaris muscle predicted higher odds of undergoing TKR, whereas hotspots in the medial and lateral tibiofemoral joint, meniscus and anterior cruciate ligament portended decreased odds of undergoing TKR. A hotspot refers to a portion of the image that the model assigns a weight to for decision-making, but it is not known how that portion of the image directly affects the final prediction owing to the ‘black box’ nature of artificial intelligence algorithms. Identifying model hotspots only informs the reader that the model is utilizing specific regions in different ways from other knee structures for its final decision. For example, the negative odds of needing TKR for the anterior cruciate ligament hotspot only denotes that this pixel location is used in determining the presence or absence of future TKR, but it is not known in which of the two directions it contributes to this prediction. Reprinted from REF.¹¹⁶, CC BY 4.0 (<https://creativecommons.org/licenses/by/4.0/>).

Gradient boosting

A machine learning technique used for regression and classification. Starting from multiple prediction models, gradient boosting is used to create a prediction model in the form of an ensemble of those models.

Occlusion maps

An image overlay representing the change in probability for a model’s prediction as a function of position in the image.

Multitask learning

Training a machine learning algorithm to simultaneously learn to perform more than one task at a time, which forces the algorithm to identify a more general model for the data.

necessarily undergo MRI solely to assess OA, as X-ray imaging is often sufficient to inform management decisions and is more cost-effective than MRI. Furthermore, MRI can potentially exaggerate the severity of knee OA by illuminating many more abnormalities than are detectable in radiographically mild-appearing osteoarthritic knees, and abnormalities found by MRI might not necessarily be meaningful for clinical management. MRI-based AI research efforts are useful for clinical trials (that is, for research) but are not immediately relevant for routine day-to-day clinical practice.

There is an overall paucity of trajectory analysis to predict OA prognosis with MRI, and it is important to highlight X-ray applications, in which AI models possess seemingly higher potential for clinical translation. A multitask model has been developed to predict two outcomes, namely baseline KL grade and receiving a TKR within 9 years of initial radiographic assessment, by training a single model using multitask learning¹¹⁹. Multitask learning entails training one neural network to predict two mutually inclusive outcomes that are hypothesized a priori to share parameter spaces. Multitasking saves computational time and avoids data over-fitting by

ensuring that model parameters are sufficiently generalizable to enable accurate prediction of each outcome. This multitask model incorporated regions of high importance to predict TKR in knees with different KL grades. Another DL framework predicted three groups of OA progression that were defined using rate of change in KL grade between follow-ups: no progression, quick progression and slow progression¹¹⁰. The AI’s prediction probabilities for progression were then combined with medical history and clinical examination results into a subsequent gradient-boosting algorithm to make a final hybrid prediction of whether a patient’s KL grade would increase in the next year. Projections from AI alone may not capture all the pertinent information for characterizing prognosis (for example, clinical evaluation), which is why ML models that use multiple data inputs, one of which is the output from a neural network, might prove more accurate as research in this area progresses. Clinical trials with longer-term follow-up will improve evaluation of disease progression and prognostication in DL studies.

Conclusions

AI in OA imaging has been extensively used with the ultimate goal of improving patient management. Reduction of the duration of MRI acquisition time, post-processing of data, disease diagnosis and prognosis are examples of areas where AI has been successfully applied. As discussed in this Review, studies demonstrate that advancements in DL have great potential to decrease patient discomfort, by reducing MRI acquisition time through accelerated MRI and super-resolution imaging techniques, which should also result in reducing the costs of patient care. DL has been used to process large datasets such as from the OAI and to analyse knee bone shape, T_2 relaxation values and cartilage thickness, which previously required labour-intensive, non-AI approaches.

Overall, the development of AI in the field of clinical imaging has the potential to bolster the utility of MRI in OA research and clinical application. By automating acquisition and reducing the required scan times, MRI protocols can be dynamically adapted and tailored to a patient’s needs, thereby moving closer to achieving real-time precision imaging. Accurate extraction of quantitative features such as cartilage thickness and T_2 values, including the presence of abnormalities, will no longer rely on time-consuming acquisitions or non-scalable post-processing procedures.

AI-based imaging has advantages and has demonstrated potential; however, thorough clinical validation is necessary at this point in time. Availability of datasets involving large cohorts of participants that include diverse normal and pathological morphologies, as well as multi-institutional collaborations, are fundamental to improving the generalizability of AI’s technological promise. Future research will likely be devoted to improving the interpretability and estimation of the uncertainty of DL models, so that clinicians can ultimately feel comfortable relying on AI support in patient care routines.

Published online 30 November 2021

1. Link, T. M., Neumann, J. & Li, X. Prestructural cartilage assessment using MRI. *J. Magn. Reson. Imaging* **45**, 949–965 (2017).
2. LeCun, Y., Bengio, Y. & Hinton, G. Deep learning. *Nature* **521**, 436–444 (2015).
3. Erickson, B. J., Korfiatis, P., Akkuz, Z. & Kline, T. L. Machine learning for medical imaging. *Radiographics* **37**, 505–515 (2017).
4. Liang, S. et al. Deep-learning-based detection and segmentation of organs at risk in nasopharyngeal carcinoma computed tomographic images for radiotherapy planning. *Eur. Radiol.* **29**, 1961–1967 (2019).
5. Assefa, D. et al. Robust texture features for response monitoring of glioblastoma multiforme on-weighted and-FLAIR MR images: a preliminary investigation in terms of identification and segmentation. *Med. Phys.* **37**, 1722–1736 (2010).
6. Razmjoo, A. et al. T2 analysis of the entire osteoarthritis initiative dataset. *J. Orthop. Res.* **39**, 74–85 (2021).
7. Iriondo, C. et al. Towards understanding mechanistic subgroups of osteoarthritis: 8 year cartilage thickness trajectory analysis. *J. Orthop. Res.* **36**, 1305–1317 (2020).
8. Desai, A. D. et al. The international workshop on osteoarthritis imaging knee MRI segmentation challenge: a multi-institute evaluation and analysis framework on a standardized dataset. *Radiol. Artif. Intell.* **3**, e200078 (2021).
9. Goodfellow, I., Bengio, Y. & Courville, A. *Deep learning* (MIT Press, 2016).
10. Caliva, F., Iriondo, C., Martinez, A. M., Majumdar, S. & Pedoia, V. Distance map loss penalty term for semantic segmentation. Preprint at *arXiv* <https://arxiv.org/abs/1908.03679> (2019).
11. Hansen, M. S. & Kellman, P. Image reconstruction: an overview for clinicians. *J. Magn. Reson. Imaging* **41**, 573–585 (2015).
12. Chaudhari, A. S. et al. Rapid knee MRI acquisition and analysis techniques for imaging osteoarthritis. *J. Magn. Reson. Imaging* **52**, 1321–1339 (2020).
13. Deshmene, A., Gulani, V., Griswold, M. A. & Seiberlich, N. Parallel MR imaging. *J. Magn. Reson. Imaging* **36**, 55–72 (2012).
14. Jakob, P. M., Griswold, M. A., Edelman, R. R. & Sodickson, D. K. AUTO-SMASH: a self-calibrating technique for SMASH imaging. *Magn. Reson. Mater. Phys. Biol. Med.* **7**, 42–54 (1998).
15. Lustig, M., Donoho, D. & Pauly, J. M. Sparse MRI: the application of compressed sensing for rapid MR imaging. *Magn. Reson. Med.* **58**, 1182–1195 (2007).
16. Otazo, R., Candes, E. & Sodickson, D. K. Low-rank plus sparse matrix decomposition for accelerated dynamic MRI with separation of background and dynamic components. *Magn. Reson. Med.* **73**, 1125–1136 (2015).
17. Hammernik, K. & Knoll, F. Machine learning for image reconstruction. in *Handbook of Medical Image Computing and Computer Assisted Intervention* 25–64 (Elsevier, 2020).
18. Hammernik, K. et al. Learning a variational network for reconstruction of accelerated MRI data. *Magn. Reson. Med.* **79**, 3055–3071 (2018).
19. Souza, R., Lebel, R. M. & Frayne, R. A hybrid, dual domain, cascade of convolutional neural networks for magnetic resonance image reconstruction. *PMLR* **102**, 437–446 (2019).
20. Liang, D., Cheng, J., Ke, Z. & Ying, L. Deep MRI reconstruction: unrolled optimization algorithms meet neural networks. Preprint at *arXiv* <https://arxiv.org/abs/1907.11711> (2019).
21. Recht, M. P. et al. Using deep learning to accelerate knee MRI at 3 T: results of an interchangeability study. *Am. J. Roentgenol.* **215**, 1421–1429 (2020).
22. Subhas, N. et al. Diagnostic interchangeability of deep convolutional neural networks reconstructed knee MR images: preliminary experience. *Quant. Imaging Med. Surg.* **10**, 1748 (2020).
23. Wang, S. et al. Accelerating magnetic resonance imaging via deep learning. in *2016 IEEE 13th International Symposium on Biomedical Imaging (ISBI)* 514–517 (IEEE, 2016).
24. Yang, Y., Sun, J., Li, H. & Xu, Z. Deep ADMM-Net for compressive sensing MRI. in *Advances in Neural Information Processing Systems*. 10–18 (MIT Press, 2016).
25. Han, Y. et al. Deep learning with domain adaptation for accelerated projection-reconstruction MR. *Magn. Reson. Med.* **80**, 1189–1205 (2018).
26. Lee, D., Yoo, J. & Ye, J. C. Deep residual learning for compressed sensing MRI. in *2017 IEEE 14th International Symposium on Biomedical Imaging (ISBI)* 15–18 (IEEE, 2017).
27. Yu, S. et al. Deep de-aliasing for fast compressive sensing MRI. Preprint at *arXiv* <https://arxiv.org/abs/1705.07137> (2017).
28. Yang, G. et al. DAGAN: Deep de-aliasing generative adversarial networks for fast compressed sensing MRI reconstruction. *IEEE Trans. Med. Imaging* **37**, 1310–1321 (2017).
29. Jin, K. H., McCann, M. T., Froustey, E. & Unser, M. Deep convolutional neural network for inverse problems in imaging. *IEEE Trans. Image Process.* **26**, 4509–4522 (2017).
30. Quan, T. M., Nguyen-Duc, T. & Jeong, W.-K. Compressed sensing MRI reconstruction using a generative adversarial network with a cyclic loss. *IEEE Trans. Med. Imaging* **37**, 1488–1497 (2018).
31. Liu, F., Samsonov, A., Chen, L., Kijowski, R. & Feng, L. SANTIS: sampling-augmented neural network with incoherent structure for MR image reconstruction. *Magn. Reson. Med.* **82**, 1890–1904 (2019).
32. Han, Y., Sunwoo, L. & Ye, J. C. k-Space deep learning for accelerated MRI. *IEEE Trans. Med. Imaging* **39**, 377–386 (2019).
33. Akçakaya, M., Moeller, S., Weingärtner, S. & Ugurbil, K. Scan-specific robust artificial-neural-networks for k-space interpolation (RAKI) reconstruction: database-free deep learning for fast imaging. *Magn. Reson. Med.* **81**, 439–453 (2019).
34. Schlemper, J., Caballero, J., Hajnal, J. V., Price, A. N. & Rueckert, D. A deep cascade of convolutional neural networks for dynamic MR image reconstruction. *IEEE Trans. Med. Imaging* **37**, 491–503 (2017).
35. Zhu, B., Liu, J. Z., Cauley, S. F., Rosen, B. R. & Rosen, M. S. Image reconstruction by domain-transform manifold learning. *Nature* **555**, 487–492 (2018).
36. Chandler, D. M. Seven challenges in image quality assessment: past, present, and future research. *Int. Sch. Res. Not.* **2013**, 1–54 (2013).
37. Wang, Z. & Bovik, A. C. Mean squared error: love it or leave it? A new look at signal fidelity measures. *IEEE Signal. Process. Mag.* **26**, 98–117 (2009).
38. Wang, Z., Bovik, A. C., Sheikh, H. R. & Simoncelli, E. P. Image quality assessment: from error visibility to structural similarity. *IEEE Trans. Image Process.* **13**, 600–612 (2004).
39. Zbontar, J. et al. fastMRI: an open dataset and benchmarks for accelerated MRI. Preprint at *arXiv* <https://arxiv.org/abs/1811.08839> (2018).
40. Zhao, H., Gallo, O., Frosio, I. & Kautz, J. Loss functions for image restoration with neural networks. *IEEE Trans. Comput. Imaging* **3**, 47–57 (2016).
41. Genzel, M., Macdonald, J. & März, M. Solving inverse problems with deep neural networks — robustness included? Preprint at *arXiv* <https://arxiv.org/abs/2011.04268> (2020).
42. Wang, Z., Simoncelli, E. P. & Bovik, A. C. Multiscale structural similarity for image quality assessment. in *The Thirty-Seventh Asilomar Conference on Signals, Systems & Computers*, 2003 **2**, 1398–1402 (IEEE, 2003).
43. Sheikh, H. R. & Bovik, A. C. A visual information fidelity approach to video quality assessment. in *The First International Workshop on Video Processing and Quality Metrics for Consumer Electronics* **7**, 2 (Academia, 2005).
44. Cheng, K. et al. Addressing the false negative problem of deep learning MRI reconstruction models by adversarial attacks and robust training. in *Medical Imaging with Deep Learning* 121–135 (PMLR, 2020).
45. Antun, V., Renna, F., Poon, C., Adcock, B. & Hansen, A. C. On instabilities of deep learning in image reconstruction and the potential costs of AI. *Proc. Natl. Acad. Sci. USA* **117**, 30088–30095 (2020).
46. McAlindon, T. E. et al. OARSI guidelines for the non-surgical management of knee osteoarthritis. *Osteoarthritis Cartilage* **22**, 363–388 (2014).
47. Wang, Z., Chen, J. & Hoi, S. C. H. Deep learning for image super-resolution: a survey. *IEEE Trans. Pattern Anal. Mach. Intell.* **43**, 3365–3387 (2020).
48. Chaudhari, A., Fang, Z., Lee, J. H., Gold, G. & Hargreaves, B. Deep learning super-resolution enables rapid simultaneous morphological and quantitative magnetic resonance imaging. in *International Workshop on Machine Learning for Medical Image Reconstruction* 3–11 (Springer, 2018).
49. Liu, F., Feng, L. & Kijowski, R. MANTIS: model-augmented neural network with incoherent k-space Sampling for efficient MR parameter mapping. *Magn. Reson. Med.* **82**, 174–188 (2019).
50. Eckstein, F. et al. Quantitative MRI measures of cartilage predict knee replacement: a case-control study from the Osteoarthritis Initiative. *Ann. Rheum. Dis.* **72**, 707–714 (2013).
51. Bowes, M. A. et al. Precision, reliability, and responsiveness of a novel automated quantification tool for cartilage thickness: data from the Osteoarthritis Initiative. *J. Rheumatol.* **47**, 282–289 (2020).
52. Bredbenner, T. L. et al. Statistical shape modeling describes variation in tibia and femur surface geometry between control and incidence groups from the Osteoarthritis Initiative database. *J. Biomech.* **43**, 1780–1786 (2010).
53. Morales Martinez, A. et al. Learning osteoarthritis imaging biomarkers from bone surface spherical encoding. *Magn. Reson. Med.* **84**, 2190–2203 (2020).
54. Pedoia, V., Lee, J., Norman, B., Link, T. M. & Majumdar, S. Diagnosing osteoarthritis from T2 maps using deep learning: an analysis of the entire Osteoarthritis Initiative baseline cohort. *Osteoarthritis Cartilage* **27**, 1002–1010 (2019).
55. Carballido-Gamio, J. et al. Spatial analysis of magnetic resonance and relaxation times improves classification between subjects with and without osteoarthritis. *Med. Phys.* **36**, 4059–4067 (2009).
56. Carballido-Gamio, J., Joseph, G. B., Lynch, J. A., Link, T. M. & Majumdar, S. Longitudinal analysis of MRI T2 knee cartilage laminar organization in a subset of patients from the osteoarthritis initiative: a texture approach. *Magn. Reson. Med.* **65**, 1184–1194 (2011).
57. Fink, A., Koscoff, J., Chassin, M. & Brook, R. H. Consensus methods: characteristics and guidelines for use. *Am. J. Public Health* **74**, 979–983 (1984).
58. Tibrewala, R. et al. Computer-aided detection AI reduces interreader variability in grading hip abnormalities with MRI. *J. Magn. Reson. Imaging* **52**, 1163–1172 (2020).
59. Smith, C. P. et al. Intra- and interreader reproducibility of PI-RADSv2: a multireader study. *J. Magn. Reson. Imaging* **49**, 1694–1703 (2019).
60. Dunn, W. R. et al. Multirater agreement of arthroscopic meniscal lesions. *Am. J. Sports Med.* **32**, 1937–1940 (2004).
61. Harolds, J. A., Parikh, J. R., Bluth, E. I., Dutton, S. C. & Recht, M. P. Burnout of radiologists: frequency, risk factors, and remedies: a report of the ACR commission on human resources. *J. Am. Coll. Radiol.* **13**, 411–416 (2016).
62. Prasoon, A. et al. Deep feature learning for knee cartilage segmentation using a triplanar convolutional neural network. in *International conference on medical image computing and computer-assisted intervention* 246–253 (Springer, 2013).
63. Norman, B. et al. Use of 2D U-Net convolutional neural networks for automated cartilage and meniscus segmentation of knee MR imaging data to determine relaxometry and morphometry. *Arthritis Rheumatol.* **79**, 3184–3189 (2018).
64. Liu, F. et al. Deep convolutional neural network and 3D deformable approach for tissue segmentation in musculoskeletal magnetic resonance imaging. *Magn. Reson. Med.* **79**, 2379–2391 (2018).
65. Çiçek, Ö., Abdulkadir, A., Lienkamp, S. S., Brox, T. & Ronneberger, O. 3D U-Net: learning dense volumetric segmentation from sparse annotation. in *International conference on medical image computing and computer-assisted intervention* 424–432 (Springer, 2016).
66. Milletari, F., Navab, N. & Ahmadi, S.-A. V-net: fully convolutional neural networks for volumetric medical image segmentation. in *2016 Fourth International Conference on 3D Vision (3DV)* 565–571 (IEEE, 2016).
67. Jørgensen, D. R., Lillholm, M., Genant, H. K. & Dam, E. B. On subregional analysis of cartilage loss from knee MRI. *Cartilage* **4**, 121–130 (2015).
68. Zeng, G. et al. Latent3DU-Net: Multi-level latent shape space constrained 3D U-net for automatic segmentation of the proximal femur from radial MRI of the hip. in *International Workshop on Machine Learning in Medical Imaging* 188–196 (Springer, 2018).
69. Gaj, S., Yang, M., Nakamura, K. & Li, X. Automated cartilage and meniscus segmentation of knee MRI with conditional generative adversarial networks. *Magn. Reson. Med.* **84**, 437–449 (2020).
70. Wirth, W. et al. Accuracy and longitudinal reproducibility of quantitative femorotibial cartilage measures derived from automated U-Net-based

- segmentation of two different MRI contrasts: data from the Osteoarthritis Initiative healthy reference cohort. *Magn. Reson. Mater. Phys. Biol. Med.* **34**, 337–354 (2021).
71. Cheng, R. et al. Fully automated patellofemoral MRI segmentation using holistically nested networks: implications for evaluating patellofemoral osteoarthritis, pain, injury, pathology, and adolescent development. *Magn. Reson. Med.* **83**, 139–153 (2020).
 72. Schock, J. et al. A method for semantic knee bone and cartilage segmentation with deep 3D shape fitting using data from the Osteoarthritis Initiative. in *International Workshop on Shape in Medical Imaging* 85–94 (Springer, 2020).
 73. Ambellan, F., Tack, A., Ehlike, M. & Zachow, S. Automated segmentation of knee bone and cartilage combining statistical shape knowledge and convolutional neural networks: data from the osteoarthritis initiative. *Med. Image Anal.* **52**, 109–118 (2019).
 74. Liu, F. SUSAN: segment unannotated image structure using adversarial network. *Magn. Reson. Med.* **81**, 3330–3345 (2019).
 75. Perslev, M., Dam, E. B., Pai, A. & Igel, C. One network to segment them all: a general, lightweight system for accurate 3D medical image segmentation. in *International Conference on Medical Image Computing and Computer-Assisted Intervention* 30–38 (Springer, 2019).
 76. Mortazi, A., Karim, R., Rhode, K., Burt, J. & Bagci, U. CardiacNET: segmentation of left atrium and proximal pulmonary veins from MRI using multi-view CNN. in *International Conference on Medical Image Computing and Computer-Assisted Intervention* 377–385 (Springer, 2017).
 77. Chen, L.-C., Zhu, Y., Papandreou, G., Schroff, F. & Adam, H. Encoder-decoder with atrous separable convolution for semantic image segmentation. in *Proceedings of the European conference on computer vision (ECCV)*. Springer Science+Business Media. 801–818 (Springer, 2018).
 78. Caliva, F. et al. Breaking speed limits with simultaneous ultra-fast MRI reconstruction and tissue segmentation. *Proc. Mach. Learn. Res.* **1**, 17 (2020).
 79. Brui, E. et al. Deep learning-based fully automatic segmentation of wrist cartilage in MR images. *NMR Biomed.* **33**, e4320 (2020).
 80. Deniz, C. M. et al. Segmentation of the proximal femur from MR images using deep convolutional neural networks. *Sci. Rep.* **8**, 1–14 (2018).
 81. Zeng, G. et al. Entropy guided unsupervised domain adaptation for cross-center hip cartilage segmentation from MRI. in *International Conference on Medical Image Computing and Computer-Assisted Intervention* 447–456 (Springer, 2020).
 82. Medina, G., Buckless, C. G., Thomasson, E., Oh, L. S. & Torriani, M. Deep learning method for segmentation of rotator cuff muscles on MR images. *Skeletal Radiol.* **50**, 683–692 (2021).
 83. Boutillon, A., Borotikar, B., Burdin, V. & Conze, P.-H. Combining shape priors with conditional adversarial networks for improved scapula segmentation in MR images. in *2020 IEEE 17th International Symposium on Biomedical Imaging (ISBI)* 1164–1167 (IEEE, 2020).
 84. Conze, P. H., Brochard, S., Burdin, V., Sheehan, F. T. & Pons, C. Healthy versus pathological learning transferability in shoulder muscle MRI segmentation using deep convolutional encoder-decoders. *Comput. Med. Imaging Graph.* **83**, 101733 (2020).
 85. Cantarelli Rodrigues, T. et al. Three-dimensional MRI bone models of the glenohumeral joint using deep learning: evaluation of normal anatomy and glenoid bone loss. *Radiol. Artif. Intell.* **2**, e190116 (2020).
 86. Di Giacomo, G., de Gasperi, N. & Scarso, P. Bipolar bone defect in the shoulder anterior dislocation. *Knee Surg. Sports Traumatol. Arthrosc.* **24**, 479–488 (2016).
 87. Eckstein, F. et al. Cartilage thickness change as an imaging biomarker of knee osteoarthritis progression data from the FNIH OA biomarkers consortium. *Arthritis Rheumatol.* **67**, 3184 (2015).
 88. Samek, W., Montavon, G., Vedaldi, A., Hansen, L. K. & Müller, K.-R. *Explaining AI: interpreting, explaining and visualizing deep learning*. Vol. **11700** (Springer Nature, 2019).
 89. Peterfy, C. G. et al. Whole-organ magnetic resonance imaging score (WORMS) of the knee in osteoarthritis. *Osteoarthritis Cartilage* **12**, 177–190 (2004).
 90. Hunter, D. J. et al. The reliability of a new scoring system for knee osteoarthritis MRI and the validity of bone marrow lesion assessment: BLOKS (Boston–Leeds Osteoarthritis Knee Score). *Ann. Rheum. Dis.* **67**, 206–211 (2008).
 91. Hunter, D. J. et al. Evolution of semi-quantitative whole joint assessment of knee OA: MOAKS (MRI osteoarthritis knee score). *Osteoarthritis Cartilage* **19**, 990–1002 (2011).
 92. Lee, S. et al. Scoring hip osteoarthritis with MRI (SHOMRI): a whole joint osteoarthritis evaluation system. *J. Magn. Reson. Imaging* **41**, 1549–1557 (2015).
 93. Liu, F. et al. Deep learning approach for evaluating knee MR images: achieving high diagnostic performance for cartilage lesion detection. *Radiology* **289**, 160–169 (2018).
 94. Pedoia, V. et al. 3D convolutional neural networks for detection and severity staging of meniscus and PFJ cartilage morphological degenerative changes in osteoarthritis and anterior cruciate ligament subjects. *J. Magn. Reson. Imaging* **49**, 400–410 (2019).
 95. Roblot, V. et al. Artificial intelligence to diagnose meniscus tears on MRI. *Diagn. Interv. Imaging* **100**, 243–249 (2019).
 96. Fritz, B., Marbach, G., Civardi, F., Fucetese, S. F. & Pfirrmann, C. W. A. Deep convolutional neural network-based detection of meniscus tears: comparison with radiologists and surgery as standard of reference. *Skeletal Radiol.* **49**, 1207–1217 (2020).
 97. Namiri, N. K. et al. Deep learning for hierarchical severity staging of anterior cruciate ligament injuries from MRI. *Radiol. Artif. Intell.* **2**, e190207 (2020).
 98. Liu, F. et al. Fully automated diagnosis of anterior cruciate ligament tears on knee MR images by using deep learning. *Radiol. Artif. Intell.* **1**, 180091 (2019).
 99. Bien, N. et al. Deep-learning-assisted diagnosis for knee magnetic resonance imaging: development and retrospective validation of MRNet. *PLoS Med.* **15**, e1002699 (2018).
 100. Astuto, B. et al. Automatic deep learning assisted detection and grading of abnormalities in knee MRI studies. *Radiol. Artif. Intell.* **3**, e219001 (2021).
 101. Jordan, J. M. et al. Prevalence of hip symptoms and radiographic and symptomatic hip osteoarthritis in African Americans and Caucasians: the Johnston County Osteoarthritis Project. *J. Rheumatol.* **36**, 809–815 (2009).
 102. Panfilov, E., Tiulpin, A., Klein, S., Nieminen, M. T. & Saarakkala, S. Improving robustness of deep learning based knee MRI segmentation: mixup and adversarial domain adaptation. in *Proceedings of the IEEE International Conference on Computer Vision Workshops. Computer Vision Foundation (CVF)*. (IEEE, 2019).
 103. Shah, R. F., Bini, S. A., Martinez, A. M., Pedoia, V. & Vail, T. P. Incremental inputs improve the automated detection of implant loosening using machine-learning algorithms. *Bone Jt. J.* **102**, 101–106 (2020).
 104. Deng, J. et al. Imagenet: a large-scale hierarchical image database. in *2009 IEEE conference on computer vision and pattern recognition* 248–255 (IEEE, 2009).
 105. Liu, B., Luo, J. & Huang, H. Toward automatic quantification of knee osteoarthritis severity using improved Faster R-CNN. *Int. J. Comput. Assist. Radiol. Surg.* **15**, 457–466 (2020).
 106. Tiulpin, A., Thevenot, J., Rahtu, E., Lehenkari, P. & Saarakkala, S. Automatic knee osteoarthritis diagnosis from plain radiographs: a deep learning-based approach. *Sci. Rep.* **8**, 1–10 (2018).
 107. Norman, B., Pedoia, V., Noworolski, A., Link, T. M. & Majumdar, S. Applying densely connected convolutional neural networks for staging osteoarthritis severity from plain radiographs. *J. Digit. Imaging* **32**, 471–477 (2019).
 108. Xue, Y., Zhang, R., Deng, Y., Chen, K. & Jiang, T. A preliminary examination of the diagnostic value of deep learning in hip osteoarthritis. *PLoS One* **12**, e0178992 (2017).
 109. von Schacky, C. E. et al. Development and validation of a multitask deep learning model for severity grading of hip osteoarthritis features on radiographs. *Radiology* **295**, 136–145 (2020).
 110. Tiulpin, A. et al. Multimodal machine learning-based knee osteoarthritis progression prediction from plain radiographs and clinical data. *Sci. Rep.* **9**, 1–11 (2019).
 111. Huang, Z., Ding, C., Li, T. & Yu, S. P.-C. Current status and future prospects for disease modification in osteoarthritis. *Rheumatology* **57**, iv108–iv123 (2018).
 112. Loeser, R. F., Goldring, S. R., Scanzello, C. R. & Goldring, M. B. Osteoarthritis: a disease of the joint as an organ. *Arthritis Rheum.* **64**, 1697 (2012).
 113. Neogi, T. et al. Magnetic resonance imaging–based three-dimensional bone shape of the knee predicts onset of knee osteoarthritis: data from the Osteoarthritis Initiative. *Arthritis Rheum.* **65**, 2048–2058 (2013).
 114. Kohn, M. D., Sassoon, A. A. & Fernando, N. D. Classifications in brief: Kellgren–Lawrence classification of osteoarthritis. *Clin. Orthop. Relat. Res.* **474**, 1886–1893 (2016).
 115. Bowes, M. A. et al. Machine-learning, MRI bone shape and important clinical outcomes in osteoarthritis: data from the Osteoarthritis Initiative. *Ann. Rheum. Dis.* **80**, 502–508 (2020).
 116. Tolpadi, A. A., Lee, J. J., Pedoia, V. & Majumdar, S. Deep learning predicts total knee replacement from magnetic resonance images. *Sci. Rep.* **10**, 1–12 (2020).
 117. Roemer, F. W. et al. MRI-based screening for structural definition of eligibility in clinical DMOAD trials: rapid osteoarthritis MRI eligibility score (ROAMES). *Osteoarthritis Cartilage* **28**, 71–81 (2020).
 118. Namiri, N. K. et al. Deep learning for large scale MRI-based morphological phenotyping of osteoarthritis. *Sci. Rep.* **11**, 1–10 (2021).
 119. Leung, K. et al. Prediction of total knee replacement and diagnosis of osteoarthritis by using deep learning on knee radiographs: data from the osteoarthritis initiative. *Radiology* **296**, 584–593 (2020).
 120. Friedman, B. R., Jones, J. P., Chavez-Munoz, G., Salmon, A. P. & Merritt, C. R. B. *Principles of MRI*. (McGraw-Hill Health Professions Division, 1989).
 121. Uecker, M. et al. ESPIRiT — an eigenvalue approach to autocalibrating parallel MRI: where SENSE meets GRAPPA. *Magn. Reson. Med.* **71**, 990–1001 (2014).
 122. Lustig, M., Donoho, D. L., Santos, J. M. & Pauly, J. M. Compressed sensing MRI. *IEEE Signal. Process. Mag.* **25**, 72 (2008).
 123. Sodickson, D. K. & Manning, W. J. Simultaneous acquisition of spatial harmonics (SMASH): fast imaging with radiofrequency coil arrays. *Magn. Reson. Med.* **38**, 591–603 (1997).
 124. Griswold, M. A. et al. Generalized autocalibrating partially parallel acquisitions (GRAPPA). *Magn. Reson. Med.* **47**, 1202–1210 (2002).
 125. Ronneberger, O., Fischer, P. & Brox, T. U-net: convolutional networks for biomedical image segmentation. in *International Conference on Medical image computing and computer-assisted intervention* 234–241 (Springer, 2015).
 126. Goodfellow, I. J. et al. Generative adversarial networks. *Adv. Neural Inf. Process. Syst.* **3**, 1–9 (2014).

Author contributions

The authors contributed equally to all aspects of the article.

Competing interests

The authors declare no competing interests.

Peer review information

Nature Reviews Rheumatology thanks E. B. Dam, F. Berenbaum, and the other, anonymous, reviewer(s) for their contribution to the peer review of this work.

Publisher's note

Springer Nature remains neutral with regard to jurisdictional claims in published maps and institutional affiliations.

RELATED LINKS

FASTMRI challenge: <http://fastmri.med.nyu.edu/>
MC-MRRec challenge: <https://sites.google.com/view/calgary-campinas-dataset/mr-reconstruction-challenge>

© Springer Nature Limited 2021